The role of phytotoxic and antimicrobial compounds of *Euphorbia gummifera* in the cause and maintenance of the fairy circles of Namibia

by

Nicole Galt

Submitted in partial fulfillment of the requirements for the degree Magister Scientiae

Department of Plant and Soil Sciences

Faculty of Natural and Agricultural Sciences

University of Pretoria

Pretoria

Supervisor: Prof. J.J.M. Meyer

March 2018

UNIVERSITEIT VAN PRETORIA
UNIVERSITY OF PRETORIA
YUNIBESITHI YA PRETORIA

The role of phytotoxic and antimicrobial compounds of *Euphorbia gummifera* in the cause and maintenance of the fairy circles of Namibia

by

Nicole Galt

Department of Plant and Soil Sciences

Faculty of Natural and Agricultural Sciences

University of Pretoria

Pretoria

Supervisor: Prof. J.J.M. Meyer

Degree: MSc Medicinal Plant Science

Abstract

Fairy circles (FC) are unexplained botanical phenomena of the pro-Namib desert and parts of the West Coast of South Africa. They are defined as circular to oval shaped anomalies of varying sizes that are left bereft of vegetation. Even though there are several distinctly different hypotheses that have aimed to explain the origin of fairy circles, none have done so to satisfaction of the scientific community. The aim of this study was to determine if phytotoxic and antibacterial properties of a co-occurring *Euphorbia* species, *E. gummifera* plays a role in the creation of fairy circles. Representative soil samples (from inside-, outside fairy circles and underneath dead *E. gummifera* plants) and plant samples (aerial

parts of *E. gummifera* and intact grasses, *Stipagrostis uniplumis*) were collected from the area. The collected samples were used for a several biological assays. A soil bed bio-assay was done using the three collected soil types. A germination inhibition study was done using a methanolic *E. gummifera* extract. A soil-agar bio-assay was done with collected soil as well as with rhizosphere soil from grass roots. All data was analyzed statistically. The *E. gummifera* methanolic extract was used to test its antibacterial activity against several bacterial species. Among the tested bacteria were two isolates from the rhizosphere soil that were identified through 16S rRNA sequencing. Several compounds with biological activity of interest were identified through silica column chromatography and gas chromatography mass spectrometry in the *E. gummifera* methanolic extract.

The results from the germination inhibition assay indicated that *E. gummifera* does possess phytotoxic properties in terms of significant germination inhibition (P-value <0.05) at concentrations between 40mg/ml to 10mg/ml extract if the seeds were water stressed. The results of the soil bed bio-assay further corroborated the synergistic theory. The phytotoxic soil from underneath *E. gummifera* prevented germinated seeds to transition to mature seedlings when water stressed. The soil-agar bio-assay indicated that rhizosphere soil had a stimulatory effect on germination while the dead plant soil and soil from inside FCs inhibited germination significantly. The methanolic extract exhibited antibacterial activity against the two identified rhizosphere isolates, *Kocuria polaris* and *Pseudomonas paravulva*, as well as other bacterial species tested in the study. Several compounds that have previously been found in other studies to have antibacterial and phytotoxic activity were identified.

In conclusion, due to *E. gummifera*'s phytotoxicity (possibly allelopathy) and antibacterial activity, especially under water stressed conditions, a possible cause for the creation of fairy circles has been identified in the southern parts of Namibia where fairy circles co-occur with *E. gummifera*.

Table of contents

Chapter 3: The chemical constituents of *Euphorbia gummifera*

Chapter 4: The antibacterial properties of *Euphorbia gummifera*

Acknowledgements

I would like to thank:

God for always guiding me on the path he chose for me.

My family for supporting me and encouraging me during my six years of studying.

My supervisor Professor Marion Meyer for this opportunity and all it has offered me.

My friends and colleagues at the Plant and Soil Sciences Department.

The NRF for my funding.

CHAPTER 1

Introduction

Table of Contents

List of figures

List of tables

1.1 Introduction

Among the unexplained botanical phenomena of the world, fairy circles are probably among the ones at the top of the list. Fairy circles are usually associated with debates and intense disagreement, making this scientific anomaly one of the most controversial of its time. The main reason for this is the nature of this phenomenon. Fairy circles (Figure 1.1) are broadly defined as circular to oval shaped anomalies of varying sizes that have been left bereft of any form of flora (Getzin et al., 2015a) and occur in the pro-Namib desert (Figure 1.2) and parts of the West Coast of South Africa (Van Rooyen et al., 2004). Fairy circles have recently also been recorded to occur in the Western Australia outback (Getzin et al., 2016), although this matter is surrounded by some controversy.

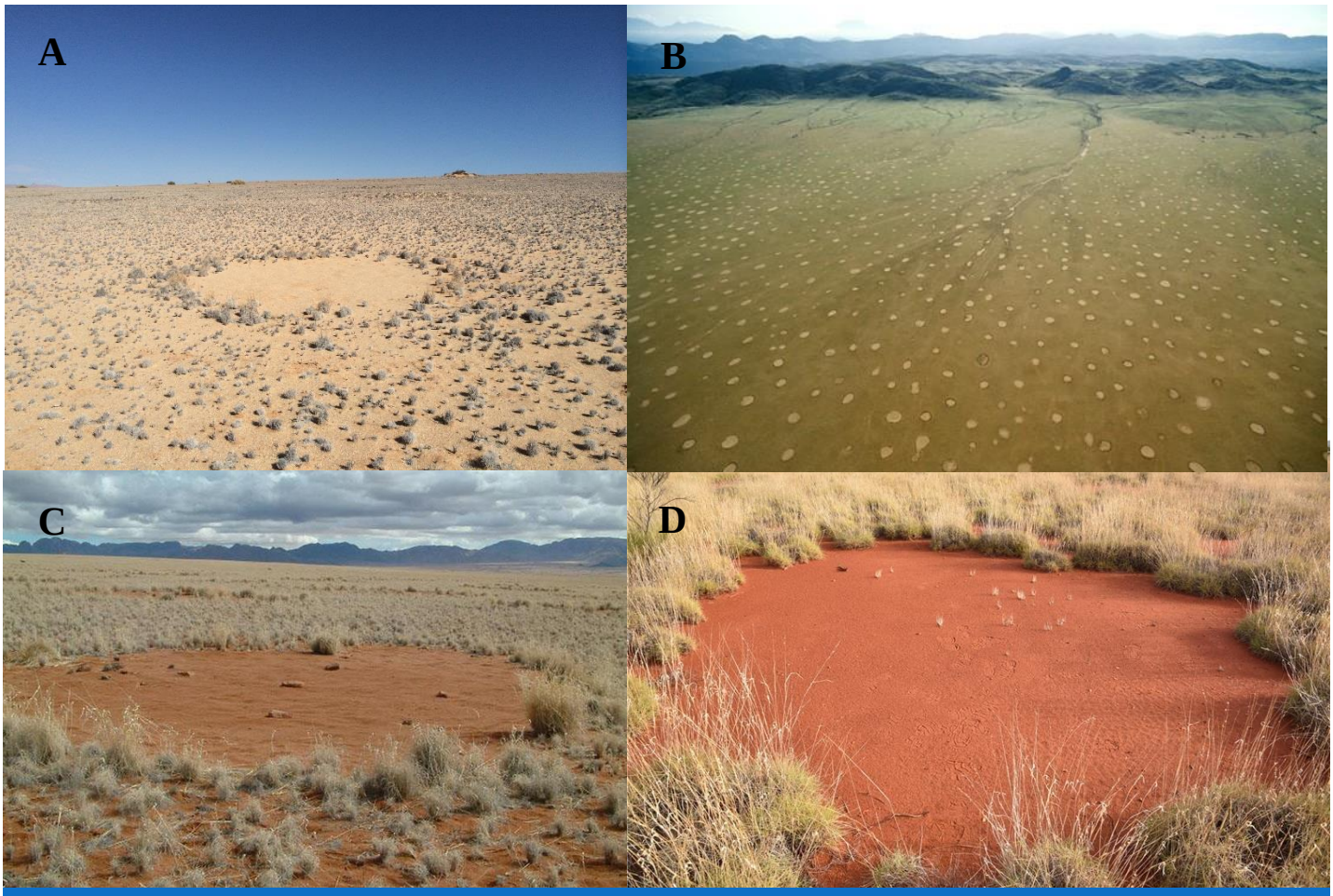

Figure 1.1: A. A fairy circle photographed during a field collection in the Garub area of southern Namibia. B. An aerial view of scattered fairy circles (Getty images, 2009). C. Fairy circle surrounded by more abundant grass growth (Livescience, 2012). D. The fairy circles discovered in the western part of Australia (Getzin et al., 2016).

This contentious scientific anomaly has led to contradicting theories put forth by a diverse set of global scientists, over the better part of the last 45 years (Figure 1.3). Even with such world class research no single theory has been accepted/proven, further baffling the scientific community.

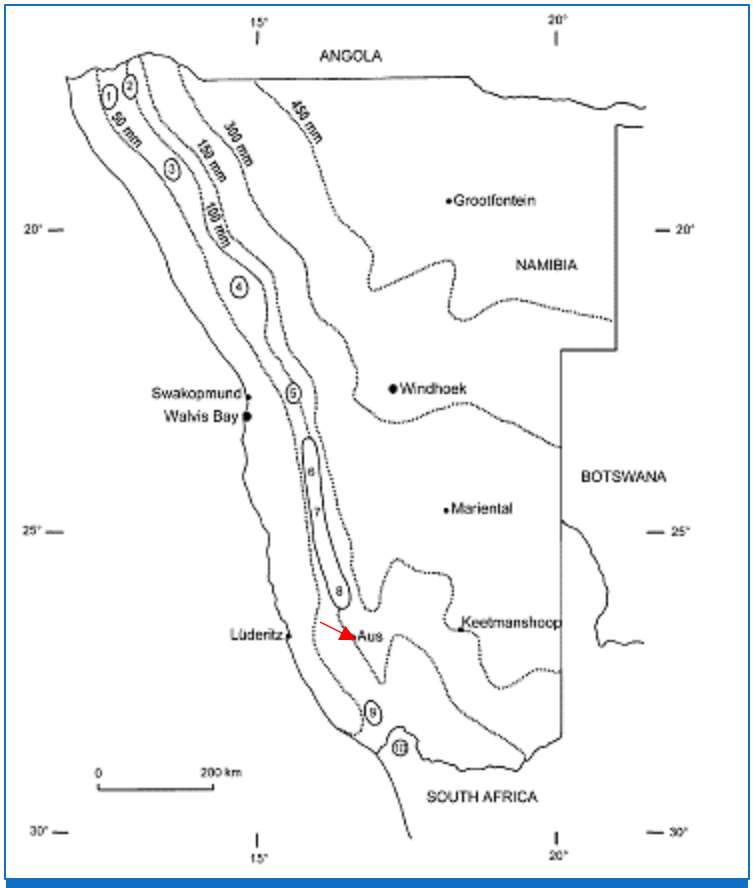

Figure 1.2: Fairy circle distribution map. The numbers indicate areas of known fairy circle locations. The red arrow indicates an addition area where fairy circles occur (Van Rooyen et al., 2004).

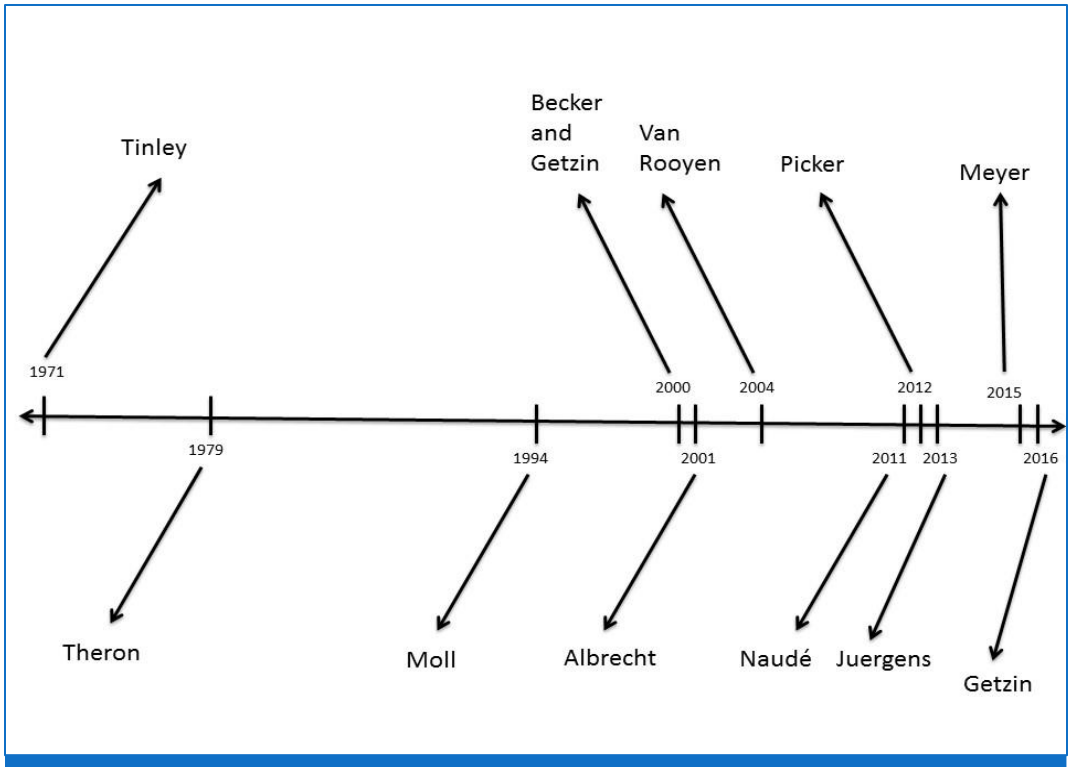

Figure 1.3: Timeline representing the various fairy circle theories developed over the last 45 years.

1.2 Literature review: Fairy circle theories

There are four main theories explaining the origin of fairy circles: social insects (ants/termites), vegetation patterning, volatile gas emissions, microbial and plant based allelopathy.

1.2.1 Insect related theories

One of the main theories that aim to explain the genesis of the fairy circle phenomenon involves the role that insects, such as termites and ants, play. The first scientific publication concerning fairy circles, hypothesized that the fairy circles were remnants of fossilized termite nests that formed when these areas had experienced higher than average rainfall (Tinley et al., 1971). More than 20 years passed then, without any research focusing on fairy circles, until Moll (1994) published his article.

Figure 1.4: The termite *H. mossambicus* (Biomes of South Africa).

Moll hypothesized that termites were the causative agent behind the occurrence of fairy circles. The three possible termite culprits were *Hodotermes mossambicus* (Figure 1.4), *Psammotermes allocerus* or *Baucaliotermes hainsei*. His hypothesis was formulated on the basis of the physical and chemical cues he observed. This included the foraging behavior of the ants near their termitaira that he linked to the apparent lack of vegetation from fairy circles. After studying aerial photographs of areas where fairy circles occur, he noted that not all circles were equally bereft of vegetation. Thus he concluded that fairy circles were sporadically appearing and disappearing as a result of the lifespan of termite nests which were in turn dependent on seasonal rainfall. Thus during times of flourishing grass cover termites fed adjacently to their nest leading to circle formation and vice versa. Also, after comparing the patterns of termite distribution with the occurrence of fairy circles he deduced that the termite *P. allocerus* and *H. mossambicus* were most likely the causative agents involved in the genesis of fairy circles. Moll (1994) also concluded that fairy circles mainly occur on substrates of a sandy nature.

Becker and Getzin (2000) reviewed the previous work done on fairy circles in terms of termites. Their study consisted of three main parts: the origin of fairy circles, their distribution as well as some of their striking characteristics. An in depth study of the distribution of fairy circles in the

Kaokoland was done through studying a series of aerial photographs from 1996 as well as Landsat TM images. Through analysis of these visual aids they found that fairy circles were more widely distributed over western Koakoland than previously indicated (Moll, 1994). The wider distribution indicated that fairy circles occur on different substrates (Aeolian and Alluvial of origin). This directly contradicts Moll (1994) statement that fairy circles are restricted to sandy substrates. The amount of precipitation decreases in these areas from east to west and as a result the densities of fairy circles also decrease (Becker and Getzin, 2000). A large part of their study focused on the unique characteristics of the fairy circles. In their specific study area they found that the grass that forms the prominent edge effect of the circles and the grass forming the matrix in between circles are of the same species. This intriguing fringe of densely growing grass that is clearly distinct from the matrix grass is one of the most confounding aspects of fairy circles. As part of their research they aimed to explain the occurrence of this unique characteristic.

Fairy circles are characteristically devoid of vegetation. The barren patches thus provide an uncontested source of water and nutrients to the grasses on growing on the edge. Thus the fringe grasses thrive due to favorable conditions as compared to the matrix grasses that need to compete for resources (Juergens, 2013).

Desert environments are arid and are mostly shaped by Aeolian forces. A combination of wind and the apparent lack of vegetation cover inside circles causes a sunken or concave appearance. Thus the barren patches act as water traps where water can penetrate into deeper parts of the soil contributing to the average soil moisture. Fringe grass roots can utilize the higher soil moisture that is not available to matrix grass (Becker and Getzin, 2000).

Desert environments are associated with stress and severe competition. Among scares resources, nutrients are among the most important. Due to the lack of water and wind movement, decomposition of natural matter is a rare occurrence. Grasses growing on the edge of circles have the greatest chance of trapping such organic matter. Here the organic matter decomposes and contributes to the soil nutrients available to these grasses further enabling them to thrive (Becker

and Getzin, 2000).Lastly they focused origin of fairy circles. They focused on both the allelopathy theory as well as the termite related theory. For the purpose of this section only the research focused on termites is discussed. They specifically focused on the biology of the *H. mossambicus* termite. Through their review they noted that this foraging termite feeds mainly on surface grass (also on leaves and non-woody substrates) in dry regions. During their field work they did observe the termite, yet the surface foraging activity of the termite was not observed very frequently. Using their collected background information on *H. mossambicus*, they used a model to describe how this termite is involved in the genesis of fairy circles (Figure 1.5). This model also accounts for their dynamic nature.

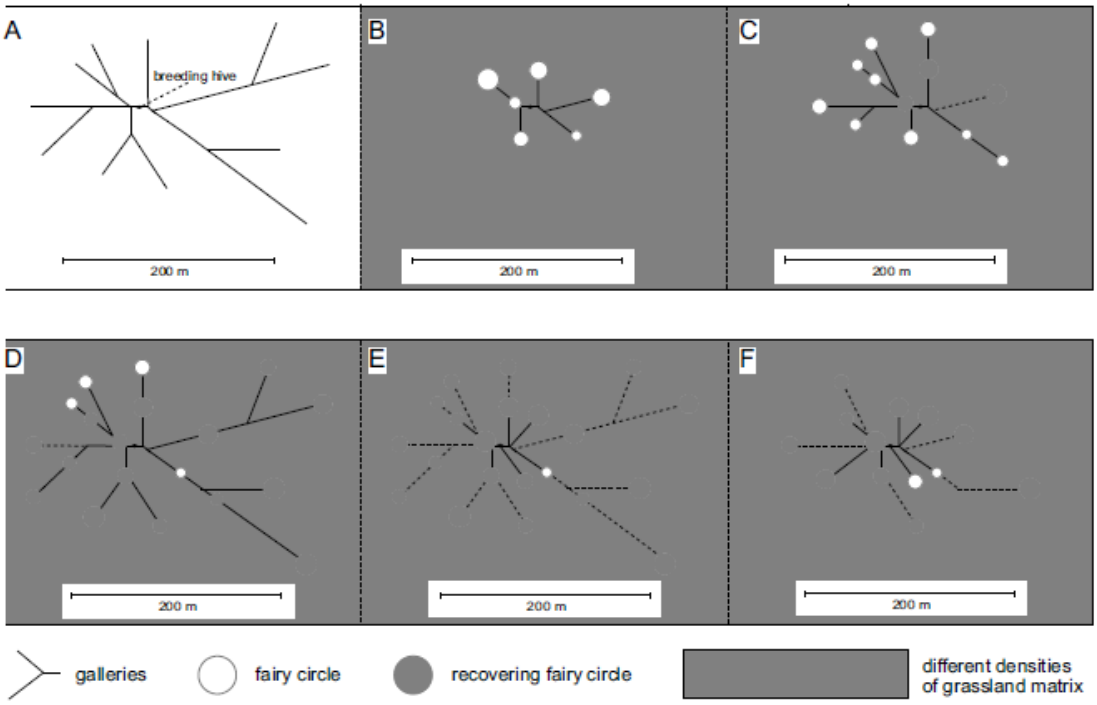

Figure 1.5: Becker and Getzin (2000)'s model describing how the harvester termite *H. mossambicus*' feeding and nesting system is involved in the genesis of fairy circles. A: Visual representation of the nesting system of the harvester termite with the breeding hive in the center. B: During years of average rainfall the feeding behavior of the termite at the end of the galleries in close proximity to the hive leads to the formation of barren patches. C: During years of less than average rainfall galleries are extended further outward from the breeding hive giving rise to new barren patches. D: In the case of even more dire environmental conditions the feeding galleries are stretched out even further. As a result some of the barren patches close to the breeding hive that were abandoned are able to recover thus closing the barren patches. E: When rainfall parameters return to normal or as a result of less feeding, foraging returns to areas in close proximity to the feeding hive and those areas further out are abandoned. Subsequently these abandoned patches can also recover. F: Eventually disused circles transition completely and start to form part of the matrix in between barren patches.

According to their model the barren patches are maintained due to the lack of soil nutrients. This is a result of organic matter from the barren patches as well as the mentioned before the conditions in the desert constantly move organic matter with the wind. Recovery of these areas thus doesn't happen overnight due to its dependence on various factors. Not all fairy circles are similar in shape and most if not all differ in the average diameter. They explained this feature of fairy circles due to the differences in the intensity of the feeding of the harvester termite which is in turn affected by environmental and biological factors such as soil temperature and predators. Overall they concluded that the harvester termite *H. mossambicus* is the main factor causing the formation of fairy circles.

Albrecht et al. (2001) had an alternative approach to the termite related hypothesis as compared to Moll's research. Their research was based on the hypothesis that a biological factor (possibly semi-volatile in nature) directly/indirectly associated with termite nests is responsible for the formation of fairy circles. Their research had several different puzzle pieces that would ultimately paint a picture explaining their hypothesis. This included: analysis of aerial photographs, determining potential differences in the soil moisture of fairy circles soil versus matrix soil, determining the natural progression of the circles, microscopically studying root morphology and germination experiments with collected soil.

Analysis of aerial photographs enabled them to determine the distribution, density and average size of the fairy circles. Using the distance to nearest neighbor method and the R-value it yields, the type of distribution of the fairy circles could be deduced. An R-value equal to zero indicates that all studied objects are arranged in a clump, a value of 1.0 indicates a random distribution and a value of 2.149 indicates a perfect hexagonal distribution pattern. To link their measurements with termites, their results were compared to a similar natural phenomenon thought also to be associated with termites (Figure 1.6). This natural phenomenon is known as 'heuweltjies'/mima mounds found in parts of the Cape.

A comparison of their features and important values can be found in Table 1.1.

Figure 1.6: A. The phenomenon known as heuweltjies/mima mounds in the area of Clanwilliam in the Cape province of South Africa. B. The characteristic fairy circle with the well-defined fringe grass surrounding the barren patch.

It is clear from Table 1.1 that there are some striking similarities as well as distinct differences between these two phenomena. The R-values of the fairy circles and the 'heuweltjies' are very similar and thus further supported their hypothesis of a termite related origin for both. However, the nearest neighbor values are very different.

Using the Adobe Photoshop software, scanned image of areas with fairy circles were analyzed. Using manipulation techniques circles could clearly be distinguished from the landscape. After studying the circles' average diameters they determined that in their study area most circles fall in the parameter of between 3 to 9 m. What was interesting was that their study revealed that there was a wide array of different diameter sizes. In comparison, "heuweltjies"/mima mounds have an average diameter of 20m (Cramer et al., 2016). The difference in soil moisture of fairy circle soil compared to matrix soil was also investigated. Their results indicated that on average soil collected from the center of fairy circles (at a depth of one meter) contained five times more moisture than its counterpart from the matrix. However, these results could be an inaccurate representation of the true differences as prior to sampling the area received extensive rain.

Table 1.1: Comparison of fairy circles to heuweltjies/mima mounds based on important characteristics.

Feature	Fairy circle	"Heuweltjies"/mima mounds	References
Basic description/ features	Circular to oval shaped anomalies of varying sizes that have been left bereft of any form of flora, surrounded by a dense fringe of taller grass.	The mounds are characterized by vegetation that grows more densely inside them than the areas in between mounds. The mounds are usually covered by grass. Thus the mounds can support a higher number of plants versus the areas in between.	Albrecht et al., 2001; Cramer et al., 2012; Knight et al., 1989; Lovergrove and Siegfried, 1989; Van Rooyen et al., 2004
Distribution areas	Pro-Namib desert and parts of the West Coast of South Africa.	Western and southern parts of the Cape province of South Africa. Similar mounds to the 'heuweltjies' are found around the world.	

Feature	Fairy circle	"Heuweltjies"/mima mounds	References
R-value	1.68 (± 0.05)	1.7	Albrecht et al., 2001; Cramer et al., 2012; Knight et al., 1989; Lovergrove and Siegfried, 1989; Van Rooyen et al., 2004
Average nearest-neighbour distance	14.4 m	47.14 m	
Density of phenomena in area studied	3484/km^2 (7.3% of surface area of area of interest for the study)	335.37/km^2	
Explanation for phenomenon	Termites, ants, plant based allelopathy, vegetation patterning and gas-related theories.	Differences in the fertility of the "heuweltjie" soil versus the soil in between, termites and rodents (due to their non-random distribution a biological agent, specifically faunal is implicated), erosion resulting in islands of fertility.	

The differences in diameter lengths led them to investigate the lifespan of the fairy circles. Their results and background study led them to believe that fairy circles evolve as most things in the natural world do. This natural evolution progresses from genesis to development to maturation to the inevitable death. They also distinguished each of the stages on the basis of a circles physical attributes (Figure 1.7)

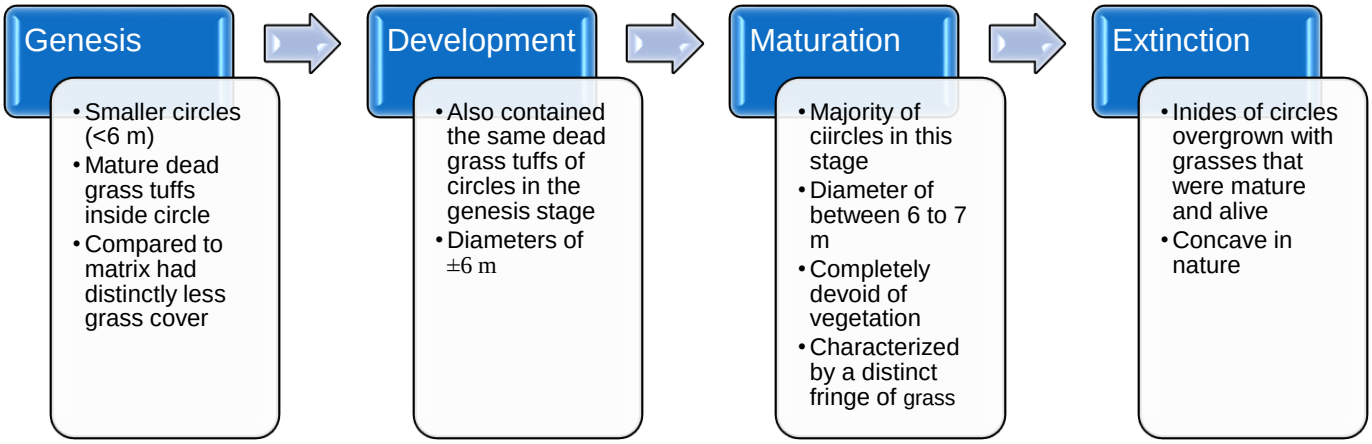

Figure 1.7: Natural evolutionary progression of fairy circles from genesis to extinction (adapted from information originally published by Albrecht et al., 2001).

To study the root morphology of the grass *Stipagrostis uniplumis*, intact plants were carefully removed from both the inside and outside of thirteen fairy circles. The extensive rains prior to their field collection enabled grasses to grow on the inside of the circles. These, however, grew in closer proximity to the edge than the center of the circles and these could clearly be distinguished from the dead grasses. After close inspection with and without a dissection microscope, it became evident that there were marked differences between the rhizospheres of the grasses from the different locations. The roots from the matrix were covered with an extensive soil sheath, while the roots from inside fairy circles lacked such a soil layer.

Finally Albrecht et al. (2001) conducted a germination experiment using different soil types collected during their field trip. There were 7 different types (Figure 1.8). An aliquot of 30 grams of each soil type was placed in an ice tray. A 100 *Cynodon dactylon* seeds were sown and the soil was moistened with distilled water. The soil was kept moist and no statistically significant differences could be detected on day 15 and 22 when the trays were moved to direct sunlight. The seedlings were put under water stress conditions for a day but no differences could be detected again. Following this, the seedlings were subjected to continuous dehydration and hydration for 12 days. As this process progressed differences became more prominent. Results indicated that those seedlings growing in soil types 1, 7, 6 and 2 could survive such dehydration brought on by the water stress. This indicated to Albrecht et al. (2001) that a biological factor (possibly semi-volatile in nature) could be responsible for preventing plants growing inside circles to resist such dehydration stress associated with desert environments. However, such a factor could not directly be linked to termites/termite nests.

Figure 1.8: The locations in and around a fairy circle from where soil was collected. 1: On the outside of the circle, 3 m from the edge. 2: On the edge of the circle. 3: Equidistantly from the edge and the center of the circle. 4: In the center of the circle. 5: Equidistantly from the center and the opposite edge of the circle. 6: The opposite edge of the circle. 7: On the outside of the circle, 3 m from the opposite edge (information Albrecht et al., 2001).

Picker et al. (2012) proposed an alternative hypothesis contradicting the termite hypothesis. They proposed that ants were the causative agent of this phenomenon. Six different fairy circle sites were chosen for their research of which the NamibRand was their main research area. At the sites the association of the termite *H. mossambicus* with fairy circles as well as the association of ants and ant nests with fairy circles was investigated. Picker et al. (2012) found that termites were rarely encountered and sometimes virtually absent from their main research area, whereas at some of the other sites they were more abundant. This could be explained by the fact the

rainfall patterns differed between the sites, which is known to affect termites activity (Albrecht et al., 2001). The large black pugnacious ant, *Anoplolepis steingroeveri* was found to be the most abundant of the eleven sampled ant species. Overall the ants were found to be more abundant inside circle than outside circles. In addition to these finding Picker et al. (2001 found several correlations between ant nest and circles in terms of spatial distribution and moisture content. The conclusion that Picker et al. (2001) made was that ants were the causative agent and more importantly linked them to the gas theory (Naudé et al., 2011).

Juergens (2013) focused on water availability inside fairy circles and how these levels relate to termite activity. Previous studies had noted that even though the fairy circles are devoid of any vegetation, their soil moisture content is much higher than the surrounding areas (Albrecht et al., 2001; Van Rooyen et al., 2004). Juergens aimed to provide supporting quantitative data to support these claims. He did so by measuring the soil water content within fairy circles as well as at surrounding sites, over a period of four years (2006-2012). He found higher soil water content in fairy circles and hypothesized that this is a result of the lack of vegetation. He also mentioned that an absence of vegetation leads to less transpiration compared to the matrix and that the nature of the soil (grain and pore sizes) and the absence of vegetation cause rapid percolation of water which leads to the concentrated source of perennial water. This deep source of water helps maintain the matrix vegetation (Figure 1.9).

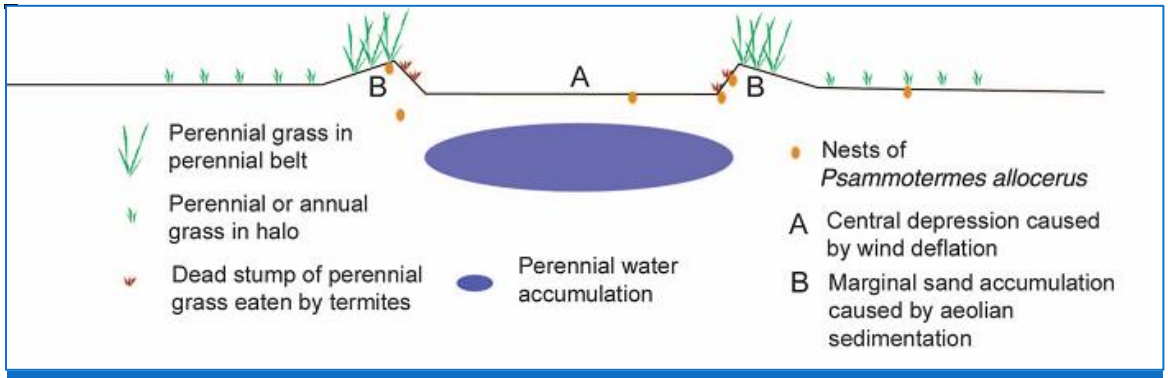

Figure 1.9: Visual representation of Juergens (2013)' hypothesis.

Juergens' results led him to believe that some form of biogenic ecosystem engineer is responsible for the formation of fairy circles which is related to the higher soil moisture levels found. During several field trips, 30 to 100 fairy circles were investigated to establish which organisms had a direct link to them. He compared his results to distribution maps of the organisms sampled. Only the termite *P. allocerus* was sampled at all the fairy circle locations. Other termites previously linked to fairy circles, such as *H. mossambicus* and *M. viator*'s involvement in this phenomenon was dismissed due to discrepancies in terms of their distribution compared to fairy circle distribution. Low frequency of ant sampling eliminated them as being involved in the origin of fairy circles. Overall *P. allocerus* had the best distribution data: these termites were found in and around 80 to 100% of fairy circles studied as well as their nests and galleries. To dismiss claims that such results merely reflect termite colonization of bare patches Juergens found that termites can be found associated with circles in any stage of development such as initial development shown in newly formed circles. The main role of the termite was hypothesized to be to forage on grass roots as a means to keep the fairy circles devoid of vegetation and thus prevent transpiration. Thus the action of the termite ensures a water source which can sustain them as well a matrix grasses (which they also can feed on). Their foraging behavior is responsible for the gradual widening of the circles from their origin to established circles. Fairy circles thus act as unique ecosystems in a very hostile environment. Fairy circles ensure the persistence of accumulation of perennial water which in turns leads to the formation of the perennial grass fringe around the circles. This subsequently causes a burst in biodiversity in fauna and flora due to the favorable conditions in the desert environment. Juergens thus equated the allogenic power of the termite *P. allocerus* to that of the well-known ecosystem engineer, beavers.

The most important aspect that distinguishes the findings of Vlieghe et al. (2015) from the previous termite theories is that their theory clearly focuses on the origin and maintenance of fairy circles. They aimed to provide supporting data as well as explanations for both genesis and maintenance by combining the rational of Albrecht et al. (2001) and Tschinkel (2012). Tschinkel provided evidence that supports the hypothesis that fairy circles develop from origin to death. He estimated that fairy circles have an average life span of 41 years, where after they are fully integrated back into the grassland matrix.

Vlieghe et al. (2015) study site focused on the fairy circle occurring in the NamibRand Nature Reserve. One of their field work and sampling excursions was done after extensive rains in February 2011 which might have affected some of their findings. Their study consisted of five different parts:

1. Termite abundance, soil moisture as well as the process of circle formation and different stages thereof.
2. Feeding trails with termites.
3. Seed numbers in fairy circles.
4. Estimating the relative age of fairy circles.
5. Abundance of other associated organisms.

Similarly to Albrecht et al. (2001), Vlieghe et al. (2015) divided fairy circles into distinctly different sequential stages (Figure 1.10). These were new, young, mature and senescent.

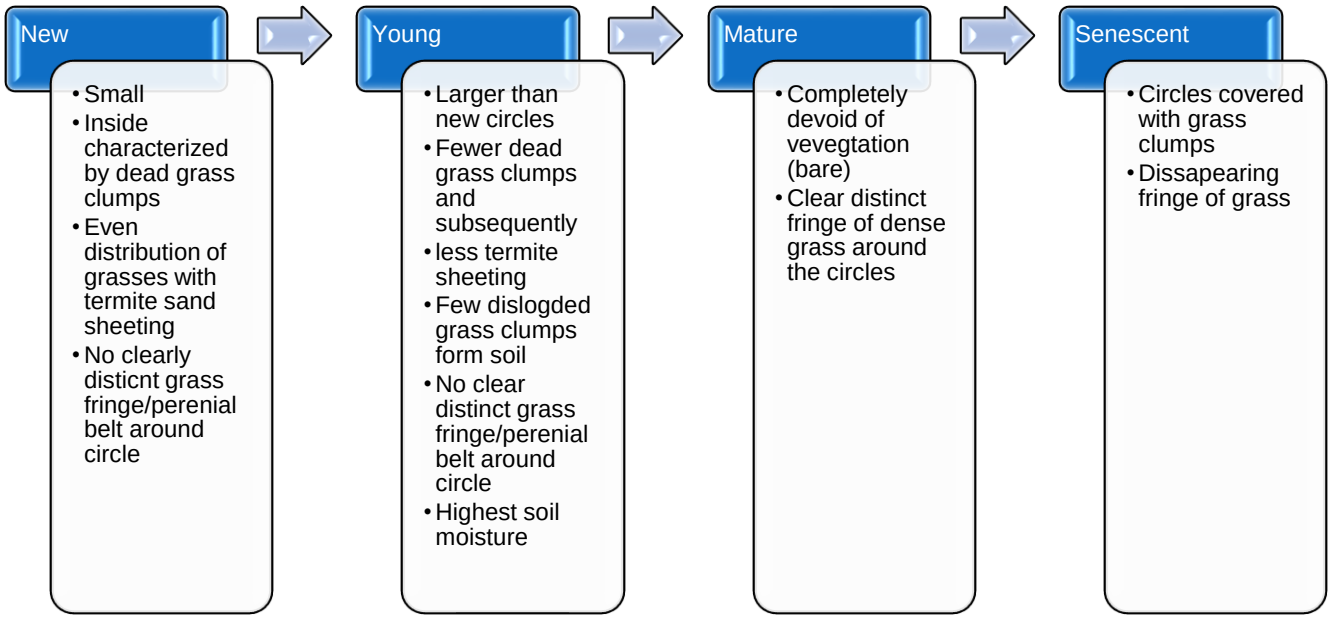

Figure 1.10: Sequential stages of fairy circle development.

Each distinct stage was also studied by Vlieghe et al. (2015) in terms of area, soil moisture, glass clump abundance, termite sheeting and amount of living termites encountered. For each of these criteria ten circles were studied. The area of the circles gradually increased as they developed with largest being in the mature stage. Soil samples of 500 cm^3 were collected at a depth of 50 cm from the center of ten circles as well as in between these circles. An aliquot of 100g was dried to determine the soil moisture. The results indicated that of all the developmental stages the young circles contained the highest soil moisture even when compared to the matrix. Circles in the senescent stage had the lowest soil moisture content, which was approximately the same as the matrix. Termite activity was the most abundant in new circles and as circles matured these numbers decreased. Once their numbers started to decrease (lowest in mature and senescent stages) the termite activity shifted from the inside of circles to the fringe of grass surrounding circles.

In an attempt to demonstrate that the foraging and feeding behavior of the termite *P. allocerus* matches that observed on the field, Vlieghe et al. (2015) conducted an herbivory trail. The termites were obtained from a collection trip when ten intact nests were harvested near Vanrhynsdrop in the Western Cape of South Africa. Sand was also collected from their study site in Namibia. There were three different treatments: ten pots containing sand only was frozen to kill all possible termites, ten pots contained sand plus termite nests and ten control pots contained only sand. The bio-indicator was wheat plants (three seedlings) whose roots, leaves as well as inflorescence were monitored in terms of amounts and size. After a five week growth period the differences between the three treatments were compared. The results indicated that termite activity significantly reduced root and leaf numbers. Of the controls, 100% survived as compared to the 33.3% mortality of the live nest treatment. The frozen soil had improved growth (higher number of inflorescence and leaf length) as compared to those containing termites. Overall the reduction in roots was as a result of direct feeding of termites on roots at soil surface which indirectly decreased leaf numbers as a result of subsequent stress exerted on plants.

In terms of seed abundance, results indicated that fairy circles contained a very low amount of seeds (*S. ciliata* and *S. obtuse*) when compared to the matrix and grass fringe. Vlieghe et al. (2015) estimated that on average most circles stayed 50 years in the young and mature stages combined and it takes an average of 16 years to reach the senescent stage. They found no

significant difference in the *A. steingroeveri* ant numbers between the bare circles, the fringe and the matrix. They did, however, find that even though there were no differences between the different stages of circle development the ant numbers did increase after significant rains. Vlieghe et al. (2015) hypothesized that the ants are more involved in the maintenance of fairy circles than their origin.

Due to the fact that fairy circles evolve though a developmental process, any proposed theory for the origin of fairy circles needs to clearly be associated with all stages (Tschinkel, 2012). Without this, a proposed theory can merely be seen as an association. Their results clearly demonstrated this in terms of termite abundance in all developmental stages.

1.2.1.1 Shortcomings and discrepancies of the insect related theories

With such an intriguing phenomenon, it comes as no surprise that each theory is extensively scrutinized by the scientific community. Because no concrete undisputed theory has been put forth a few important shortcomings and discrepancies of each theory, including the termite/ant theory, needs to be addressed.

Figure 1.11: *H. mossambicus* termites. The smaller dark pigmented termites are the workers in their colony (Czech University of Life Science Prague, Faculty of forestry and Wood Science, 2012).

Moll (1994) was the first to put forth comprehensive research for a termite related origin of fairy circles. The major shortcoming of his theory is that he was unable to directly connect his main causative insect species, *H. mossambicus*, to fairy circles in the field due to the fact that he did not successfully encounter and subsequently harvest the termite during field work. The worker termites responsible for foraging are pigmented (Figure 1.11) (Mitchell et al., 1993) which would make their surface foraging discernable during field surveillance.

This was corroborated by field observations of Becker and Getzin (2000) and Jankowitz et al. (2008). The few species that Moll (1994) did, however, find (*P. allocerus* and *B. hansei*) would not be able to be responsible for forming fairy circles through their foraging behavior. Moll also did not clearly distinguish the genesis of fairy circles from there maintenance. According to his hypothesis, termites are involved in both aforementioned stages. He explained that termites

extensively forage on grass seeds which subsequently maintain the bare characteristic of circles. Yet Van Rooyen et al. (2004) point out that after sufficient rain some grass seeds do germinate but are unable to survive. Thus a lack of seeds cannot be responsible for maintaining circles' bare nature. Van Rooyen also pointed out some irregularities when comparing the *H. mossambicus*'s distribution versus that of fairy circles in terms of their rainfall region local. This termite mainly inhabits areas receiving an average of 400 to 600 mm of rain annually (Coaton, 1958) which transcends that of the drier areas where fairy circles occur (Becker and Getzin, 2000).

Even though Becker and Getzin (2000) put forth a comprehensive model explaining fairy circle origin, it was scrutinized quite extensively by Grube (2002) as well as Van Rooyen et al. (2004). The aspects upon which the model, foraging behavior of the termites and their heat sensitivity, was based was especially discussed. The unique behavior of the harvester termite would make it troublesome to observe its foraging behavior in the field. These termites prefer to be hidden from sight, especially those higher up in the hierarchy of the colony (breeders and king/queen) (Grube, 2002). Becker and Getzin's (2000) remark that these termites only forage a minimum distance from their nest in order to stay close has not yet been observed and recorded in literature. Moreover, the nesting system is usually characterized by sub-units that are connected to the nest's different entrances (Leuthold et al., 1976). This in turn leads to a multitude of feeding sites (Harrison, 2011), contradicting the proposed models foraging predictions that the termites foraging is centered closely around the nest. Overall there is a lack of knowledge of the specifics of this termites nest physiology as well as feeding behavior, which Becker and Getzin (2000) overlooked. A few other noteworthy points were also addressed by Grube (2002).

One evident characteristic of fairy circles is that they are of various sizes, their diameters ranging from 3 m to 9 m (Albrecht et al., 2001; Theron, 1979). Becker and Getzin (2000) hypothesized that this was a result of varying feeding intensities of the termites as well as their temperature sensitivity. In terms of their feeding behavior specifically, the proposed model assumed that the termites are restricted to feeding on grasses, feed in circular patterns and feed with different intensities. Nel and Hewitt (1969) did a study on the different types of food the *H. mossambicus* termite consumes in the field. They found that the termite eats both grasses and shrubs. Harvester termites are also important ecosystem engineers through their detritivorious behavior.

Based on field observations, Grube (2000) concluded that the termite does not necessity forage in circular patterns and that their feeding only results in clearly visible barren patches when foraging occurs in areas sparsely covered with grass. Mitchell et al. (1993) did a study on the temperature sensitivity of the *H. mossambicus* termite to determine its critical thermal maxima (CTmax) and the critical thermal minimum (CTmin). Their observations indicated that that of most worker termites (pigmented major and minor workers) were between 43.5 °C to 48.53 °C. Field observations recorded by Grube (2002) supported this. Termites were found to forage during peak summer at temperatures higher than 44 °C which contradicts Becker and Getzin's (2001) observation that *H. mossambicus* has limited surface activity at temperatures at and above 40 °C. Altogether, these observations disprove the link between fairy circle diameters and termite heat sensitivity that Becker and Getzin (2001) hypothesized. Various different factors can possibly affect the termite's temperature sensitivity. Mitchell et al. (1993) concluded that biological factors such as size, age and matureness of termites as well as thermal history and certain environmental conditions affect termite foraging, thus making any assumptions regarding a link between temperature sensitivity and fairy circle size speculatory.

Albrecht et al. (2001), as discussed previously, linked fairy circles to termites through a hypothesized semi-volatile compound (among other things discussed previously) released by a mechanism of termites. Nonetheless, this hypothesized compound has yet to be found and successfully identified, leaving questionable gaps in their hypothesis. Their results from their germination experiment using collected soil from in and around fairy circles and their conclusion was also questionable. Most previous germination experiments done using soil from inside as well as outside fairy circles indicated that inside fairy circle soil has an inhibitory effect on growth, independent of water stress or the watering schedule.

One of the first research articles on fairy circles by Theron (1979) reported on a soil bioassay using soil collected from three distinct localities in and amongst fairy circles (Figure 1.12). *Eragrostis teff* seeds were planted in soil from inside fairy circles, the edge of the circles and in between circles. He found that the grass growing in the soil from inside grew substantially slower compared to its counterparts.

Figure 1.12: The bioassay Theron (1979) conducted using different types of soil collected from in and around fairy circles. Left: Soil from inside fairy circles. Middle: Soil from the edge of fairy circles. Right: Soil from in between fairy circles

Van Rooyen et al. (2004) also conducted a soil bioassay with soil from Giribes Plain, Hartsmann's Valley and Marienfluss, these areas are amongst the most well-known fairy circle localities. They used *Lolium multiflorum* Lam. as a bio-indicator for this soil bioassay. There was a significant difference between the results of the bioassay done on soil from inside fairy circles as compared to soil from the edge of the circles. A bioassay of soil from inside fairy circles exhibited a strong inhibitory effect on the growth of the bio-indicator. In contrast, the bioassay of soil collected from the edge exhibited a stimulatory effect on bio-indicator growth. Van Rooyen et al. (2004 emphasized the need for further research focusing specifically on the nature of this stimulatory and inhibitory effect. Joubert (2008) conducted a bioassay on soil collected from the Giribes plan. *S. uniplumis* was used as bio-indicator and planted in soil from the inside of circles, the edge and matrix. There were also significant differences between the grass grown in soil from inside circles and grass grown in soil from the matrix (in terms of biomass and length).

Picker et al. (2012) rejected the termite theory on the basis of an apparent lack of termite observation inside fairy circles in the field (NamibRand) or scant numbers (northern fairy circle localities). The same was found for termite foraging holes. As discussed previously, they formulated an ant-related fairy circle theory focused on the black pugnacious ant, *A. steingroeveri.* This ant's distribution area covers drier areas of South Africa as well as south

west- and central Africa (Prins, 1982). Even though the ant is accustomed to drier environmental conditions, Picker et al. (2012) could not explain the apparent lack of ant observation at Marienfluss.

Fairy circles are characterized by a band of taller grass forming their margins (Juergens, 2013). This aspect of fairy circle morphology was not investigated and explained by Picker et al. (2012) even though they encountered a multitude of ants on the periphery. It could be argued that the ants are merely associated with the higher grass density of the circle margins (as their food source) and not the circles themselves.

Picker et al.'s (2012) investigations into the difference in soil moisture indicated higher soil moisture content as compared to the matrix and a noteworthy finding to point out is that the periphery also had lower soil moisture content than anywhere inward toward the circle center. Ants are important ecosystem engineers and play a pivotal part in ecosystems (Folgarait, 1998). The construction of ant nests, whether above-ground or subterranean, is accompanied by severe changes in the soil structure. Ant nests are characterized by the construction of a complex set of underground networks and chambers/galleries (Tschinkel, 2003) which could increases soil porosity (Frouz and Jilkova, 2008; McCahon and Lockwood, 1990), leading to higher water infiltration rates (Kutílek, 2004). A study done by Rogers and Lavine (1974) into the difference in soil moisture above ant nests as compared to the surroundings indicated that there was no significant differences between them in terms of the top 20 cm of soil. This repudiates some of Picker et al.'s (2012) findings. If nests were situated beneath fairy circles, this would cause the soil to have a lower moisture content, which was not what Picker et al. (2012) found.

Ants also play a central role in modifying the chemical and biological structure of soil (Folgarait, 1998). Some ants are known to enrich the soil microbial profile by interacting with different microbes either directly or indirectly. Friese and Allen (1993) did a study on the interactions between harvester ants and arbuscular mycorrhiza in a semi-arid environment. They concluded, based on their results, that the harvester ant *Pogonomyrmex occidentalis* had an enrichment effect on arbuscular mycorrhiza and once nest systems were abandoned, the mycorrhizal density was significantly higher than before. Thus ant nests, through mutualistic relationships with certain microbes, improve soil fertility which facilitates establishment of plants.

More recently Juergens (2013) connected fairy circles to the sand termite *P. allocerus*. One of the most significant counter arguments to his theory was documented in Getzin et al. (2015a & b). According to them fairy circles have the following spatial characteristics: fairy circles have a hexagonal spatial arrangement, which indicates a very high degree of ordering. They noted that even though the termite theory can account for the regularity of the fairy circle it fails to account for the highly ordered distribution. Thus concluding that *P. allocerus*, and other fairy circle associated termites, do not have the ability to produce fairy circles with such specific spatial characteristics.

Overall there is confusion regarding the different insect related theories of fairy circles. The most prominent being in terms of the termite nests themselves. Some theories state that such termite nests are located directly beneath fairy circles (Albrecht et al., 2001; Moll, 1994) whereas others state that they are located in between the circles (Becker and Getzin, 2000;) or on the periphery of circles (Juergens, 2013). Another confusing and contradicting aspect of this branch of theories is with regards to the specific site of foraging on grasses. *H. mossambicus* related theories are centered around above-ground foraging whilst *P. allocerus* related theories on the other hand focus on subterranean foraging on roots.

1.2.2 Vegetation patterning

The use of mathematical models to study scientific anomalies is a fairly new and sometimes overwhelming approach. The approach depends on the use of digital imagery and analytical software (Juergens, 2015) to analyze patterns observed in nature. This is an alternative approach to studying the elicit fairy circles.

Cramer and Barger (2013) were the first to approach the study of fairy circles using this new technique. They hypothesized that fairy circles are spatial patterns forming as a result of vegetation self-organization in an environment with strenuous resource competition, especially subterranean. The barren patches facilitate movement of water to nearby plants, enhancing their growth. Over time these barren patches accumulate soil water and nutrients thus acting as valuable resource reservoirs. Such reservoirs help taller grass species flourish leading to the development of fairy circle peripheral grass ring.

Cramer and Barger's (2013) study site focused on areas in the NamibRand Nature reserve where fairy circles occur. Here soil samples were collected for further study. These studies included soil analysis and a bioassay. Additionally aerial photographs were analyzed using Matlab. Finally, Cramer and Barger used the boosted regression tree analysis to establish a model for fairy circle presence and or absence.

The most significant result from their soil analysis was the significant difference in the soil moisture content of the matrix soil versus that of soil taken from the center of a fairy circle. Cramer and Barger (2013) ascribed this to less moisture utilization in the barren zone due to the absence of vegetation. The matrix soil contained 2 to 3 times less moisture than the inside of fairy circles as well as significant differences in soil water holding capacities. There were a minor differences in terms of the chemical profiles of the two distinct soil types. Fairy circles soils had a markedly lower content of soil organic carbon (SOC) (C_4-grass origin), total soil nitrogen (N) and soil potassium (K) while having higher levels of available phosphorus (P) than the matrix soil. In terms of the soil physical properties, there were no significant differences. The lower SOC and N was hypothesized to be a result of circles being devoid of vegetation. However, their bioassay yielded noteworthy results.

For the purpose of Cramer and Barger's (2013) bioassay, wheat was grown in soil from both inside fairy circles as well as from the matrix. There was no difference in their growth tempos but there were differences with regards to biomass. Wheat grown in the matrix soil had 1.4 times more accumulated biomass than wheat grown in fairy circle soil due to reduced root growth. These results were linked to the minor differences in soil nutrients described above. Cramer and Barger (2013) concluded that a combination of: lower levels of nutrients, absence of certain microorganisms, herbivory by termites and ants as well as environmental conditions may have a hand in maintaining fairy circles over time.

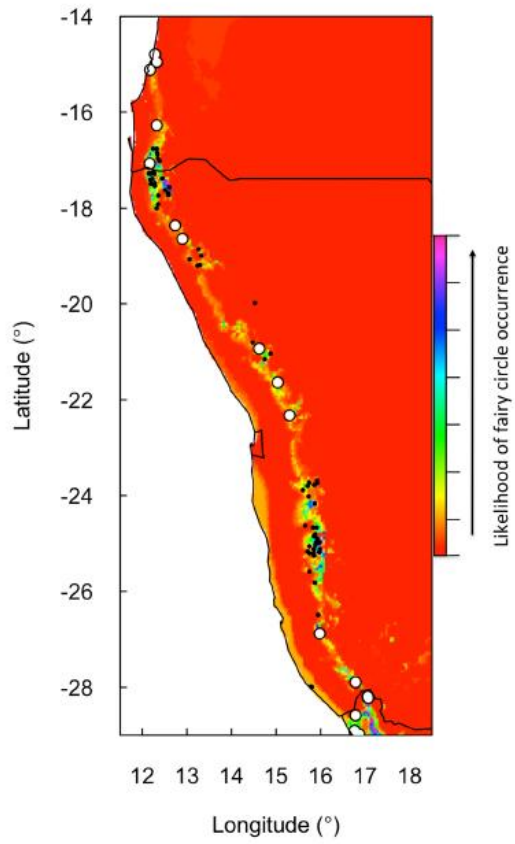

Figure 1.13: Fairy circle prediction map produced by the model of Cramer and Barger (2013). Black spots indicate the areas with fairy circles utilized to produce their model whereas the white spots are other known sites where fairy circles occur. From the map it is clear that fairy circle occur and can develop in a narrow band along the coast (Cramer and Barger, 2013).

Using the boosted regression tree and a set of different parameters (mean annual precipitation, an enhanced vegetation index and temperature seasonality) they developed a model that would predict where fairy circles would occur. Their model predicted that fairy circles would occur on a narrow band along the western parts of Namibia (Figure 1.13) (including South Africa and Angola).

The data obtained from aerial photographs were used to calculate the area's specific R-value. This value provided vital information on the distribution pattern. Of all the fairy circles analyzed 58% had R-values indicating an over-dispersed distribution (R=1.67) while the rest had a clumped distribution (R=0.58). The R-value according to their observations, are highly dependent on landscape occupancy.

Due to the nutrient insufficient nature of arid ecosystems, Cramer and Barger (2013) explained that competition for the scant available nutrients, among dominant flora, is to be expected. As with previous fairy circle studies, they noted that their sizes are not consistent. This led them to hypothesize that circles sizes vary due to different levels of resources recorded.

Many fairy circle researchers have stated that fairy circles are "dynamic" in nature meaning they appear and disappear over time (Albrecht et al., 2001; Becker and Getzin, 2000; Moll, 1994; Vlieghe et al., 2015). Cramer and Barger (2013) explained that the gradual closure of fairy circles are a result of a collection of different factors including, varying rainfall and termite herbivory.

Overall Cramer and Barger (2013) concluded that fairy circles arise due to vegetation spatial patterning which is a consequence of intense resource competition in such an arid ecosystem. Due to the resulting pattern the barren patches act as resource islands in a sea of infertility created by a complex interplay of fauna, flora and prevailing environmental conditions.

Getzin et al. (2015a) continued with Cramer and Barger's (2013) approach to uncovering the mystery behind fairy circles. Their research focused on the spatial patterns produced by fairy circles which they hypothesized is a direct result of vegetation self-organization. They also reviewed other theories' ability to recreate their observed spatial pattern.

Getzin et al. (2015a) study primarily made use of aerial photographs from which they identified three sample squares (identified study area of 500 x 500 m). One plot was identified from an aerial photograph of Marienfluss while the others were of two areas in the Giribes plain. All fairy circles identified inside their respective squares were given specific parameters (x, y coordinates, area and perimeter). The collected data was used for spatial point pattern analysis.

The first analysis Getin et al. (2015a) conducted was the Voronoi tessellations for point patterns. This produces Voronoi tiles or cells that provide important information regarding the regularity of the pattern and the distribution. Following this, they used the pair-correlation function to give the critical scales of the specific pattern. Values of r =1 indicates complete spatial randomness, r<1 indicates regularity and r>1 indicates aggregation. They used the L-function to give a visual representation of the regularity of the pattern observed. Finally Getzin et al. (2015a) used the mark-correlation function to assess whether there is a link between the sizes of nearby fairy circles and the distance between them. If a value of $k_{mm}(r) = 1$ is computed it indicates no spatial correlation, a value of $k_{mm}(r) < 1$ indicates a negative correlation while $k_{mm}(r) > 1$ indicates a positive correlation. In order to evaluate whether the pattern produced by fairy circles correlated with patterns predicted by spatial models for describing vegetation self-organization, the Gilad et al. (2004, 2007) mathematical model was employed. This was done by analyzing the patterns produced by the model in the same way as the fairy circle patterns.

Analysis of the aerial photographs of the three sample squares revealed that the diameters of the circles range from 1.98 to 15.38 m and the tiles produced by the Voronoi tessellation indicated a majority of hexagonal pattern. The pair correlation function produced a regularity that is not

usually associated with biological systems. The L-function revealed that no large scale patterns could be observed at distances beyond 60 m. The mark-correlation function showed that there was a negative correlation between circle sizes and the distances between them (up to 12.5-13.5 m). There was a general match between the characteristics of the fairy circle patterns with that generated by the model. The models had tiles with a lesser degree of hexagonality. The pair correlation function revealed that the model generated pattern had a more ordered regular nature.

In an attempt to review the credibility of previous hypotheses (gas and insect theories) in terms of their novel approach, the fairy circle patterns were compared to those generated by each theory's causative agent. With regards to the hydrocarbon microseepage theory, Getzin et al. (2015a) concluded that patterns previously observed does not match that of fairy circles. On the other hand, their research indicated that insects can produce vegetation self-organization patterns in similar environments as fairy circles but that these patterns does not match the observed pattern in terms of its hexagonal nature.

Overall Getzin et al.'s (2015a) research supported their vegetation self-organization theory. They hypothesized that when fairy circles are located a distance away from each other (more than 13m) the matrix vegetation experiences extreme competition for water as a result of the great distance between the bare patches which act as water traps. Fairy circles accumulate water due to the fact that water infiltrates at a much slower rate in the absence of vegetation (Rietkerk et al., 2002). The specific area where competition is the most intense, bare patches develop as a result of matrix vegetation mortality. Nearby grass extend their roots up to and into the bare area to utilize stored water, this leads to bigger fairy circles diameters. In contrast, circles located in closer proximity to one another are smaller due to less competition for water. In terms of the maintenance of fairy circles, Getzin et al. (2015a) did not rule out the possibility that insects and/or differences in nutrient could play a role.

1.2.2.1 Shortcomings and discrepancies of the vegetation patterning theories

Juergens (2015) pointed out some shortcoming in the vegetation self-organization model. Firstly he mentioned that the plant competition on which the model is largely based is limited to 13m while fairy circle diameters can reach 35 m with distances of 30 m between them. The question he thus poses is whether competing plants could produce such large bare gaps over such large distances. Secondly, he questioned the reasoning that grass roots can extend over 70 cm to acquire water from fairy circles and suggested that root length limitations should be added as a parameter to the model.

Juergens et al. (2015) was one of the biggest critics of the vegetation patterning theory. Being a supporter of the termite related theory they compared these two competing theories with each other in terms of five aspects they deemed important to this phenomenon. This included the following: the relationship between rainfall and fairy circle development, the role of the fairy circle in its unique ecosystem, the origin of the perennial grass band, the role sand termites play in circle origin (explained in section 2.1), desert ecosystem grass interaction and spatial patterns of insects versus that of fairy circles.

Research done by both Juergens (2015) and Juergens et al. (2015) indicated that there was a positive correlation between fairy circle development and rainfall. During years of increased rainfall development of new fairy circles were clearly visible while during drought years the opposite was observed (Figure 1.14). This could be explained at the hand of the termite feeding behavior. During years of increased rainfall grass growth is stimulated. The main role of the termite was hypothesized to be to forage on grass roots as a means to keep the fairy circles devoid of vegetation and thus prevent transpiration. Thus the action of the termite ensures a water source which can sustain them as well a matrix grasses (which they also can feed on). Their foraging behavior is responsible for the gradual widening of the circles from their origin to established circles. In contrast to that described previously, Getzin et al. (2015a) ascribed new fairy circle development to the severe competition for water by matrix grass which results in grass death and finally the development of bare patches. This is supported by predictions of Cramer and Barger (2013) that fairy circle death would occur during years with sufficient rainfall when resource competition has eased off. They also pointed out that during their study a significant number of circles that had not been undergoing closure was associated with low

numbers of termite activity. However, this could not be supported by scientific evidence, as was done for the converse.

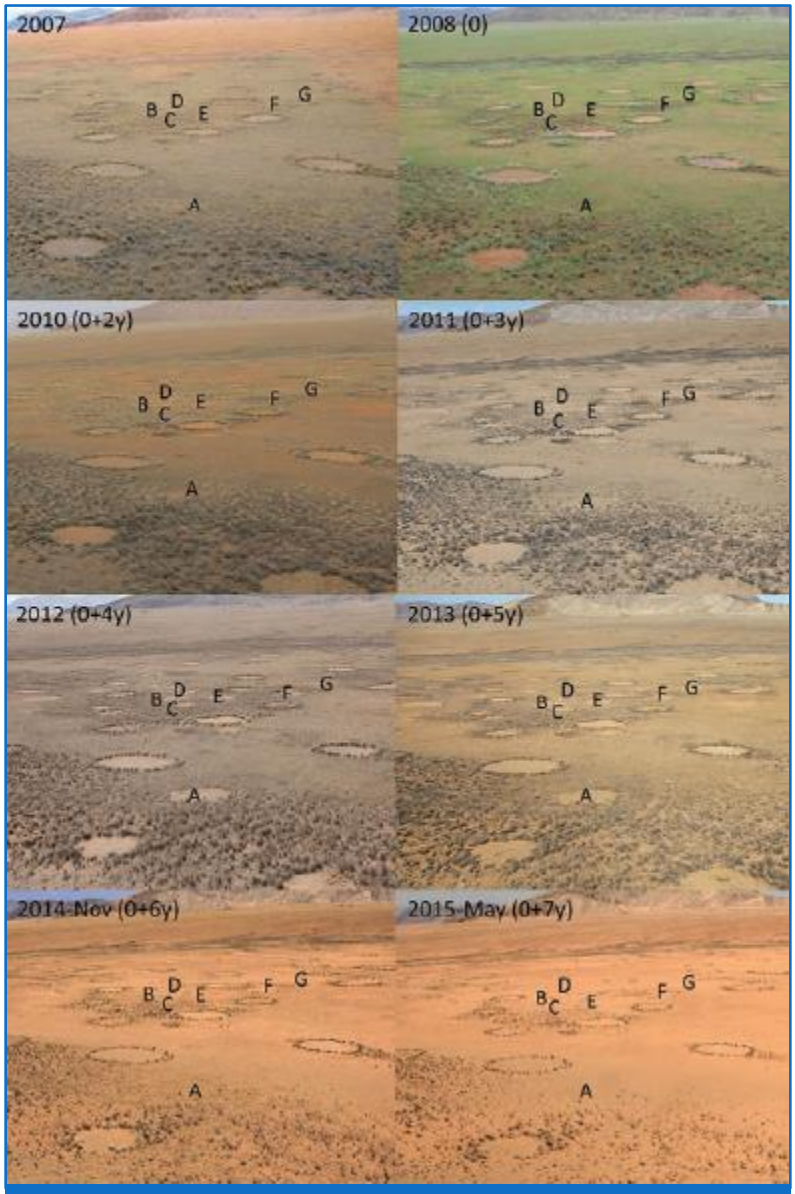

Figure 1.14: Differences in fairy circle occurrence during years of high and low rainfall. The year 2008 to 2011 experienced good rainfall followed by 3 drier years. (Adapted from Juergens et al., 2015).

According to the research of Juergens (2013), fairy circles ensure the persistence of accumulation of perennial water which in turns leads to the formation of the perennial grass fringe around the circles. This subsequently causes a burst in biodiversity in fauna and flora due to the favorable conditions in the desert environment. Thus fairy circles are unique niches supporting survival in a harsh ecosystem. In contrast, the vegetation self-organization theory sees fairy circles merely as water traps/reservoirs.

The ring of taller grass surrounding fairy circles is an aspect of this phenomenon that is often overlooked. According to the termite theory, the perennial grass band develops due to the fact that the grasses there experience the most favorable conditions (Figure 1.8 previously) i.e. easy access to water source, lack of competition as well as not being the food source for termites. On the other hand the vegetation self-organization theory sees the perennial grass band differently. New fairy circles provide a rich supply of water due to the lack

of vegetation and thus transpiration which supports the growth of the perennial grass belt. This was again questioned by Juergens et al. (2015), due to fact that it is hard to comprehend that the grass species that grows in the matrix can successfully colonize the periphery of circles yet also prevent grass establishment inside circles.

Another drawback of this theory, according to Juergens et al. (2015), is the fact that even though it is rooted in competition among plants, it contradicts itself in terms of viewing fairy circles as water traps, yet the circles stay devoid of vegetation. Thus if circles were a permanent source of water, competition would lend itself to grass establishing where there is a water source i.e. the fairy circles themselves. Additionally they noted that there are very similar ecosystems to the fairy circle distribution range around the world, and it would be expected that similar vegetation patterns would arise, which has yet to be reported.

Finally Juergens et al. (2015) applied the pair correlation function that was used to find the spatial distribution pattern of fairy circles by Getzin et al. (2015a), to fairy circles in Giribes, nest systems of social insects as well as existing vegetation gaps/spots and compared their results to those of heuweltjies (hypothesized to be social insects in origin) and Getzin et al.'s (2015a) results. This was done in an attempt to establish if social insects could reproduce the observed pattern of fairy circles.

With regard to the number of hexagons, the results of the fairy circles in Giribes, vegetation spots and heuweltjies matched that computed for fairy circles by Getzin et al. (2015a) indicating these are in the same range of regularity. The values computed for the remaining (vegetation gaps and social insect nests) were less regular. Instead of viewing these results as indication that social insects cannot recreate fairy circle spatial distribution patterns, they instead pointed out flaws in Getzin et al. (2015a) approach to ignoring the effect environmental gradients have on distribution patterns. Recently however Tarnita et al. (2017) modeled social-insect self-organization and found that it could reproduce the spatial distribution pattern of fairy circles modeled by Getzin et al. (2015a). They took it further by developing a model that combines social insect and vegetation self-organization (discussed in alternative theories section below).

1.2.3 Hydrocarbon microseepage and other gas related theories

Jankowitz et al. (2008) proposed that semi-volatile gas and the inhibiting effect it has on native grass growth could explain the phenomenon of fairy circles on the basis of Albrecht et al.'s (2001) hypothesis regarding a semi-volatile agent associated with termite nests. Their study site was two distinct circles located in the NamibRand nature reserve. They conducted a simple pot experiment with mature *S. ciliata* grass seedlings, which tested three different factors: soil origin, presence/effect of gas and position of pots relative to fairy circles (Figure 1.15). To assess the differences in growth patterns of the different pot types, a vitality score (0 to 10) was used which was followed by statistical analysis (SAS Software Version 8.2). Overall Jankowitz et al. (2008) found that when pots, especially open containers, were placed inside circles they experienced a negative growth inhibitory effect. However, the origin of the soil did not seem to have an effect. They concluded that a semi-volatile gas, whose growth inhibitory effect is not retained in soil, is responsible for the fairy circle phenomenon thus in part supporting Albrecht et al.'s (2001) hypothesis. Jankowitz et al. (2008) were ,however, unsure if the gas could be linked to termite nests or other factors.

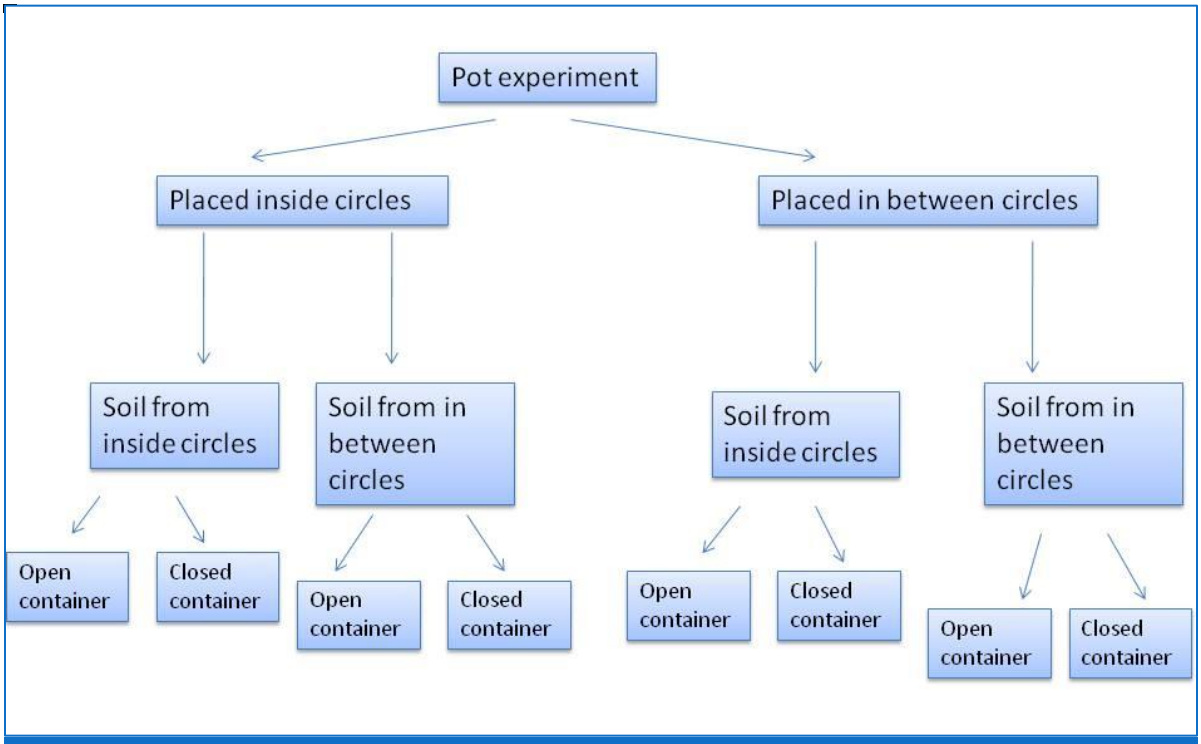

Figure 1.15: The different pot experiments conducted by Jankowitz et al. (2008).

Naudé et al. (2011) also proposed a gas related hypothesis that explained the origin of fairy circles in response to research by Albrecht et al. (2001) and Jankowitz et al. (2008). They hypothesized that in order for such a substance (whether or not gaseous in nature) to create the circular barren patches, it had to be released regularly and diffuse to the surface, thus leading to their theory that fairy circles are surface footprints that result from geochemical hydrocarbon microseepage.

A single study site, the NamibRand Nature reserve, was chosen on the basis of the results obtained from the bioassay conducted by Van Rooyen et al. (2004). Due to the fact that the same results were obtained using soil from a vast array of different fairy circle location, the subsequent results supported their reasoning. Inside their chosen study site, five distinct fairy circles were identified for the purpose of their research (in field gas measurements and sample collection). Fairy circles 1 to 3 were established barren patches devoid of any vegetation whereas fairy circle 4 was characterized by several dead grass tuffs and fairy circle 5 contained both dead and chlorotic grass tuffs (Figure 1.16).

Figure 1.16:
Fairy circles in the NamibRand Nature Reserve differing in their appearance. A. A characteristic fairy circle devoid of any vegetation (Jen Guyton, 2017). B. Fairy circle characterized by several dead grass tuffs (Janine Avery, 2013). C. A fairy circle characterized by both dead and dying grass tuffs (New York Times, 2017).

Soil samples were collected from both inside the five fairy circles as well as the matrix on different soil levels. Inside circles 4 and 5, soil was collected in the center at a depth of 50 cm. Two of the characteristic barren patches were selected, however, it is unclear which ones as initially the circles are referred to as 1, 2 and 3, followed by referring to them as 1.3 and 2.1.Nonetheless soil was collected from circle 1.3 in the center and its matrix at a depth of 1 m, while soil was collected from the center of circle 2.1 and its matrix at the surface layer.

To conduct field gas measurements, they made use of the Greenline 8000 Portable gas analyser (Figure 1.17). The measurements were taken over a three day period during different time of the day:

- For circles 1-3, measurements were taken on day one between 15:00 and 16:00, on day two between 17:00 and 18:00 and on day three between 11:40 and 12:05 as well as between 16:30 and 16:50.
- For circles 4 and 5, measurements were only taken on day three between 12:12 and 12:30, 15:50 and 16:15 as well as 17:50 and 18:50.
- Measurements were also taken in the matrix to act as control, yet it was not mentioned when this occurred over the three day period.

Figure 1.17: The Greenline 8000 Portable gas analyser (Eurotron).

The collected soil samples were subjected to stir bar sorptive extraction with twister, which is a solventless extraction process aimed at extracting hydrocarbons from soil. However, this chosen method proved to be problematic due to the adherence of an unknown black magnetic substance. To overcome this issue they employed an alternate novel solventless extraction method. The obtained extracts were subjected to gas chromatography-mass spectrometry (GC-MS).

The results of the infield gas measurements are in Tables 1.2, 1.3 and 1.4. The control site for circles 4 and 5 is not shown in the respective tables as this site had a constant O_2 measurement of 20.9% and CO was not detected. The gas analyser was not equipped to detect methane and/or other combustible gases.

Table 1.2: The results of the infield gas measurements taken over three days for fairy circles 1, 2 and 3 (data from Naudé et al., 2011)

	Gas measurement results			
Day and time	Circle 1	Circle 2	Circle 3	Control
1 (between 15:00 and 16:00)	Drop in O_2 from 20.9% to 20.8% followed by CO emission of 0.0001%	Drop in O_2 from 20.9% to 20.8% followed by CO emission of 0.0001%	Drop in O_2 from 20.9% to 20.8%. No CO measurements.	Measurements not conducted.
2 (between 17:00 and 18:00)	Drop in O_2 of 0.1% followed by CO emission of 1 part per million (ppm)	Drop in O_2 of 0.1% followed by CO emission of 1 part per million (ppm)	Drop in O_2 of 0.2%. No CO measurements.	O_2 level of 20.9%. No CO measurements.
3 midday (between 11:40 and 12:05)	Drop in O_2 of 0.2% followed by CO emission of 0.005%	Drop in O_2 of 0.2%. No CO measurements.	Drop in O_2 of 0.2% followed by CO emission of 0.007%	O_2 level of 20.9%. No CO measurements.
3 late afternoon (between 16:30 and 16:50).	Drop in O_2 of 0.1-0.2%. No CO measurements.	Drop in O_2 of 0.1-0.2%. No CO measurements.	Drop in O_2 of 0.1-0.2%. No CO measurements.	Drop in O_2 of 0.2%. No CO measurements.

Table 1.3: The results from the field gas measurement for fairy circle 4 (data from Naudé et al., 2011)

Time (all measurement taken on day 3)	Gas measurement results for circle 4
12:12-12:30	Drop in O_2 of 0.2% followed by CO emission of 0.028%.
15:50	Drop in O_2 of 0.2% followed by CO emission of 0.001.
17:55	Drop in O_2 of 0.3% followed by 0 ppm CO.
18:50	O_2 levels constant and CO not detected.

Table 1.4: The results from the field gas measurement for fairy circle 5 (data from Naudé et al., 2011)

Time (all measurement taken on day 3)	Gas measurement results for circle
16:03-16:15	Drop in O_2 of 0.1% followed by CO emission of 0.032%
17:50	Drop in O_2 of 0.1% followed by 0 ppm CO.

From the results it was evident to Naudé et al. (2011) that the emission of CO does not happen at a constant rate or at a specific time and that CO emissions did not always exactly match the decrease in O_2. This led Naudé et al. (2011) to believe that other gasses are also emitted (could not be verified with gas analyser). CO is a common by product of the oxidation of hydrocarbons, thus CO was used as a marker compound.

The GC-MS results (Figure 1.18) indicated that there were differences in terms of alkenes and alkanes. From the chromatogram, Naudé et al. (2011) came to the conclusion that the barren fairy circles represent dormant seepage vents that could become active in future, while circle 4 (dead vegetation) is indicative of a new seepage vent and circle 5 (both dead and chlorotic vegetation) of a new seepage with a recent period of activity. The latter conclusion was made based on the ratio of alkanes/alkenes in circles 4 versus 5 that were 7 and 72 respectively. The GC-MS also detected phytane (Ph) in circles 4 and 5. Chlorophyll is broken down into phytane and pristine, thus reflecting the remnants of organic matter in the circles.

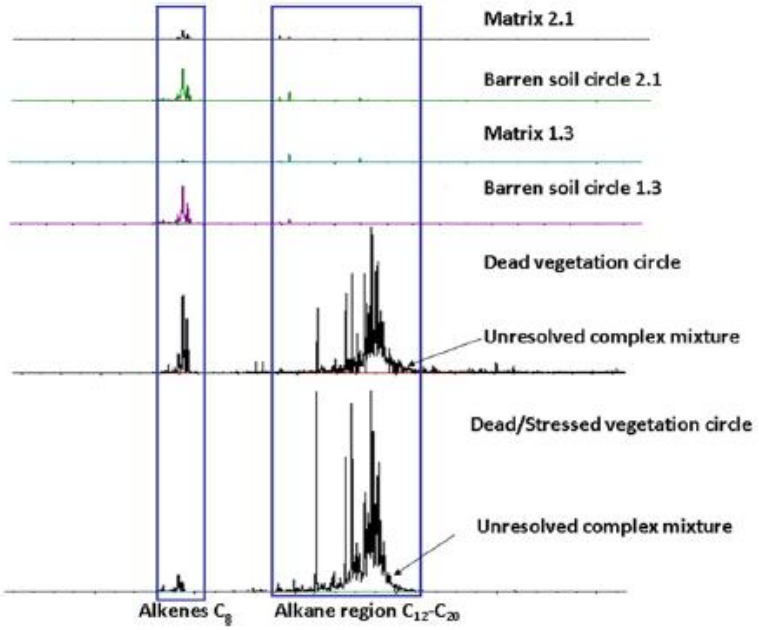

Figure 1.18: The fairy circle soils had more alkenes as compared to the matrix soil. Fairy circle 4 (containing dead vegetation) and 5 (containing dead and chlorotic vegetation) had additional unresolved alkanes (indicated by arrows) (Naudé et al., 2011).

The differences in terms of alkane versus alkene content in the different soil was attributed to hydrocarbon degrading microorganisms (Heider et al.,1999; Naudé et al., 2011) believed to be active inside fairy circles. Alkenes are the byproduct when alkanes are the hydrocarbon being utilized as food source under anoxic conditions (Grossi et al., 2008; Mbadinga et al., 2011). They supported this hypothesis on the basis of results from Eicker et al. (1982) who found differences in the activity of anaerobic bacteria versus aerobic bacteria in and around fairy circles.

This led Naudé et al. (2011) to explain the characteristic taller grass periphery surrounding fairy circles at the hand of their hydrocarbon microseepage theory. Their reasoning (depicted in Figure 1.19) was that the edge of fairy circle represents the most favorable conditions for plant growth and survival.

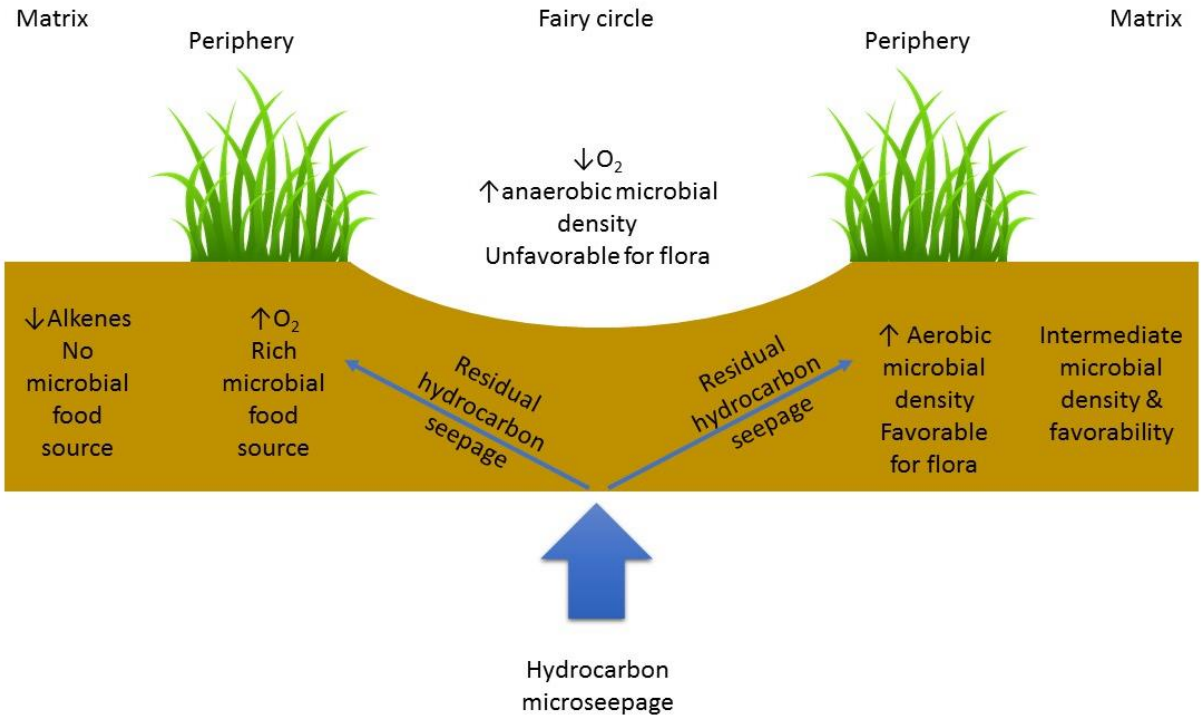

Figure 1.19: Naudé et al. (2011)'s explanation for the characteristic grass periphery surrounding fairy circles.

Thus overall Naudé et al. (2011) concluded that fairy circles are the visual consequence of natural gas emission that alter soil chemical and biological properties. Theses natural gasses include non-hydrocarbon CO as well as alkenes and alkanes. Microbial degradation of alkanes to alkenes may be responsible for the different level observed between fairy circles and the matrix. Higher ratios of alkanes/alkenes are associated with "new" circles and thus active microseeps.

1.2.3.1 Shortcomings and discrepancies of the gas-related theory

The biggest shortcoming of the method used by Jankowitz et al. (2008) was in terms of the vitality scores used to grade the plants. This is not a very scientifically accurate and reproducible method, as scoring is done based on individual perception. The results of pot experiments are usually compared in terms of dry weight, germination percentage, root/shoot ratios, length of shoot and/or roots. This is a much more accurate way of analyzing and comparing data. Additionally Jankowitz et al.'s (2008) results were inconclusive.

One of the biggest drawbacks of methods employed by Naudé et al. (2011) was the sampling technique. Initially they identified five fairy circles, differing in appearance, inside their study area. Yet soil collection and gas measurements were only done for four circles and three control (matrix) sites. Soil samples were also collected at different depths for some of the circles, thus making their sampling inconsistent. It would have been more accurate to collect at two different depths consistently for at least five circles of each appearance.

The gas measurements were taken at different times of the day for fairy circles 1 to 3 versus 4 and 5. There were four measurements taken for fairy circles 1 to 4 while only two measurements were taken for fairy circle 5. Thus, overall the gas measurements were taken inconsistently. Finally there were only three matrix locations used for gas measurements, differing in measurement amounts and times.

The same problem spills over into Naudé et al.'s (2011) GC-MS analysis where the inconsistent soil samples of four fairy circles were compared to two matrix samples. Meyer et al. (2015) also conducted GC-MS analysis on soil collected from fairy circle in the Garub area. Meyer et al. (2015) collected soil from 10 different fairy circles at two different depths, as well as in between these circles, thus providing a more representative sample group.

The isoprenoid hydrocarbon phytane was detected in circles 4 and 5 and was linked to hydrocarbon microseepage by the authors. However, Meyer et al. (2015) pointed out that phytane can indicate a plant related link to fairy circles as this hydrocarbon is a byproduct of chlorophyll degradation.

Finally, Naudé et al. (2011) had a very descriptive hypothesis to explain the occurrence of the taller grass periphery yet no soil was collected for GC-MS analysis or gas measurements on the edge for that matter. For example they hypothesized that the periphery is high in O_2 yet this cannot be backed up by field data. Naudé et al.'s (2011) hypothesis is also based on different microbial densities in the matrix, periphery and fairy circles, which is only based on old research done by Eicker et al. (1982) which may not be applicable anymore as they only focused on culturable microorganisms. Their research should have included metagenomics studies on the different soils to support their hypothesis. It would be surprising if such small differences in CO and O_2 concentrations would prevent the grasses from growing. Bioassays in controlled CO and O_2 concentrations are required to prove the gas theory.

1.2.4 Microbial related theories

Even though this theory is sometimes categorized as one of the lesser accepted fairy circle origin theories it is nonetheless as important as any other supported by the fact that it is often used in conjunction with other theories.

Eicker et al. (1982) did a microbiological study on the fairy circles of the Giribes plain to determine if there were differences in the microbial population of fairy circles and their surroundings. Soil samples were collected from the top 30 mm of ten fairy circles and their peripheries as well as 10 matrix locations chosen at random. For each location the 10 samples were pooled and mixed thoroughly to obtain a 1 kg representative sample for each.

To determine bacterial population densities, 5 g soil was suspended in 95 cm^3 sterile distilled water and placed on a shaker for 30 minutes. A dilution series was made for each. For each dilution, 1 cm^3 was pipetted in 10 sterile petri dishes a mixed with melted agar (50 °C) and left to solidify. Two different types of agar were used: peptone-yeast extract agar for mesophilic and thermophilic bacteria, as well as sucrose-yeast extract-salt agar for anaerobic bacteria. For the

growth of mesophilic bacteria, plates were incubated at 25 °C for 7 days. For thermophilic bacteria plates were incubated at 50 °C for 7 days. To grow aerobic bacteria plates were incubated in Brewer anaerobic flask with Gaspak oxygen absorber at 25°C for 7 days.

To determine fungal population densities, a modified dilution series was made by suspending 25 g of each soil type in 250 cm^3 sterile distilled water and shaken for 30 minutes. The suspension was diluted up to 5000 times and an aliquot of 1 cm^3 was placed in a petri dish, mixed with agar and left to solidify. The media was Czapek-Doxagar which contained antibiotics to prevent bacterial growth. The plates were incubated at 25 °C for 3 weeks even though the colonies were identified after only one week. Subcultures were grown on potato dextrose agar and potato carrot agar.

Eicker et al.'s (1982) results (Figure 1.20) indicated that other than anaerobic bacteria, fairy circles had a lower microbial density than the periphery and matrix. The periphery looked to support the highest density of microorganisms. They hypothesized that it contained a higher level of organic matter that might support the growth of the microorganisms. Another interesting finding was the high number of pigmented microorganisms found in the soil. Pigmentation is an adaption of desert microorganisms to resist the harmful ultraviolet rays. Eicker et al. (1982) concluded that their results could not shed any light in terms of the origin and/or maintenance of fairy circles.

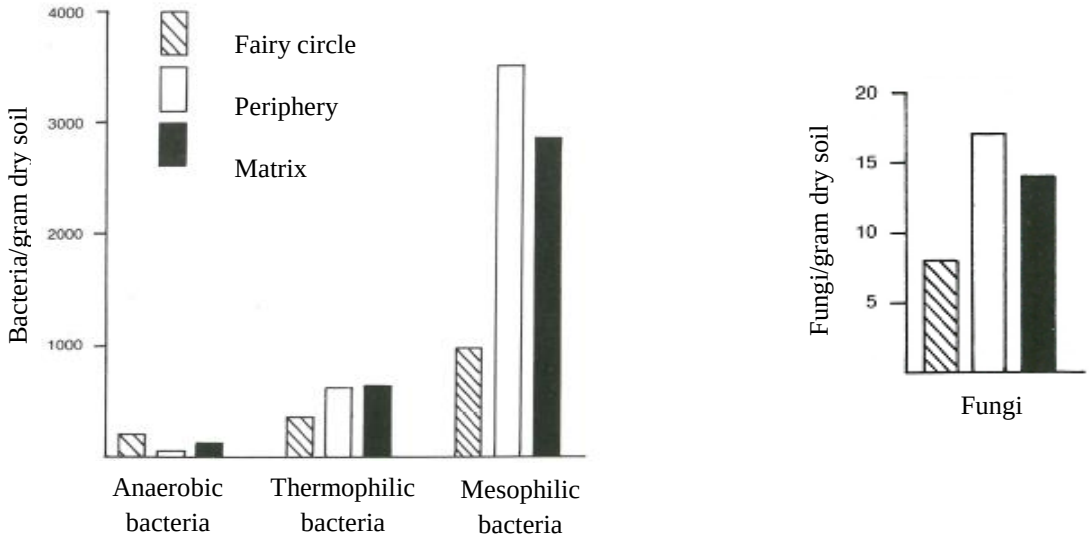

Figure 1.20: The results of the microbial study done by Eicker et al. (1982). To the left is the results for the bacterial densities and to the right is the fungal densities.

Ramond et al. (2014) formulated a hypothesis that edaphic microorganisms could be involved in the origin and /or maintenance of fairy circles. Their study focused exclusively on gravel plain fairy circles instead of the extensively studied dune sand fairy circles.

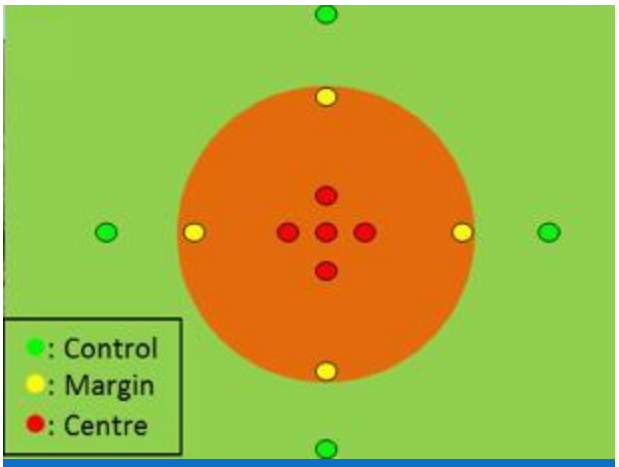

Figure 1.21: Soil collection layout followed by Ramond et al. (2014).

Ramond et al.'s (2014) study site was near the Gobabeb Research and Training Center. Here they selected five fairy circles from which 13 soil samples were collected near the surface. Of the eleven samples, four were taken from the matrix (controls), four on the periphery and five from the center of the circle (Figure 1.21) and stored at 4 °C during transport. For the purpose of molecular analysis a 1 g subsample of each collected sample was stored at -80 °C and the rest (for chemical analysis) at 4 °C before experimental use.

Chemical analysis was conducted to determine the pH, organic carbon, exchangeable ammonium and nitrate, organic phosphorus and ion concentrations (iron, calcium, potassium, magnesium and sodium). A principal component analysis was conducted to see how the different locations group in terms of their chemistry.

Total DNA was extracted from each soil type using the Powersoil DNA isolation kit and the DNA concentrations were determined using a Nanodrop spectrophotometer. The 16S rRNA genes of the extracted DNA was amplified using a polymerase chain reaction (PCR) with universal bacterial primers followed by purification and restriction enzyme digested. A terminal-restriction fragment length polymorphism (T-RFLP) analysis was conducted and the results were statistically analysed.

A PCA plot indicated to Ramond et al. (2014) that there were differences in the soil chemistry of the three different zones analysed due to the fact that they grouped separately. Their results in conjunction with the soil chemistry results of Van Rooyen et al. (2004) and the results from Naudé et al. (2011) led them to the conclusion that gas emissions could possibly have a direct or indirect hand in fairy circle formation and/or maintenance in conjunction with edaphic microorganisms.

The statistical analysis of the metagenomics study of the soil indicated that there were significant differences in the bacterial and fungal communities of the matrix versus that of the center of the fairy circles. Ramond et al. (2014) ascribed these differences to the barren nature of fairy circle i.e. the absence of vegetation and subsequently a rhizosphere zone. Interestingly enough they also found significant differences between individual circles in terms of the microbial communities.

Each fairy circle was then statistically analysed as an individual where each zone was compared to the other: center versus margin, center versus control and control versus margin for each of the five circles. These results indicated that all circles (excluding fairy circle 2's fungal community) the control and the fairy circle center microbial communities differed significantly. For some of the circles there were also significant differences between the margin and the center as well as the control and the margins. This led Ramond et al. (2014) to the conclusion that each individual fairy circle supports the growth of a unique edaphic microbial community significantly different to other fairy circles which cannot be satisfactory explained only by the absence of a rhizosphere zone. Instead, because fairy circles are dynamic (Cramer and Barger, 2013) the surface soil microbial communities are also constantly changing as fairy circles progress through their lifecycle which is shaped by environmental changes/drivers (hydrocarbon gas seepage, pathogens or toxins).

Using their results (including results that indicated that fairy circle centers house microbial communities that where more variable than the other zones) and research on the dynamic nature of fairy circles, Ramond et al. (2014) proposed two models (Figure 1.22) to explain the differences in microbial communities of the gravel plain fairy circles. Even though their results were substantial, Ramond et al. (2014) could not directly link bacteria and/or fungi to the origin and/or maintenance of fairy circles. They instead suggested the need for extensive chemical (soil and gas) and biological studies of both gravel and sand fairy circles soil (at deeper levels).

Van der Walt et al. (2016) did a study aimed at determining the differences between gravel plain fairy circles and dune fairy circles in terms of microbial community structure and soil physiochemical properties. They hypothesized that if they could identify unique microorganisms present in each of the fairy circles (gravel versus dune) that this could be linked to fairy circle formation and/or maintenance.

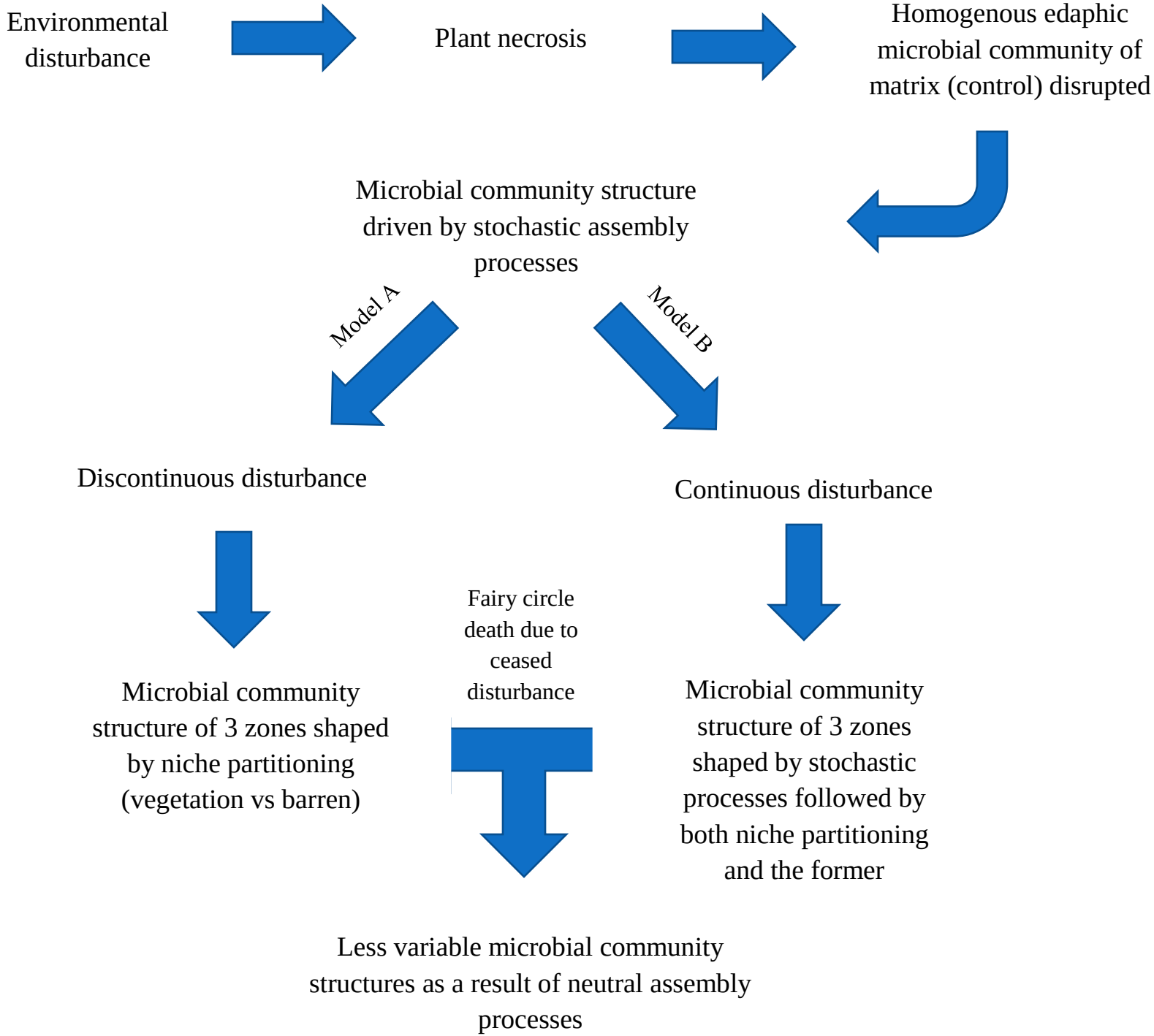

Figure 1.22: Summary of the two models proposed by Ramond et al. (2014) to explain the differences in the edaphic microbial communities of fairy circles and their surroundings.

Van der Walt et al. (2016) collected soil from both gravel plain and dune fairy circles in Namibia. Five fairy circles in each location were identified from which three samples (combined into one sample) were collected in the center and three in the matrix (at a depth of 0 to 5 cm) giving a total of 20 samples at each. After collection the samples were stored at -20 °C.

A subsample of 50 g was taken from each sample collected and sieved through a 2 mm sieve before physiochemical analysis. Their chemical analysis was done by Bemlab (Pty) Ltd. (Strand, Western Cape, South Africa) which included soil pH, conductivity, sodium (Na), potassium (K), calcium (Ca), magnesium (Mg), chloride (Cl), sulfate (SO_4), phosphorus (P), ammonium (NH_4) and nitrate (NO_3). They also determined carbon content (Walkey-Black method) and particle size (hydrometer method) themselves. All data was statistically analysed.

DNA was extracted from the soil using the Poweroil DNA isolation kit and DNA concentrations determined with Qubit 3.0 flourometer. A PCR aimed at amplifying the bacterial/archaeal 16S rRNA gene and a PCR aimed at amplifying the fungal ITS1 gene region. Sequencing was done using an Illumina MiSeq platform. Obtained sequences were analysed with the QIIME platform as well as statistically.

Based on the groupings of samples on a constructed PCA plot (clear separation between sites), the overall physiochemical properties of the two sites (gravel planes versus dune) differed significantly. The two sites also differed in soil physical properties: dune soils had larger particles sizes compared to gravel plain soil. When comparing the matrix soil with that of the fairy circle soil at both sites, no significant differences could be found.

Van der Walt et al.'s (2016) results indicated that each sites housed a microbial community significantly distinct from the other. Within the dune ecosystem there were significant differences between the fairy circles and their matrix counterpart in terms of edaphic bacterial and archaeal communities, whereas no significant differences could be found between gravel plain fairy circles and their matrix counterpart. Fungal community structure differed significantly over all sites and locations.

In response to the results obtained for the physiochemical and microbial differences, Van der Walt et al. (2016) aimed to determine which soil physiochemical properties drive edaphic microbial community structure in gravel and dune fairy circle ecosystems. For the dune microbial communities the percentage sand, pH and carbon content were the driving forces influencing community structure while gravel plain microbial communities were shaped by P-, Na-, S concentrations as well as by the percentage carbon and soil physical properties (percentage silt and clay). Van der Walt et al.'s (2016) data also suggested that other factors either of abiotic or biotic nature could shape the differences between fairy circle and their corresponding matrix (microelements such as Fe, Zn, Al or toxins or unknown stochastic processes).

Van der Walt et al. (2016) also analysed the microbial community richness at each site and compared the results. Overall the results indicated that the edaphic bacterial communities were more diverse as compared to the bacterial and archaeal communities. Fungal communities were more species rich in the gravel plains than the dune counterparts. They also found fairy circle (both dune and gravel plane) specific phylotypes: nine bacterial, one archaeal and 57 fungal phylotypes unique to fairy circles.

Taking all their results into consideration, Van der Walt et al. (2016) formulated the hypothesis that certain microorganisms could interact negatively with plants through their pathogenic nature and therein have a role in fairy circle origin and/or maintenance. Due to the fact that each site has its own processes shaping its soil physiochemical properties, the microbial community at each site has to adapt leading to significantly different edaphic microbial communities. Whereas bacterial and archaeal community structure could be shaped by soil physiochemical properties and/or other random processes, fungal community structure is thought to be primarily shaped by niche partitioning or environmental disturbances. Van der Walt et al. (2016) concluded that, based on the unique microorganisms identified inside fairy circles, these may be implicated in the origins and/or maintenance of fairy circles.

1.2.5 Allelopathy theory

Theron (1979) was the first researcher that proposed a hypothesis that explained the occurrence of fairy circles. He proposed that there was a direct link between the native poisonous *Euphorbia damarana* plant and fairy circles as the circles occurred among these plants in the Giribes plain (northern Namibia). He measured the diameter of ten circles as well as ten *E. damarana* plants. There was a striking similarity between the average diameter of a fairy circles and *E. damarana* plants. He hypothesized that when these *E. damarana* plants started to die, large quantities of an allelopathic compound were released in to the soil. The allelopathic compound subsequently prevented any plant from colonizing the barren circular patch where an *E. damarana* plant once grew. To assess the allelopathic nature of the soil, *E. teff* seeds were planted in soil collected from inside fairy circles, the edge of the circles and in between circles. He found that the grass growing in the soil from inside fairy circles grew substantially slower compared to its counterparts.

Meyer et al. (2015) conducted research on the relationship between the occurrence of fairy circles and the *E. gummifera* plant in the Garub region (southern Namibian pro-desert) (Figure 1.23). Their main objective was to find a characteristic chemical compound known to be present in this plant inside the fairy circles.

Figure 1.23: The co-occurrence of fairy circles and *E. gummifera* plants in the Garub area in the south of Namibia.

Euphol (Figure 1.24) has been successfully identified in several *Euphorbia* spp.: *E. tirucalli* (Lin et al., 2000; Vuong et al., 2015), *E. kansui* (Yasukawa et al., 2000) and *E. nerifolia* and *E. antiquorum* (Mallavadhani et al., 2006). Thus euphol was chosen as the marker compound. They collected soil from inside ten randomly selected circles as well as in between circles. *E. gummifera* material was also collected. Soil and plant material collected were subjected to speed extraction with hexane. Once dried, the samples were subjected to GC-MS. Euphol was detected in significant amounts in 19 out of 20 soil samples from inside fairy circles, while it was only detected in miniscule amounts in outside (matrix) soil samples. In addition to their chemical analysis they also conducted geographical studies on the area with the use of Google Earth. As with Theron (1979), they found a striking similarity in the average size of 60 fairy circles as compared to 60 *E. gummifera* plants. Furthermore, close inspection of Google Earth images of the area from 2003, 2004, 2010, 2012 and 2013 clearly showed plants that were present initially are transitioning into barren patches or have already transformed in to one. As a result of their data, they concluded that the theory of Theron (1979) is the most probable.

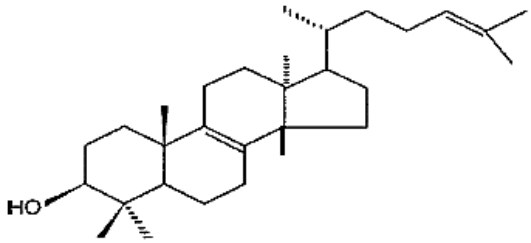

Figure 1.24: The chemical structure of euphol (Mallavadhani et al., 2006).

One of the main reasons the allelopathy theory was condemned by so many scientists is observation that *Euphorbia* species such as *E. damarana* favour rocky habitats and it would be unlikely that they would occur in sandy habitats where fairy circles occur (Van Rooyen, 2004). However the basis for these claims is not based on concrete sources. Both *E. damarana* and *E. gummifera* have been found to grow on both hills as well as plains that have rocky or sandy substrates (Figure 1.25 A and B) (Curtis and Mannheimer, 2005) as well as the fact that fairy circles also occur on gravel plains (Ramond et al., 2014; Van der Walt et al., 2016). Meyer et al. (2015) also found that *Euphorbia* spp. do in fact co-occur in areas where fairy circles area found. This directly contradicts the reason for discrediting the allelopathy theory by Van Rooyen et al. (2004) and several others.

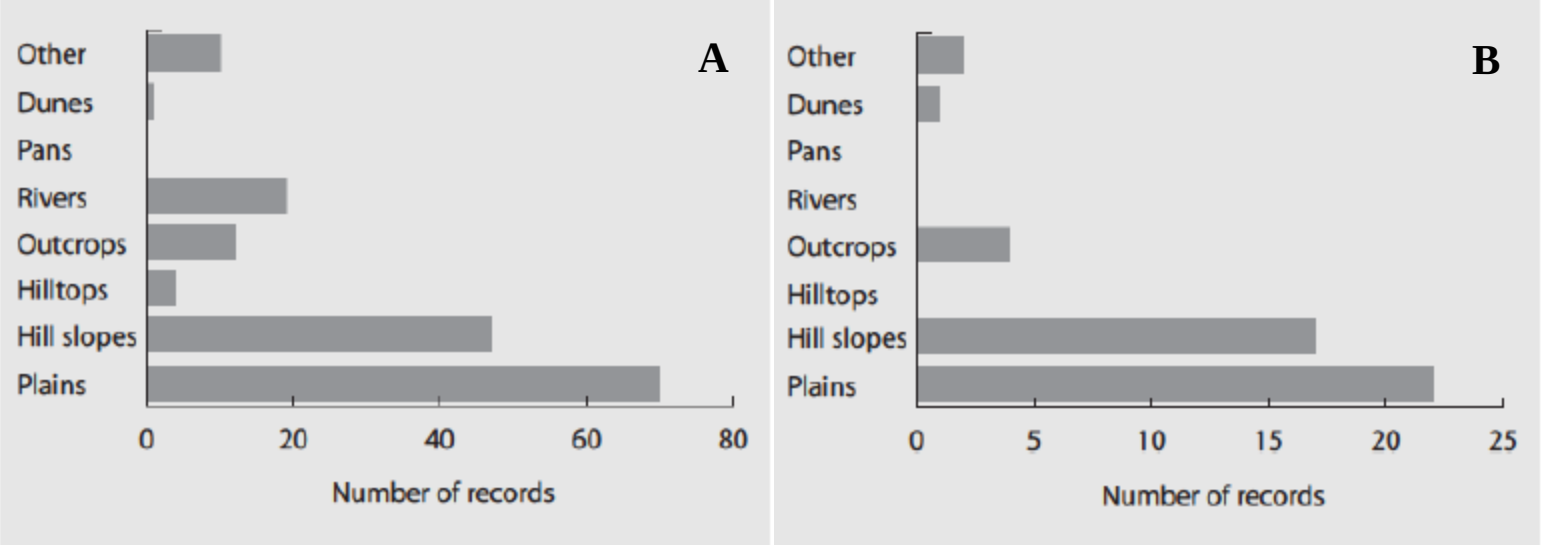

Figure 1.25: The different habitats favoured by two *Euphorbia* spp. A. The occurrence of *E. dammarana* in different habitat types in Namibia. B. The occurrence of *E. gummifera* in different habitat types in Namibia (Curtis and Mannheimer, 2005).

1.3 Aims and objectives

The aim of this project was to link the following concepts (Figure 1.26):

1. The allelopathic and antimicrobial effects of the *E. gummifera* plant,
2. The differences in the soil microbial profile of soil from inside and outside fairy circles
3. The remnants of such effects in soil (such as fairy circle soil)

to the prolonged persistence of fairy circles in the Garub area of southern Namibia.

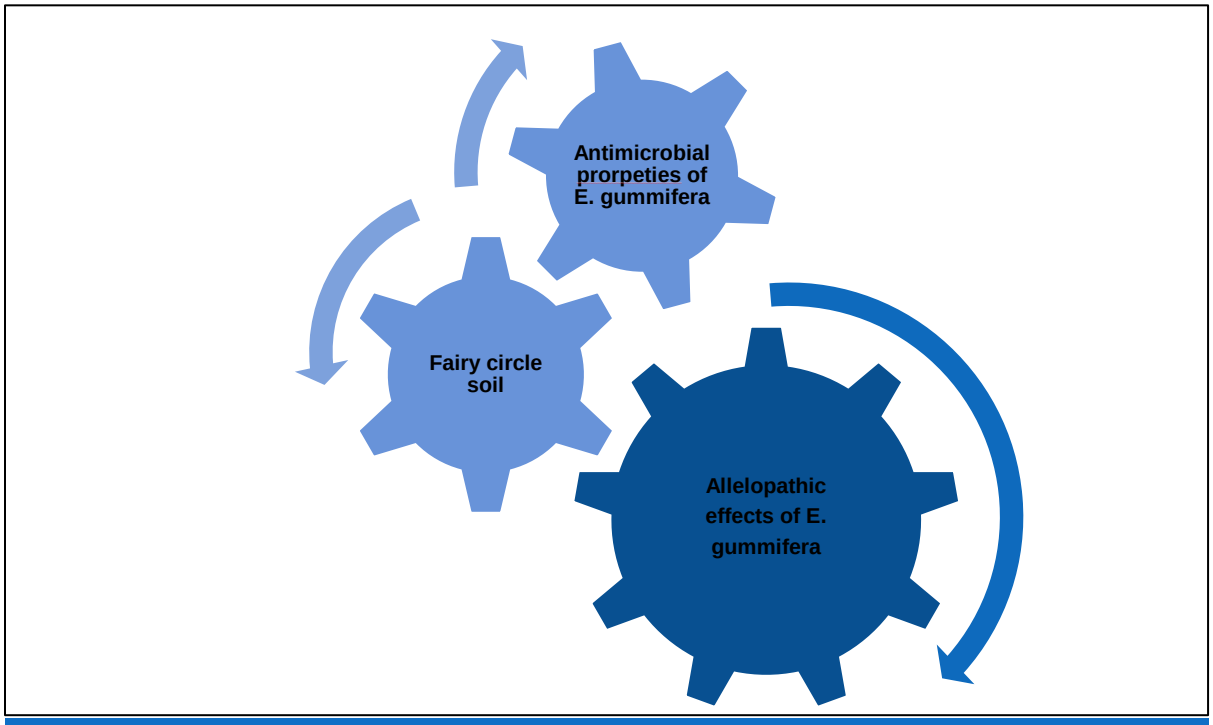

Figure 1.26: The three main concepts underlying this project.

This was achieved by following these set of objectives:

- *E. gummifera* based allelopathy:
  - Preparations of an *E. gummifera* methanolic extract using a speed extractor and gene vac evaporator.
  - Crude extract was used to make a dilution series that was subsequently used in a germination inhibition study with *E. teff* seeds as a bio-indicator.
  - Prepared extract was used to do column chromatography so separate compounds that were present.
  - Fractions that showed promising activity were investigated further for possible identification of compound(s) of interest.

- Antimicrobial properties of *E. gummifera*
  - Two bacteria previously isolated from fairy circle soil was identified using the 16S rRNA based sequencing technique.

- Prepared extract was used in an antimicrobial study by employing the microtiter method and the two identified isolates.
- Possible antimicrobial activity was further investigated by spraying TLC plates from the column chromatography with the susceptible bacteria to determine which specific bands/compound(s) possesses antimicrobial activity.

- Fairy circle soil
  - Soil was collected from the Garub area of southern Namibia. This consisted of soil from both inside and outside fairy circles as well as beneath a dead *E. gummifera* plant
  - A soil-bed bioassay and soil-agar bioassay was conducted using all three types of soil collected and *E. teff* as bio-indicator to investigate the allelopathic nature of the soils.

1.4 References

Albrecht, C.F., Joubert, J.J., De Rycke, P.H. 2001. Origin of the enigmatic, circular, barren patches ('Fairy Rings') of the pro-Namib. South African Journal of Science 97, 23-27.

Becker T. and Getzin S. 2000. The fairy circles of Kaokoland (North-West Namibia) – origin, distribution, and characteristics. Basic and Applied Ecology 1, 149-159.

Berendsen, R.L., Pieterse, C.M.J., Bakker, P.A.H.M. 2012. The rhizosphere microbiome and plant health. Trends in Plant Science 17 (8), 478-486.

Coaton, W.G.H. 1958. The HODOTERMID harvester termites of South Africa. Department of Agriculture, Division of Entomology, Science Bulletin No. 375.

Cramer, M.D. and Barger, N.N. 2013. Are Namibian "Fairy Circles" the consequence of self-organizing spatial vegetation patterning? Public Library of Science (PLOS one) 8(8), 1-12.

Cramer, M.D., Innes, S.N., Midgley, J.J. 2012. Hard evidence that heuweltjie earth mounds are reticule features produced by differential erosion. Paleogeography, Paleoclimatology, Paleoecology 350-352, 189-197.

Cramer, M.D., Von Holdt, J., Khomo, L., Midgley, J.J. 2016. Evidence for Aeolian origins of *heuweltjies* from buried gravel layers. South African Journal of Science, 112(2), 1-10.

Curtis, B. and Mannheimer, C. 2005. Tree Atlas of Namibia. National Botanical Research Institute, Windhoek.

Eicker, A., Theron, G.K., Grobbelaar, N. 1982. n' Mikrobiologiese studie van 'kaal kolle' in die Giribesvlakte van Koakoland, S.W.A.- Namibië. South African Journal of Botany 1, 69-74.

Folgarait, P.J. 1998. Ant biodiversity and its relationship to ecosystem functioning: a review. Biodiversity and Conservation 7, 1221-1244.

Friese, C.F. and Allen, M.F. 1993. The interaction of harvester ants and vesicular- arbuscular mycorrhizal fungi in a patchy semi-arid environment: the effects of mound structure on fungal dispersion and establishment. Functional Ecology 7, 13-20.

Frouz, J. and Jilkova, V. 2008. The effects of ants on soil properties and processes (Hymenoptera: Formicidae). Myrmecological News 11, 191-199.

a) Getzin, S., Wiegand, K., Wiegand, T., Yizhaq, H., Von Hardenberg, J., Meron. E. 2015. Adopting a spatially explicit perspective to study the mysterious fairy circles of Namibia. Ecography 38, 1-11.

b) Getzin, S., Wiegand, K., Wiegand, T., Yizhaq, H., Von Hardenberg, J., Meron. E. 2015. Clarifying misunderstandings regarding vegetation self-organization and spatial patterns of fairy circles in Namibia: a response to recent termite hypotheses. Ecological Entomology 40, 669-675.

Getzin, S., Yizhaq, H., Bell, B., Erickson, T.E., Postle, A.C., Katra, I., Tzuk O., Zelnik, Y.R., Wiegand, K., Wiegand, T., Meron, E. 2016. Discovery of fairy circles in Australia supports self-organization theory. Proceedings of the Natural Academy of Science (PNAS) 113(13), 3551-3556.

Gilad, E., Von Hardenberg, J., Provenzale, A., Shachak, M., Meron, E. 2004. Ecosystem engineers: from pattern formation to habitat creation. Physical Review Letters 93.

Gilad, E., Von Hardenberg, J., Provenzale, A., Shachak, M., Meron, E. 2007. A mathematical model for plants as ecosystem engineers. Journal of Theoretical Biology 244(4), 680–691.

Grossi, V., Cravo-Laureau, C., Guyoneaud, R., Ranchou-Peyruse, A., Hirschler-Réa, A. 2008. Metabolism of n-alkanes and n-alkenes by anaerobic bacteria: A summary. Organic Geochemistry 39, 1197-1203.

Grube, S. 2002. The fairy circles of Koakoland (Northwest Namibia) – is the harvester termite *Hodotermes mossambicus* the prime causal factor in circle formation? Basic and Applied Ecology 3, 367-370.

Harrison, T. 2011. Paleontology and Geology of Laetoli: Human Evolution in Context: Volume 2: Fossil Hominins and the Associated Fauna Vertebrate Paleobiology and Paleoanthropology. Springer, Netherlands.

Heider, J., Spormann, A.M., Beller, H.R., Widdel, F. 1999. Anaerobic bacterial metabolism of hydrocarbons. FEMS Microbiology Reviews 22, 459-473.

Jankowitz, W.J., Van Rooyen, M.W., Shaw, D., Kaumba, J.S., Van Rooyen, N. 2008. Mysterious circles in the Namib Desert. South African Journal of Botany 74, 332-334.

Joubert, A., 2008. Investigation on Selected Biotic and Abiotic Factors in the Maintenance of the Fairy Circles‘(Barren Patches) of Southern Africa. (M.Sc. dissertation). University of Pretoria, Pretoria.

Juergens, N. 2013. The biological underpinnings of Namib desert fairy circles. Science 339, 1618-1621.

Juergens, N. 2015. Exploring common ground for different hypotheses on Namib fairy circles. Ecography 38, 12-14.

Juergens, N., Vlieghe, K.E.P., Bohn, C., Erni, B., Gunter, F., Oldeland, J., Rudolph, B., Picker, M.D. 2015. Weakness in the plant competition hypothesis for fairy circle formation and evidence supporting the sand termite hypothesis. 2015. Ecological Entomology 40, 661-668.

Knight, R.S., Rebelo, A.G., Siegfried, W.R. 1989. Plant assemblages on Mima-like earth mounds in the Clanwillian district, South Africa. South African Journal of Botany 55(5), 465-472.

Kutílek, M. 2004. Soil hydraulic properties as related to soil structure. Soil and Tilage Research, 79, 175-184.

Leuthold, R.H., Bruinsma, O., Van Huis, A. 1976. Optical and Pheromonal Orientation and Memory for Homing Distance in the Harvester Termite Hodotermes mossambicus (Hagen). Behavioral Ecology and Sociobiology 1, 127-139.

Lin, J.H., Ku, Y.R., Lin, Y.T., Teng, S.F., Wen, K.C., Liao, C.H., 2000. Preparative isolation and gas chromatography–mass spectrometry analysis of triterpenoids in Kansui Radix. Journal of Food and Drug Analysis 8, 278–282.

Lovergrove B.G. and Siegfried W.R. 1989. Distribution and Formation of Mima-like earth mounds in the Western Cape Province of South Africa. South African Journal of Science 82, 432-436.

Mallavadhani, U.V., Satyanarayana, K.V.S., Mahapatra, A., Sudhakar, A.V.S., Narasimhan, K., Pandey, D.K., Thirunavokkarasu, M. 2006. Development of Diagnostic Microscopic and Chemical Markers of Some *Euphorbia* Latexes. Journal of Integrated Plant Biology 48(9), 1115-1121.

Mbadinga, S.M., Wang, L., Zhou, L., Liu, J., Gu, J., Mu, B. 2011. Microbial communities involved in anaerobic degradation of alkanes. International Biodeterioration and Biodegradation 65, 1-13.

McCahon T.J. and Lockwood J.A. 1990. Nest architecture and pedoturbation of *Formica obscuripes* FOREL (Hymenoptera, Formicidae). Pan-Pacific Entomologist 66, 147-156.

Meyer J.J.M., Senejoux F., Heyman H.M., Meyer N.L., Meyer M.A. 2015. The occurrence of triterpenoids from *Euphorbia gummifera* inside the fairy circles of Garub in the southern Namibian pro-desert. South African Journal of Botany 98, 10-15.

Mitchell, J.D., Hewitt, P.H., Van der Linde, T.C.De.K. 1993. Critical Thermal Limits and Temperature Tolerance in the Harvester Termite *Hodotermes mossambicus* (Hagen). Journal of Insect Physiology 39(6), 523-528.

Moll, E.J., 1994. The origin and distribution of fairy rings in Namibia. In: Seyani, J.H., Chikuni, A.C. (Eds.), Proceedings of the 13th Plenary Meeting AETFAT, Malawi, pp. 1203–1209.

Naudé, Y., Van Rooyen, M.W., Rohwer, E.R. 2011. Evidence for a geochemical origin of the mysterious circles in the Pro-Namib desert. Journal of Arid Environments, 75, 446–456.

Nel, J.J.C. and Hewitt, P.H. 1969. A study of the food eaten by a field population of the Harvester termite, *Hodotermes mossambicus* (Hagen) and its relation to population density. Journal of Entomological Society of Southern Africa 32(1), 123-131.

Picker M.D., Ross-GillespieV., Vlieghe K., Moll E. 2012. Ants and the enigmatic Namibian fairy circles – cause and effect? Ecological Entomology 37, 33-42.

Prins, A.J. 1982. Review of *Anoplolepsis* with reference to male genitalia, and notes on *Acropyga* (Hymenoptera, Formicidae). Annals of the South African Museam 89(3), 215-246.

Ramond, J., Pienaar, A., Armstrong, A., Seely, M., Cowan, D.A. 2014. Niche-partitioning of edaphic communities in the Namib Desert gravel plain fairy circles. Public Library of Science (PLOS ONE) 9(10), 1-9.

Rietkerk, M., Boerlijst, M.C., Van Langevelde, F., HilleRisLambers, R., Van de Koppel, J., Kumar, L., Prins, H.H.T., De Roos, A.M. 2002. Self-Organization of vegetation in arid ecosystems. The American Naturalist 160(4), 524-530.

Rogers, L.E. and Lavigne, R.J. 1974. Environmental effects of western harvester ants on the shortgrass plains ecosystem. Environmental Entomologist 3, 994–997.

Tarnita, C.E., Bonachela, J.A., Sheffer, E., Guyton, J.A., Coverdale, T.C., Long, R.A., Pringle, R.M. 2017. A theoretical foundation for multi-scale regular vegetation patterns. Nature 541, 398-414.

Theron, G.K., 1979. Die verskynsel van kaal kolle in Kaokoland, SuidWes-Afrika. Journal of the South African Biological Society 20, 43–53.

Tinley, K.L. 1971. Etosha and the Koakoveld. African Wild Life 25, 1-16.

Tschinkel, W.R. 2003. Subterranean ant nests: trace fossils past and future? Palaeogeography, Palaeoclimatology, Palaeoecology 192, 321-333.

Tshinkel, W.R. 2012. The lifecycle and life span of Namibian fairy circles. *PLoS One* 7, e38056.

Turner, T.R., James E.K., Poole P.S. 2013. The plant microbiome. Genome Biology 14 (209), 1-10.

Van der Walt, A.J., Johnson, R.M., Cowan, D.A., Seely, M., Ramond, J. 2016. Unique microbial phylotypes in namib desert dune and gravel plain fairy circle soils. Applied and Environmental Microbiology 82(15), 45.92-4601.

Van Rooyen M.W., Theron G.K., Jankowitz W.J., Matthews W.S. 2004. Mysterious circles in the Namib Desert: Review of Hypotheses on their origin. Journal of Arid Environments (57), 467-485.

Vlieghe, K., Picker, M., Ross-Gillepsie, V., Erni, B. 2015. Herbivory by subterranean termite colonies and the development of fairy circles in SW Namibia. Ecological Entomology 40, 42-49.

Vuong, Q.V., Nguyen, V.T., Thanh, D.T., Bhuyan, D.J., Goldsmith, C.D., Sadeqzadeh, E., Scarlett, C.J., Bowyer M.C. 2015. Optimization of ultrasound-assisted extraction conditions for euphol from the medicinal plant, *Euphorbia tirucalli*, using response surface methodology. Industrial crops and Products 63, 197-202.

Yasukawa, K., Akihisa, T., Yoshida, Z., Takido, M. 2000. Inhibitory Effect of euphol, a triterpene alcohol from the roots of *Euphorbia kansui*, on tumour promotion by 12-*O*-tetradecanoylphorbol-13-acetate in two-stage carcinogenesis in mouse skin. Jounal of Pharmacy and Pharmacology 52(1), 119-124.

CHAPTER 2

Allelopathic properties of *Euphorbia gummifera*

Table of Contents

List of figures

List of tables

2.1 Introduction

Communication is often the key to survival for most living organisms. Communication *per se* is not necessarily verbal. Many organisms have evolved to communicate through chemical signals. Pheromones are chemical-based communication signals utilized within species that are involved in attracting a suitable mate or indicating desirable fertility (Wyatt, 2003). Mammals are known to leave a strong scent as a means to mark their territory (Gosling and Roberts, 2001). Some bacteria are known to modulate population density through chemical signals through the process known as quorum sensing (Miller and Bassler, 2001). Plants have evolved their own forms of chemical communication, one of them being allelopathy.

Allelopathy encompasses the chemical based-interactions through the release of secondary metabolites (Haig, 2008; Cipollini et al., 2012). Molisch (1937) introduced the term allelopathy. These chemicals can elicit a negative or positive effect in the receiving organisms through direct or indirect routes (Lau et al., 2008). Even though Molisch coined the term to cover both beneficial and negative plant-based chemical interactions, most scientific studies have solely been concerned with the negative effects of allelopathy and thus most definitions followed suit (Wills, 2007). Some consider this mode of communication to be confined to the plant kingdom (Muller, 1970). Even though allelopathy has been at the center of controversy and disagreement, it is not a new term. It dates back to the time of the father of botany, Theophrastus (Colquhoun, 2006).

2.1.1 History of plant allelopathy

During the third century Theophrastus, the philosopher, proposed that one plant could have an effect on another even though he did not at the time comprehend the science behind such interactions (Cipollini et al., 2012). He made the observation that the chickpea plant had the ability to negatively affect the growth of co-occurring plants, which was later again observed by Plinus Secundus (Colquhoun, 2006). At that time it was believed that the plants that could elicit such an inhibitory growth effects, achieved this by release of a repelling scent or odor (Aliotta et al., 2008). Many other scientists of their time also mentioned such negative growth effects by one plant on others in their ancient Greek and Roman as well as Japanese writings.

Other allelopathic-like findings include: Culpeper (1633) noted that the basil plant and rue never co-occur in natural systems as well as grape and cabbage; Young (1804) observed that once clover plants had been cultivated in a location successively, subsequent cultivation proved to be unsuccessful; Decandolle (1832) observed "soil sickness" for several agricultural important crops such as oats, rye and wheat and explained this at the hand of possible exudates from plants; Stikney and Hoy (1881) observed that the growth of vegetation under the walnut tree was severely impaired as compared to others growing in similar conditions. These are just a few reports noted in literature and a vast majority of such reports could have been lost over the decades.

It was only after the beginning of the 1900's that allelopathy could be investigated and demonstrated in a scientific environment; During this time the majority of plants thought to be allelopathic was proven so as well as other historically important medicinal plants (Rice, 2012).

2.1.2 Important aspects of the allelopathic process in the environment

When studying allelopathy there are a few important aspects that needs to be fully explained and understood: the release of the allelochemical into the environment, effect on the target plant and the fate of the allelochemical in the environment. It is a common misconception that allelopathy and competition are one and the same. However, allelopathy involves the release of a chemical(s) into the environment whereas competition involves removing a factor which has limited availability (Rice, 2012).

2.1.2.1 Release of allelochemicals into the environment

Release of allelochemicals into the environment is not as simple as chemicals entering the environment and eliciting an effect (Inderjit et al., 2011). There is a complex network of different ecosystem factors affecting (enhancing or reducing) the amount, release, chemical form and subsequent uptake of these secondary metabolites (Inderjit et al., 2011) (Figure 2.1). Allelochemical effects on the receiver can be a result of: released chemical(s) having a direct effect, degradation and/or transformation of released product(s) elicit an effect, released chemical(s) affects other factors (physical, biological and/or chemical) or involvement of a third party as a result of released compound(s) (Inderjit and Weiner, 2001). Allelochemicals enter the environment directly through active release by leaching, root exudation and release of volatiles

or indirectly through the decomposition of plant material (foliage and/or roots) which also leaches allelochemicals (Zang et al., 2010; Haig, 2008; Inderjit and Nilsen, 2003; Einhellig, 1995a).

Certain abiotic and biotic factors determine the amounts of allelochemicals present in plants and thus the amount that is released as well as the severity of the effect on the donor plant (Kobayashi, 2004; Kruse et al., 2000; Wardle et al., 1998, Einhellig, 1996a).

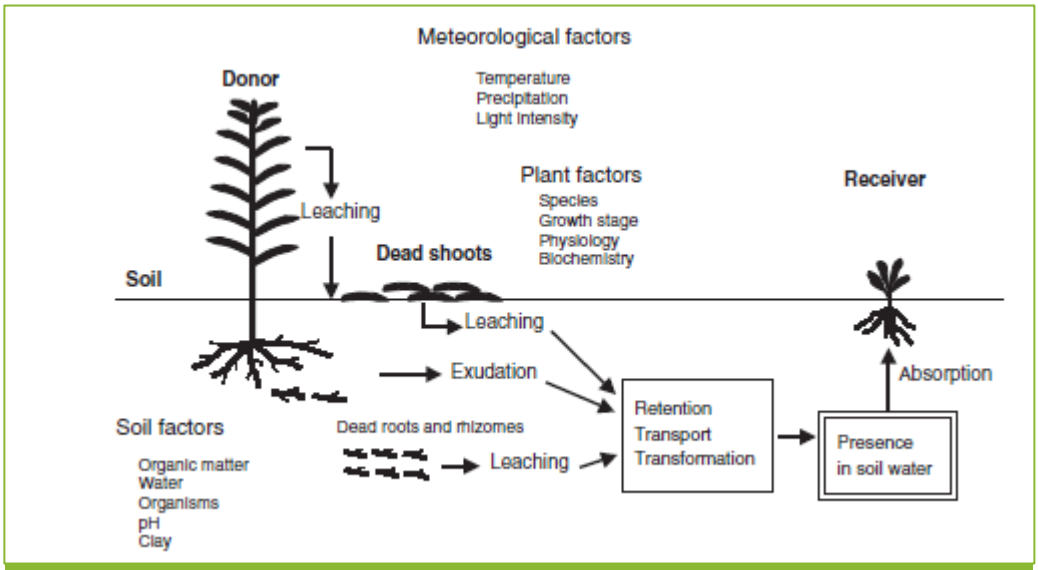

Figure 2.1: The complex process of the release of allelochemicals from the donor plant as well as all the factors affecting this process and the subsequent uptake by the receiver plant (Kobayashi, 2004).

These abiotic factors include temperature, light intensity, water availability and soil properties, whereas the biological properties include plant physiological properties and other organisms (Tesio and Ferrero, 2010; An et al., 2003; Kruse et al., 2000; Einhellig, 1996a). As allelochemicals are secondary metabolites, some environmental stress factors have been demonstrated to enhance their content (An et al., 2003) and effect in some plants (Tesio and Ferrero, 2010). Research done on the purple nutsedge (*Cyperus rotundas* L.) by Tang et al. (1995) demonstrated that the phytotoxic allelochemical content of both its tissue culture and root exudates was enhanced by water stress. Einhellig (1996a) reported that barley was more susceptible to the phytotoxic effect of vanillic and ρ-coumaric acids under nutrient (nitrogen and

phosphorus) deficient growth conditions. The mathematical model developed by An et al., to explain the link between environmental stresses and allelopathy demonstrated that allelochemical content decreases with age.

Once allelochemicals enter the environment they enter this complex network of ecosystem factors that further have a hand in this process. Thus the fate of an allelochemical in the environment is complex, as explained in the next section.

2.1.2.2 Fate of allelochemicals in the environment

One of the biggest problems and counter arguments against allelopathy is that a plant may demonstrate phytotoxic allelopathic effects on other plants in its natural habitat, yet upon investigation under laboratory conditions the same plant fails to reproduce such effects. The answer lies in the complex transformation the compound(s) undergo once released from the donor plant into the environment. There are several factors such as soil properties (Kobayashi, 2004) microorganisms (Cipollini et al., 2012; Inderjit, 2005) and environmental conditions that influence the allelochemicals, their bioavailability and their eventual effect (Inderjit, 2005).

The transformation of allelochemicals can occur as a results of chemical processes such as oxidation, reduction, ionization, volatilization, hydrolysis, acetylation and polymerization (Zang et al., 2010; Blum, 2004; Vidal and Bauman, 1997). These processes are the result of the action of organic matter, inorganic ions, reactive mineral surfaces, ion-exchange capacity and biotic barriers present in the soil, as well as microbial enzymatic reactions or physical factors such as UV radiation and seasonal variation (Bonanomi et al., 2006; Inderjit, 2005; Vidal and Bauman, 1997).

Allelochemicals are not only transformed but they are also broken down and/or inactivated by the processes described above. Soil microorganisms are known to utilize the released allelochemicals present in root exudates as source of organic carbon (Inderjit and Callaway, 2003). Such an example is the microbial utilization of phenolics such as salicylate, ferulic, p-coumaric, p-hydroxybenzoic and vanillic acids (Schmidt et al., 2000). Thus the release of allelochemicals can induce soil microbial enrichment (Inderjit and Weiner, 2001) and subsequently have an effect on emergence of other plants (Inderjit and Callaway, 2003; Schmidt and Ley, 1999). This suggests that released allelochemicals and microorganisms work

synergistically to have an effect on the receiver plant(s). The inactivation of the quinone, sorgoleone (Hess et al., 1992), is an example of microbial inactivation of allelochemicals. Microorganisms are also known to degrade released allelochemicals into more inhibitory compounds, thus increasing the allelopathic effect (Inderjit, 2005). Such an example is the environmental (pH, light intensity, temperature) (Tanrisever et al., 1987; Obara et al. 1989; Williamson et al. 1992) and microbial degradation (Fischer et al. 1994) of the inactive non-allelopathic phenolic compound, ceratiolin, into active allelochemicals hydrocinnamic acid (Inderjit and Weiner, 2001) and acetophenone respectively (Williamson et al., 1992)

2.1.2.3 Phytotoxic effects/mode of action of allelochemicals on target plant

The phytotoxic effects or detrimental modes of action of allelochemicals are as diverse as the chemical compounds themselves. These mechanisms include inhibition of key enzymes involved in amino acid production, pigment production, lipid synthesis, nucleic acid synthesis, nutrient uptake, photosynthesis (Figure 2.2 A) and respiration to name just a few (Inderjit and Duke, 2003; Vyvyan, 2002) as well as affecting pivotal processes such as metabolite and hormone production, germination, root elongation, shoot growth, and cellular membrane integrity (Figure 2.2 B) (transport, fluidity, elongation of cells) (Weir et al., 2004; Einhellig, 1996b). Disrupting even one of a target plant's key processes can severely affect is ability to survive. Several secondary metabolites have been identified as being allelopathic (Table 2.1)

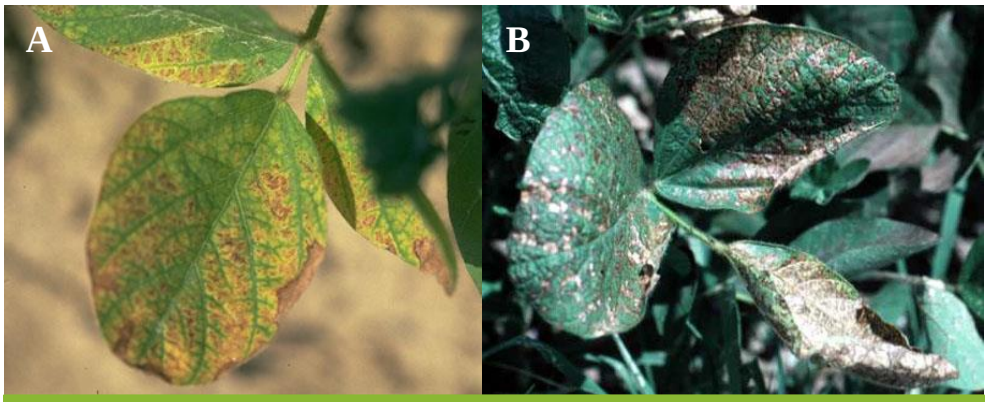

Figure 2.2: A. A plant exhibiting symptoms as a result of photo-inhibition. B. A plant exhibiting symptoms as a result of cell membrane disruption (Department of Botany and Plant Pathology, University of West Lafayette, 2015).

Table 2.1: Known allelochemicals, their distribution and effects

Secondary metabolite group	Examples	Producing plants	Mode of action/ effect on target	References
Cyanogenic glycosides	○ Linamarin (widespread in many plant families) ○ Dhurrin (sorghum) ○ Amgydalin (rosaceous plants) ○ Lotaustralin (lotus flower)	○ Plant families such as Fabaceae, Rosaceae, Linaceae, Compositae and others ○ Cassava ○ White clover ○ Sorghum	Production and subsequent release of hydrogen cyanide (HCN) that inhibits key enzymes of respiration through interacting with protein structure.	Taiz and Zeiger, 2010; Vetter, 2000
Glucosinolates	○ Allyl isothiocyanate (rape seed) ○ 4-Methylsulfinyl-3-butenylglucosinolate (raddish ○ Allylglucosinolate (mustard seed) ○ Allyl and 2-hydroxy-3-butenylglucosinolate (cabbage)	○ *Brassica* vegetables (cabbage, lettuce, rapeseed, raddish, broccoli)	Germination inhibition, give rise to phytotoxins that damage cells, targets enzymes of glycolysis and respiration.	Choesin and Boerner, 1991; Brown and Morra, 1997; Colquhoun,2006; Haig, 2008

Secondary metabolite group	Examples	Producing plants	Mode of action/ effect on target	References
Phenolic compounds	○ Caffeic acid ○ Ferulic acid ○ Psoralen ○ Scopoletin ○ Umbelliferone ○ Esculentin ○ Chlorogenic acid ○ Protocatechuic acid (3,4-dihydroxybenzoic acid) ○ Gallic acid ○ 3,4 Dihydroxy-benzaldehyde, *p*-hydroxybenzoic acid ○ 3,5-Dinitrobenzoic acid ○ ρ-Coumaric acid ○ Anisic acid ○ Gentisic acid ○ Syringic acid ○ Vanillic acid ○ Cathecol	○Celery, parsnip, parsley ○ *Delonix regia* ○ Billy goat weed ○ *Eucalyptus* genus (*Eucalyptus tereticornis, E. camaldulensis, E. polycarpa* and *E. microtheca)* ○ *Euphorbia* species (*E. supine, E. maculata*)	○ Germination inhibition (laboratory conditions) ○ Decreases shoot and root length as well as weight ○ Generalized cytotoxicity, change cell wall permeability and possibly interact with other more toxic substances. ○ General reduced rate of growth and yield.	Li et al., 2010; Taiz and Zeiger, 2010; Batish et al., 2008; Haig, 2008; Einhellig, 2004; Sasikumar et al., 2002; Rimando et al., 2001; Chou et al., 1992

Secondary metabolite group	Examples	Producing plants	Mode of action/ effect on target	References
Terpenoids	○ Cineole (rosemary) ○ Borneol (rosemary) ○ Carvacrol (thyme) ○ Thymol (savory) ○ á-Terpineol, linalool, thymol, and geraniol (tomato) ○ Limonene (lemon) ○ Menthol (peppermint) ○ Artemisinin (sweet wormwood) ○ Cineoles (*Artemisia* species and *Eucalyptus* species	○ Herbs (rosemary, thyme) ○ Tomatoes ○ Peppermint ○ Lemon ○ *Artemisia* species and *Eucalyptus* species ○ Liverwort	○ Germination inhibition ○ Certain terpenoids can inhibit key stages of cell division ○Act synergistically together and with other secondary metabolites.	Kim and Kil, 2001; Angelini et al., 2003; Haig, 2008; Taiz and Zeiger, 2010

Secondary metabolite group	Examples	Producing plants	Mode of action/ effect on target	References
Alkaloids	○ Scopolamine and hyoscyamine (thornapple) ○ Gramine and hordenine (barley) ○ Berberine ○ Ergotamine ○ Quinine ○ Coniine ○ Colchicine	○ Plant families: Fabaceae, Apocynaceae, Asteraceae, and Borginaceae ○ Legumes	○ Inhibits germination ○ Retards growth of seedlings ○ By binding to and interacting with DNA, RNA and proteins key enzymes of photosynthesis, respiration, transcription, protein synthesis, membrane stability, signal transduction, electron transport, and replication are affected.	Lovett and Hoult, 1995; Wink and Latz-Bruning, 1995; Haig, 2008; Taiz and Zeiger, 2010

2.1.3 The *Euphorbia* genus and allelopathy

The genus *Euphorbia*, belonging to the Euphorbiaceae family, comprises a very diverse group of plants in terms of their physiology and structure (Tanveer et al., 2013). This genus includes several plants with physiologically important activities such as allelopathic and antimicrobial (Chapter 3) capabilities. Both these have been studied extensively in this genus.

Hong et al. (2003) found that *E. hirta* (Figure 2.3) could suppress the germination and growth of radish seeds to some extent. *E. hirta* was found by Jabeen and Ahmad (2009) to possess allelopathic properties through its ability to affect maize growth through retarded germination and decreased chlorophyll content and protein production.

Figure 2.3: *E. hirta* (Plants for a future, 2012).

E. heterophylla (Figure 2.4) has been found be able to successfully outcompete co-occurring plants that result in yield losses of crops (Tanveer et al., 2013). Meschede et al. (2002) found that the plant caused severe losses when grown in close proximity to soybean. This was attributed it to *E. heterophylla*'s ability to use water more effectively and thus subsequently photosynthesize more optimally than soybeans (Procopio et al., 2004).

Figure 2.4: *E. heterophylla* (Plantnet, 1990).

Kumbhar and Dabgar (2011) found that *E. thiamifolia* aqueous extract significantly inhibited the germination of pigeon pea, as well as its overall growth. They found that an extract made from stems was the most effective.

Investigations into the allelopathic properties of *E. granulata* (Figure 2.5) by Hussain (1980) demonstrated that its aqueous extract had the ability to significantly inhibit germination and subsequent radicle development of several bio-indicators in a laboratory bioassay. This activity was later confirmed through experiments conducted by Sadaqa et al. (2010). They found that the plant residue when incorporated into soil of a bioassay significantly inhibited germination of onions.

Figure 2.5: *E. granulata* (Floraofqatar, 2014).

Qin et al. (2006) investigated the allelopathic and phytotoxic properties of the roots and root exudates from *E. esula* (Figure 2.6). They identified several compounds and their derivatives (jatrophane diterpenes and ellagic acid derivatives) whose phototoxic and allelopathic effects caused necrosis and reduced root development.

Figure 2.6: *E. esula* (The Nature Conservancy, Bugwood.org, 2014).

Figure 2.7: *E. prostata* (MBG.Research, 2017).

Alsaadawi et al. (1990) found that soil obtained from underneath an *E. prostata* (Figure 2.7) plant was able to significantly inhibit germination and growth of several test species. Further investigation showed that extracts as well as root exudates and plant residues were all able to display the same inhibitory effects as the soil. Elmetwally and Mansour (1994) also conducted experiments that showed that *E. prostata* exhibited allelopathic

activity against several plants (ornamental plants and turf grasses) in terms of germination inhibition, growth and development. They identified several compounds: ellagic and chlorogenic phenolic acids, rutin, Q-3 glucoside and Q-3 galactoside flavonide that belong to known classes of allelopathic compounds.

2.2 Aims and objectives

The aim of this chapter was to investigate the possible allelopathic properties of *Euphorbia gummifera*, as well as soil collected from inside fairy circles, by following these objectives:

- Collecting both plant and soil samples from an area known for fairy circles
- Preparing a methanol extract of the collected plant material
- Using the extract in a germination inhibition assay
- Using the soil for both a soil-bed bioassay and soil-agar bioassay
- Compare results to relevant control using statistical programmes

2.3 Materials and methods

2.3.1 Field collection

During March 2016 a field collection trip to the Garub area, where fairy circles occur, in the southern part of Namibia was undertaken. The field collection consisted of both soil and plant collection.

2.3.1.1 Soil collection

Ten fairy circles were selected at random. Soil was then collected from the surface of these ten circles (Figure 2.8) as well as in between (the matrix) the circles. Soil was also collected from underneath dead/decaying *E. gummifera* plants. Collected soil was transported in labeled airtight plastic jars (volume ± 500 g). After the field collection, the jars with the soil were stored in a basement cellar in plastic

Figure 2.8: Soil collection from inside a fairy circle's surface.

crates at room temperature. Specifics of the collection (coordinates, dates, fairy circle characteristics etc.) can be found in Appendix A.

2.3.1.2 Plant collection

Aerial parts of *E. gummifera* plant were collected in the same location as mentioned above (herbarium voucher PRU124383 University of Pretoria, H. G. W. J. Schweickerdt herbarium). Due to the poisonous nature of this plant, extreme caution was taken during harvesting. This included wearing protective gloves, avoiding direct contact with the plant's milky latex, wearing protective glasses and using shears to remove the plant parts. After harvesting the plant material, it was placed in double paper bags and transported to the University of Pretoria. After the field collection the plant material was placed in paper bags in a 5.5 °C fridge until used.

Figure 2.9: An intact *S. uniplumis* plant.

The dominant grass species of this area, *Stipagrostis uniplumis*, was also harvested (herbarium voucher PRU124384 University of Pretoria, H. G. W. J. Schweickerdt herbarium). Using a shovel the plant was loosened from the soil and the whole plant (roots intact) was harvested (Figure 2.9). The grass plants were placed in airtight plastic zip lock bags and transported in this manner. The plant material was stored in a 5.5 °C fridge.

2.3.2 Extract preparation

The aerial parts (Figure 2.10) of the *E. gummifera* was placed in a -80 °C freezer for two days before freeze drying for a week (United Science Pty Ltd. Freeze drier). Following the freeze drying the extraction process was conducted using a Speed Extractor (Büchi E-916) with methanol as solvent. The extraction

Figure 2.10: Aerial parts of *E. gummifera*

was done at 50 °C and 100 kPa with four cycles of extraction using 40 ml extraction tubes. The extraction's first three cycles consisted of 1 minute heat up, 15 minute hold and 5 minute solvent discharge while the last cycle differed only in terms of the hold, which was for 9 minutes.

Samples were collected in 240 ml glass bottles, where-after they were dried using a Genevac EZ-2 Plus personal evaporator. The aerial parts of the grass, *S. uniplumis* was placed in a -80 °C fridge for 24 hours followed by freeze drying (for a week). The same extraction process was followed as described above. A total of 14.0986 g of plant material was extracted to yield 0.5598 g extract. Thus 1 g dry plant material yielded 3.97 mg of extract.

2.3.3 Germination inhibition assay

A 1 g/ml *E. gummifera* extract (whole extract) solution was made using methanol as solvent. The solution was sonicated for 15 minutes in a heated water bath. This solution was used to make a dilution series of the following concentrations: 20 mg/ml, 10 mg/ml, 5 mg/ml, 2.5 mg/ml, 1.25 mg/ml and 0.625 mg/ml. A control of 100% methanol was also used. Each concentration had five replicates. To a Petri dish (9 cm) (individual replicate) containing a Whatmann no.1 filter paper (9 cm), 2 ml of each respective concentration was added. The dishes were left for 2-3 days to allow the methanol to evaporate from the filter paper. The filter papers were moistened with 2 ml of distilled water. In each plate, 30 *Eragrostis teff* seeds were evenly spaced out and the plates were incubated at 25 °C for 48 hours. A stereo microscope was used to count the germinated versus non-germinated seeds. The data was statistically analysed with Graph Pad Prism (GraphPad Software Inc., San Diego CA.) to determine any significant differences using a two-way Anova analysis with a 95% confidence interval (Tukey comparative post-hoc test).

The entire process was repeated three more times but with adjustments. Firstly, instead of moistening the filter papers with 2 ml of distilled water, 1 ml was used and the dilution series was started at a concentration of 40 mg/ml. Following this the extract was separated (see Section 2.4.1) by decanting the top layer using a glass pipet. The process was repeated for both types of the extract using 1 ml water for moistening and starting at a concentration of 40 mg/ml.

The process was again repeated using the *S. uniplumis* methanol extract using 1 ml of water for moistening and starting at a concentration of 40 mg/ml to rule out the possible allelopathic properties of the co-occurring grass species.

2.3.4 Soil-bed bioassay

For the purpose of this experiment the three soil types: inside and outside fairy circles as well as soil from underneath a dead *E. gummifera* were used. Each soil type had 5 replicates. Inside each petri dish a Whatmann no.1 filter paper was placed to which 2 ml of distilled water was added. To this 20 g of soil was added. The plates were shaken lightly back and forth to spread out the soil evenly. On the surface of the soil 30 *E. teff* were evenly spaced out. The plates were incubated at 25 °C for 48 hours. A stereo-microscope was used to count the germinated versus non-germinated seeds. The plates were then left for an additional seven days in the incubator to determine whether the germinated seeds could develop into established seedlings without additional water. The data was statistically analysed Graph Pad Prism using a one-way Anova analysis with a 95% confidence interval (Tukey comparative post-hoc test).

2.3.5 Soil-agar bioassay

This method to evaluate allelopathy, is a modified method of Yoshiharu et al. (2005). Four soil types were used for this assay: soil from inside and outside fairy circles, soil from underneath a dead *E. gummifera* as well as soil harvested from the roots of *S. uniplumis*. In order to obtain the soil from the *S. uniplumis* grass, the roots were gently rolled lengthwise in between glove-covered fingers. Each soil type had 5 replicates. Of each soil type 6 g of soil was used per Petri dish (9 cm). The soil was mixed with 15 ml of cooled nutrient agar (Merck) (15 g powder dissolved in 1 L distilled water followed by autoclaving) and placed in a 9cm petri dish. The petri dishes were left to solidify overnight in a laminar flow chamber under UV light. The UV light prevented any microbial growth. After 24 hours the plates were overlaid with an additional agar layer of 9ml. The plates were left to solidify overnight under the same conditions as described above. After the plates had solidified, 30 *E. teff* seeds were placed on the surface of each plate, evenly spaced out. The plated were sealed with parafilm and incubated at 25 °C for 48 hours.

The percentage germination of each plate was calculated and the data was analyzed statistically with Graph Pad Prism using a one-way Anova analysis with a 95% confidence interval. The entire process was repeated but instead of using nutrient agar, pure agar (15 g powder) (Merck) dissolved in 1 L distilled water followed by autoclaving) was used at the same percentage used for the nutrient agar.

2.4 Results

2.4.1 Extract preparation

A total of 84.7586 g of plant material was extracted (Figure 2.11A) and dried (Figure 2.11) to yield 7.11644 g of extract. Thus 1 g of dry plant material yields 0.0839 g extract.

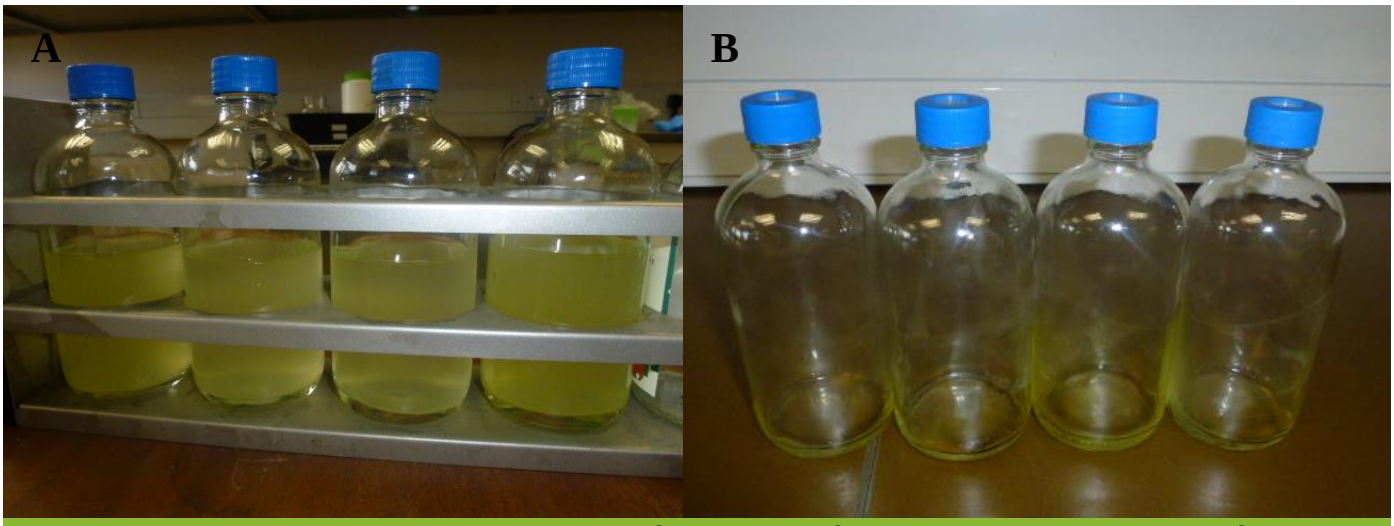

Figure 2.11: A. The methanol based *E. gummifera* extract after the extraction process, before being dried. B. The dried extract before transferal to a single polytop.

Figure 2.12: A. The separating extract before drying and B. after drying

The whole extract had two distinct layers: (Figure 2.12) a milky cream colored part and a brown colored sticky part which separated spontaneously when left to stand after the extraction process as well as after the drying process. Parts of the extract were separated for a germination bioassay but in response to results it was decided to keep the complete extract for further experiments.

2.4.2 Germination inhibition assays

2.4.2.1 Germination inhibition assay- Not water stressed

From the results (Table 2.2) it was clear that there were no significant differences (P-value < 0.05) between the control and treatment or between the different concentrations themselves (Appendix B). It was unclear whether or not this was due to the starting concentration, the amount of moisture or a combination of these two parameters. Thus both were adjusted.

Table 2.2: Methanol extract germination inhibition assay results using 2ml of water (unstressed) for moistening

Concentration	Germination percentage					Average germination percentage
	1	2	3	4	5	
Methanol control	73.33%	96.67%	90.00%	76.67%	86.67%	84.67%
0.626 mg/ml	96.67%	93.33%	93.33%	83.33%	83.33%	90.00%
1.250 mg.ml	93.33%	100.00%	93.33%	90.00%	100.00%	95.33%
2.500 mg/ml	93.33%	90.00%	96.67%	80.00%	90.00%	90.00%
5.000 mg/ml	93.33%	90.00%	90.00%	90.00%	86.67%	90.00%
10.000 mg/ml	100.00%	93.33%	93.33%	96.67%	96.67%	96.00%
20.000 mg/ml	80.00%	96.67%	96.67%	83.33%	86.67%	88.67%

2.4.2.2 Germination inhibition assay- Water stressed

The subsequent results proved to be more interesting. From the results in Table 2.3 and Figure 2.13 it was clear that there were significant results (P-values < 0.05) (Appendix B) that could indicate possible phyto-toxicity and indications of allelopathy of the *E. gummifera* plant. From the results it was evident that there were significant differences between the three highest

concentrations and the control, as well as between the three highest concentrations and some of the lower concentrations. There was even a significant difference between the percentage germination of 20 mg/ml and 40 mg/ml. The results could thus indicate that there is a specific threshold in terms of concentration where *E. gummifera* exhibits phyto-toxicity/allelopathy. In order to rule out the possibility that a co-occurring plant (such as the *S. uniplumis* grass plant) could be responsible for the 'allelopathy' linked to fairy circles, another germination inhibition assay needed to be conducted.

Table 2.3: Methanol extract germination inhibition assay results using 40mg/ml starting concentration and 1ml of water (stressed) for moistening

Concentration	Germination percentage					Average germination percentage
	1	2	3	4	5	
Methanol control	90.00%	86.67%	86.67%	90.00%	90.00%	88.67%
0.626 mg/ml	73.33%	76.67%	76.67%	76.67%	46.67%	70.00%
1.250 mg.ml	90.00%	80.00%	56.67%	83.33%	50.00%	72.00%
2.500 mg/ml	46.67%	83.33%	63.33%	80.00%	73.33%	69.33%
5.000 mg/ml	60.00%	80.00%	76.67%	63.33%	56.67%	67.33%
10.000 mg/ml	53.33%	70.00%	53.33%	53.33%	50.00%	56.00%
20.000 mg/ml	26.67%	30.00%	40.00%	50.00%	10.00%	31.33%
40.000 mg/ml	6.67%	26.67%	33.33%	23.33%	26.67%	23.33%

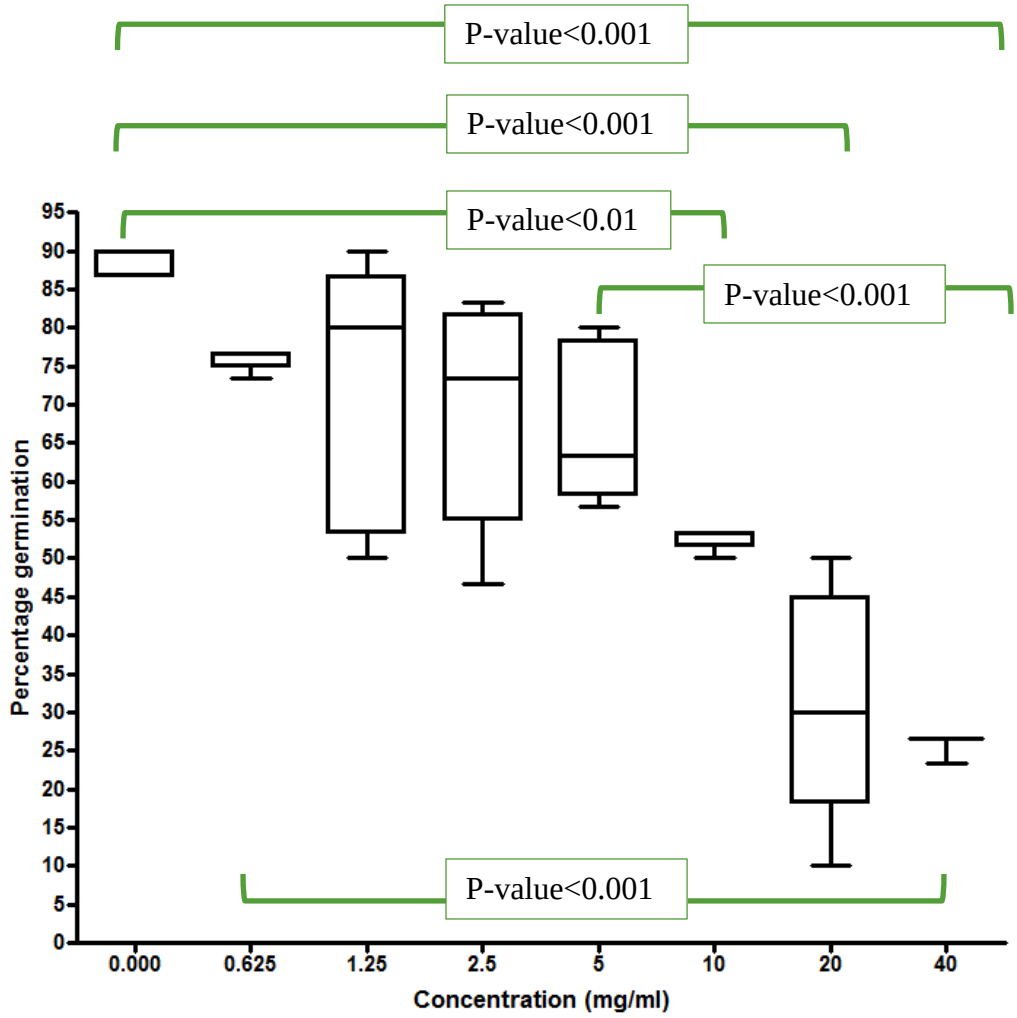

Figure 2.13: Box and whisker diagram of the germination data- Starting concentration 40mg/ml and 1ml water used

2.4.2.3 Germination inhibition assay using *S. uniplumis* extract

The results (Table 2.4 and Appendix B) from the germination inhibition assay using a *S. uniplumis* extract and the same parameters as in the bioassay with water stress above, it was clear that there was of no significant differences (p-value < 0.05). This indicated that the *S. uniplumis* could not be linked to the fairy circle allopathy theory.

Table 2.4: Germination inhibition assay results using *S. uniplumis* methanol extract

Concentration	Germination percentage					Average germination percentage
	1	2	3	4	5	
Methanol control	90.00%	86.67%	86.67%	83.33%	83.33%	86.00%
0.626 mg/ml	93.33%	90.00%	90.00%	93.33%	83.33%	90.00%
1.250mg.ml	90.00%	93.33%	90.00%	83.33%	83.33%	88.00%
2.500 mg/ml	76.67%	100.00%	90.00%	100.00%	80.00%	89.33%
5.000 mg/ml	66.67%	86.67%	96.67%	90.00%	90.00%	86.00%
10.000 mg/ml	90.00%	90.00%	86.67%	86.67%	90.00%	88.67%
20.000 mg/ml	93.33%	83.33%	86.67%	73.33%	86.67%	84.67%
40.000 mg/ml	76.67%	80.00%	80.00%	93.33%	83.33%	82.67%

2.4.2.4 Germination inhibition assay with the separated *E. gummifera* extract

In an attempt to determine which part of the *E. gummifera* extract (milky cream coloured part and/or brown colored sticky part) was the most active, the separated extracts were tested separately for their germination inhibition ability (starting concentration 40 mg/ml and 1 ml water for moistening). The results (Tables 2.5 and 2.6) indicated that once the extract was separated into its two distinct parts, it lost its germination inhibitory activity. There were no significant differences between the values for either type of extract (Appendix B).

Table 2.5: Germination inhibition assay results using the milky cream colored part of the *E. gummifera* methanol extract

Concentration	Germination percentage					Average germination percentage
	1	2	3	4	5	
Methanol control	86.67%	76.67%	86.67%	90.00%	83.33%	82.67%
0.626 mg/ml	86.67%	76.67%	93.33%	96.67%	83.33%	87.33%
1.250 mg.ml	86.67%	86.67%	90.00%	86.67%	90.00%	88.00%
2.500 mg/ml	96.67%	83.33%	90.00%	76.67%	90.00%	87.33%
5.000 mg/ml	80.00%	93.33%	93.33%	86.67%	73.33%	85.33%
10.000 mg/ml	90.00%	86.67%	90.00%	83.33%	93.33%	88.67%
20.000 mg/ml	86.67%	83.33%	90.00%	80.00%	80.00%	84.00%
40.000 mg/ml	90.00%	83.33%	86.67%	80.00%	73.33%	82.67%

Table 2.6: Germination inhibition assay results using the brown colored sticky part of the *E. gummifera* methanol extract

Concentration	Germination percentage					Average germination percentage
	1	2	3	4	5	
Methanol control	96.67%	90.00%	93.33%	93.33%	86.67%	92.00%
0.626 mg/ml	93.33%	76.67%	86.67%	90.00%	90.00%	87.33%
1.250 mg.ml	86.67%	90.00%	96.67%	80.00%	93.33%	89.33%
2.500 mg/ml	90.00%	86.67%	90.00%	90.00%	93.33%	90.00%
5.000 mg/ml	96.67%	96.67%	83.33%	66.67%	86.67%	86.00%
10.000 mg/ml	86.67%	83.33%	96.67%	96.67%	80.00%	88.67%
20.000 mg/ml	83.33%	83.33%	83.33%	90.00%	53.33%	85.00%
40.000 mg/ml	70.00%	93.33%	86.67%	86.67%	83.33%	84.00%

2.4.3 Soil-bed bioassay

The initial results from the soil-bed bioassay in terms of germination indicated that there were no significant differences between the three different soil types used after the initial 48 hour incubation. However, after the additional seven day incubation significant differences (P-value < 0.05) were observed (table 2.7 and Figure 2.14) between the established seedlings of the outside fairy circle soil versus that of the dead plant soil.

Table 2.7: Results of the soil-bed bioassay showing the germination percentage and the percentage of established seedlings

Replicate	Soil type					
	Inside fairy circle soil		Outside fairy circle soil		Dead plant soil	
	Germinated seeds	Established seedlings	Germinated seeds	Established seedlings	Germinated seeds	Established seedlings
1	96.67%	96.67%	96.67%	83.33%	86.67%	60.00%
2	90.00%	70.00%	93.33%	73.33%	76.67%	16.67%
3	100%	53.33%	86.67%	90.00%	80.00%	56.67%
4	93.33%	80.00%	83.33%	76.67%	83,33%	43.33%
5	73.33%	50.00%	93.33%	76.67%	73.33%	56.67%
Average	90.67%	70.00%	90.67%	80.00%	80.00%	46.67%

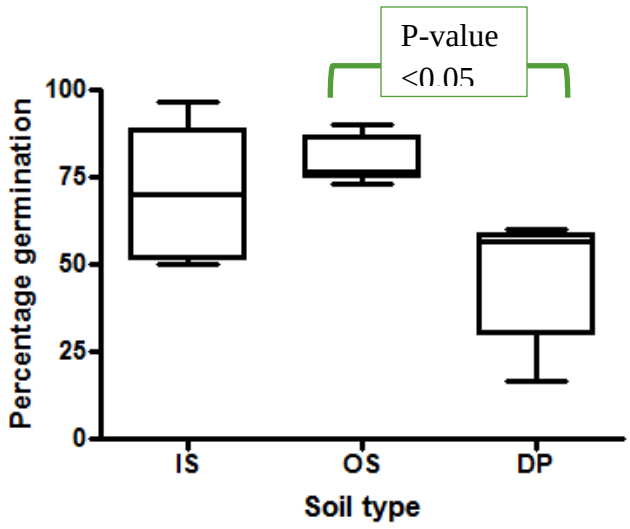

Figure 2.14: Box and whisker diagram for the establishment of seedlings data of the soil-bed bioassay

2.4.4 Soil-agar bioassay

2.4.4.1 Soil-agar bioassay using nutrient agar

The results from the soil-agar bioassay using nutrient agar (table 2.8 and Appendix B) indicated that there were significant differences (P-value < 0.05). The significant differences were observed for the following:

- Control vs Inside fairy circle soil (P value < 0.05)
    - The control had a much higher germination percentage than that of the inside fairy circle soil.
- Control vs Dead plant soil (P-value < 0.001)
    - The control had a much higher germination percentage than that of the dead plant soil.
- Outside fairy circle soil vs Dead plant soil (P-value < 0.05)
    - The outside fairy circle soil had an average percentage germination which was double that of the dead plant soil.
- Dead plant soil vs Rhizosphere soil (P-value < 0.01)
    - The rhizosphere soil had an average percentage germination which was double that of the dead plant soil

Overall the results indicated that the control, outside fairy circle soil and rhizosphere soil enabled a higher germination percentage while the inside fairy circle soil and the dead plant soil appeared to inhibit germination.

Table 2.8: Germination results for the soil-agar bioassay using nutrient agar

Soil type	Germination percentage					Average germination percentage
	1	2	3	4	5	
Control	73.33%	93.33%	83.33%	83.33%	83.33%	83.33%
Inside fairy circle soil	56.67%	60%	66.67%	50.00%	43.33%	55.33%
Outside fairy circle soil	63.33%	66.67%	53.33%	70.00%	53.33%	61.33%
Dead plant soil	46.67%	60.00%	16.67%	40.00%	6.67%	34.00%
Rhizosphere soil	63.33%	76.67%	63.33%	60.00%	60.00%	64.67%

2.4.4.2 Soil-agar bioassay using pure agar

From the results for the soil-agar bioassay using pure agar (Table 2.9 and Appendix B) no significant differences could be observed, indicating that the type of agar used had an effect on the results.

Table 2.9: Germination results for the soil-agar bioassay using pure agar

Soil type	Germination percentage					Average germination percentage
	1	2	3	4	5	
Control	86.67%	93.33%	90.00%	93.33%	86.67%	90.00%
Inside fairy circle soil	96.67%	90.00%	90.00%	93.33%	86.67%	91.33%
Outside fairy circle soil	83.33%	93.33%	100.00%	93.33%	90.00%	92.00%
Dead plant soil	83.33%	100.00%	93.33%	96.67%	86.67%	92.00%
Rhizosphere soil	90.00%	93.33%	96.67%	96.67%	90.00%	93.33%

2.5 Discussion

2.5.1 Germination inhibition assays

2.5.1.1 Germination inhibition assay- Not water stressed

The results from this germination inhibition assay indicated that there was no significant differences and thus possibly no allelopathic or phytotoxic properties linked to the *E. gummifera* plant. This might not be the case. Inderjit and Nilsen (2003) emphasized the importance of concentration in filter paper-based germination inhibition assays. As with this experiment, they noted that when germination was unaffected by different concentrations it could be ascribed to allelopathy and resource limitation (in this case water availability) counteracting each other. For this reason it was decided to adjust both the starting concentration and the amount of water used for the following germination inhibition experiment to help distinguish between the effects of allelopathy and/or resource limitation.

2.5.1.2 Germination inhibition assay- Water stressed

Once the starting concentration and the amount of water was adjusted, the results for the germination inhibition experiment changed drastically. The higher concentrations (40, 20 and 10 mg/ml) differed significantly from the control which had the highest germination values. Germination inhibition decreased as the dilution increased, indicating that allelopathy could be the cause (Inderjit and Nilsen, 2003). However, the amount of water given was also adjusted indicating that allelopathy and water stress might work synergistically. It has been found that water stress can enhance allelopathy of certain plants. Water stress was found to enhance the allelopathic properties of the purple nutsedge plant through increasing the amount of allelochemicals in both the plants tuber and rhizosphere (Kohl, 1993).

Several species belonging to the *Euphorbia* genus have been documented to have allelopathic properties manifested in germination inhibition, much in the same way as with this experiment. Germination inhibition experiments conducted by Husain (1980) with whole aqueous extracts of *E. granulata* significantly inhibited germination (p-value < 0.05) of several different plant species. Their results support the findings of this experiment, the difference being that their experiment used a whole extract versus a much lower concentration for this experiment. Husain (1980) concluded that their results were due to phytotoxins present in the plant which could also be present in *E. gummifera* but possibly in much higher concentrations or more than one allelochemical. Tanveer et al. (2010) also explained their germination inhibition results to other in this way.

Elmetwally and Mansour (1994) studied the allelopathic properties of three weeds of which *E. prostata* was among them. Their three different solvent based extracts (aqueous, ethanol and acetone) of different parts of the plant inhibited germination of several flowering plants and turf grasses. Their results led them to isolate and identify known allelopathic compounds which were: ellagic and chlorogenic phenolic acids, rutin, Q-3 glucoside and Q-3 glactoside flavonides. Even though the chemistry of *E. gummifera* has not yet been studied, compounds belonging to the same secondary metabolite groups as those identified in *E. prostata* could be linked to its germination inhibitory properties.

Many other *Euphorbia* species have been shown to be successful in inhibiting germination of several test organisms: *E. hirta*, *E. helioscopia*, *E. thiamifolia* (Kumbhar and Dabgar, 2010; Tanveer et al., 2010; Jabeen and Ahmad, 2009) and furthermore several additional allelochemicals have been also identified. These include phenolics (*E. supine* and *E. maculata*) (Elmore and Paul, 1983), gallic acid (*E. supina*) (Rice, 1969), di- and tri-terpenoids and tannins (*E. esula and E. helioscopia*) (Jiangbo et al, 2010; Zhi Qiang et al., 2008).

Thus overall all these studies support the theory that the *E. gummifera* plant does contain allelopathic and/or phytotoxic compounds that can be linked to its germination inhibitory activity.

2.5.1.3 Germination inhibition assay using *S. uniplumis* extract

The results from this assay indicated that a link between *S. uniplumis* and allelopathy (especially germination inhibition) is unlikely. As explained by Inderjit and Nilsen (2003), when germination increases with dilution then the inhibition is likely due to resource limitation. Even though there was no significant difference in germination between the control and the test concentrations, as well as the test concentrations themselves, differences even small and insignificant can be ascribed due to nutrient limitations or water stress.

2.5.1.4 Germination inhibition assays with the two parts of the *E. gummifera* extract

Neither part of the whole extract (milky cream coloured or brown colored sticky part) could significantly inhibit germination at any concentration. Subsequently it could not be deduced which part of the extract contained the compound(s) responsible for the germination inhibition and would be used for chemical studies.

It is known that most instances of allelopathy cannot be linked to a single compound (Einhellig, 1996). Several different allelochemicals work synergistically to inhibit growth (Tesio and Ferrero, 2010). Research done by Tanveer et al., 2013 led to the conclusion that the same allelochemical(s) that inhibit germination at high concentration can stimulate germination at low concentrations. Once the extract had been separated the concentrations of the allelochemicals could be affected, leading to a stimulation of germination instead of inhibition.

2.5.2 Soil-bed bioassay

The soil collected from underneath decaying *E. gummifera* plants significantly inhibited germinated seeds to progress to established seedlings when compared to the soil from outside fairy circles. This experiment shed light on the possible mode of action of the allelochemicals(s) present in this plant. Rather than it being germination inhibition, instead it could be retarding growth of germinated seeds preventing their transition into seedlings.

Several studies have been done on soil collected from underneath *Euphorbia* species hypothesized to contain allelochemicals. Hussain (1980) did a similar soil-bed bioassay using soil collected from underneath an *E. granulata* plant. Their results were similar to our results in that the soil underneath *E. granulata* retarded the growth of its test species significantly as compared to its control (soil not containing plant residues). They concluded that the plant deposits toxic residues through its natural decaying process which is responsible for its allelopathic activity. This reasoning is in line with that which is hypothesized for the *E. gummifera* plant.

Alsaadawi et al. (1990) also encountered similar results with *E. prostata*. Soil collected from underneath the plant inhibited both germination and growth of *Cynodon dactylon* (L.) seedlings. Tanveer et al. (2010) found that soil containing *E. helioscopia* residues significantly affected the overall growth of wheat, chickpea and lentil. Sadaqa et al. (2010) corroborated the findings of Hussain (1980) by demonstrating that soil containing *E. granulata* residues had the same effects on onions.

2.5.3 Soil-agar bioassay

For this bioassay significant differences were only observed when nutrient agar was used versus when pure agar was used. Nutrient agar's constituents are as follows: meat extract (1 g/L), peptone (5 g/L), yeast extract (2 g/L), sodium chloride (8 g/L), agar (15 g/L) (Merck). The pure agar growth media was made up of 15g pure agar dissolved in 1L distilled water, thus both growth media had the same concentration of agar. The difference was rather the constituents added to the nutrient agar. Meat extract, peptone and yeast contribute carbohydrates to the media (Thermo Fischer, Oxoid Microbiology Products). Van der Wheele (2002) did a study on the water potential of nutrient agar media and the effects it has on the growth of *Arabidopsis thaliana* in tissue culture. They found that adding low molecular weight solutes to agar, such as

carbohydrates, decreases the water potential of the growth media. This in turn causes water deficit conditions, which put the plants under stress.

These results further corroborated the hypothesis that allelopathy and water stress conditions could work synergistically to inhibit germination and overall growth.

2.6 Conclusion

The overall results from this chapter indicated that the *E. gummifera* plant does contain allelochemicals. Furthermore it appeared that during the plants natural decaying process a high amount of the compounds are deposited into the soil. Initially these compounds are present in high concentrations which causes germination and growth inhibition. Yet as a web of biotic and abiotic factors shape and breakdown these compounds, their concentrations dwindle down to a level where it could cause the opposite effects (demonstrated by the germination percentage of the lower concentrations of the *E. gummifera* methanol extract in Table 2.3) on plants until finally disappearing from the environment.

2.7 References

Aliotta, G., Mallik, A.U., Pollio, A., 2008. Historical Examples of Allelopathy and Ethnobotany from the Mediterranean Region, in: Zeng, R.S., Mallik, A.U., Luo, S. (Eds.), Allelopathy in sustainable agriculture and forestry. Springer-Verlag, New York.

Alsaadawi, I.S., Sakeri, F.A.K., Al-Dulaimy, S.M., 1990. Allelopathic inhibition of *Cynodon dactylon* (L.) PERS. and other plants by *Euphorbia prostata* L. Journal of Chemical Ecology 16(9), 2747-2754.

Angelini, L.G., Carpanese, G., Cioni, P.L., Morelli, I., Macchia, M. and Flamini, G., 2003. Essential oils from Mediterranean Lamiaceae as weed germination inhibitors. Journal of Agriculture and Food Chemistry 51, 6158–6164.

An, M., Liu, D.L., Johnson, I.R., Lovett, J.V. 2003. Mathematical modelling of allelopathy: II. The dynamics of allelochemicals from living planys in the environment.

Batish, D.R., Kaur, S., Singh, H.P., Kohli, R.K. 2008. Role of root-mediated interactions in phytotoxic interference of *Ageratum conyzoides* with rice (*Oryza sativa*). Flora 204, 388-395.

Blum, U. (2004) Fate of phenolic allelochemicals in soils – the role of soil and rhizosphere microorganisms, in: Macias, F.A., Galindo, J.C.G., Molinillo, J.M.G., Cutler, H.G. (Eds.), Allelopathy: Chemistry and Mode of Action of Allelochemicals. CRC Press, Boca Raton, Florida.

Brown, P.D. and Morra, M.J., 1997. Control of soil-borne plant pests using glucosinolate-containing plants in: Advances in Agronomy. Academic Press, New York.

Choesin, D.V. and Boerner, R.E.J., 1991. Allyl isothiocyanate release and the allelopathic potential of *Brassica napus* (Brassicaceae). American Journal of Botany 78, 1083–1090.

Chou, C.H., Leu, L.L. 1992. Allelopathic substances and interactions of *Delonix regia* (BOJ) RAF. Journal of Chemical Ecology 18, 2285-2303.

Cipollini, D., Rigsby, C.M., Barto, E.K., 2012. Microbes as targets and mediators of allelopathy in plants. Journal of Chemical Ecology 38, 714-727.

Colquhoun, J.B., 2006. Allelopathy in weeds and crops: myths and facts, in: Proc. of the 2006 Wisconsin Fertilizer, Aglime and Pest Management Conference, Madison, Wisconsin (Vol. 1719, p. 318320).

Culpeppe, N. 1633. English Physitian and Complete Herball. Foulsham, London.

Einhellig, F.A., 2004. Mode of allelochemical action of phenolic compounds in: Macias, F.A., Galindo, J.C.G., Molinillo, J.M.G., Cutler, H.G (EDs.), Allelopathy: Chemistry and Mode of Action of Allelochemicals. CRC Press, Boca Raton, Florida.

Einhellig, F.A. 1996. Interactions involving allelopathy in cropping systems. Agronomy Journal 88, 886-893.

a) Einhellig, F.A. 1995. Allelopathy: Current Status and Future Goals, in: Inderjit, K. M. M. Dakshini, F.A. Einhellig (Eds.), Allelopathy: Organisms, processes and applications. American Chemical Society, Washington, D.C.

b) Einhellig, F.A. 1995. Mechanisms of action of allelochemicals in allelopathy, in: Inderjit, K. M. M. Dakshini, F.A. Einhellig (Eds.), Allelopathy: Organisms, processes, and applications. American Chemical Society, Washington, DC.

Elmetwally, M.H., and Mansour, A.A. 1994. Allelopathic effects of certain weeds on some ornamental and turf grass plants. The 5th Mediterranean Symposium: Weed control in sustainable agriculture in the Mediterranean area, Perugia.

Elmore, C.D. and Paul, R.N. 1983. Phenolic deposits and kranz syndrome in leaf tissues of spotted (*Euphorbia maculata*) and prostrate (*Euphorbia supina*) spurge. Weed Science 31(1), 509-516.

Fischer, N.H., Williamson, G.B., Weidenhamer, J.D., Richardson, D.R. 1994. In search of allelopathy in Florida scrub: The role of terpenoids. Journal of Chemical Ecology 20, 1355–1380.

Gosling, L.M. and Roberts, S.C. 2010. Scent-marking by male mammals: Cheat-proof signals to competitors and mates. Advances in the Study of Behavior 30, 169-217.

Haig T., 2008. Allelochemicals in plants, in: Zeng, R.S., Mallik, A.U., Luo, S. (Eds.), Allelopathy in sustainable agriculture and forestry. Springer-Verlag, New York.

Hess, D.E., Ejeta, G., Buttler, L.G. 1992. Selecting sorghum genotypes expressing a quantitative biosynthetic trait that confers resistance to *Striga*. Phytochemistry 31, 493-497.

Hong, N.H., Xuan, T.D., Tsuzuki, E., Hiroyuki, T., Mitsuhiro M., Khanh, T.D., 2003. Screening for allelopathic potential of higher plants from Southeast Asia. Crop Protection 22(6), 829-836.

Hussain, F., 1980. Allelopathic effects of Pakistani weeds: *Euphorbia granulate* Forssk. Oecologia 45(2), 267-269.

Inderjit and Duke, S.O. 2003. Ecophysiological aspects of allelopathy. Planta 217, 529-539.

Inderjit and Nilsen, E.T. 2003. Bioassays and field studies for allelopathy in terrestrial plants: progress and problems. Critical reviews in Plant Science, 22(3), 221-238.

Inderjit and Weiner, J. 2001. Plant allelochemical interference or soil chemical ecology? Perspectives in Plant Ecology, Evolution and Systematics 4(1), 3-12.

Inderjit, Wardle, D.A., Karban, R., Callaway, R.M. 2011. The ecosystem and evolutionary contexts of allelopathy. Trends in Ecology and Evolution 26(12), 655-662.

Inderjit. 2005. Soil microorganisms: An important determinant of allelopathic activity. Plant and Soil 274, 227-236.

Inderjit. 2001. Soil environment effects on allelochemical activity. Agronomy Journal 93, 79-84.

Jabeen, N. and Ahmad, M., 2009. Possible allelopathic effects of three different weeds on germination and growth of maize (*Zea mays* L.) cultivars. Pakistan Journal of Botany 41(4), 1677-1683.

Jiangbo, H., Hua-Jie, Z., Gui-Fen, L., Guang-Ming, L., Hao, C., Yan, L., Shaopeng, C., Xin, L., Guochun, Z., Yong-Xian, C. 2010. New compounds from *Euphorbia helioscopia* and absolute configuration determination by computational methods. Bulletin of the Korean Chemical Society 31(8), 2211-2214.

Kim, Y.S. and Kil, B.-S. 2001. Allelopathic effects of some volatile substances from the tomato plant. Journal of Crop Production 4, 313–321.

Kobayashi, K. 2004. Factors affecting phytotoxic activity of allelochemicals in soil. Weed Biology and Management 4, 1-7.

Kohl, I.C. 1993. Allelopathy and water stress of purple nutsedge *(Cyperus rotundus L.).* M.S. thesis, University of Hawaii, Honolulu.

Kruse, M., Strandberg. M., Strandberg, B. Ecological effects of allelopathic plants – a review. 2000. National Environmental Research Institute 315, 1-68.

Kumbhar, B.A., and Dabgar, Y.B., 2011. Allelopathic effects of aqueous extracts of *Euphorbia thiamifolia* L. on germination and seedling growth of *Cajanus cajan* L. Journal of Bioscience Research 2(2), 62-66.

Lau, J.A., Puliafico, K.P., Kopshever, J.A., Steltzer, H., Jarvis E.P., Schwarzländer, M., Strauss, S.Y., Hufbauer, H.A., 2008. Inference of allelopathy is complicated by effects of activated carbon on plant growth. New Phytologist 178, 412-423.

Li, Z., Wang, Q., Ruan, X., Pan, C., Jiang, D. 2010. Phenolics and plant allelopathy. Molecules 15, 8933-8952.

Lovett, J.V. and Hoult, A.H.C.1995. Allelopathy and self-defense in barley in: Dakshini, K.M.M., and Einhellig F.A. (Eds.), Allelopathy: Organisms, Processes, and Applications. American Chemical Society Symposium Series 582, Washington.

Meshede, D. K., Oliveira, R.S., Constantin, J., Scapim, C.A., 2002. Critical period of interference of *Euphorbia heterophylla* in soybean crop under low seeding rate. Planta Daninha 20(3), 381-387.

Miller, M.B. and Bassler, B.L., 2001. Quorum sensing in bacteria. Annual Reviews Microbiology 55, 165-199.

Molisch,H. 1937. Der Einfluss einer Pflanze auf die andere Allelopathie. Gustav Fisher, Jena.

Muller, C.H., 1970. Phytotoxins as plant habitat variables. Recent Advances in Phytochemistry 3, 106-121.

Obara, H., Onodera, J., Yusa, K. 1989. Synthesis of Ceratiolin, a constituent of *Ceratiola ericoides*. Bulletin of the Chemical Society of Japan 62, 3771–3372.

Procópio, S.O, Santos, J.B., Silva, A.A., Martinez, C.A., Werlang, R.C. 2004. Physiological characteristics of soybean and common bean crops and three weed species. Planta Daninha, 22(2), 211-216.

Qin, B., Perry, L.G., Broeckling, C.D., Du, J., Stermitz, F.R., Paschke, M.W., Vivanco, J.M., 2006. Phytotoxic Allelochemicals from roots and root exudates of leafy spurge (*Euphorbia esula* L.). Plant Signalling and Behaviour 1(6), 323-327.

Rice, E.L. 2012. Allelopathy, second edition. Academic Press.

Rice, E. L. 1969. Inhibition of nitrogen – fixing and nitrifying bacteria by seed plants. III. Inhibitors from *Euphorbia supina*. Physiology Plantarum 22 (6), 1175-1183.

Rimando, A.M., Olofsdotter, M., Dayan, F.E., Duke, S.O., 2001. Searching for rice allelochemicals: an example of bioassay-guided isolation. Agronomy Journal 93, 16–20.

Sadaqa, E.A., Bawazir, A.A., Qasem, J.R., 2010. Allelopathic activity of some common weeds species in onion fields. Allelopathy Journal 26(2), 175-184.

Sasikumar, K., Vijayalakshmi, C., Parthiban, K.T. 2002. Allelopathic effects of *Eucalyptus* on blackgram (*Phaseolus mungo* L.). Allelopathy Journal 9, 205-214.

Schmidt, S.K. and Ley, R.A. 1999. Microbial competition and soil structure limits the expression of phytochemicals in nature, in: Inderjit, Dakshini, K.M.M., Foy, C.L. (Eds.), Priciples and Practices in Plant Ecology: Allelochemical Interactions. CRC Press, Boca Raton, Florida.

Schimdt, S.K., Lipson, D.A., Raab, T.A. 2000. Effects of willows (*Salix brachyearpa*) on populations of salicylate-mineralizing microorganism in alpine soils. Journal of Chemical Ecology 26, 2049-2057.

Stickney, J.S. and Hoy, P.R. 1881. Toxic action of black walnut. Transactions of the Wisconsin Horticultural Society 11,166–167.

Taiz, L., and Zeiger, E., 2010. Secondary metabolites and defence in Plant Physiology 5th edition. Sinauer Associates Inc., Sunderland, Massachusetts.

Tang, C., Cai, W., Kohl, K., Nishimoto, R.K. 1995. Plant stress and allelopathy, in: Inderjit, K. M. M. Dakshini, Frank A. Einhellig (Eds.), Allelopathy: organisms, processes and applications. American Chemical Society.

Tanrisever, N., Fronczek, F.R., Fischer, N.H., Williamson, G.B. 1987. Ceratiolin and other flavonoids from *Ceratiola ericoides*. Phytochemistry 26, 175–179.

Tanveer, A., Khaliq, A., Javaid, M.M., Chaudhry M.N., Awan, I. 2013. Implications of weeds of genus *Euphorbia* for crop production: A Review. Planta Daninha 31(3), 723-731.

Tanveer, A., Rehman, A., Javaid, M.M.J., Abbas, R.N., Sibtain, M., Ahmad, A.U.H., Ibin-I-Zamir, M.S, Chaudhary, K.M., Aziz, A. 2010. Allelopathic potential of *Euphorbia helioscopia* L. against wheat (*Triticum aestivum* L.), chickpea (*Cicer arietinum* L.) and lentil (*Lens culinaris*Medic.). Turkish Journal of Agriculture and Forestry34, 75-85.

Tesio, F. and Ferrero, A. 2010. Allelopathy, a chance for sustainable weed management. International Journal of Sustainable Development and World Ecology 17(5), 377-389.

Van der Wheele, C.M., Spollen, W.G., Sharp, R.E., Baskin, T.I. 2000. Growth *of Arabidopsis thaliana* seedlings under water deficit studied by control of water potential in nutrient-agar media. Journal of Experimental Botany 51(350), 1555-1562.

Vetter, J., 2000. Plant cyanogenic glycosides. Toxicon 38, 11-36.

Vidal, R.A. and Bauman, T.T. 1997. Fate of allelochemicals in the soil. Ciência Rural 27(2), 351-357.

Wardle, D.A., Nilsson, M., Gallet, C., Zackrisson, O. 1998. An ecosystem level perspective of allelopathy. Biological Reviews 73, 305–319.

Weir, T.L., Park, S.W., Vivanco, J.M. 2004. Biochemical and physiological mechanisms mediated by allelochemicals. Current Opinions in Plant Biology7, 472–479.

Williamson, G.B., Obee, E.M., Weidenhamer, J.D. 1992. Inhibition of *Schizachyrium scoparium* (Poaceae) by the allelochemical hydrocinnamic acid. Journal of Chemical Ecology 18, 2095–2105.

Wills, R.J. 2007. What is allelopathy? in: History of Allelopathy. Springer Science and Business Media, Dordrecht.

Wink, M. and Latz-Bruning, B., 1995. Allelopathic properties of alkaloids and other natural products: possible modes of action in: Dakshini, K.M.M., and Einhellig F.A., Allelopathy: Organisms, Processes, and Applications. American Chemical Society Symposium Series 582, Washington.

Wyatt, T.D. 2003. Animals in a chemical world in: Pheromones and animal behavior. Cambridge University Press.

Yoshiharu, F., Akihiro, F., Syuntaro, H., 2005. Rhizosphere soil method: a new bioassay to evaluate allelopathy in the field. [Online]. Availible: http://www.regional.org.au/au/allelopathy/2005/2/3/2535_fujiiy.htm. [Cited: 22 May 2017].

Young, A. 1804. The Farmers Calendar. London.

Zang, Z.Y., Pan, L.P., Li, H.H. 2010. Isolation, identification and characterization of soil microbes which degrade phenolic allelochemicals. Journal of Applied Microbiology 108, 1839-1849.

Zhi-Qiang, L., Min, Y., Jin-Qiang, Z., Guang-Tong, C., Hui-Lian, H., Shu-Hong, G., Chao, M., Xuan, L., De-An, G. 2008. Ingenane diterpenoids from *Euphorbia esula*. Phytochemistry 69, 812-819.

CHAPTER 3

The chemical constituents of *Euphorbia gummifera*

Contents

List of figures

List of tables

3.1 Introduction

Euphorbia gummifera is not known for much except its association with the fairy circles of southern Namibia. The plant is closely related to *E. damarana* and *E. gregaria* and they bear some striking similarities to each other in terms of appearance (Leach, 1975) and association with fairy circles. The *Euphorbia* genus falls under the Euphorbiaceae family (Kirbag et al., 2013) this is the sixth largest flowering plant family (Al-Mughrabi, 2003; Bruyns et al., 2006; Horvath et al., 2011).

E. gummifera, more commonly known as "gommelkbos" or "stinkmelkbos" or "taaimelkbos" are succulent leafless shrubs of 1-1.5m in height and 2m in diameter with an irritant milky latex (Curtis and Mannheimer, 2005; Leach, 1975; Red List of South African Plants, 2010). They are mainly restricted to habitats such as plains and slopes consisting of sandy or rocky substrates such as desert and succulent Karoo (Curtis and Mannheimer, 2005; Red List of South African Plants, 2010). The plant's distribution range is confined to winter rainfall areas in the south-west of Namibia that are about 80km inwards from the coast (Leach, 1975).

Yet even though this plant's morphology, distribution and habitat range have been studied, its chemistry has not been investigated. No studies have been conducted to investigate the chemical makeup and compound range of any aspect of *E. gummifera* or its closely related counterparts such as *E. damarana* and *E. gregaria*, even though these plants are exploited industrially to produce fibers (Van Zyl, 2000).

3.2 The *Euphorbia* genus

The *Euphorbia* genus has been characterized as one of the most species rich and diverse among the flowering plant's genera (Horvath et al., 2011). Species belonging to this genus are known to be rich in secondary metabolites (Shi et al., 2008) that have vast functions to the plant as well as for exploitation for commercial use. All species belonging to this genus produce latex (Jassbi, 2006) which is how the genus was botanically named (Horvath et al., 2011).

The genus name is believed to have been modified from Euphorbus, who was an ancient Greek physician serving King Juba II of Numidia where he supposedly utilized the medicinal properties

of latex in his practices (Mozaffarian, 1996).Today these plants are not only used for their diverse medicinal properties (antibacterial, anticancer, antiHIV, analgesic, enzyme inhibition and anitfeedant) (Jassbi, 2006) but also as ornamentals as well as for the production of biofuel, rubber (Horvath et al., 2011; Sneider, 2009) and fiber (Van Zyl, 2000).

This genus can be taxonomically subdivided into four subgenera: *Esula*, *Rhizanthium*, *Euphorbia*, and *Chamaesyce* based on ITS (internal transcribed spacer) and psbA-trnH sequence data and *Euphorbia* can again be subdivided into sections *Euphorbia, Monadenium, Goniostema* and *Tirucalli Boiss* (Bruyns et al., 2006). All three Namibian euphorbs: *E. gummifera*, *E. damarana* and *E. gregaria* belong to the subgenus *Euphorbia* section. *Tirucalli Boiss.*

3.2.1 Chemistry of the latex

The milky sap (Figure 3.1) abundantly produced in specialized organs known as laticifers and exuded by euphorbs when mechanically damaged is referred to as latex (Horvath et al., 2011, Pintus et al., 2010). The latex is rich in diverse types of secondary metabolites such as: terpenoids (di-and triterpenoids) and alkaloids (Jassbi, 2006; Mallavadhani et al., 2006; Rizk, 1987; Shi et al., 2008) as well as starch grains, rubber, resins and protein polymers (Horvath et al., 2011). The latex produced by *Euphorbia* species is toxic and an irritant which has been demonstrated by several studies of the latex and the compounds it contains (Table 3.1).

Figure 3.1: The milky sap, latex, exuded from an *E. tirucalli* plant (Da Silva et al., 2011)

Table 3.1: Characteristics of latex from different *Euphorbia* species

Euphorbia species	Compounds isolated and identified from latex/plant parts containing latex	Isolation and identification methods	Biological activity	References
E. antiquorum	○ Nerifoliene ○ Euphol	○ Silica gel column chromatography ○ Libermann-Buchard test for terpenoids ○ Ultraviolet (UV) spectra ○ Infrared (IR) spectra ○ NMR ○ Mass spectrometry (MS)	Not investigated.	Mallavadhani et al., 2006
	○ Eupha-7,9(11),24-trien-3ß-ol (antiquol C) ○ 19(10→9) Abeo-8α,9ß,10α-eupha-5,24-dien-3ß-ol (antiquol B) ○ Euphol ○ Lemmaphylla-7,21-dien-3ß-ol ○ Isohelianol ○ Camelliol	○ Column chromatography on silica- and octadecyl silica gel ○ Reversed-phase HPLC ○ Gas-liquid chromatography (GLC) ○ NMR	Inhibition of Epstein-Barr Virus Activation	Akihisa et al., 2002

Euphorbia species	Compounds isolated and identified from latex/plant parts containing latex	Isolation and identification methods	Biological activity	References
E. antiquorum	○ Euphol 3-*O*-cinnamate ○ Antiquol A ○ Antiquol B ○ Euphol ○ 24-Methylene cycloarthanol ○ Cyclo-eucalenol ○ (*Z*)-9-nonacosene ○ Sitosterol ○ ρ-Acetoxyphenol	○ Silica gel column chromatography ○ HPLC ○ GC-MS ○ NMR	Not investigated	Gewali et al., 1990
E. tirucalli	○ Euphol	○ Silica gel column chromatography ○ Libermann-Buchard test for terpenoids ○ Ultraviolet (UV) spectra ○ Infrared (IR) spectra ○ NMR ○ Mass spectrometry (MS)	Not investigated.	Mallavadhani et al., 2006

Euphorbia species	Compounds isolated and identified from latex/plant parts containing latex	Isolation and identification methods	Biological activity	References
E. tirucalli	○ Eutirucallin (carbohydrate binding protein)	○ Ion exchange chromatocgraphy ○ MS	Ribosomal inactivating properties	Santana et al., 2014
	○ Campesterol ○ ß-Sitosterol ○ Euphol ○ ß-Amyrin ○ Glutinol	○ GC-MS	Not investigated	Uchida et al., 2010
	○ 3,7,12-Tri-0-acecy1-8-isovaleryl-ingol	○ Silica column chromatography ○ MS ○ NMR	Not investigated	Khan and Malik, 1990
	○ Euphorcinol	○ Silica gel chromatography ○ NMR	Not investigated	Khan et al., 1998
	○ Cyclo-euphordenol (4α,14α,24β-trimethyl-9β: 19-cyclocholest-20-en-3β-ol)	○ UV spectra ○ Silica column chromatography ○ NMR	Not investigated	Khan et al., 1988

Euphorbia species	Compounds isolated and identified from latex/plant parts containing latex	Isolation and identification methods	Biological activity	References
E. bothae	○ 12-Deoxyphorbol-13-isobutyrate-20-acetate ○ 2-Deoxyphorbol-13-(2-methylbutyrate)-20-acetate ○ 12-Deoxyphorbol-13-isobutyrate-16-angelate-20-acetate ○ 12-Deoxyphorbol-13-(2-methylbutyrate)-16-angelate-20-acetate	○ Reversed-phase separation ○ Silica gel chromatography ○ HPLC ○ NMR	Investigated opioid receptor binding (negative results)	Popplewell et al., 2010
E. nerifolia	○ Eurifoloids A to R ○ Ingenane ○ Abietane ○ Isopimarane ○ *ent*—Atisane type compounds	○ Colomn chromatography (D101-macroporous absorption resin, an MCI gel column and normal and reverse phase silica gel) ○ NMR ○ IR spectra ○ UV spectra ○ HPLC	Anti-HIV activity (eurifoloid E and F)	Zhao et al., 2014

Euphorbia species	Compounds isolated and identified from latex/plant parts containing latex	Isolation and identification methods	Isolation and identification methods	References
E. nerifolia	○ Euphonerins A to G ○ 3-*O*-Acetyl-8-*O*-tigloylingol ○ 3,12-di-*O*-Acetyl-8-*O*-tigloylingol ○ (24R)-Cycloartane-3β,24,25-triol ○ 5,4′-Dihydroxy-3,7,3′,5′-tetramethoxyflavone ○ Pachypodol (5,4′-dihydroxy-3,7,3′-trimethoxyflavone) ○ Combretol (5-hydroxy-3,7,3′,4′,5′-pentamethoxyflavone)	○ Diaion HP20 (7 × 23 cm) column chromatography ○ NMR ○ HPLC ○ IR spectra ○ UV spectra	Death-Receptor Expression-Enhancing Activity (cell ceath/apoptosis) in DLD-1/SacI cells	Toume et al., 2012
	○ Neriifolin (a serine protease)	○ Ammonium sulfate precipitation ○ Cation exchange chromatography ○ Gel filtration	Enzymatic activity and other chemical characteristics lends itself to possible use in food, dairy and textile industries	Yadav et al., 2011

Euphorbia species	Compounds isolated and identified from latex/plant parts containing latex	Isolation and identification methods	Isolation and identification methods	References
E. nerifolia	○ Nerifoliene (9,19-cyclolanost-22(22'), 24-diene-3ß-ol) ○ Euphol	○ Silica gel chromatography ○ IR spectra ○ UV spectra ○ NMR ○ MS	Not investigated	Mallavadhani et al., 2004
E. resinifera	○ Euphorol A to I ○ Kansenone ○ Kansenonol ○ (20R,23E)-Eupha-8,23- diene-3β,25-diol ○ (24R)-eupha-8,25-diene-3β,24-diol ○ Kansenol ○ 3β,25-Dihydroxy-tirucalla-7,23-diene	○ UV spectra ○ IR spectra ○ NMR ○ RP-HPLC ○ Silica gel and ODS column chromatography	Anticancer (antitumour) activity, assessed through cytotoxicity against cancer cell lines	Wang et al., 2016

Euphorbia species	Compounds isolated and identified from latex/plant parts containing latex	Isolation and identification methods	Isolation and identification methods	References
E. resinifera	○ Ingenol monoester (ingenol 3-[2,6-dimethylnonanoate]) ○ Ingol ester (ingol 3,7,12-triacetate 8-[phenylacetate]) ○ 12-Deoxy-phorbol esters (12-deoxyphorbol 13-isobutyrate 20-acetate) ○ Resiniferonol orthophenyl acetate ○ Euphol ○ Euphorbol ○ Euphorbioside A and B ○ Aglycone	○ UV spectra ○ Silica gel chromatography ○ NMR ○ MPLC (medium pressure LC) ○ HPLC ○ GC-MS	Not investigated	Fattorusso et al., 2002

3.3 Aims and objectives

The aim of this chapter was to investigate the chemical constituents of an *E. gummifera* methanol extract. The chemistry of the plant could then possibly be linked back to its allelopathic and/or antimicrobial activity.

The objectives were:

- Preparing a methonolic *E. gummifera* extract (Chapter 2).
- Conducting a test silica column chromatography experiment to optimize and troubleshoot procedures.
- Running a silica column chromatography to separate compounds based on polarity.
- Subjecting collected fractions to gas chromatography mass spectrometry (GC-MS) analysis to identify separated compounds.

3.4 Materials and methods

3.4.1 Silica column chromatography

The *E. gummifera* and the *S. uniplumis* methanol extracts were prepared as described in Chapter 2's Method and materials section. As a result of the problematic nature of the *E. gummifera* extract (extremely thick and sticky) a full scale silica column could not be run without optimizing the process and eliminating possible technical difficulties. Thus a smaller test column was run. Before any column could be run, a series of thin layer chromatography (TLC) experiments were conducted to establish the optimal solvent ratio to be used as a starting point. Both of the methanol extracts were dissolved in methanol and used for the TLC experiment. The grass extract was used as a standard to compare to that of the *E. gummifera* extract. The ratios tested were as follows:

- ✓ 100% hexane
- ✓ Hexane: ethyl acetate 9:1
- ✓ Hexane: ethyl acetate 7:3
- ✓ Hexane: ethyl acetate 5:5
- ✓ 100% methanol

The TLCs were visualized with both short (254 nm) and long (365 nm) UV wave length as well as vanillin. Vanillin was prepared by completely dissolving 7.5 g of vanillin powder in 250 ml ethanol followed by carefully dripping (one drop at a time) 5 ml sulfuric acid (H_2SO_4) into the solution.

3.4.1.1 Test silica column

As mentioned above, the *E. gummifera* extract was very arduous to work with. This was further exacerbated by the fact that the extract only dissolved in solvent at temperatures above 75 °C. As a result all aspects of the experiment involved heating. Solvents were heated in a water bath of 40 to 45 °C and the exterior of the column was heated with a hairdryer to 45 °C whilst the column was running (Figure 3.2).

Figure 3.2: The test silica column setup.

The test column used was 30 cm in length and 1 cm in diameter. The ratio of sample to silica was 0.1 g sample to 2 g silica (1:20). The column was packed using the slurry method whereby the column was filled with hexane three quarters of the full length. Before adding the silica slurry, the column was adjusted to be completely level. The silica was mixed with hexane to make a viscous mixture. The slurry was gently poured in small aliquots. Time was allowed for the silica to settle and the slurry was mixed again. The tap was opened when the column was filled to provide more space to pack the column. This was continued until the column was filled half way with silica. All of the silica was rinsed with hexane using from the glass above the slurry using a glass pipette. The column tap was opened and the hexane was allowed to run through until the meniscus reached the top of the silica.

The plant extract (1 g) was dissolved in 1 ml methanol by heating in a water bath (75 °C) until completely dissolved. Using a heated glass pipette, the plant sample was carefully added on top of the packed column to obtain an even thin layer. The first solvent ratio was added carefully by swirling the pipette tip all around the inside of the column and the tap was opened to collect fractions (7-10 ml). The column was run using different ratios of hexane, ethyl acetate and

methanol. TLC's were continually spotted, developed and visualized to determine the progression of solvent ratios.

3.4.1.2 Experimental silica column chromatography

Following the success of the test column, a full scale silica column was run. Due to the larger scale of the experiment, heated air (45 °C) was applied to the outside of the column from three different equidistant points. The solvents used were again heated in a water bath, at temperatures from 40 to 45 °C.

The column was packed and ran following the same steps as described for the test column. The experimental column was 95 cm in length and 3.5 cm in diameter. The ration of sample to silica was 5 g sample to 50 g silica (1:10). The collected fractions (15-20 ml) were dried and weighed. After examination of the TLC's, fractions that yielded identical band(s) were pooled, dried and weighed. After pooling, the fractions were again spotted on TLC and developed.

3.4.2 GC-MS

For the purpose of the GC-MS analysis, 1 mg/ml of each of the major fractions were made up in 1.5 ml GC-MS bottles. Fractions 1 to 70 was dissolved in hexane while the remaining fractions were dissolved in methanol. Wash samples consisted of 1 ml hexane and 1ml methanol.

The details for the GC-MS apparatus were as follows: Shimadzu GC-MS QP 2010. The GC-MS was powered by an electrical current of 70 eV. The GC column, using helium as carrier gas, was a RTX column with a diameter of 29.3 m, thickness of 0.25 µm and diameter of 0.25 mm that had a splitless injection of 1 µl. The program was as follows: initial over temperature of 50 °C held for two minutes, followed by a temperature increase to 280 °C at a rate of 10 °C/minute, once 280 °C was reached it maintained it of two minutes followed by a temperature increase to 300 °C at a rate of 25 °C/minutes and finally this temperature was held for five minutes. A total of 33 minutes was needed to run each sample. The obtained spectra were analysed using Shimadzu GC-MS post-run analysis program.

3.5 Results

3.5.1 Silica column chromatography

The series of TLCs developed with different solvent ratios as mobile phase indicated that the ideal solvent ratio to start the column chromatography experiment was hexane: ethyl acetate (9:1). The TLC plates developed with 100% hexane (Figure 3.3) and methanol (Figure 3.4) yielded problematic results. Using 100% hexane resulted in the samples spotted being confined to the baseline whereas using 100% methanol resulted in a smear rather than clear bands.

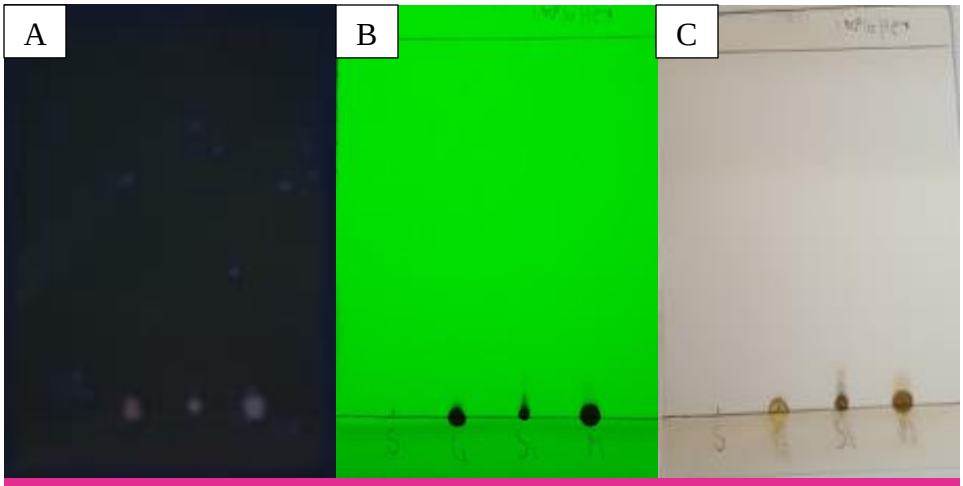

Figure 3.3: The TLC plate developed with 100% hexane as mobile phase. The order of samples spotted on the baseline is first lane solvent, second lane grass extract, third lane 3 spots and fourth lane six spots *E. gummifera* extract respectively. A. Visualization with UV wavelength of 254 nm (short wave length). B. Visualization with UV wavelength of 365 nm (long wave length). C. TLC plate after development with vanillin.

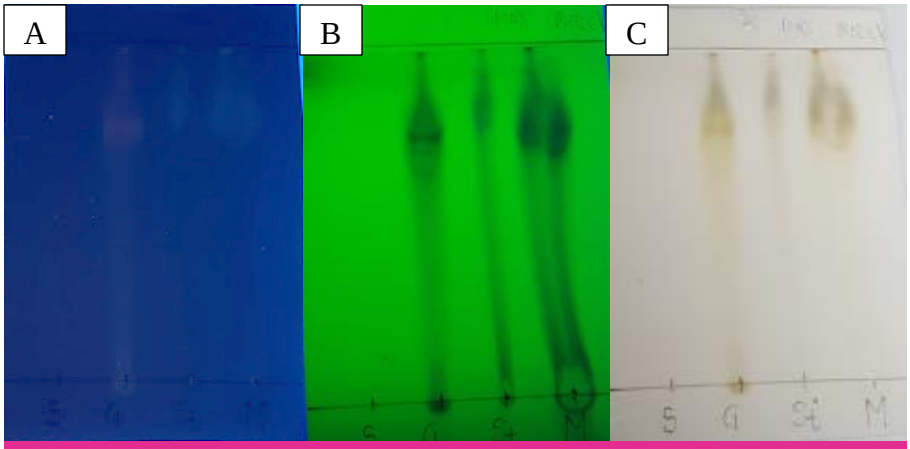

Figure 3.4: The TLC plate developed with 100% methanol as mobile phase. The order of samples spotted on the baseline is first lane solvent, second lane grass extract, third lane 3 spots and fourth lane six spots *E. gummifera* extract respectively. A. Visualization with UV wavelength of 254 nm (short wave length). B. Visualization with UV wavelength of 365 nm (long wave length). C. TLC plate after development with vanillin.

After comparing the banding pattern of the TLCs with different ratios of hexane and ethyl acetate (9:1, 7:3 and 5:5) as mobile phase, a ratio of 9:1 yielded the best initial separation (Figure 3.5). The banding pattern of the TLC with mobile phase 7:3 (Figure 3.6) was not a distinct as compared to 9:1 whereas at 5:5 (Figure 3.7) the bands clustered at the top closer to the solvent line. Thus hexane: ethyl acetate (9:1) was chosen as the starting solvent for the silica column chromatography.

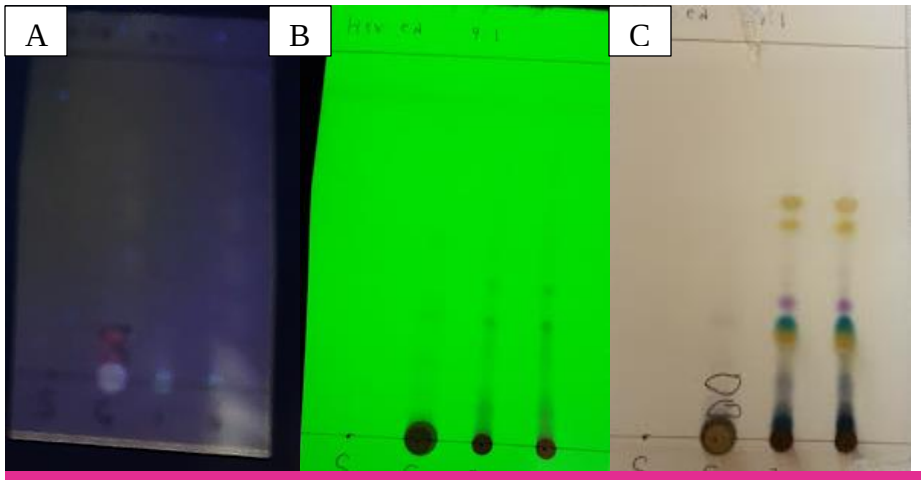

Figure 3.5: The TLC plate developed with hexane: ethyl acetate (9:1) as mobile phase. The order of samples spotted on the baseline is first lane solvent, second lane grass extract, third lane 3 spots and fourth lane six spots *E. gummifera* extract respectively. A. Visualization with UV wavelength of 254 nm (short wave length). B. Visualization with UV wavelength of 365 nm (long wave length). C. TLC plate after development with vanillin.

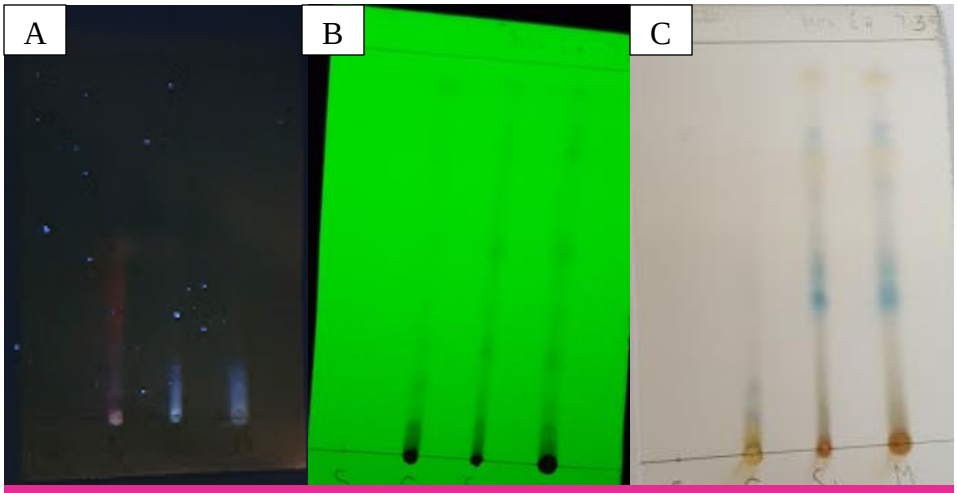

Figure 3.6: The TLC plate developed with hexane: ethyl acetate (7:3) as mobile phase. The order of samples spotted on the baseline is first lane solvent, second lane grass extract, third lane 3 spots and fourth lane six spots *E. gummifera* extract respectively. A. Visualization with UV wavelength of 254 nm (short wave length). B. Visualization with UV wavelength of 365 nm (long wave length). C. TLC plate after development with vanillin.

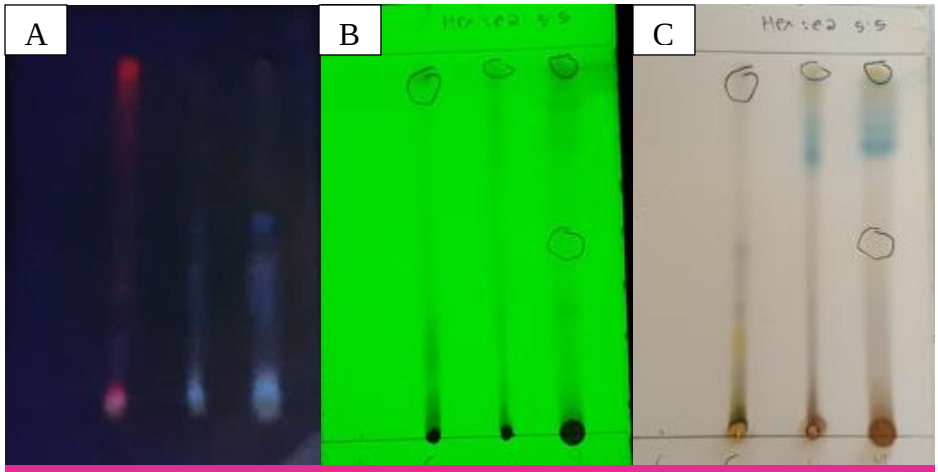

Figure 3.7: The TLC plate developed with hexane: ethyl acetate (5:5) as mobile phase. The order of samples spotted on the baseline is first lane solvent, second lane grass extract, third lane 3 spots and fourth lane six spots *E. gummifera* extract respectively. A. Visualization with UV wavelength of 254 nm (short wave length). B. Visualization with UV wavelength of 365 nm (long wave length). C. TLC plate after development with vanillin.

3.5.1.1 Test silica column

The test column was successfully developed with the adjustment of heated solvents and air. A total of 69 fractions (8 ml) were collected and TLC's were developed to visualize isolated compounds. The solvents hexane, ethyl acetate and methanol were used in ratios of increasing polarity (Table 3.2).

Fractions 2 and 3 yielded clearly separated compounds visible under UV light as wells as vanillin treatment (Figure 3.8). From fraction 4 to 21 no compounds could be visualized with either UV light or vanillin.

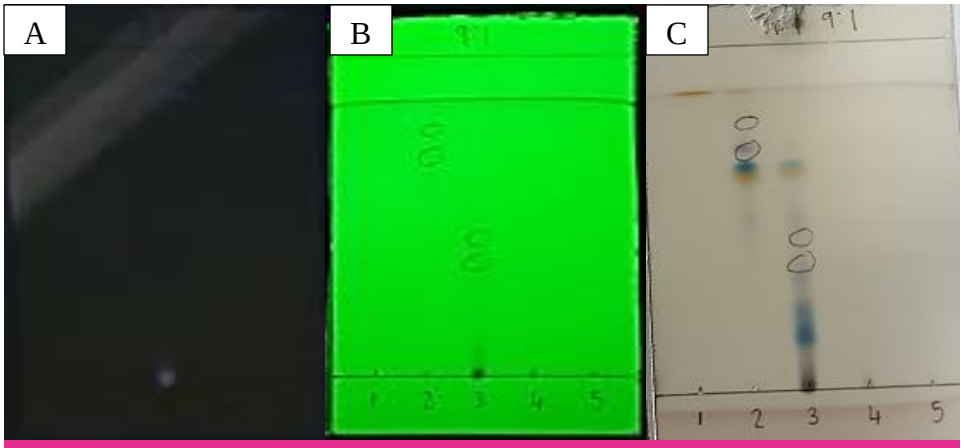

Figure 3.8: The TLC plate for fractions 1 to 5 developed with hexane: ethyl acetate (9:1) as mobile phase. A. Visualization with UV wavelength of 254 nm (short wave length). B. Visualization with UV wavelength of 365 nm (long wave length). C. TLC plate after development with vanillin. Encircled areas indicate bands that fluoresced under UV light.

Table 3.2: The solvent ratios used for test column

Solvent combination	Fractions
100% Hexane	Fraction 1
Hexane 9: ethyl acetate 1	Fractions 2-13
Hexane 7: ethyl acetate 3	Fractions 14-21
Hexane 5:ethyl acetate 5	Fractions 22-25
Hexane 3: ethyl acetate 7	Fractions 26-28
Hexane 1: ethyl acetate 9	Fractions 29-33
Ethyl acetate 9: methanol 1	Fractions 34-37
Ethyl acetate 7: methanol 3	Fractions 38-41
Ethyl acetate 5: methanol 5	Fractions 42-45
Ethyl acetate 3: methanol 7	Fractions 46-50
Ethyl acetate 1: methanol 9	Fractions 51-54
100% Methanol	Fractions 55-69

As the polarity of the mobile phase increased the compounds were increasingly more visible under UV light and did not react with vanillin. This was demonstrated by the visualization of fractions 33 to 36 (Figure 3.9). No compounds were visible with either UV light or vanillin development for the rest of the collected fractions.

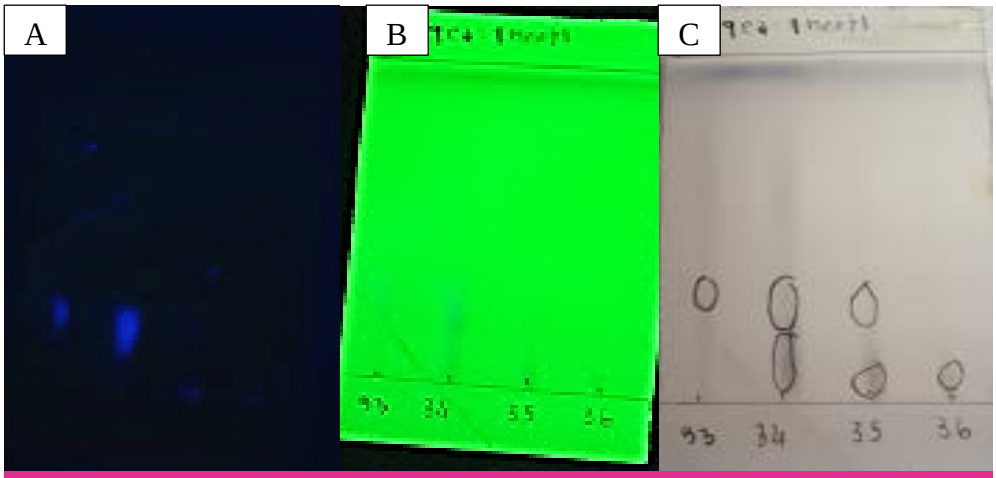

Figure 3.9: The TLC plate for fractions 33 to 36 ran with ethyl acetate: methanol (9:1) as mobile phase. A. Visualization with UV wavelength of 254 nm (short wave length). B. Visualization with UV wavelength of 365 nm (long wave length). C. TLC plate after development with vanillin. Encircled areas indicate bands that /fluoresced under UV light.

Overall the test silica column chromatography proved to be successful in terms of troubleshooting. The application of heat in all experimental procedure proved to aid in the success of the column as reflected by the visualized compounds on the TLC's. Even though several fractions did not react with the visualization techniques, the aim was to evaluate the feasibility of the application of heat and whether or not this would enable a large scale column, which it did.

3.5.1.2 Experimental silica column chromatography

The troubleshooting and success of the test column aided in running the full scale silica column chromatography experiment successfully. A total of 267 minor fractions of 15-20 ml were collected, subjected to TLC (Table 3.3), dried and weighed. Fractions with similar banding patterns were combined, dried and weighed (Appendix C) to yield 35 major fractions. The major fractions were subjected to TLC to yield visual representations that would aid in subsequent experiments (Table 3.4).

Table 3.3: Thin layer chromatography results for the full scale silica column.

Solvent ratio	Fractions	Thin layer chromatography silica plates		
		Short wave UV light	**Long wave UV light**	**Vanillin treatment**
Hexane 9: ethyl acetate 1	1 to 10	No visible bands	No visible bands	No visible bands
Hexane 9: ethyl acetate 1	11-18	No visible bands		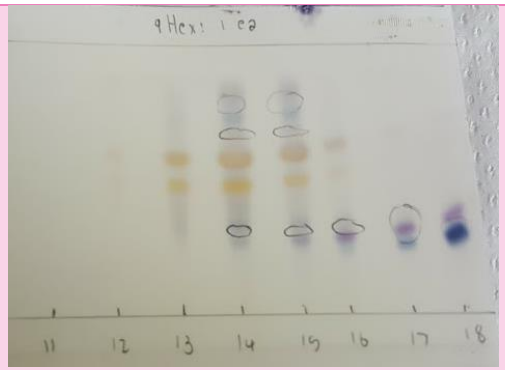

Solvent	Fractions	Thin layer chromatography silica plates		
		Short wave UV light	**Long wave UV light**	**Vanillin treatment**
Hexane 9: ethyl acetate 1	19-27	No visible bands	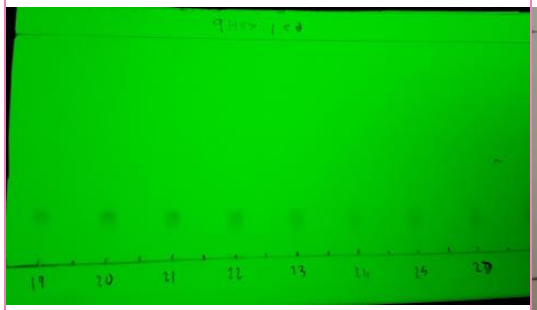	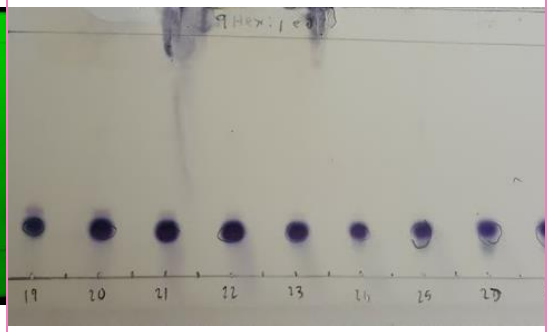
Hexane 9: ethyl acetate 1	28-34	No visible bands	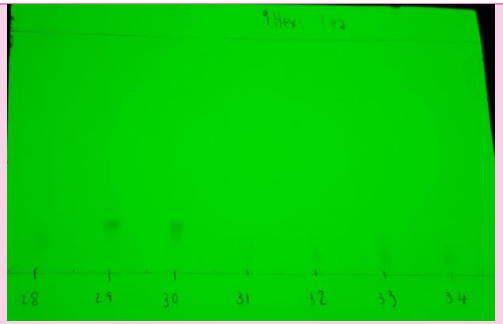	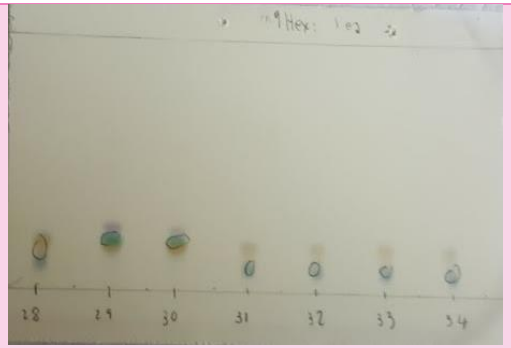

Solvent	Fractions	Thin layer chromatography silica plates		
		Short wave UV light	**Long wave UV light**	**Vanillin treatment**
Hexane 7: ethyl acetate 3	35-44	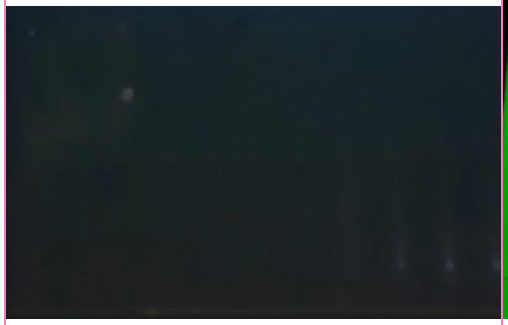	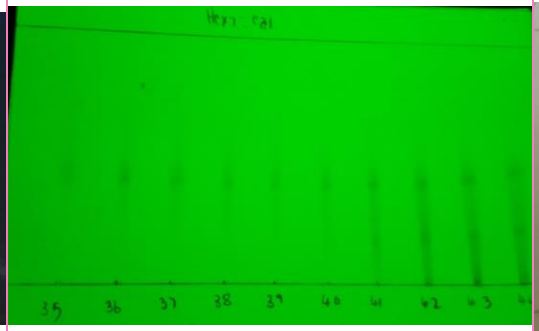	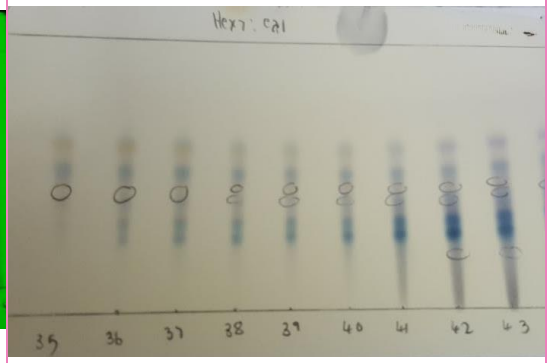
Hexane 7: ethyl acetate 3	45-52	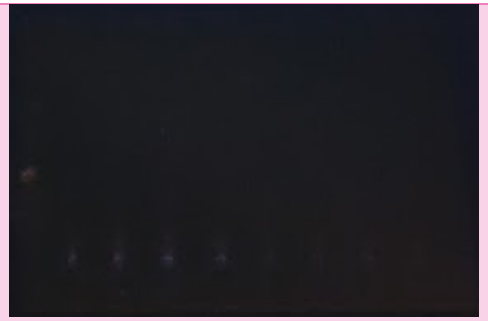	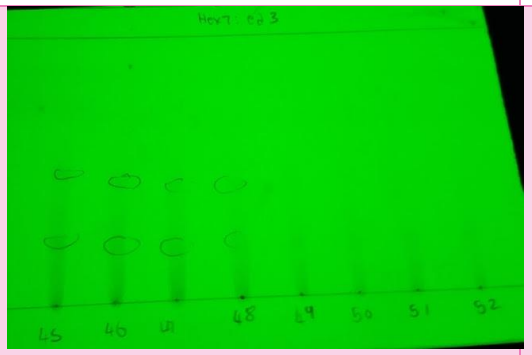	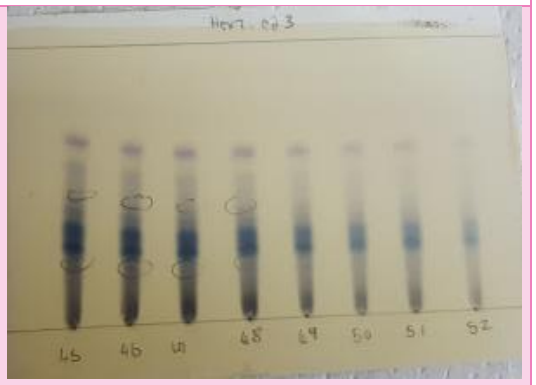

Solvent	Fractions	Thin layer chromatography silica plates		
		Short wave UV light	**Long wave UV light**	**Vanillin treatment**
Hexane 7: ethyl acetate 3	53-60	No visible bands	No visible bands	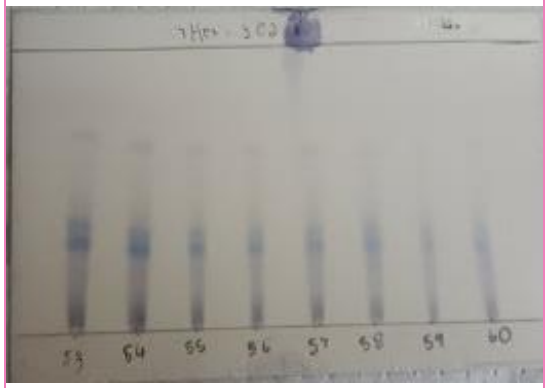
Hexane 7: ethyl acetate 3	61-70	No visible bands	No visible bands	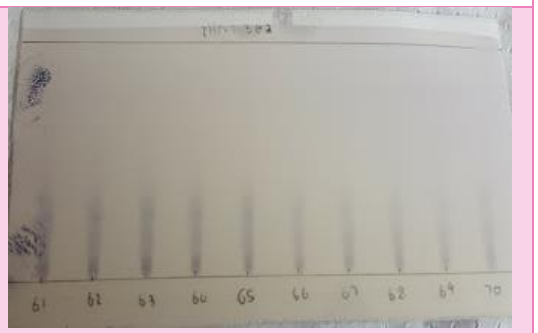

Solvent	Fractions	Thin layer chromatography silica plates		
		Short wave UV light	**Long wave UV light**	**Vanillin treatment**
Hexane 5: ethyl acetate 5	71-80		No visible bands	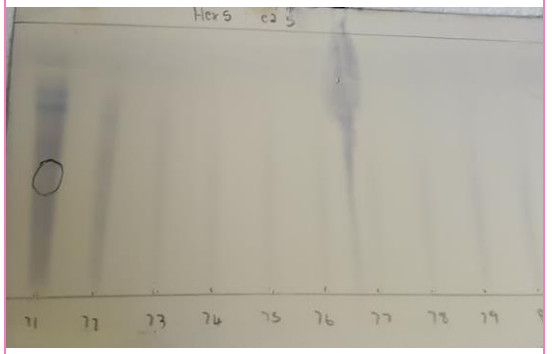
Hexane 5: ethyl acetate 5	81-89	No visible bands	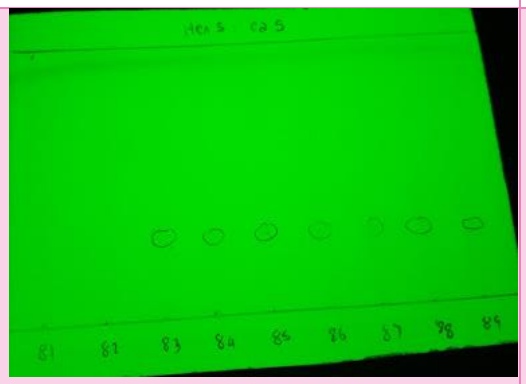	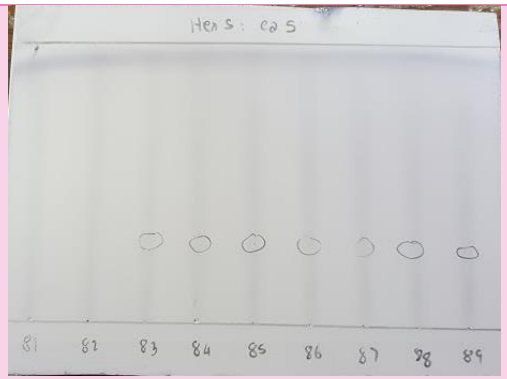

Solvent	Fractions	Thin layer chromatography silica plates		
		Short wave UV light	**Long wave UV light**	**Vanillin treatment**
Hexane 5: ethyl acetate 5	90-99	No visible bands	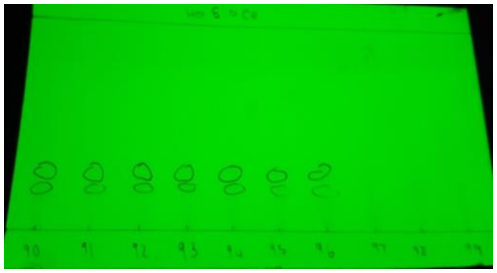	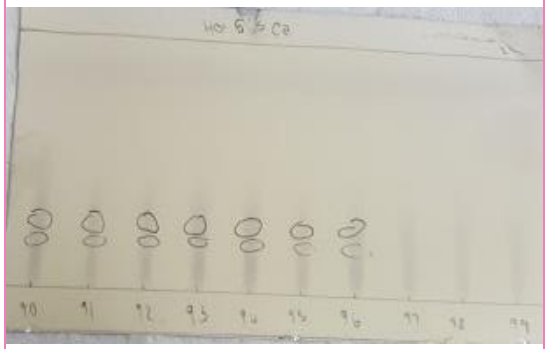
Hexane 3: ethyl acetate 7	100-110	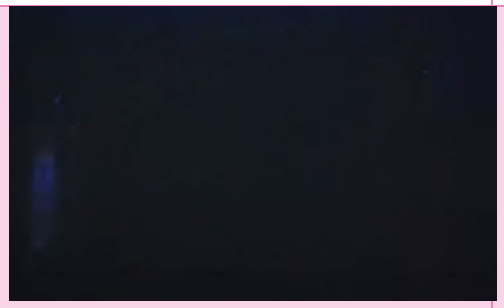	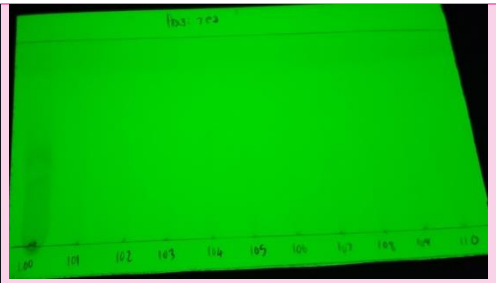	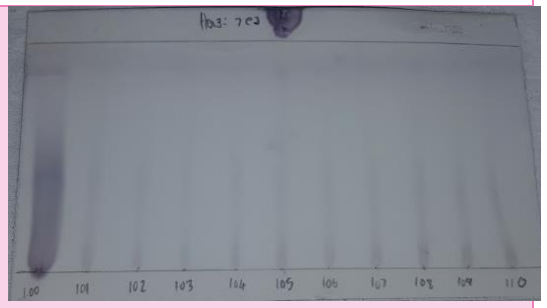

Solvent	Fractions	Thin layer chromatography silica plates		
		Short wave UV light	**Long wave UV light**	**Vanillin treatment**
Hexane 3: ethyl acetate 7	111-120	No visible bands	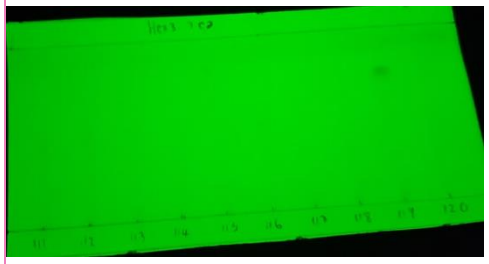	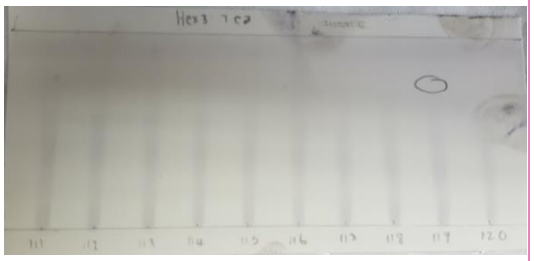
Hexane 1: ethyl acetate 9	121-131	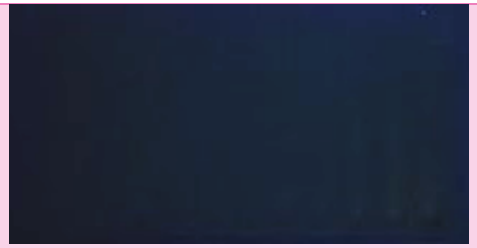	No visible bands	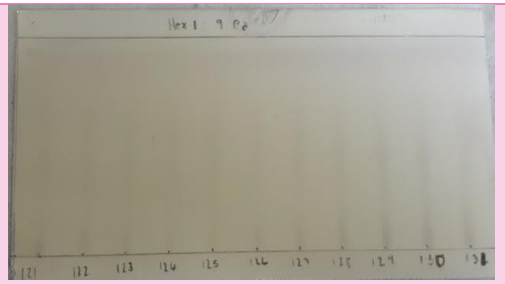

Solvent	Fractions	Thin layer chromatography silica plates		
		Short wave UV light	**Long wave UV light**	**Vanillin treatment**
Hexane 1: ethyl acetate 9	132-139	No visible bands	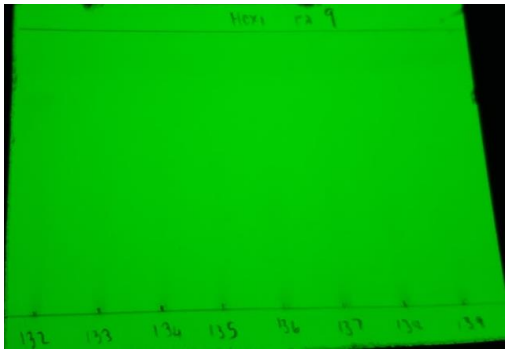	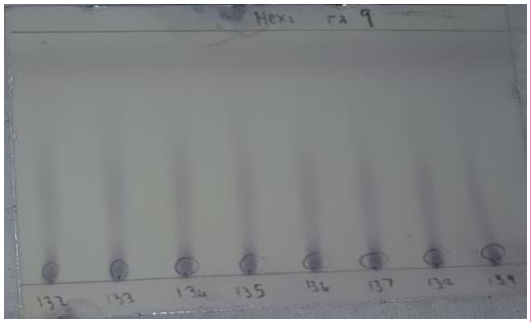
100% ethyl acetate	140-147	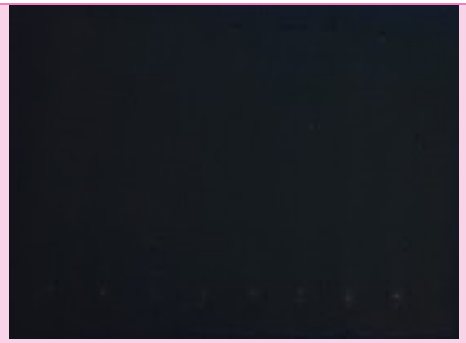		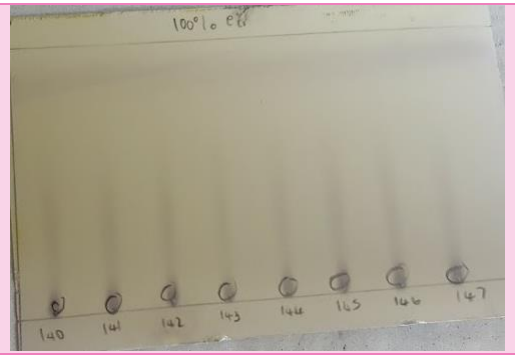

Solvent	Fractions	Thin layer chromatography silica plates		
		Short wave UV light	**Long wave UV light**	**Vanillin treatment**
Ethyl acetate 9: methanol 1	148-158		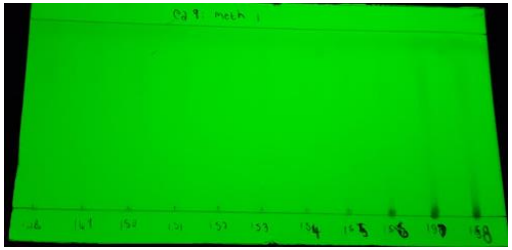	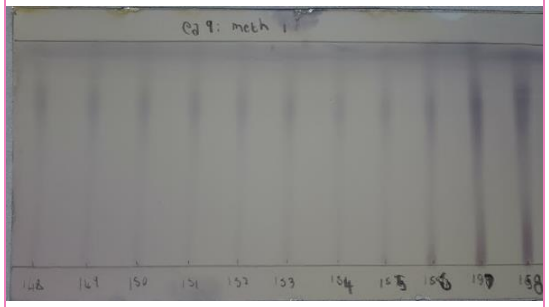
Ethyl acetate 9: methanol 1	159-160	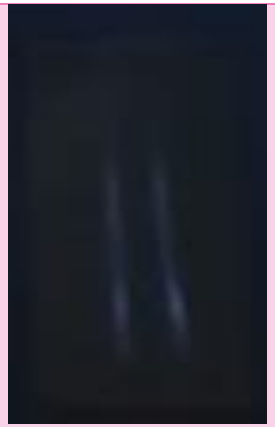	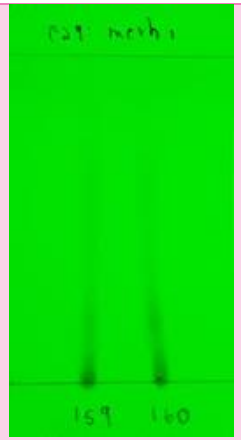	

Solvent	Fractions	Thin layer chromatography silica plates		
		Short wave UV light	**Long wave UV light**	**Vanillin treatment**
Ethyl acetate 9: methanol 1	161-168		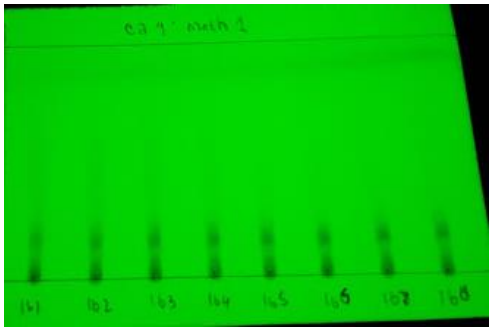	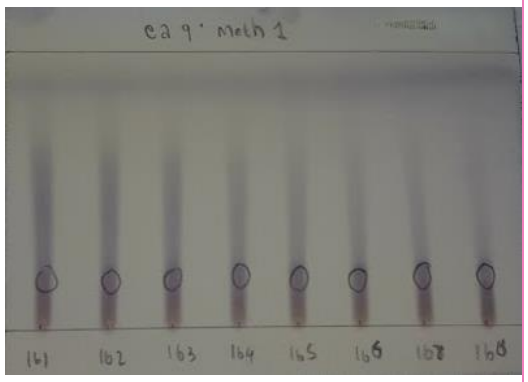
Ethyl acetate 9: methanol 1	169-172		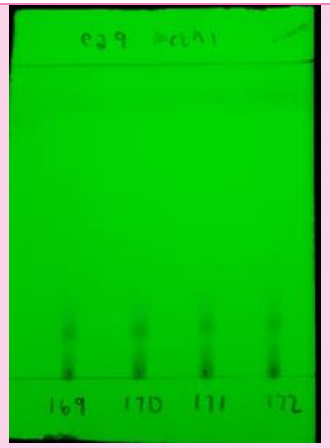	

Solvent	Fractions	Thin layer chromatography silica plates		
		Short wave UV light	**Long wave UV light**	**Vanillin treatment**
Ethyl acetate 7: methanol 3	173-182	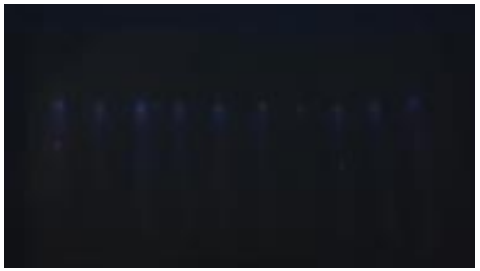	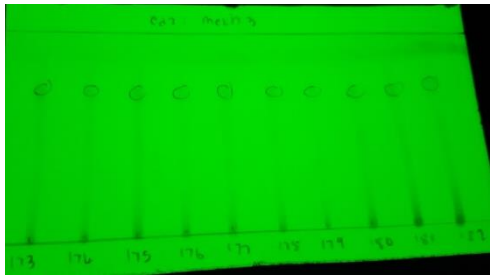	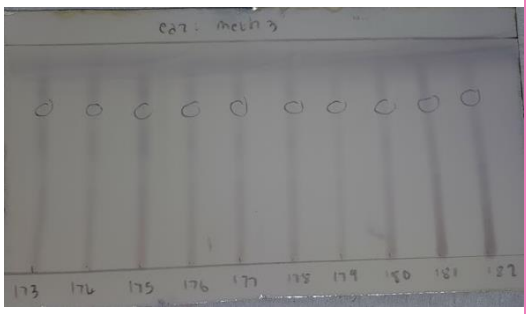
Ethyl acetate 7: methanol 3	183-192		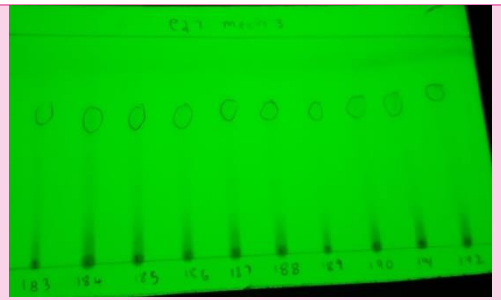	

Solvent	Fractions	Thin layer chromatography silica plates		
		Short wave UV light	**Long wave UV light**	**Vanillin treatment**
Ethyl acetate 7: methanol 3	193-200		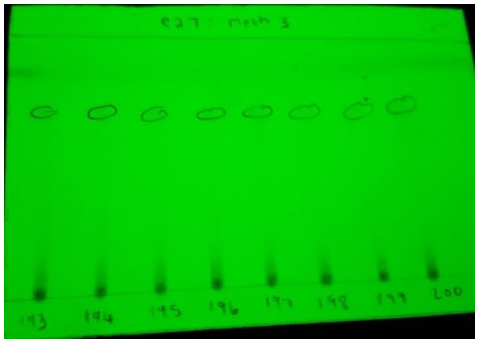	
Ethyl acetate 7: methanol 3	201-205	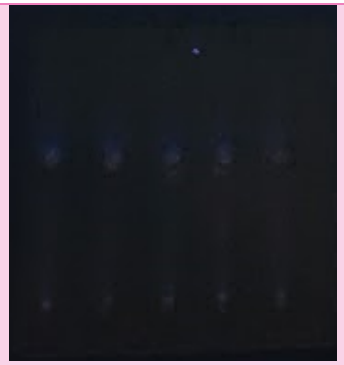	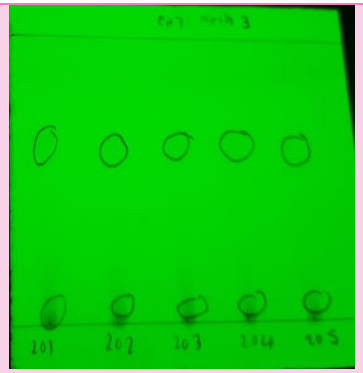	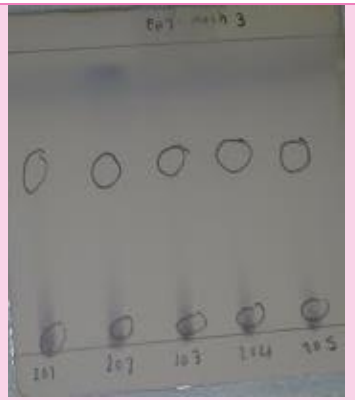

Solvent	Fractions	Thin layer chromatography silica plates		
		Short wave UV light	**Long wave UV light**	**Vanillin treatment**
Ethyl acetate 5: methanol 5	206-215		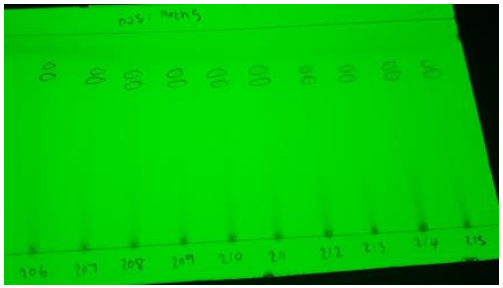	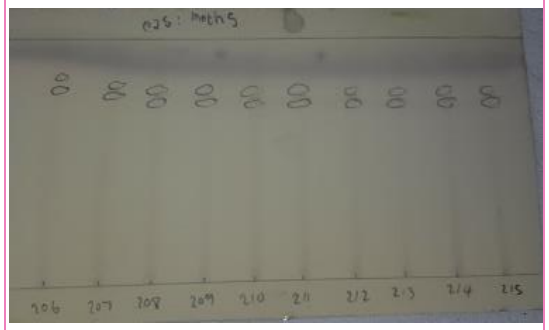
Ethyl acetate 5: methanol 5	216-224		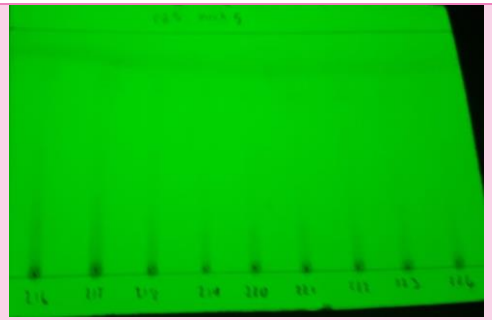	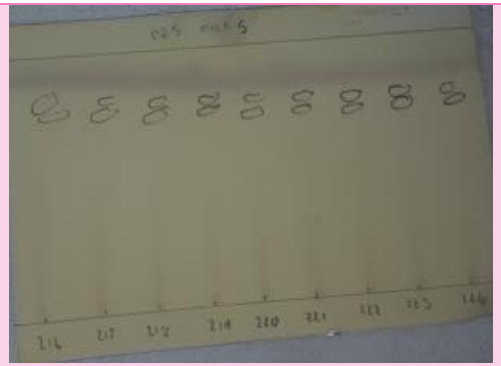

Solvent	Fractions	Thin layer chromatography silica plates		
		Short wave UV light	**Long wave UV light**	**Vanillin treatment**
Ethyl acetate 5: methanol 5	225-234	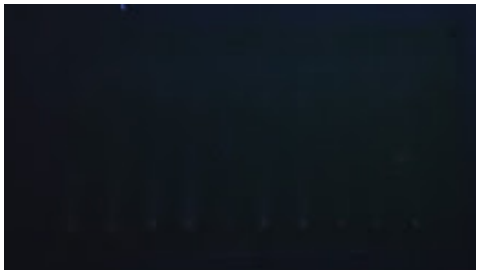	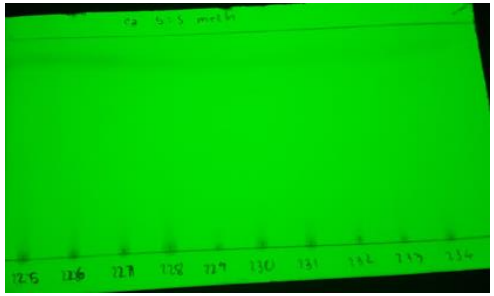	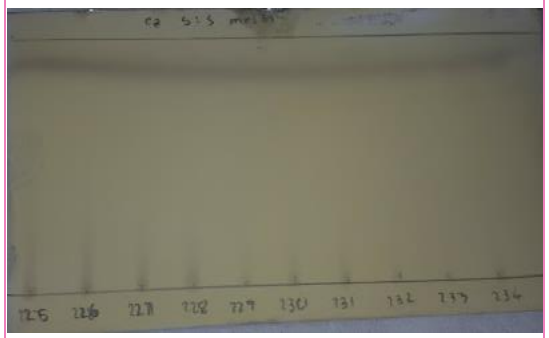
Ethyl acetate 3: methanol 7	235-244	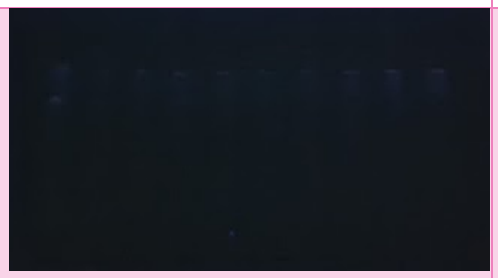	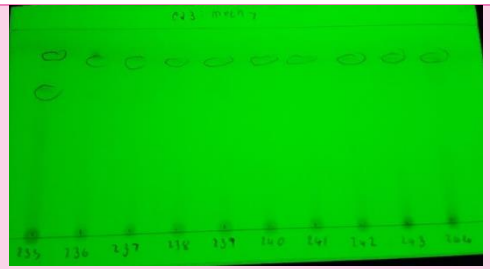	No visible bands

Solvent	Fractions	Thin layer chromatography silica plates		
		Short wave UV light	**Long wave UV light**	**Vanillin treatment**
Ethyl acetate 3: methanol 7	245-250		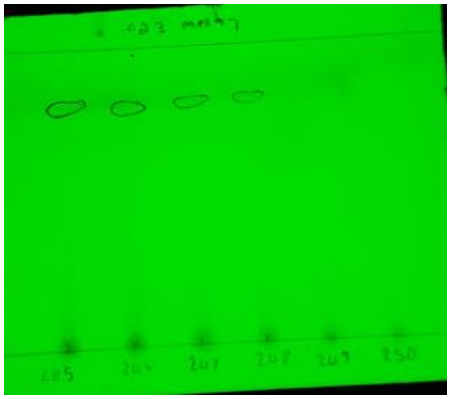	No visible bands
Ethyl acetate 1: methanol 9	251-260		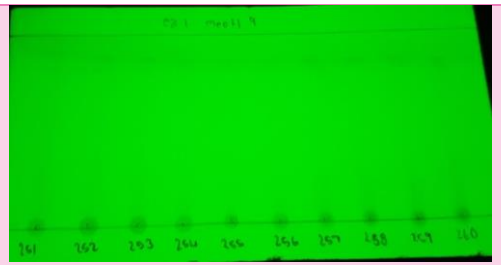	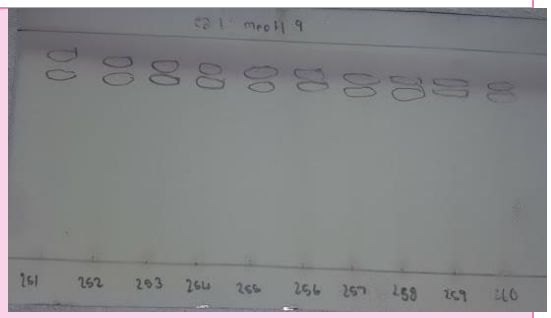

Solvent	Fractions	Thin layer chromatography silica plates		
		Short wave UV light	**Long wave UV light**	**Vanillin treatment**
Ethyl acetate 1: methanol 9	261-268	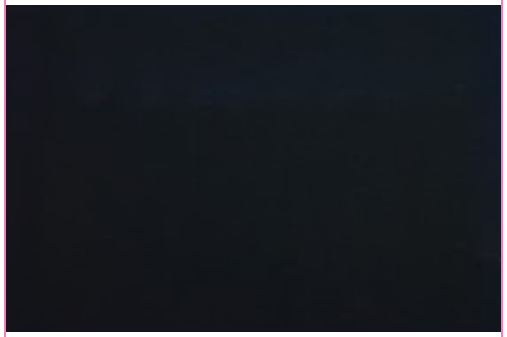	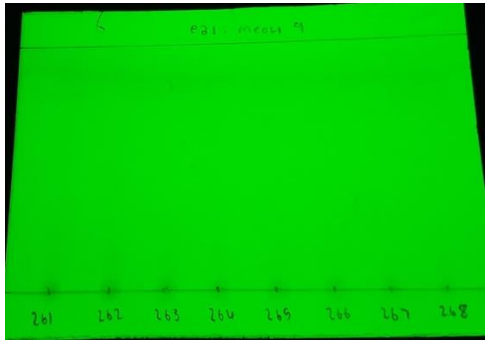	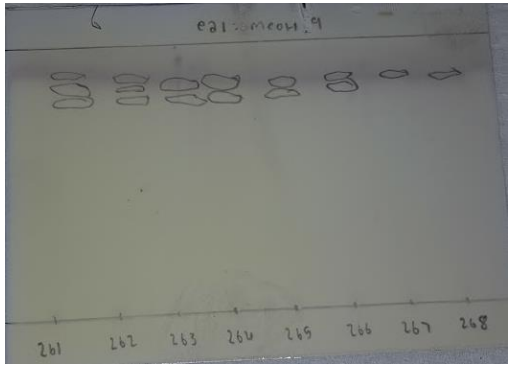

The pooled fractions were combined and renamed as follows:

- Fraction A (fractions 1 to 12)
- Fraction B (fractions 13 to 16)
- Fraction C (fractions 17 to 18)
- Fraction D (fractions 19 to 28)
- Fraction E (fractions 29 to 30)
- Fraction F (fractions 31 to 34)
- Fraction G (fractions 35 to 37)
- Fraction H (fractions 38 to 41)
- Fraction I (fractions 42 to 44)
- Fraction J (fraction 45 to 48)
- Fraction K (fraction 49 to 60)
- Fraction L (fraction 61 to 70)
- Fraction M (fraction 71)
- Fraction N (fraction 72 to 82)
- Fraction O (fraction 83 to 89)
- Fraction P (90 to 96)
- Fraction Q (97 to 99)
- Fraction R (fraction 100)
- Fraction S (fraction 101 to 118)
- Fraction T (fraction 119)
- Fraction U (fraction 120 to 131)
- Fraction V (fraction 132 to 147)
- Fraction W (fraction 148 to 155)
- Fraction X (fraction 156 to 158)
- Fraction Y (fraction 159 to 172)
- Fraction Z (fraction 173 to 182)

- Fraction AA (fraction 183 to 200)
- Fraction BB (fraction 201 to 205)
- Fraction CC (fraction 206 to 224)
- Fraction DD (fraction 225 to 234)
- Fraction EE (fraction 235)
- Fraction FF (fraction 236 to 248)
- Fraction GG (fraction 249 to 250)
- Fraction HH (fraction 251 to 266)
- Fraction II (fraction 267 to 268)

Table 3.4: The TLC results for the combined/major fractions

Fractions	Thin layer chromatography		
	Short UV wavelength	Long UV wavelength	Vanillin
Fraction A to K		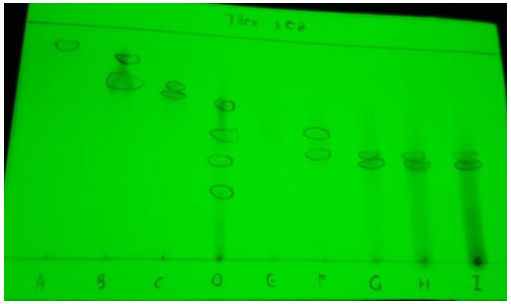	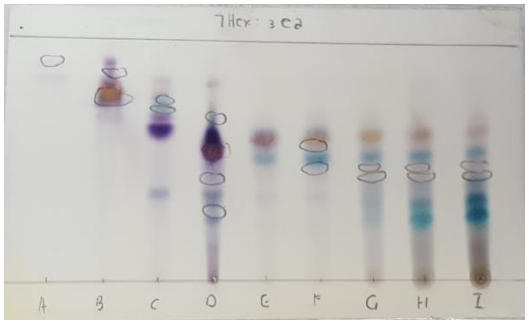
Fraction J to R		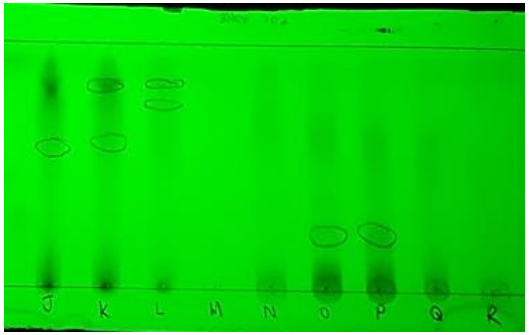	

Fractions	Thin layer chromatography		
	Short UV wavelength	Long UV wavelength	Short UV wavelength
Fraction S to AA	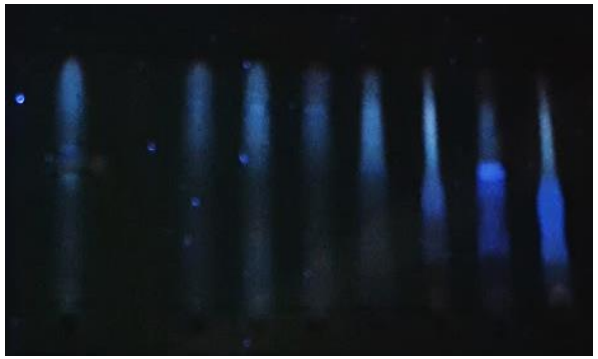	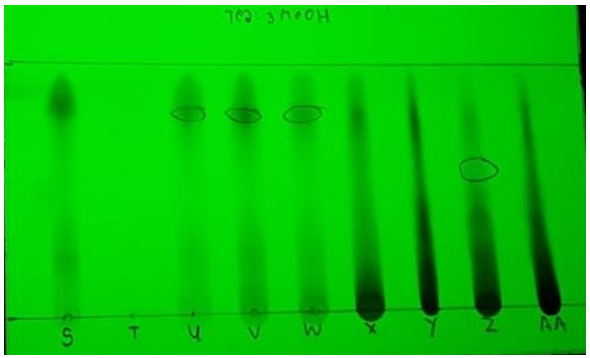	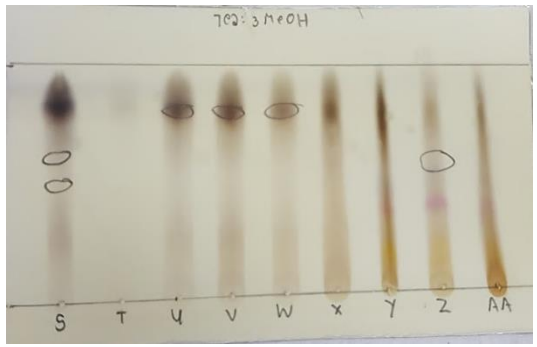
Fraction BB to II		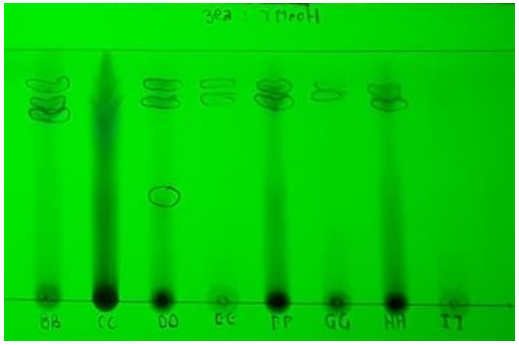	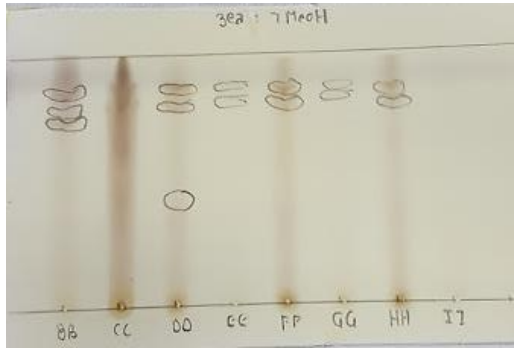

3.5.2 GC-MS

The data obtained from the GC-MS was analysed using the Shimadzu GC-MS post run analysis program. Each fraction's spectrum was analysed to identify compounds present. A total of 216 compounds were identified (Appendix E). The compounds were researched for previous literature reports of biological activity of interest (allelopathy Chapter 2 and antimicrobial Chapter 4) as well as their previous reported presence in the *Euphorbia* genus (Table 3.5).

Table 3.5: Compounds previously found in *Euphorbia* species, other species (plants and microorganisms) and identified in the *E. gummifera* methanol extract by GC-MS analysis

Compounds	Present in fraction(s) and hit % of each	Species previously reported in	Reference
Hopenone b (A'-Neogammacer-22(29)-en-3-one) 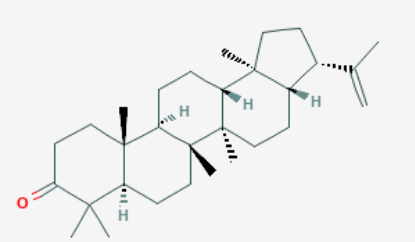	B (80%)	*E. cyparissias*	Oksüz et al., 1994
Olean-12-en-3-one 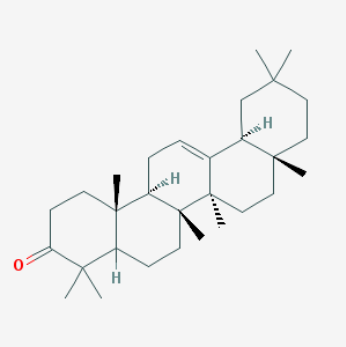	A (91%) B (93%) K (76%)	*E. bivonae*	Stefano et al., 2011
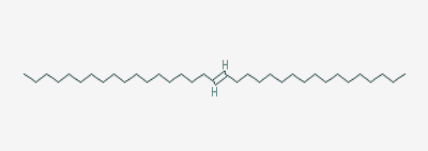 **17-Pentatriacontene**	A (96%) C (97%) D (91%)	*E. grandialata, E. macroclada*	Ertas et al., 2015; Ismail et al., 2017

Compounds	Present in fraction(s) and hit % of each	Species previously reported in	Reference
Hexatriacontane	A (95%)	*E. gaillardotii, E. macroclada, E. regis-jubae*	Ertas et al., 2015; Hmimid et al., 2012
Tetracontane	A (96%)	*E. gaillardotii, E. macroclada*	Ertas et al., 2015
Nonacosane	A (97%)	*E. grandialata, E. hirta, E. dendroides, E. characias, E. rigida, E. apios, E. helioscopia, E. antiquirum*	Fokialakis et al., 2003; Gewali et al., 1990; Gnecco, 1996; Ismail et al., 2017
Tetracosane	A (96%)	*E. dendroides, E. rigida, E. heliscopia, E. acanthothamnas*	Fokialakis et al., 2003
Eicosane	A (96%) EE (89%) II (90%)	*E. helioscopia*	Fokialakis et al., 2003
Heneicosane	A (98%)	*E. grandialata, E. demdroides, E. characias, E. rigida, E. apois, E. heliscopia, E. acanthamnos*	Fokialakas et al., 2003; Ismail et al., 2017

Compounds	Present in fraction(s) and hit % of each	Species previously reported in	Reference
Eicosanoic acid, methyl ester 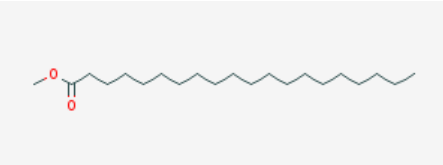	B (80%)	*E. helioscopia E. acanthothamnos, E. lathyris*	Fokialakas et al., 2003; Sosa et al., 2016
Octadecanal 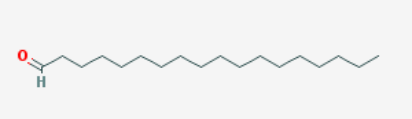	B (87%) C (85%)	*E. dendroides, E. rigida, E. apios, E. helioscopia*	Fokialakas et al., 2003
Tetracosanoic acid methyl ester (Methyl lignocerate) 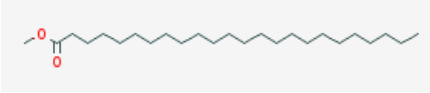	B (93%) C (85%)	*E. helioscopia*	Fokialakas et al., 2003
Methyl stearate 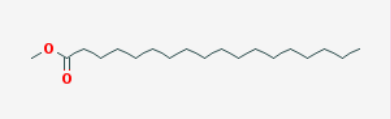	B (92%) BB (82%) DD (90%) EE (93%) FF (90%) GG (95%) HH (94%) II (96%)	*E. grandialata*	Ismail et al., 2017
Docosane	L (91%) N (91%) Q (90%) R (90%) T (92%) U (89%) V (93%) W (89%) BB (86%) FF (90%) GG (89%)	*E.grandialata, E. dendroides E. characias, E. apios, E. helioscopia ,E. acanthothamnos*	Fokialakas et al., 2003; Ismail et al., 2017

Compounds	Present in fraction(s) and hit % of each	Species previously reported in	Reference
Methyl behenate (Docosanoic acid, methyl ester) 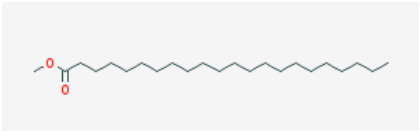	N (80%) U (80%)	*E. heliscopia*	Fokialakas et al., 2003
Heptacosane	V (88%)	*E. dendroides E. characias E. rigida E. apios E. helioscopia E. acanthothamnos, E. hirta*	Fokialakas et al., 2003, Gnecco, 1996
Pentadecane 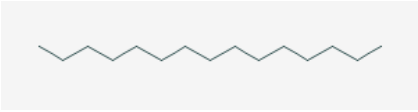	W (93%)	*E. helioscopia*	Fokialakas et al., 2003
Tricosane	X (90%)	*E. dendroides, E. characias, E. rigida, E. apios, E. helioscopia, E. acanthothamnos*	Fokialakas et al., 2003
Desulphosinigrin 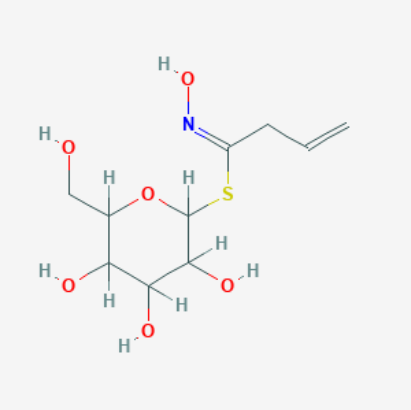	Z (76%)	*E. lathyris*	Sosa et al., 2016

Compounds	Present in fraction(s) and hit % of each	Species previously reported in	Reference
Lucenin 2 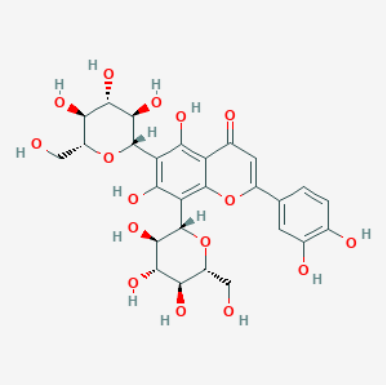	J (76%) O (80%) P (81%) Q (82% R (79%) S (81%) T (79%) U (80%) V (77%)	Mosses (*Bartramia pomiformis*, *Hedwigia ciliate*, *Polytrichum affine*, *P. cuspidatum*, *Dicranum scoparium*)	Basile et al., 1999
Octatriacontyl pentafluoropropionate 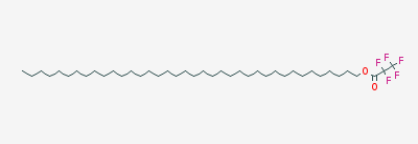	A (95%)	*Symplocos crataegoides* Buch, *Mangifera indica*, *Pisonia grandis*	Govindarajan et al., 2016; Oluwayiose et al., 2015; Pradheesh et al., 2017
Heptacosanol 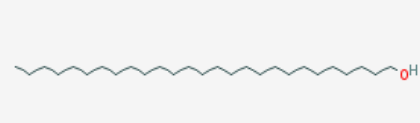	A (97%) C (97%) D (96%) F (89%)	*Strobilanthes crispus*	Koay et al. 2013

Compounds	Present in fraction(s) and hit % of each	Species previously reported in	Reference
Lupeol 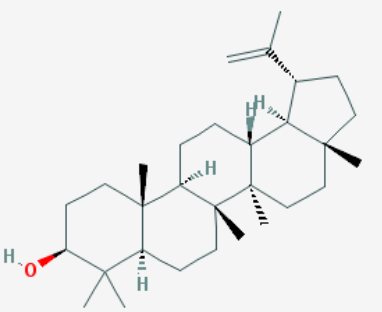	B (80%) C (89%) E (90%) G (90%) H (90%) I (89%) J (87%) K (87%) L (87%) M (74%) N (81%) O (83%) P (85%) Q (86%) R (83%) V (73%) W (77%)	*E. larica*, *E. hirta*, *E. chamaesyce*, *E. tirucalli*, *E. lagascae*, *E. bivonae*, *E. damarana*	Duarte, 2008; Gupta et al., 2013; Jassbi, 2006; Joubert, 2008; Ragasa and Cornelio, 2013; Stefano et al., 2011; Tanaka et al., 1999; Wal et al., 2015
Quinic acid 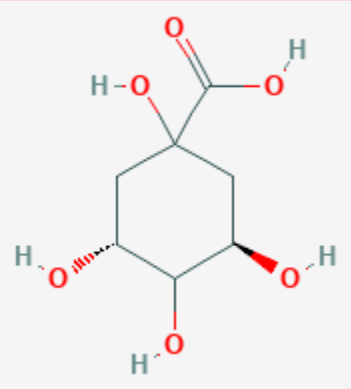	CC (83%) DD (83%) FF (80%)	*E. macroclada*, *E. gaillardotii*, *E. hirta*	Ertas et al., 2015; Gopi et al., 2015

Compounds	Present in fraction(s) and hit % of each	Species previously reported in	Reference
α- Amyrin 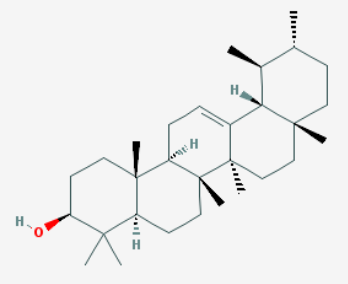	H (92%)	*E. hirta, Stevia rebaudiana* Bert., *E. grandialata, E. characias*	Ahmad et al., 2002a,b; Fernandes-Freire et al., 1990; Ismail et al., 2017; Jassbi, 2006; Kumar et al., 2010; Martínez-Vázquez et al., 1999; Ragasa and Cornelio, 2013; Stefano et al., 2011; Vázquez et al., 2012; Verma and Batra, 2013;
β- Amyrin 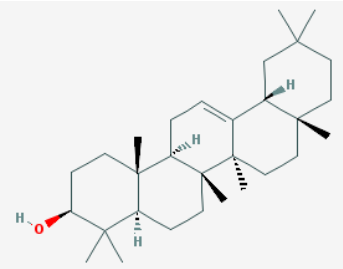	C (92%) E (93%) F (94%) G (93%)	*E. decipiens, E. larica, E. falcata* L., *E. hirta*	
Betulin 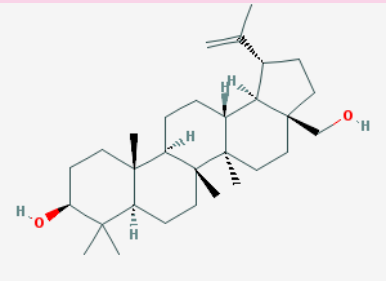	D (83%) E (79%) G (77%) H (89%) I (84%) J (84%) L (80%) X (85%)	*E. teheranica, E. heteradena, E. rigida, E. latifolia, Euphorbia myrsinites*	Ahmad et al., 2002b; Gherraf et al., 2010; Jassbi, 2006; Jassbi, 2000; Öksüz et al., 1995

Compounds	Present in fraction(s) and hit % of each	Species previously reported in	Reference
Roridin E 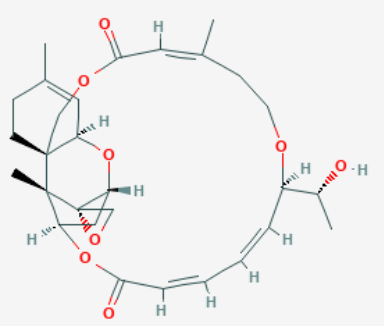	R (76%) CC (78%)	*Myrothecium* spp. including *M. verrucaria*, *M. roridum*	Jarvis and Wang, 1999; Wagenaar and Clardy, 2001; Xu et al., 2006
Lanosterol 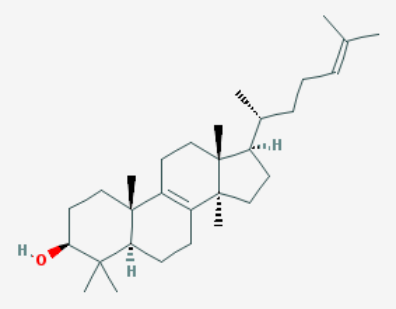	C (90%) D (90%) F (90%)	*E. peplus*, *E. lathyris*, *E. pekinensis*, *E. characias*, *E. tirucalli*	Fernandes-Freire et al., 1990; Giner et al., 2000; Giner et al., 1995; Gupta et al., 2013; Kong and Min, 1996; Zhang et al., 2006
Lupeol acetate 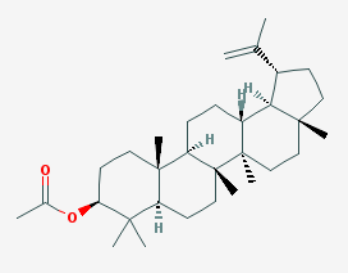	B (94%) D (94%) E (89%) I (88%) J (85%)	*E. larica*; *E. geniculata* Ortega; *E. quinquecostata*	Eliza et al., 2016; Jassbi, 2006; Mbwambo et al., 1996

Several of the identified compounds have not been recorded in literature asbeing identified in *Euphorbia* spp. and this is the first record of them is this genus. Some of the identified compounds have been found in other plants where as other in insects and microorganisms. Octatriacontyl pentafluoropropionate (Govindarajan et al., 2016; Khoushika and Chitra, 2016; Oluwayiose et al., 2015; Pradheesh et al 2017), heptacosanol (Koay et al., 2013) and lucenin 2 (Basile et al., 1999) have been identified in plants other than *Euphorbia* spp. Roridin E has been identified in fungi (Jarvis and Wang, 1999; Wagenaar and Clardy, 2001; Xu et al., 2006).

3.6 Discussion

Following an overall inspection of the chromatography results encompassing the *E. gummifera* extract, it was evident that this ill studied plant housed a wealth of different compounds.

Using methanol as an extracting solvent enabled good extraction of metabolites (Sarker et al., 2006). The three solvents used were of non-polar (hexane), medium polarity (ethyl acetate) and polar (methanol) nature (Tsuda, 2004) as a means to separate the wealth of compounds effectively as this plant has not yet been studied in terms of its chemistry. Hexane has been reported to be responsible for eluting hydrophobic, lipophilic compounds such as hydrocarbons, fatty acids, pigments, terpenoids, alkaloids, and coumarins, while ethyl acetate eluted alkaloids and flavonoids and methanol eluted all other compounds left such as amino acids and carbohydrates (Sarker et al., 2006; Tsuda, 2004).

Different detection methods are often employed to provide information on the types of compounds eluted. UV light and vanillin were employed. There are specific compounds that are able to absorb UV light and as a result are visible as dark spots on a light background while other molecules emit a distinctive blue light (Sarker et al., 2006). Such molecules were visibly on several of the TLC silica plates during the column chromatography experiment. These include compounds with aromatic, alipathic and alicyclic functional groups and conjugated double bonds (Sharma, 2000). Quinoline, isoquinoline and indole type compounds have the ability to fluoresce in solution (Khopkar, 1998). Several compounds with such functional groups were identified

through GC-MS (Appendix E). It is, however, important to note that many compounds (non-polar compounds) are not visible under UV light. This became evident during the bioautography experiment of Chapter 4. Another important obstacle encountered is the smearing of bands on TLC plates which is due to the acidity of compounds while basic compounds may have trouble reacting positively to TLC (Sarker et al., 2006).

Vanillin is known as a universal detector (Sarker et al., 2006). This method is known to show amine, hydroxyl and carbonyl functional groups effectively (Pirrung, 2016). Terpenes are known to produce red and blue colour in bands while compounds lacking functional groups don not react (Sarker et al., 2006). A few of the TLC plates did have such coloured bands. As with most experiment, improvements can always be made. A methanolic extract and fractions are best suited for high performance liquid chromatography (HPLC) (Sarker et al., 2006).

The GC-MS analysis yielded 216 compounds spread out over 35 major fractions. Some of these compounds are known to possess antimicrobial properties that will be discussed in detail in Chapter 4. Many of these compounds have been previously identified in *Euphorbia* species (Table 3.5) which support their identification in *E. gummifera*. Several other compounds, however, are more common to alternative sources. Pentatriacontane and tertacontane have been found in *E. paralais* (Rizk et al., 1974), *E. Gaillardotii* and *E. macroclada* (Ertas et al., 2015) respectively. Nelson et al. (2003) isolated the pentatriacontane from the cuticle of adult beetles belonging to *Aphthona lacertosa* and *A. nigriscutis,* after feeding on an *E. esula* plant. These beetles act as a biocontrol against the *E.esula* plant. Crude oil is known to be a source of hydrocarbons such as tetracontane and tetracosane (Owunari, 2010), which were also found some of the fractions.

Octatriacontyl pentafluoropropionate has also not been identified in any *Euphorbia* species but was found in fraction A. Sources of this compound include *Symplocos crataegoides* Buch (Govindarajan et al., 2016), *Pisonia grandis* (Pradheesh et al 2017), *Mangifera indica* (Khoushika and Chitra, 2016) and crude oil (Oluwayiose et al., 2015).

This is also the first instance of identifying heptacosanol in an *Euphorbia* species. The compound was found in fractions A, C, D and F. Koay et al. (2013) identified heptacosanol in *Strobilanthes crispus.* This compounds is also part of the mixture of C23 to C38 aliphatic

alcohols that form part of the anticholesterolelmic drug policosanol (Granja et al., 1997; Martínez et al., 1999).

Nonacosane is a prominent compound in many *Euphorbia* species. This compound is speculated to be toxic due to its accumulation along with other long chain alkanes in the viscera of a male patient that died suddenly (Salvayre et al., 1988).

Lucenin 2 is a flavonoid that is found in mosses (Basile et al., 1999) that was demonstrated to have allelopathic activity against *Tortula muralis* HEDW and *Raphanus sativus* L. by Basile et al. (2003). Allelopathic activity manifested as significant inhibition of germination and seedling development. This could be applicable to Chapter 2.

The compounds identified and investigated for previously reported biological activity are a mere fraction of the 216 compounds identified. Due to the time constraints only the compounds showing biological activity of interest for the aim of this study are showed in this chapter and the following Chapter 4. There are, however, a wealth of compounds that still need to be investigated.

3.7 Conclusion

A wealth of different types of compounds was identified *E. gummifera* methanol extract. Some can be linked to closely-related species whereas others cannot. Several compounds have antibacterial activity (Chapter 3), allelopathic activity (lucenin 2) and toxicity. Future work could involve HPLC, which as mentioned previously is the best analytical technique for methanolic extracts and fractions as well as isolating toxic compounds such as phorbol esters (Goel et al., 2007).

3.8 References

a) A). Ahmad, V.U., Hussain, H., Hussain, J., Jassbi, A.R., Bukhari, I.A.,Yasin, A., Choudhary, M.I., Dar, A., 2002. New bioactive diterpenoids from *Euphorbia decipiens.* Zeitschrift für Naturforschung 57, 1066–1071.

b) B.) Ahmad, V.U., Zahid, M., Khan, T., Asim, M., Ahmad, A. 2002. Chemical constituents of *Euphorbia heteradenia* Boiss. Proceedings of the Pakistan Academy of Sciences. 39, 201–205.

Akihisa, T., Kithsiri Wijeratne, E.M., Tokuda, H., Enjo, F., Toriumi, M., Kimura, Y., Koike, K., Nikaido, T., Tezuka, Y., Nishino, H. 2002. Eupha-7,9 (11),24-trien-3ß-ol ("Antiquol C") and other triterpenes from *Euphorbia antiquorum* latex and their inhibitory effects on epstein-barr virus activation. Journal of Natural Products 65(2), 158-162.

Al-Mughrabi, K.I. 2003. Antimicrobial activity of extracts from leaves, stems and flowers of *Euphorbia macroclada* against plant pathogenic fungi. Phytopathologia Mediterranea 42(3), 245-250.

Basile, A., Sorbo, S., López-Sáez, J.A., Cobianchi, R.C. 2003. Effects of seven pure flavonoids from mosses on germination and growth of *Tortula muralis* HEDW. (Bryophyta) and *Raphanus sativus* L. (Magnoliophyta). Phytochemistry 62, 1145-1151.

Basile, A., Giordano, S., López-Sáez, J.A., Cobianchi, R.C. 1999. Antibacterial activity of pure favonoids isolated from mosses. Phytochemistry 52, 1479-1482.

Bruyns, P.V., Mapaya, R.V., Hedderson, T. 2006. A new subgeneric classification for *Euphorbia* (Euphorbiaceae) in southern Africa based on ITS and *psb*A-*trn*H sequence data. TAXON 55(2), 397-420.

Curtis B. and Mannheimer C. 2005. Tree Atlas of Namibia. National Botanical Research Institute, Windhoek.

Duarte, N. 2008. Structural characterization and biological activities of terpenic and phenolic compounds isolated from *Euphorbia lagascae* and *Euphorbia tuckeyana*. PhD Thesis Universidade de Lisboa Faculdade de Farmácia.

Eliza, E., Fatsiami, R., Yusuf, S., Ferlinahayati, F. 2016. Isolation of Triterpenoid from Katemas (*Euphorbia geniculata* Ortega) Stem Extracted using Methanol and Its Toxicity Test. Indonesian Journal of Fundamental and Applied Chemistry 1(1), 19-23.

Ertas, A., Yilmaz, M.A., Firat, M. 2015. Chemical profile by LC–MS/MS, GC/MS and antioxidant activities of the essential oils and crude extracts of two *Euphorbia* species, Supplementary material. Natural Product Research 29(6), 529–534.

Fattorusso, E., Lanzotti, V., Taglialatela-Scafati, O., Tron, G.C., Appendino, G. 2002. Bisnorsesquiterpenoids from *Euphorbia resinifera* Berg. and an expeditious procedure to obtain resiniferatoxin from its fresh latex. European Journal of Organic Chemistry 1, 71-78.

Fernandes-Freire, M., Novais, J.M., Pais, M.S.S. 1990. Free triterpenols and sterols produced by *in vitro* cultures and laticifer cells from *Euphorbia characias*. Phytochemistry 29(6), 1855-1860.

Fokialakis, N, Melliou, E., Magiatis, P., Harvala, C., Mitaku, S. 2003 Composition of the Steam Volatiles of Six *Euphorbia* spp.from Greece. Fragrance and Flavour Journal 18, 39-42.

Gewali, M.B., Hattori, M., Tezuka, Y., Kikuchi, T., Namba, T. 1990. Constituents of the latex of *Euphorbia antiquorum*. Phytochemistry 29(5), 1625–1628.

Gherraf, N., Zellagui, A., Mohamed, N. S. Hussien, T. A., Mohamed, T. A., Hegazy, M. F., Rhouati, S., Moustafa, M. F. M., El-Sayed, M. A., Mohamed, A. H. 2010. Triterpenes from *Euphorbia rigida.* Pharmacognosy Research 2(3), 159-162.

Giner, J. and Djerassi, C. 1995. A reinvestigation of the biosynthesis of lanosterol in *Euphorbia lathyris*. Phytochemistry 39(2), 333-335.

Giner, J., Berkowitz, J.D., Andersson, T. 2000. Nonpolar components of the latex of *Euphorbia peplus.* Journal of Natural Products 63, 267-269.

Gnecco, S. 1996. Distribution pattern of n-alkanes in Chilean species from the Euphorbiaceae family. Boletin de la Sociedad Chilena de Quimica, 41(3), 229-233.

Gopi, K., Renu, K., Vishwanath, B.S., Jayaraman, G. 2015. Protective effect of *Euphorbia hirta* and its components against snake venom induced lethality. Journal of Ethnopharmacology 165, 180-190.

Govindarajan, N., Cheekala, U.M.R, Arcot, S., Sundaramoorthy, S., Duraisamy, R., Raju, I. 2016. GC-MS Analysis of n-hexane extract of stem bark of *Symplocos crataegoides* Buch.-Ham. ex D. Don. Pharmacognosy Journal 8(6), 520-524.

Goel, G., Makkar, H.P.S., Francis, G., Becker, K. 2007. Phorbol esters: Structure, biological activity, and toxicity in animals. International Journal of Toxicology 26, 279-288.

Granja, A. L., Hernanadez, J.M., Quintana, D.C., Valmana, L.A., Ferreiro, R.M., Mesa, M.G.M. 1997. Mixture of higher primary aliphatic alcohols, its obtention from sugar cane wax and its pharmaceutical uses. Patent no. 5,663,156, United States of America.

Gupta, N., Vishnoi, G., Wal, A., Wal, P. 2013. Medicinal value of *Euphorbia tirucalli*. Systematic Reviews in Pharmacy 4(1), 40-47.

Hmimid, F., Lahlou, F.A., Loutfi, M., Bourhim, N. 2012. Phytochemical screening chemical composition and toxicity of *Euphorbia regis-jubae* (Webb & Berth). Journal of Toxicology and Environmental Health Sciences 4(8), 130-139.

Horvath, D., Wurdack, K., Pullin, K.L. 2011. Euphorbia, in: Chittaranjan, K (Eds.), Wild Crop Relatives: Genomic and Breeding Resources: Plantation and Ornamental Crops. Springer, Berlin.

Ismail, M., Owis, A.I., Hetta, M., Mohammed, R. 2017. Total phenolics and flavonoids content, antioxidant activity and GC/MS analyses of *Euphorbia grandialata*. Journal of Applied Pharmaceutical Science 7(6), 176-181.

Jarvis, B.B. and Wang, S. 1999. Stereochemistry of the Roridins. Diastereomers of Roridin E. Journal of Natural Products 62(9), 1284-1280.

Jassbi, A.R. 2006. Chemistry and biological activity of secondary metabolites in *Euphorbia* from Iran. Phytochemistry 67, 1977-1984.

Joubert, A. 2008. Investigation on selected biotic and abiotic factors in the maintenance of the "fairy circles" (barren patches) of southern Africa. MSc thesis, University of Pretoria, South Africa.

Khan, M.Q and Malik, A. 1990. A new macrolytic diterpene ester from the latex of *Euphorbia tirucalli*. Journal of Natural Products 53(3), 728-731.

Khan, A.Q., Rasheed, T., Kazmi, S.N., Ahmed, Z., Malik, A. 1988. Cycloeuphordenol, a new triterpene from *Euphorbia tirucalli*. Phytochemistry 27(7), 2279-2281.

Khan, A.Q., Syed, N.U.H., Ahmed, Z., Malik, A. 1989. Euphorcinol, a newpentacyclic triterpene from *Euphorbia tirucalli*. Planta Medica 55, 290–291.

Khoushika, R.R. and Chitra, P. 2016. Characterisation, Invitro and Insilico Antidiabetic activity in the leaf extract of *Mangifera indica*. World Journal of Pharmaceutical Research 5(9), 1063-1082.

Khullar, N. 2010. Antimicrobials from plants and their use in therapeutics and drug discovery. The IIOAb Journal 1(3), 31-37.

Kirbag, S., Erecevit, P., Zengin, F., Guvenc, A.N. 2013. Antimicrobial activity of some *Euphorbia* species. African Journal of Traditional, Complementary and Alternative Medicine 10(5), 305-309.

Koay, Y.C., Wong, K.C., Osman, H., Eldeen, I.M.S., Asmawi, M.Z. 2013. Chemical constituents and biological activities of *Strobilanthes crispus* L. Records of Natural Products 7(1), 59-64.

Kong, L.Y. and Min, Z.D. 1996. Studies on chemical constituents of roots of *Euphorbia pekinensis*. Acta Pharmaceutica Sinica 31(7), 524-529.

Kumar, S., Malhotra, R., Kumar, D. 2010. *Euphorbia hirta:* Its chemistry, traditional and medicinal uses, and pharmacological activities. Pharmacognosy Review 4(7), 58-61.

Leach, L.C. 1975. *Euphorbia gummifera*, *E. gregaria* and a new species from Damaraland. Bothalia 11, 495-503.

Mallavadhani, U.V., Satyanarayana, K.V.S., Mahapatra, A., Sudhakar, A.V.S., Narasimhan, K., Pandey, D.K., Thirunavokkarasu, M. 2006. Development of diagnostic microscopic and chemical markers of some *Euphorbia* latexes. Journal of Intergrative Plant Biology 48(9), 1115-1121.

Mallavadhani, U.V., Satyanarayana, K.V.S., Mahapatra, A., Sudhakar, A.V.S. 2004. A new tetracyclic triterpene from the latex of *Euphorbia nerifolia*. Natural Product Research 18(1), 33-37.

Martínez, L., Uribarri, E., Laguna, A. 1999. Characterization and compatibility studies between policosanol, a new hypocholesterolemic drug, and tablet excipients using differential Ssanning calorimetry (DSC). Archiv de Pharmazie 332(12), 439-441.

Martínez-Vázquez, M., Ramírez Apan, T.O., Lazcano, E.M., Bye, R. 1999. Anti-inflammatory active compounds from the *n*-Hexane extract of *Euphorbia hirta*. Revista de la Sociedad Química de México 43(4), 103-105.

Mbwambo, Z.H., Lee, S.K., Mshiu, E.N., Pezzuto, J.M., Kinghorn, A.D. 1996. Constituents from the stem wood of *Euphorbia quinquecostata* with phorbol dibutyrate receptor-binding inhibitory activity. Journal of Natural Products 59, 1051–1055

Mozaffarian, V. 1996. A Dictionary of Iranian Plant Names. Farhang Mo'aser, Tehran.

Nelson, D.R., Olsen, D.L., Fatland, C.L. 2003. Cuticular hydrocarbons of the flea beetles, *Aphthona lacertosa* and *Aphthona nigriscutis*, biocontrol agents for leafy spurge *(Euphorbia esula)*. Comparative Biochemistry and Physiology Part B 133, 337-350.

Oksüz, S., Gil, R.R., Chai, H., Pezutto, J.M., Cordell, G.A., Ulubelen, A. 1994. Biologically active compounds from the Euphorbiaceae; 2. Two triterpenoids of *Euphorbia cyparissias*. Planta Medica 60(6).

Öksüz, S., Gürek, F.; Gil, R. R.; Pengsuparp, T.; Pezzuto, J. M.; Cordell, G. A. 1995. Four diterpene esters from *Euphorbia myrsinites*. Phytochemistry 38, 1457-1462.

Oluwayiose, O.A., Akinsete, S.J., Ana, G.R.E.E, Omishakin, A.M. 2015. Soil contamination by refined crude oil using *Lumbricus terrestris* as toxicity indicator at a petroleum product depot, Ibadan, Nigeria. British Journal of Applied Science & Technology 9(1), 37-46.

Owunari, A.G. 2012. Crude Oil: Sweet and sour – efforts at mitigating the toxic effects. University of Port Harcourt, Inaugural Lecture Series no. 93.

Pintus, F., Medda, R., Rinaldi, A.C., Spanò, D., Floris, G. 2010. *Euphorbia* latex biochemistry: Complex interactions in a complex environment. Plant Biosystems 144(2), 381-391.

Pirrung, M.C. 2016. Following the Reaction, in: Handbook of Synthetic Organic Chemistry, 2nd Edition. Elsevier Academic Press.

Popplewell, W.L., Marais, E.A., Brand, L., Harvey, B.H., Davies-Coleman, M.T. 2010. Euphorbias of South Africa: Two new phorbol esters from *Euphorbia bothae*. South African Journal of Chemistry 63, 175-179.

Pradheesh, G., Suresh, J., Suresh, S., Alexramani, V. 2017. Antimicrobial activity and identification of potential ethanolic antimicrobial compounds from medicinal plant *Pisonia grandis R. Br*. International Journal of Pharmacy and Pharmaceutical Science 6(4), 1686-1700.

Ragasa, C.Y. and Cornelio, K.B. 2013. Triterpenes from *Euphorbia hirta* and their cytotoxicity. Chinese Journal of Natural medicine 11(5), 528-533.

Red List of South African Plants. 2010. South African Biodiversity Institute. [Online available: http://redlist.sanbi.org/species.php?species=574-160] [Date accessed: 14 August 2017].

Rizk, A.F.M. 1987. The chemical constituents and economic plants of Euphorbiaceae. Botanical Journal of the Linnean Society 94, 293–326.

Rizk, A. M., Youssef, A. M., Diab, M. A., Salem, H. M. 1974. Triterpenoids and related substances of *Euphorbia paralias*. Constituents of Egyptian Euphorbiaceae, I.

Salvayre, R., Nègre, A., Rocchiccioli, F., Duboucher, C., Maret, A., Vieu, C., Lageron, A., Polonovski, J., Douste-Blazy, L. 1988. A new human pathology with visceral accumulation of long-chain n-alkanes; tissue distribution of the stored compounds and pathophysiological hypotheses. Biochimica et Biophysics Acta 958, 477-483.

Santana, S.S., Gennari-Cardoso, M.L., Carvalho, F.C., Roque-Barreira, M.C., Da Silva Santiago, A., Alvim, F.C., Pirovani, C.P. 2014. Eutirucallin, a RIP-2 type lectin from the latex of *Euphorbia tirucalli* L. presents proinflammatory properties. Public Library of Science (PLOS ONE) 9(2), 1-12.

Santiago, A., Alvim, F.C., Pirovani, C.P. 2014. Eutirucallin, a RIP-2 Type Lectin from the latex of *Euphorbia tirucalli* L. Presents Proinflammatory Properties. PLOS ONE 9(2), 1-12.

Sarker, S.D., Latif, Z., Gray, A.I. 2006. Natural Product Isolation, 2nd ed. Humana Press Inc., Totowa, New Jersey.

Schneider, E. 2009. Trade survey study on succulent *Euphorbia* species protected by CITES and used as cosmetic, food and medicine, with special focus on *Candelilla* wax. Convention on international trade in endangered species of wild fauna and flora, Eighteenth meeting of the Plants Committee, Buenos Aires.

Sharma, B.K. 2000. Molecular luminescence fluorometry and phosphorimetry, in: Instrumental Methods of Chemical Analysis. Krishna Prakashan Media.

Shi, Q-W., Su, X-H., Kiyota, H. 2008. Chemical and pharmacological research of the plants in genus *Euphorbia*. Chemical Reviews 108(10), 4295-4327.

Sosa, A.A., Bagi, S.H., Hameed, I.H. 2016. Analysis of bioactive chemical compounds of *Euphorbia lathyrus* using gas chromatography-mass spectrometry and Fourier-transform infrared spectroscopy. Journal of Pharmacognosy and Phytotherapy 8(5), 109-126.

Stefano, V.D., Pitonzo, R., Schillaci, D. 2011. Chemical constituents and antiproliferative activity of *Euphorbia bivonae*. Chemistry of Natural Products 47(4), 660-664.

Tanaka, R., Kasubuchi, K., Kita, S., Matsunaga, S. Obtusifoliol and related steroids from the whole herb of *Euphorbia chamaesyce*. Phytochemistry 41(3), 457-463.

Toume, K., Nakazawa, T., Hoque, T., Ohtsuki, T., Arai, M.A., Koyona, T., Kowithayakorn, T., Ishibashi, M. 2012. Cycloartane triterpenes and ingol diterpenes isolated from *Euphorbia neriifolia* in a screening program for death-receptor expression-enhancing activity. Planta Medica 78(12), 1370-1377.

Tsuda, Y. 2004. Isolation of natural products. Analytical Industry Co., Ltd., Japan.

Uchida, H., Ohyama, K., Suzuki, M., Yamashita, H., Muranaka, T., Ohyama, K. 2010. Triterpenoid levels are reduced during *Euphorbia tirucalli* L. callus formation. Plant Biotechnology 27, 105-109.

Van Zyl, J.J. 2000. Producing a textile from plant fiber of arid regions. RSA patent, ZA 99-5995 19990917.

Vázquez, L.H., Palazon, J., Navarro-Ocaña, A. 2012. The Pentacyclic Triterpenes α, β-amyrins: A Review of Sources and Biological Activities, in: Rao, V. (Eds), A Global Perspective in the role Nutrition and Health, INTECH.

Verma, R.N. and Batra, A. 2013. Isolation and analytic characterization of rebaudioside A and GC-MS analysis of methanolic leaves extract of *Stevia rebaudiana* Bert. Annals of Phytomedicine 2(1), 108-114.

Wagenaar, M.M. and Clardy, J. 2001. Two new roridins isolated from *Myrothecium* sp. The Journal of Antibiotics 54(6), 517-520.

Wal, A., Srivastava, R.S., Wal, P., Rai, A., Sharma, S. 2015. Lupeol as a magical drug. Pharmaseutical and Biological Evaluations 2(5), 142-151.

Wang, S., Liang, H., Zhao, Y., Wang, G., Yao, H., Kasimu, R., Wu, Z., Li, Y., Huang, J., Wang, J. 2016. New triterpenoids from the latex of *Euphorbia resinifera* Berg. Fitoterapia 108, 33-40.

Xu, J., Takasaki, A., Kobayashi, H., Oda, T.,Yamada, J., Mangindaan, R.E.P., Ukai†, K., Nagai, H., Namikoshi, M. 2006. Four new macrocyclic trichothecenes from two strains of marine-derived fungi of the genus *Myrothecium*. The Journal of Antibiotics 59(8), 451-455.

Yadav, R.P., Patel, A.K., Jagannadham, M.V. 2011. Purification and biochemical characterization of a chymotrypsin-like serine protease from *Euphorbia neriifolia* Linn. Process Biochemistry 46(8), 1654-1662.

Zhang, L. H., Zhang, G. T., Ye, W. C., Yin, Z. Q., Zheng, D., Zhao, S. X. 2006. Chemical constituents from *Euphorbia latifolia*. Natural Product Research and Development 18, 58-60.

Zhao, J-X., Liu, C-P., Qi, W-Y., Han, M-L., Han, Y-S., Wainberg, M.A., Yue, J-M. 2014. Eurifoloids A−R, structurally diverse diterpenoids from *Euphorbia neriifolia*. Journal of Natural Products 77, 2224-2233.

Chapter 4

The antibacterial properties of *Euphorbia gummifera*

Contents

List of figures

List of tables

4.1 Introduction

The identification of the existence of microorganisms can be seen as one of the most important scientific findings of our time. Even long before these fascinating organisms were identified they existed. The origin of microorganisms can be traced back to as early as 3900 million years ago as indicated by fossils that date back to that time (Margulis and Chapman, 2009).

It comes as no surprise that the identification of disease causing microorganism (of human, animals and plant) especially bacteria, went hand in hand with the identification of agents/compounds that could eliminate them. Such agents/compounds are known as antimicrobials or antibiotics. According to the Journal of Antimicrobial Agents, antimicrobials are defined as agents/compounds that kill and/or prevent further growth and reproduction of microorganisms, while antibiotics are a sub-class of antimicrobials specifically aimed at.

Since the identification of the first antibiotic, penicillin, that inhibited the growth of *Staphylococcus aureus*, by Alexander Fleming in 1928 and its mainstream use after 1940 (Abdallah, 2011; Saga and Yamaguchi, 2009), an invisible arms race was already underway between synthetic antibiotics and their target bacteria (Figure 4.1). This has led to the worldwide problem of antibiotic resistance.

What contributed even more to the problem of bacterial resistance to antibiotics was the decline in identification of new antibiotics. The development of antibiotics experienced a boom during the 1940s to 1960s and a decline from there on (Saga and Yamaguci, 2009) to the staggering extent of only two new antibiotics were identified during the last 30 years (Figure 4.1) (World Health Organization, 2011). This problem has sparked interest in finding alternative antimicrobials and especially antibiotics from sources other than soil microbes. One such alternative source is plants.

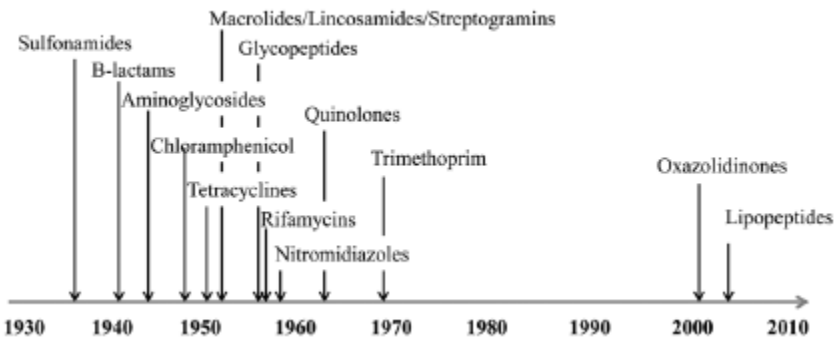

Figure 4.1: Timeline depicting the development and approved use of antibiotics over the decades (Abreu et al., 2012).

4.2 Plants: the alternative weapon against microorganisms

Through the ages plants have proven their worth through the identification of many medicinally and commercially important compounds such as morphine, atropine, ephedrine and quinine (Gilani and Atta-ur-Rahman, 2005), to name just a few. Plants thus represent an untapped source of compounds that could be alternatives to many synthetic drugs.

4.2.1 History of antimicrobial plant use

Plants have long since their origin had to "arm" themselves with ways to combat the continuous onslaught of diseases caused by microorganisms and tissue damage by other parasites, in the form of secondary metabolites (Abdallah, 2011; Abreu et al., 2012). Humans have also long depended on plants for their medicinal properties (Khullar, 2010).

The use of plants for their medicinally important properties can be traced back to the time of the Sumerians 5000 years ago (Petrovska, 2010; Swerdlow, 2000). The ancient Egyptians also utilized various different plants, shown to contain medicinally important compounds, to cure numerous ailments 3000-6000 years ago (Halberstein, 2005). There are also references to plant-based medicines in ancient Greek writings, as well as other historical cultures including China, India, Tibet, the Aztecs and the Mayans (Abreu et al., 2012; Halberstein, 2005).

All of these historical references led to a sparked interest in the possibility of plants as sources of alternatives to, or in combination with, synthetics drugs, especially antimicrobials. Various plant crude extracts and plant-derived compounds potentiate the activity of several synthetic antibiotics by either alleviating resistance to them or lower their minimum inhibitory concentration (MIC) (Awan et al., 2010; Betoni et al., 2006; Sibanda and Okoh, 2007; Stapleton et al., 2004). On the other hand, several plant crude extracts and plant derived compounds have exhibited antibacterial activity (Adwan et al., 2010; Mahesh and Satish, 2008) but at much higher MIC compared to synthetic antibiotics (Gibbons, 2004). Among these plants containing antibacterial properties are members of the *Euphorbia* genus.

4.2.2 Antibacterial properties of *Euphorbia* species

The genus *Euphorbia* falls under the sixth largest flowering plant family, Euphorbiaceae (Al-Mughrabi, 2003). This genus has been known to be exploited worldwide for its medicinal properties. Amongst these medically important properties, antimicrobial activity has been studied extensively (Table 4.1).

4.3 Aims and objectives

The aim of this chapter was to demonstrate the possible antibacterial properties of *E. gummifera* against certain plant growth promoting rhizobacteria (PGPR). The purpose of this chapter was not necessarily to identify and isolate a possible antimicrobial compound(s) but rather to determine the influence of *E. gummifera* metabolites on some soil bacteria.

The objectives were:

- Identifing two bacterial isolates that reside in the rhizosphere of *Stipagrostis uniplumis* grass that grows outside fairy circles.
- Using these isolates and other known growth promoting rhizobacteria as test organisms in a microtiter based antibacterial assay to test the antibacterial properties of *E. gummifera* methanol extract.
- Conducting a bioautography experiment with the column chromatography fractions from Chapter 3 to identify possible antibacterial fractions.
- Investigating the active fractions' GC-MS data (Chapter 3) to identify possible antibacterial compound(s).

Table 4.1: Antimicrobial activity of some *Euphorbia* species

***Euphorbia* species**	**Part of plant used**	**Extraction solvent(s) used**	**Antimicrobial activity against**	**References**
E. hirta  **Figure 4.2: *E. hirta* (Elumalia et al., 2010)**	Aerial parts	Ethanol	○ *Escherichia coli* ○ *Proteus vulgaris* ○*Pseudomonas aeruginosa* ○ *Staphylococcus aureus*.	Sudhakar et al. (2006)
	Aerial parts	Aqueous and Chloroform	○ *Bacillus subtilis* ○ *E. coli* ○ *Klebsiella pneumonia* ○ *P. aerugonosa* ○ *S. aureus*	Suresh et al. (2008)
	Whole plant	Aqueous and Methanol	○ *Bacillus cereus* ○ *S. aureus* ○ *K. pneumoniae*	Parekh and Chanda (2007)
	Leaves	Aqueous and silver nano-particles	○ *S. aureus* ○ *Bacillus cereus*	Elumalai et al. (2010)

Euphorbia species	Part of plant used	Extraction solvent(s) used	Antimicrobial activity against	References
E. segetalis  **Figure 4.3: *E. segetalis***	Whole plant	Acetone	○ Herpes simplex virus ○ African swine fever virus ○ *Candida kruzei* ○ *C. glabrata* ○ *Cryptococcus neoformans.* ○ *S. aureus* ○ *E. coli* ○ *Shigella dysentriae* ○ *Salmonella typhimurium* ○ *P. aeruginosa*	Madureira et al., 2003
E. macroclada  **Figure 4.4: *E. macroclada***	Leaves, stems and flowers	Methanol	○ *Pythium* spp. ○ *Verticillium dahlia* ○ *Fusarium oxysporum* ○ *Penicillium italicum* ○ *Rhizoctonia solani* ○ *Rhizopus stolonifer* ○ *Cladosporium* spp.	Al-Mughrabi, 2003

***Euphorbia* species**	**Part of plant used**	**Extraction solvent(s) used**	**Antimicrobial activity against**	**References**
E. macroclada	Above ground parts and latex	Methanol	○ *S. aureus* ○ *B. megaterium* ○ *P. vulgaris* ○ *K. pneumoniae* ○ *E. coli* ○ *P. aeruginosa*	Kirbag et al., 2013
E. socotrana  **Figure 4.5: *E. socotrana***	Leaves	Methanol and aqueous	○ *S. aureus* ○ *B. subtilis* ○ *Micrococuss flavus* ○ Multiresistant *Staphylococcus* strains: *Staphylococcus epidermidis* 847, *Staphylococcus haemolyticus* 535, and *S. aureus.*	Mothana et al., 2009

***Euphorbia* species**	**Part of plant used**	**Extraction solvent(s) used**	**Antimicrobial activity against**	**References**
E. balsamifera 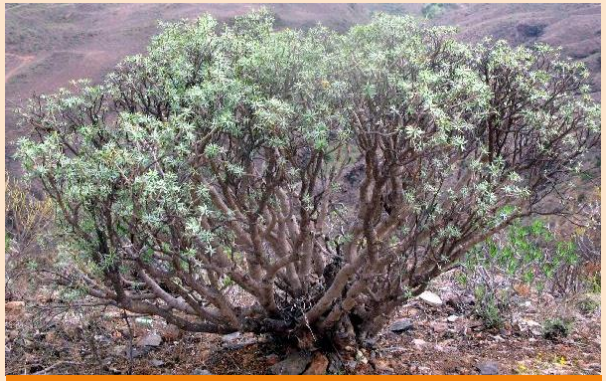 **Figure 4.6: *E. balsimifera***	Leaves, stems and root	Ethanol	○ *S. typhimurium* ○ *P. aeroginosa* ○ *Klebkkksiella spp.* ○ *E. coli* ○ *C. albicans* ○ *K. pneumoniae*	Kamba and Hassan, 2010
 **Figure 4.7: *E. tirucalli***	Stem	Aqueous and methanol	○ *B. cereus* ○ *S. aureus* ○ *Enterobacter aerogenes* ○ *E.coli* ○ *K. pneumoniae*	Parekh and Chanda, 2007
	Leaves and stems/bark	Methanol	○ *E.coli* ○ *P. aeruginosa* ○ *P. vulgaris*	Upadhyay et al., 2010

Euphorbia species	Part of plant used	Extraction solvent(s) used	Antimicrobial activity against	References
E. tirucalli	Above ground parts	n-Hexane, acetone, ethyl acetate, methanol, aqueous, gemmo-modified	○ *S. aureus* ○ *B. subtilis* ○ *E. coli*	Jahan et al., 2011
E. macrorrhiza  **Figure 4.8: *E. macrorrhiza***	Essential oils and extracts of roots	Methanol	○ *S. aureus*	Lin et al., 2012

Euphorbia species	Part of plant used	Extraction solvent(s) used	Antimicrobial activity against	References
E. pulcherima* L. (Poinsettia)**  **Figure 4.9: *E. pulcherma	Leaves, stem, inflorescence and whole plant	Ethanol	○ *Salmonella typhi* ○ *E. coli* ○ *Aspergillus niger* ○ *Trichophyton tonsurans*	Yakubu and Mukhtar, 2011
E. characias  **Figure 4.10: *E. characias* (Pisano et al., 2016).**	Leaves, stems and flowers	Ethanol and aqueous	○ *S. aureus* ○ *B. cereus* ○ *Listeria monocytogenes*	Pisano et al., 2016

4.4 Materials and methods

4.4.1 Bacterial isolation

Figure 4.11: A *S. uniplumis* plant with its intact rhizosphere sheath.

Attached rhizosphere soil particles were removed from the roots of a *S. uniplumis* (Figure 4.11) using a sterile blade. To isolated bacteria from the rhizosphere soil, 1 g of the soil was added to 9 ml of Ringers solution (Merck). This solution was mixed thoroughly by shaking vigorously. A dilution series (Figure 4.12) was made from this solution. Three replicates of each dilution was plated using the spread plate method, onto nutrient agar (Merck). The plates were incubated at 30-35 °C for 48 hours. Distinct single colonies were identified and streaked out on nutrient agar using the cross streak method. Each distinct culture was sub-cultured until pure cultures without contamination were obtained. Plates were sealed with parafilm and stored in a 5.5 °C fridge until used for the antibacterial assay. For the purpose of the antibacterial assay, a single colony of each distinct type of bacteria was picked up with a sterile loop and the loop was dipped in nutrient broth (Merck). The bacteria were then grown up in the liquid media.

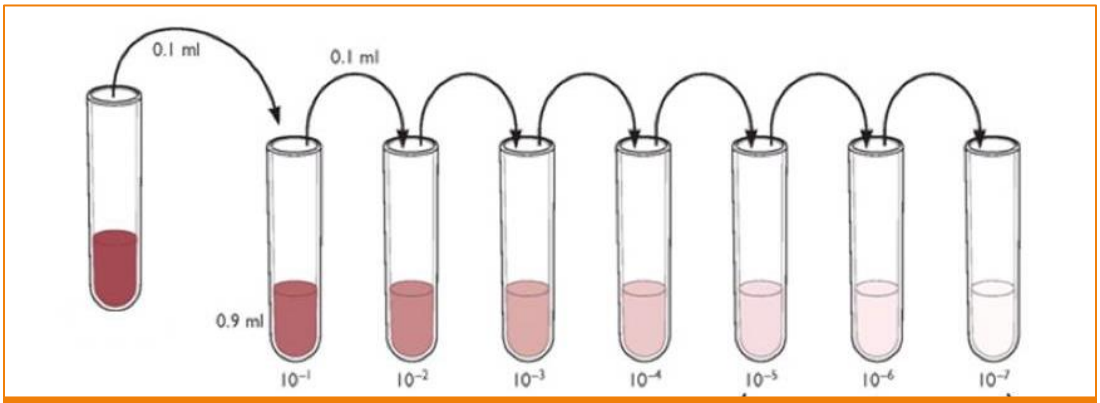

Figure 4.12: The type of dilution series method employed to isolate bacteria (Adapted from Racaniello, 2009)

4.4.2 Bacterial identification

4.4.2.1 DNA extraction

This is the first step in the bacterial identification and it is important to take great care to prevent contamination by working aseptically. The DNA extraction was done using the Zymo Research Quick-gDNA Miniprep kit (The Epigenetics Company). To a sterilized Eppendorf tube, 700 µl of genomic lysis buffer was added. Using a sterile toothpick or bacterial loop, as much as possible of the bacterial culture was scooped up and added to the lysis buffer. This mixture was vortexed for a few seconds to ensure thorough mixing. The entire mixture was transferred to a Zymo-spin 11C column in a collection tube and centrifuged at max speed in desktop microfuge for one minute. The spin column was transferred to a new tube and 200 µl of DNA pre-wash buffer was added followed by centrifugation at 10000 rpm for one minute. This was followed by addition of 400 µl g-DNA wash buffer to the spin column and centrifugation at 10000 rpm for one minute. The spin column was transferred to a clean 1.5 ml Eppendorf tube and 50 ml of DNA elution buffer was added to the spin column. The spin column was incubated at room temperature for two to three minutes followed by centrifugation at top speed (10000 rpm) for 30 seconds in order to elute the DNA into the Eppendorf tube. The collected DNA was stored in a -20 °C freezer.

4.4.2.2 Agarose gel electrophoresis

This step is necessary to deduce whether or not DNA was extracted successfully. A 1% agarose gel (0.5 g agarose plus 50 ml TDA) was set up to run the samples. A 2kb ladder (Thermo Fisher Scientific Inc.; catalogue number 15623100) was used as a reference to compare to samples that were run. The concentration of the DNA as well as its purity was tested using the Nanodrop 2000 (Thermo Fisher Scientific Inc.). The positive control used was bacterial DNA containing the 16S rRNA gene while the negative control consisted of the master mix without added bacterial DNA.

4.4.2.3 16S PCR amplification

During this experiment the reaction mixture was kept on ice to prevent any reagent from starting to react. A master mix of all the reagents (except the DNA) was made up and aliquoted into PCR reaction tubes from the Zymo Research Quick-gDNA Miniprep kit (The Epigenetics Company). Table 4.2 indicates the amount of each reagent needed for a single reaction. Thus the amount of each reagent was multiplied by the number of samples that were to be tested (in this

case by two). The master mix volume was 49 µl so to each tube 24.5 µl of master mix was added as well as 0.5 µl DNA to its respective tube to make up PCR reactions mixtures of 25 µl. To remove bubbles or droplets stuck to the side, the tubes were centrifuged for a few seconds. Details on the primers used, 27F and 1492R (Inqaba Biotech), can be found in Appendix D. The PCR reaction was then performed as follows:

- 92° C for 10 minutes
- 92 °C for 1 minute
- 58 °C for 1 minute
- 75 °C for 1 minute
- 75 °C for 5 minutes
- 4 °C §

30 cycles

Table 4.2: Amount of reagents needed for the 16S rRNA PCR amplification

Reagent	Amount
Buffer (0.5%)	2.5 µl x 2 = 5 µl
dNTPs (2.5 mM of each nucleotide)	2.0 µl x 2 = 4 µl
$MgCl_2$ (25 mM)	2.0 µl x 2 = 4 µl
Forward primer 27F (10 µM)	0.5 µl x 2 = 1 µl
Reverse primer 1492R (10 µM)	0.5 µl x 2 = 1 µl
Nuclease free water	16.85 µl x 2 = 33.7 µl
Taq DNA polymerase (2 units/µl)*	0.15 µl x 2 = 0.3 µl
DNA (1 µl/ng DNA)	0.5 µl

*Obtained from Thermo Fisher Scienific, catalogue number EP0402

4.4.2.4 Agarose gel electrophoresis

An agarose gel was set up as previously described, however, the purpose of this gel was to ascertain whether or not the 16S rRNA gene was successfully amplified during the PCR.

4.4.2.5 Clean-up and 16S rRNA PCR

The first PCR reaction was cleaned up in order to remove any primer dimers and extended adenine ends. This was done by adding 0.5 µl Exol and 2 µl FastAP from the Zymo Research Quick-gDNA Miniprep kit (The Epigenetics Company), followed by placing on a 37 °C heating

block for 15 minutes followed by 15 minutes on a 85 °C heating block. A master mix was again made, using the same principle as explained above for the sequencing reaction. The total volume with addition of the DNA was 12 µl. The PCR was performed as follows:

- 96 °C for 5 seconds
- 96 °C for 10 seconds
- 55 °C for 5 seconds
- 60 °C for 4 minutes
- 4 °C §

Table 4.3: Amount of reagents needed for second 16S rRNA PCR

Reagent	Amount
Big dye (full strength)	1.0 µl x 2= 2 µl
Sequencing buffer (5x concentration)*	2.0 µl x 2= 4.0 µl
Undiluted primer (3. 3 µM)	0.3 µl x 2= 0.6 µl
Nuclease free water	4.7 µl x 2= 9.4 µl
DNA (10 ng/100bp)	4.0 µl

* Given as 5x concentration, used as 1x

4.4.2.6 Precipitation

This step precipitated the 16S rRNA for Sanger sequencing. To a sequencing Eppendorf tube 16 µl 100% ethanol and 2 µl 3M Sodium Acetate (pH 4.8) was added. To this 12 µl of the sequencing reaction was added. The Eppendorf tube was centrifuged at maximum speed for 30 minutes. The supernatant was carefully removed and 150 µl of 70% ethanol was added to perform the wash step. The Eppendorf tube was centrifuged at maximum speed in desktop microfuge for five minutes, the supernatant was removed followed by a repeat of the wash step. Finally the Eppendorf tube was placed on a heating block set to 90 °C for three minutes to completely dry them. The sequencing tubes were stored at -20 °C until Sanger sequencing was done by the Forestry and Bio-informatics Centre (FABI), University of Pretoria.

4.4.2.7 Sequence edit and BLAST

The sequences that were obtained from Sanger sequencing were imported into the BioEdit sequence alignment programme (Hall, 1990; Ibis Therapeutics) to edit the sequences. The edited sequences were imported into the NCBI BLAST website (https://blast.ncbi.nlm.

nih.gov/Blast.cgi) where it was compared to known 16S rRNA sequence database of known bacteria.

4.4.3 Microtiter-based antibacterial assay

The method that was used to test the antibacterial properties of the *E. gummifera* methanol extract (see preparation in Chapter 2) was based on the method of Eloff (1998). The layout of the 96 well plates can be seen in Figure 4.13.

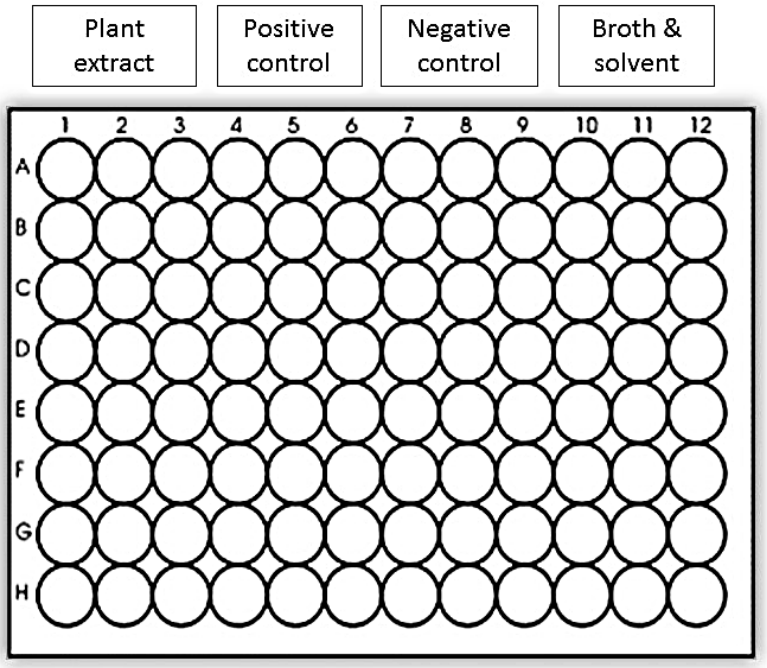

Figure 4.13: The layout of the 96 well plates used for the antibacterial assay.

The extract was tested for its antibacterial properties against nine bacteria. These included two bacteria isolated and identified from rhizosphere soil (Section 4.4.1 and 4.4.2), four unknown soil bacteria, *B. subtilis*, *P. vulgaris* and *P. aeruginosa*.

The *E. gummifera* methanol extract was prepared by weighing of 10 mg of the extract in a 2 ml Eppendorf tube. To this, 100 µl of 10% dimethylated sulfoxide (DMSO) was added. The mixture was sonicated (DSA Ultrasonic Cleaner) for 15 minutes to allow complete dissolving of the extract. Following sonication, 900 µl of ddH_2O was added to the extract mixture. The positive control was prepared by dissolving 2 mg of the antibiotic, ciprofloxacin in 10 ml of ddH_2O.

As a precaution to determine whether or not the solvent DMSO would affect the growth of the test bacteria, a 5 % DMSO solution was made up by adding 1 ml of 99% DMSO to 20 ml of ddH_2O that was tested. The densities of the bacterial cultures were determined by adding 200 µl of sterile broth and bacterial cultures to respective wells of a 96 well plate. The absorbance was read at 600 nm and the culture were adjusted (adding more broth or bacterial culture) depending on the values.

The 96 well plates were prepared as follows:

- 100 µl of nutrient broth (company) was added to all of the wells.
- 100 µl of the extract mixture was added to wells A1 to A3.
- 100 µl of the positive control was added to wells A4 to A6.
- 100 µl of the bacterial culture (negative control) was added to wells A7 to A9.
- 100 µl of 5% DMSO (solvent control) was added to wells A10 and A11.
- 100 µl of nutrient broth was added to well A12.

The contents of the plate were serially diluted from row A to row H by transferring 100 µl of content to the next row (A to B and so forth), mixing thoroughly by pipetting up and down and continuing with the process. The last 100 µl from row H was discarded. To all wells, except the negative control (A10 to H10 and A11 to H11), 100µl of bacterial culture was added. The 96 well plates were incubated at 37 °C for 48 hours.

The bacterial growth was visualized by adding 40 µl of INT (ρ-iodophenyltetrazolium) (AMRESCO) to all of the wells and incubating the plate in the dark until a colour change was visible (± 45 minutes). The minimum inhibitory concentration (MIC) was determined visually by determining at which well/ concentration no colour change occurred.\

4.4.4 Bioautography

The 35 major combined fractions from Chapter 3 were subjected to thin layer chromatography (TLC) in two separate sets. Following the development of the silica plates, each set of plates were sprayed with two isolated rhizobacteria. The plates were incubated in a humid growth chamber at 25 °C for 48 hours (Figure 4.14).

Following the incubation period, each set of plates were sprayed with INT (2 mg INT dissolved in 10 ml ddH_2O) and incubated in the dark at 25°C for 45 minute to an hour (or until a colour change was visible). Each plate was compared to its counterpart that had not been sprayed with bacteria (Chapter 3) to identify which fractions as well as bands within fractions inhibited the growth of the bacteria.

Figure 4.14: The bioautography plates incubated in a humid chamber.

4.4.5 GC-MS analysis

The compounds identified within fractions that inhibited bacterial growth on TLC plates, were investigated for antibacterial activity. Thus to identify a possible antibacterial compound present in *E. gummifera*, we worked backwards from the bio-autography to the GC-MS results.

4.5 Results

4.5.1 Bacterial isolation

One of the soil dilutions yielded a mixed bacterial culture with two distinct colonies (Figure 4.15). These two bacterial cultures were continuously streaked out to obtain pure cultures. Initially the cultures had faded colours and weren not very condensed after the incubation period at 30-35 °C (Figure 4.16 A and B). After a period of storage at 5.5 °C the colour intensified (Figure 4.16 C and D).

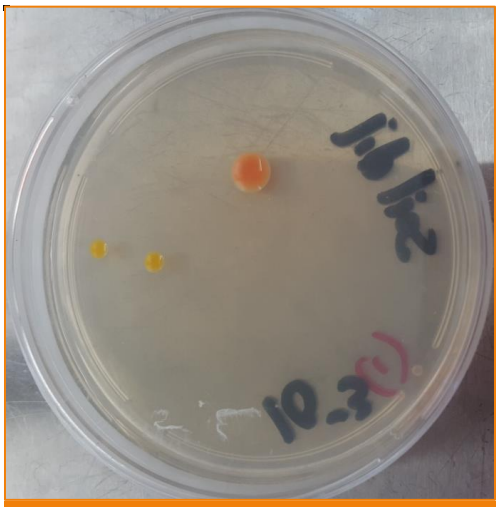

Figure 4.15: A mixed bacterial culture obtained from soil dilutions.

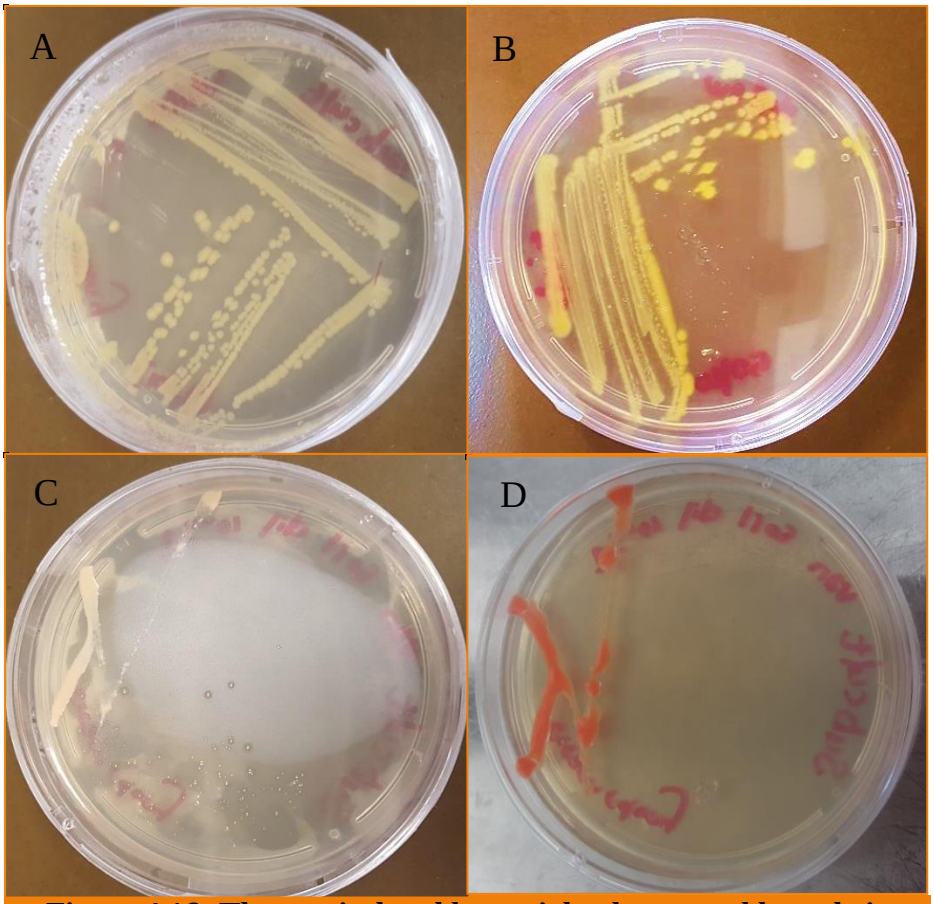

Figure 4.16: The two isolated bacterial cultures and how their appearance changed at different incubation temperatures. A. and B. are the same bacterial culture while C. and D. are the same bacterial culture. The difference being that plates A. and C. were incubated at 30-35 °C and plates C. and D. were also incubated at 35 °C followed by storage at 5.5 °C.

4.5.2 Bacterial identification

Following the DNA extraction, an agarose gel electrophoresis was run to determine if the extraction was successful. The electrophoresis indicated that DNA was successfully extracted (Figure 4.17) even though the quality of the yellow bacteria's DNA was far superior compared to the orange bacteria's DNA.

The concentration of the DNA was as follows: yellow bacteria 8.6 ng/µl and orange bacteria 39.9 ng/µl. The purity of the DNA, as indicated by the $OD_{260/280}$ values was as follows: yellow bacteria 1.84 and orange bacteria 1.79.

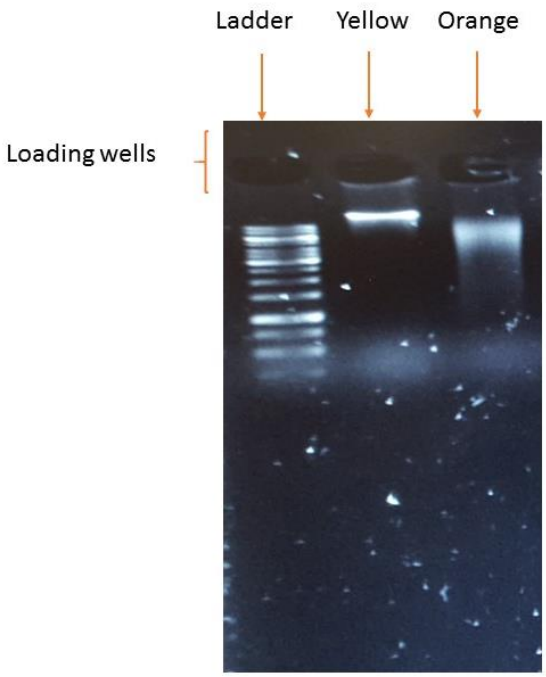

Figure 4.17: The agarose gel electrophoresis of the DNA extracted from both the yellow and orange bacteria. Both the bacteria had bands above the ladder which indicated DNA was present. The yellow bacteria had a clear thin band which indicated good quality DNA. The orange bacteria's band was smeared which indicated DNA degradation.

Both bacteria's DNA was of quality that could be subjected to a 16S rRNA PCR. After the PCR had been run a second agarose gel electrophoresis was run to establish if the desired gene had been amplified successfully. The agarose gel electrophoresis indicated that from both the bacteria's DNA the 16S rRNA gene was successfully amplified (Figure 4.18).

Once it was established that the desired gene was successfully amplified, the DNA had to be cleaned up, subjected to sequencing PCR to amplify the DNA further and the DNA had to be precipitated before it could be sequenced. The complete sequences (Appendix D) were edited using the BioEdit software programme and BLASTed to identify them.

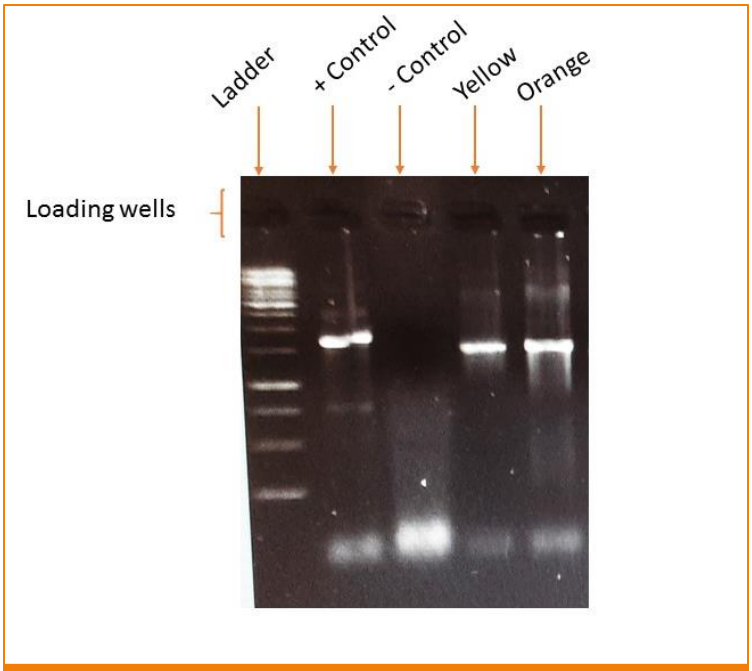

Figure 4.18: The 16S rRNA PCR gel electrophoresis. The positive control consisted of bacterial DNA which had its 16s rRNA gene successfully amplified with a PCR. The negative control was made up of the master mix without any bacterial DNA. Both the bacteria had a clearly visible band that was in line with that of the positive control, indicating a successful PCR amplification. The faint bands to the bottom indicate protein precipitation and other faint bands indicate primer dimers.

The top ten hits (all of the same genus) for both bacteria can be found in Appendix D. Due to the appearance and unique characteristics of the two bacteria, the yellow bacteria would be referred to as *Pseudomonas paravulva* and the orange bacteria *Kocuria polaris* for the purpose of this study. *P. paravulva* strain AJ 2129, accession number 04085.1, had a hit percentage of 97% and an E-value of 0.00. *K. polaris* strain CMS 76or, accession number 028924.1, had a hit percentage if 99% and an E-value of 0.00.

4.5.3 Microtiter based antibacterial assay

The *E. gummifera* methanol extract was tested for its antibacterial properties against several bacteria, including the two isolated and identified bacteria. The solvent used, DMSO, did not affect the growth of

any of the bacteria tested. The extract proved to be effective at inhibiting the growth of both *P. paravulva* and *K. polaris* at a concentration of 2.5mg/ml using INT as visualizing agent (Figure 4.19 and 4.20).

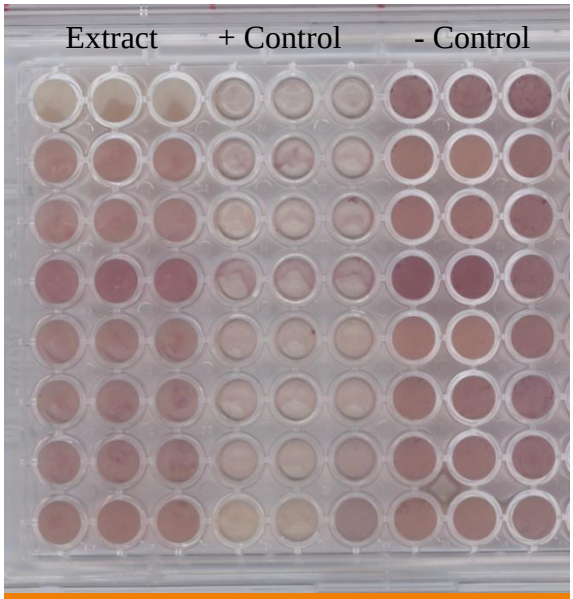

Figure 4.19: The antibacterial assay result for *P. paravulva.* Comparing the extract to both the positive and negative control, there appeared to be evident inhibition at the first row of the extract test. The MIC was calculated to be 2.5 mg/ml.

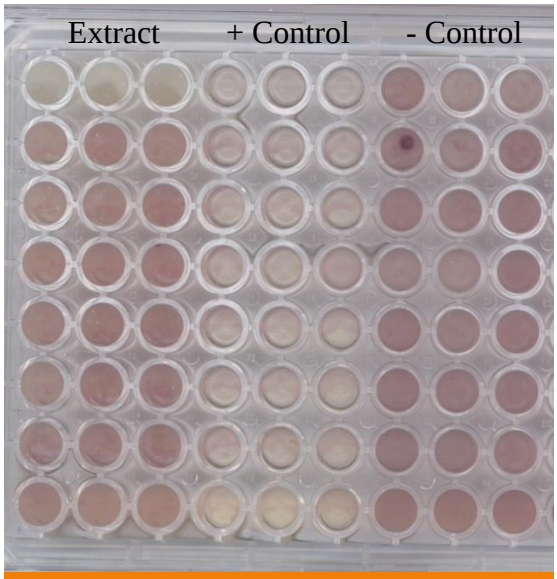

Figure 4.20: The antibacterial assay results for *K. polaris*. Comparing the extract to both the positive and negative control, there appeared to be evident inhibition at the first row of the extract test. The MIC was calculated to be 2.5 mg/ml.

The experiment proved to be more problematic for the rest of the test bacteria. The problem centered on visualizing the bacterial growth inhibition with INT. Even though there appeared to be some inhibition at high concentrations, no concise colour distinction could be made and thus as a result no MIC could be determined. Even though the results were not clear, it indicated which bacteria were more susceptible to the plant extract's antibacterial activity.

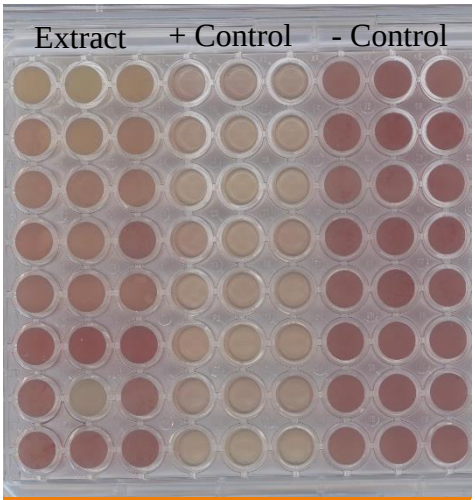

Figure 4.21: The antibacterial assay results for *P. vulgaris*.

After examining the antibacterial assay results for *P. vulgaris* (Figure 4.21), it was evident that at the highest concentration (first row) of extract, there appeared to be a degree of inhibition (2.5mg/ml) yet it was not as clear as for *P. paravulva* and *K. polaris*.

The same was found for bacteria 5 (Figure 4.22) and bacteria 10 (Figure 4.23).

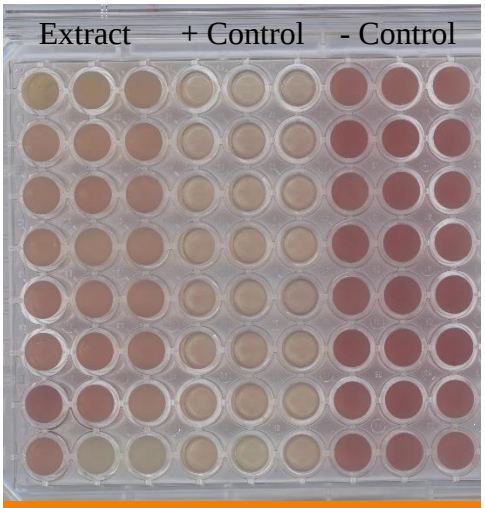

Figure 4.22: The antibacterial assay results for Bacterium 5.

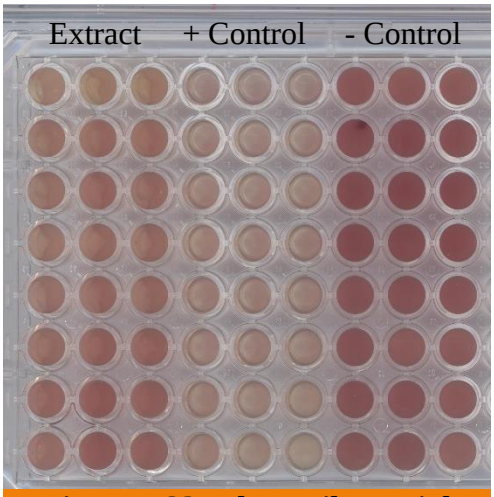

Figure 4.23: The antibacterial assay results for Bacterium 10.

The results for the rest of the bacteria: *B. subtilis*, *P. aeruginosa*, B1 and B3 were unclear.

4.5.4 Bio-autography

In order to identify which fraction had inhibitory activity on the two identified bacteria, the TLC plates from Chapter 3 were compared to those of the bio-autography analysis (Tables 4.4).

Table 4.4: The bio-autography plates compared to the fraction plates

Bacteria	Fractions	Bio-autography TLC	TLC of fractions (vanillin)	Conclusion
P. paravulva	A to I	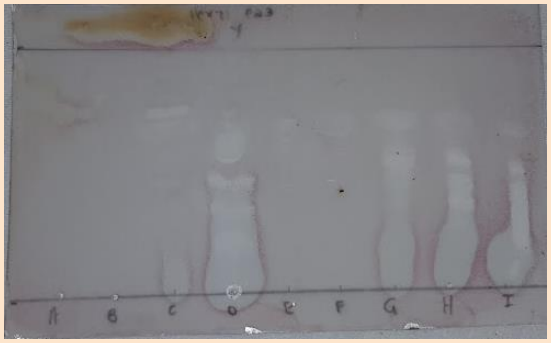	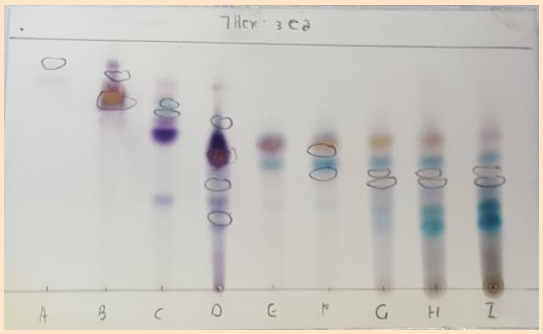	Fractions C, D, G, H, I inhibited the growth of the bacteria
	J to R	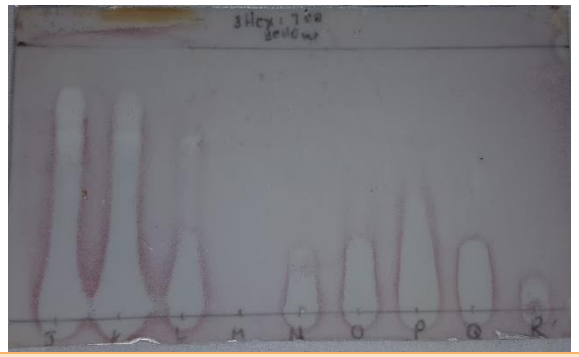	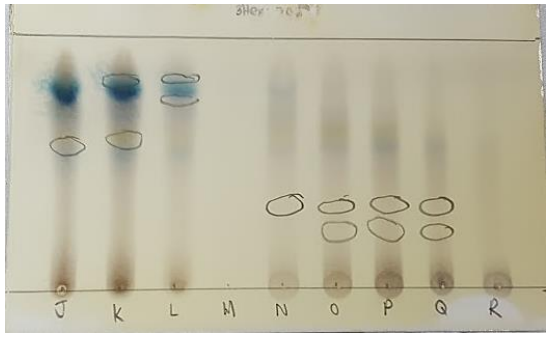	All fractions except M inhibited bacterial growth
	S to AA	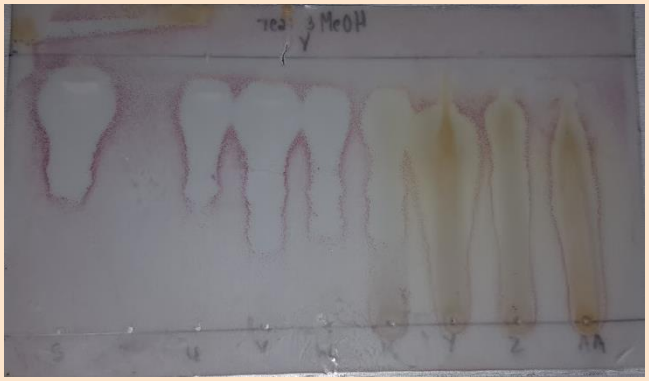	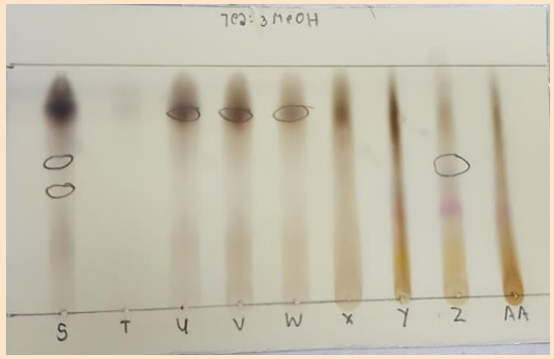	Clear inhibition at fractions S, U to AA

Bacteria	Fractions	Bio-autography TLC	TLC of fractions (vanillin)	Conclusion
P. paravulva	BB to II		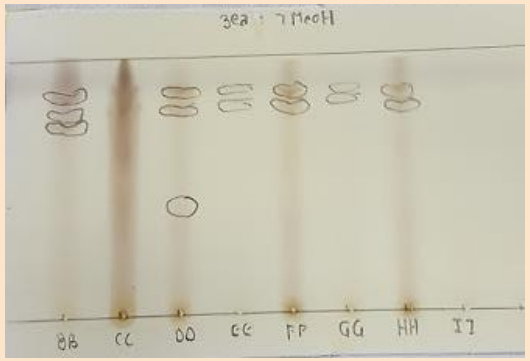	Only fraction BB inhibited bacterial growth
K. polaris	A to I	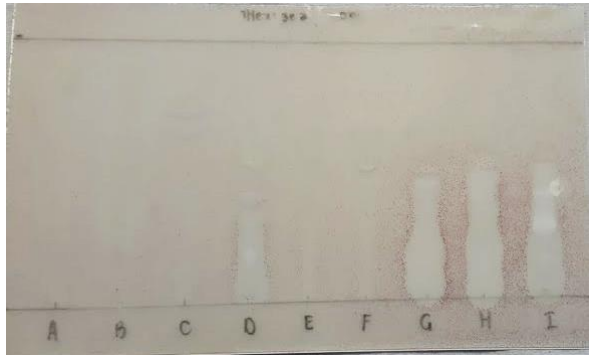	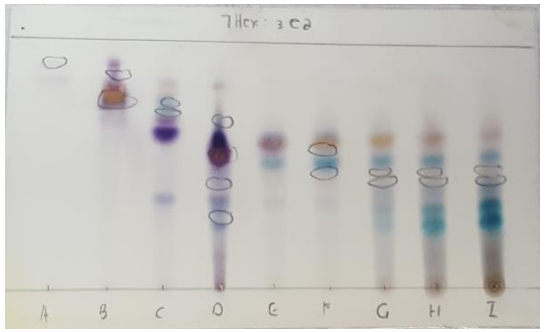	Evident inhibition visible for fractions D, G, H, I and to a lesser extent the rest of the fractions
	J to R	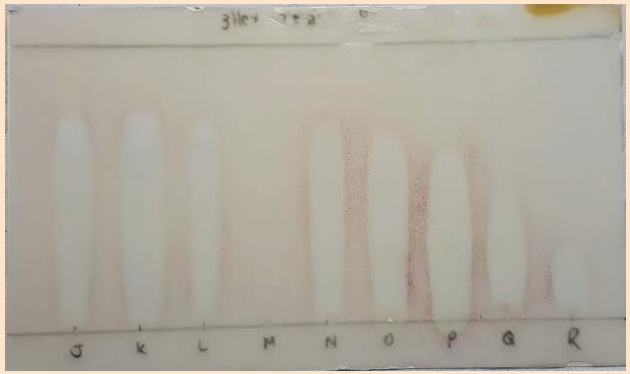		All fractions except M inhibited bacterial growth

Bacteria	Fractions	Bio-autography TLC	TLC of fractions (vanillin)	Conclusion
K. polaris	S to AA	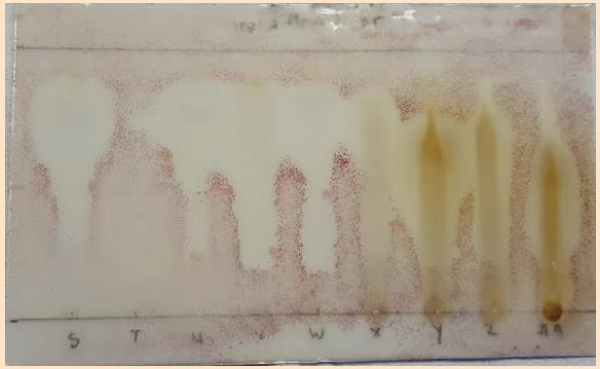	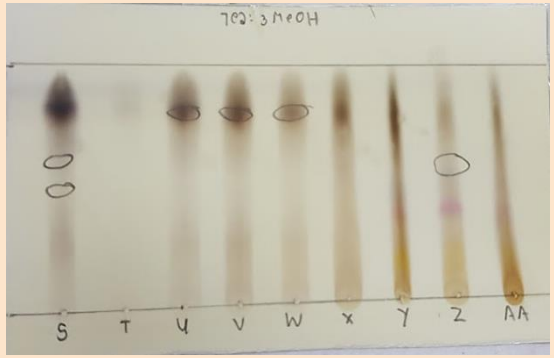	Large areas of inhibition visible for fractions S to W.
	BB to II	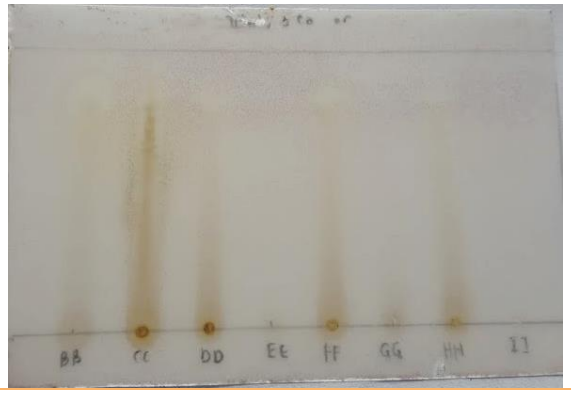	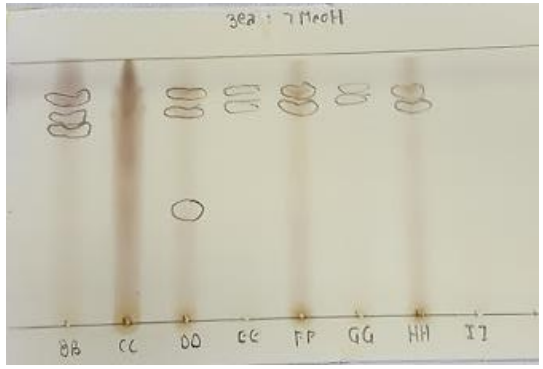	No clear inhibition.

The bio-autography results for *P. paravulva* indicated that this bacterium was more susceptible when compared to *K. polaris* due to more fractions showing activity. Fractions C, D, G, H, and I had antibacterial activity against *P. paravulva*. The inhibition by fraction C was due to compounds not visible with UV light or vanillin. The inhibition by fraction D was due to three bands, two visible under UV light and one with vanillin. The inhibition by fractions G, H and I were a result of multiple compounds. The entire fraction J and K appeared to inhibit *P. paravulva*. The inhibition by fraction N excluded that of the encircled band whereas with fractions O and Q it included the lowest most encircled band and with fraction P both encircled bands. The inhibition by fraction R was due to compound(s) stuck on the baseline. The inhibition by fraction S that was at high Rf-values included those compounds visible under UV light. Fractions U, V and W had similar inhibition zones. It appeared as if the entire fractions of X to AA inhibited growth, a slight yellow colour was visible, which made it difficult to determine bacterial inhibition. The inhibition by fraction BB was due to the uppermost encircled compound.

The inhibition for *K. polaris* was similar to that of *P. paravulva*. The inhibition by fraction D was due to lower Rf-values, most part including the encircled band. Fractions G, H, and I had similar inhibition zones that included the two encircled bands in the middle of the plate. Fractions J and K also had similar inhibition zones which included the lowermost encircled band whereas that of fraction L excluded both of its top most bands. Fractions N, O and Q had large inhibition zones that only excluded the part closest to the solvent line whereas fraction Q's inhibition zone stretched to above its two encircled bands. Fraction R's inhibition zone was due to compound(s) that were not visible with either UV light or vanillin. Fractions S to W had similar large inhibition zones. Fractions Z to AA exhibited the same problems as described for *P. paravulva*. The inhibition by fraction BB was the same as for *P. paravulva*.

4.5.5 GC-MS analysis

Several compounds (Table 4.5 and GCMS data Appendix E) were identified that had previously been identified in *Euphorbia* species whose extracts had exhibited antimicrobial activity. In addition, a few identified compounds from other species are known for having antibacterial activity.

Table 4.5: Antimicrobial compounds previously found in *Euphorbia* spp. and identified in the *E. gummifera* methanol extract by GC-MS analysis

Compound	Present in fractions and hit%	Activity against	Isolated from	Reference
Lupeol 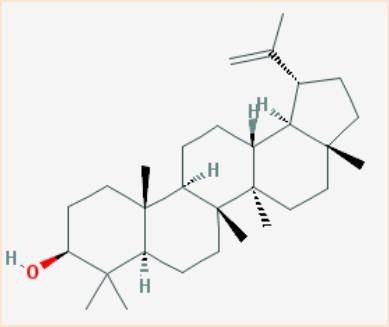	B (80%) C (89%) E (90%) G (90%) H (90%) I (89%) J (87%) K (87%) L (87%) M (74%) N (81%) O (83%) P (85%) Q (86%) R (83%) V (73%) W (77%	*P. aeruginosa*, *E. coli* (ATCC 25922 & 35218), *S. aureus* (ATCC 29213 & 25923), *Enterrococcus faecalis*, *S. typhi*, *Vibrio cholera*, *S. dysentery*, *S. flexneri*, *S. sonnei*, *S. boydii*, *P. mirabilis*	*E. larica*, *E. hirta*, *E. chamaesyce*, *E. tirucalli*, *E. lagascae*, *E. bivonae*, *E. damarana*	Ahamed et al., 2007; Duarte, 2008; Freire et al., 2008; Gupta et al., 2013; Jassbi, 2006; Joubert, 2008; Lutta et al., 2008; Ragasa and Cornelio, 2013; Stefano et al., 2011; Tamakou et al., 2012; Tanaka et al., 1999; Wal et al., 2015; Wal et al., 2011
Quinic acid 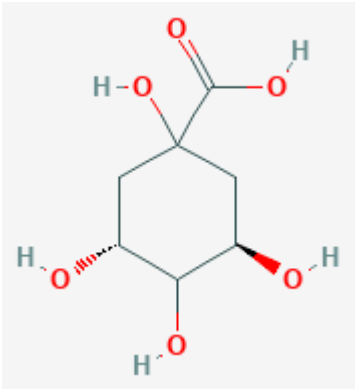	CC (83%) DD (83%) FF (80%)	*E. coli*, *P. aeruginosa*, *P. mirabilis*, *K. pneumoniae*, *Acinetobacter baumannii*, *S. aureus*, *E. faecalis*, *B. subtilis*	*E. macroclada*, *E. gaillardotii*, *E. hirta*	Ertas et al., 2015; Gopi et al., 2015; Özçelik et al., 2011

Compound	Present in fractions and hit%	Activity against	Isolated from	Reference
α- Amyrin 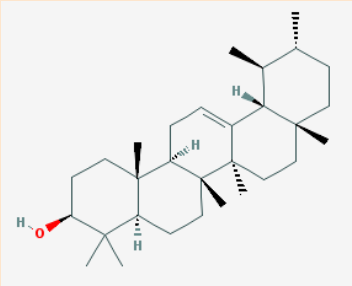	H (92%)	*S. aureus, E. faecalis*	*E. hirta, Stevia rebaudiana* Bert., *E. grandialata, E. characias*	Ahmad et al., 2002a,b; Conrado et al., 2015; Fernandes-Freire et al., 1990; Ismail et al., 2017; Jabeen et al., 2011; Jassbi, 2006; Kumar et al., 2010; Martínez-Vázquez et al., 1999; Ragasa and Cornelio, 2013; Rivero-Cruz et al., 2009; Stefano et al., 2011; Vázquez et al., 2012;Verma and Batra, 2013; Zheng et al., 2011;
β- Amyrin 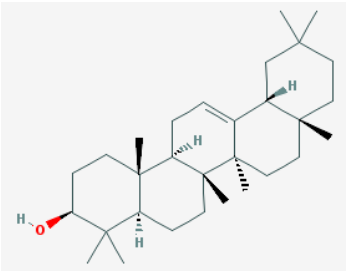	C (92%) E (93%) F (94%) G (93%)	*Ascochyta rabiei, S. mutans, Fusobacterium nucleatum, E. coli, S. aureus, E. faecium, B. subtilis, K. pneumoniae, P. aeruginosa, S. mutans,*	*E. decipiens, E. larica, E. falcata* L., *E. hirta*	
Betulin 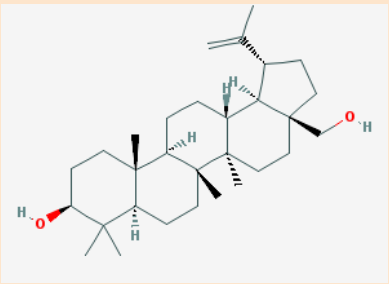	D (83%) E (79%) G (77%) H (89%) I (84%) J (84%) L (80%) X (85%)	*B. subtilis* (acid derivative), *S. aureus, S. typhi, K. pneumoniae, E. coli, E. faecium, P. aeruginosa, S. mutans*	*E. teheranica, E. heteradena, E. rigida, E. latifolia, Euphorbia myrsinites*	Ahmad et al., 2002b; Chandramu et al., 2003; Gherraf et al., 2010; Jassbi, 2006; Jassbi, 2000; Öksüz et al., 1995; Rivero-Cruz et al., 2009; Tene et al., 2009

Compound	Present in fractions and hit%	Activity against	Isolated from	Reference
Lucenin 2 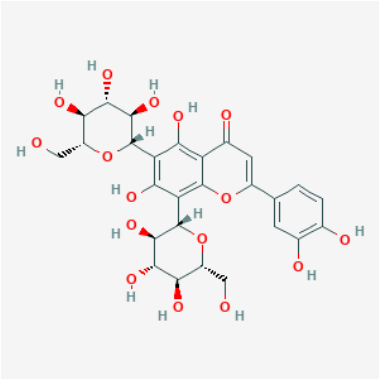	J (76%) O (80%) P (81%) Q (82% R (79%) S (81%) T (79%) U (80%) V (77%)	*P. aeruginosa, E.coli, E. aerogenes, E. cloaceae, K. pneumoniae*	Mosses (*Bartramia pomiformis, Hedwigia ciliate, Polytrichum affine, P. cuspidatum,* *Dicranum scoparium*)	Basile et al., 1999
Roridin E 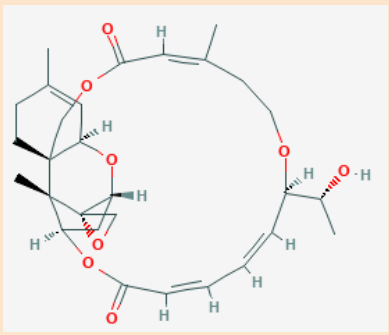	R (76%) CC (78%)	*S. cerevisiae, Candida albicans* & *Geotrichum candidum* (yeasts)	*Myrothecium* spp. including *M. verrucaria, M. roridum*	Jarvis and Wang, 1999; Wagenaar and Clardy, 2001; Xu et al., 2006
Lanosterol 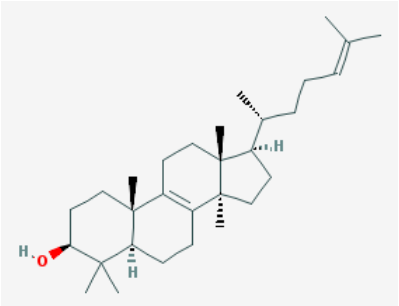	C (90%) D (90%) F (90%)	*E. coli, S, aureus*	*E. peplus, E. lathyris, E. pekinensis, E. characias, E. tirucalli*	Fernandes-Freire et al., 1990; Giner et al., 2000; Giner et al., 1995; Gupta et al., 2013; Kong and Min, 1996; Shingate et al., 2013; Zhang et al., 2006

Compound	Present in fractions and hit%	Activity against	Isolated from	Reference
Lupeol acetate 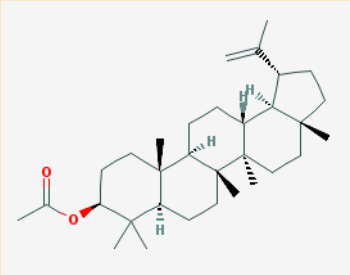	B (94%) D (94%) E (89%) I (88%) J (85%)	*B. subtilis, S. aureus, E. faecalis, E. coli, K. pneumoniae, P. aeruginosa*	*E. larica; E. geniculata* Ortega; *E. quinquecostata*	Eliza et al., 2016; Jassbi, 2006; Mbwambo et al., 1996; Muhammad et al., 2016

4.6 Discussion

4.6.1 Bacterial isolation and identification

The bacteria isolated from the rhizosphere of the *S. uniplumis* grass growing in between fairy circles were identified as *P. parafulva* and *K. polaris*. *K. polaris* a relatively recently discovered bacterial species as it was only isolated and assigned a species name in 2003 by Reddy et al. (2003). The genus itself was only introduced when Stackebradt et al. (1995) subdivided the *Micrococcus* genera into five separate genera, of which *Kocuria* was one. The bacterium was isolated from a region in Antarctica, more specifically a pond containing a cyanobacterial mat. Species belonging to the *Kocuria* genus can be described as Gram positive, aerobic coccoid bacteria that are not encapsulated, non-motile, non-spore forming, mesophilic, non-halophilic organisms (Savini et al., 2010). Yet identification of this species from the Antarctic region led to it being classified as psychrophilic. Other characteristics include positive tests for catalase but negative for coagulase and Vouges-Proskauer as well as unique cell wall composition separating it from others in the genus (Reddy et al., 2003; Savini et al., 2010).

One of the bacteria's most striking characteristics is its colour, being orange-red as a result of the production of pigments which were initially thought to be independent of any growth conditions (Reddy et al., 2003). However, a study done on the pigments produced by *K. polaris* and *K. carnippila* by Yusef et al. (2014) found that both temperature and light affected pigment production. They found that two pigments, β-carotene and echinenone, were responsible for the striking orange-red colour of *K. polaris*. Low temperatures ranging from 4 to 10 °C enhanced the production of the pigments and as temperatures

increased the production declined until its absence at temperatures above 30 °C. The absence of light also enhanced the production of the pigments.

These findings explain the colour change of the *K. polaris* bacteria plates under different growth conditions. The plates were initially incubated at temperatures between 30-35 °C where no pigments are produced thus the cream colour of the culture. Storage at 5.5 °C led to the production of the pigment and thus the orange-red colour of the culture.

Pigments such as β-carotene, echinenone and their breakdown products play pivotal roles in plants and microorganims. These include attracting pollinator's (colour and scent), regulating growth (hormones) and defense compounds for plants (Sherma et al., 1992). In harsh environmental conditions such as the arctic, desert and semi-deserts environments (such as the Garub area) pigments would be vital in absorbing harmful UV-radiation and thus aid in survival for all pigment producing organisms.

The second bacterium, identified in this study, which was initially known as *P. vulva*, was also recently characterized as a separated species now known as *P. paravulva* based on DNA and phylogenetic studies done by Uchino et al. (2001). They characterized this species as a Gram negative, rod-shaped bacterium that achieves motility though its polar flagella. It tested positive for catalase and oxidase and has a yellow colour when grown in culture. Temperatures between 4 and 37 °C will support growth. The bacteria has been isolated from paddy rice fields, where it known to exert antagonistic effects on several pathogens of rice (Liu et al., 2015) through possible secretion of secondary metabolites from biofilm formation. Biofilms play a pivotal protective role against harsh environmental conditions such as UV radiation, salinity and water-stress (Hall-Stoodley et al., 2004) that are common to desert and semi-deserts environments (Garub area).

4.6.2 Microtiter-based antibacterial assay

From the results of the microtiter-based antibacterial assay, it was evident that, of the tested bacteria, *K. polaris* and *P. paravulva* were the most susceptible.

Several extracts produced from *Euphorbia* species have been found to exert antibacterial activity on several bacteria including *Pseudomonas* species, *Micrococcus* species, *Proteus* species and *E. coli* (closely related to *K. polaris*, Reddy et al., 2003) which are all closely related to the tested bacteria (Table 4.1).

Suresh et al. (2008) investigated the antimicrobial and phytochemistry of several plants including *E. hirta*. Both aqueous and chlorophormic extracts were tested for their antibacterial activity against Gram positive and Gram negative bacteria. Both extracts were effective against all tested bacteria at a concentration as low as 25 µl and a zone of inhibition of 4 mm. Among the susceptible bacteria were *E. coli* and *P. aeruginosa*. Parekh and Chanda (2007) investigated the antimicrobial activity of selected Indian plants, among which *E. hirta* was one. The methanolic extract of the plant exhibited antibacterial activity against several bacteria, but of interest was the activity against *E. coli*. A zone of inhibition of 11 mm was observed which exceeded both the control's inhibition zone diameters (piperacillin 12 mm and gentamicin 10 mm). Sudakar et al. (2006) also investigated the antimicrobial activity of an *E. hirta* ethanol extract against several bacteria. The extract was highly effective against *E. coli*, *P. vulgaris* and *P. aeruginosa* and the zones of inhibition as well as MIC was 21 mm; 0.189 mg/ml, 19 mm; 0.200 mg/ml and 23 mm; 0.166 mg/ml respectively.

Kirbag et al. (2013) did an extensive study on the antimicrobial activity of several *Euphorbia* species. The latex as well as a methanolic extract of *E. macroclada* was tested. Both tested samples were effective against all test bacteria which included *P. vulgaris*, *E. coli* and *P. aeruginosa*. MIC values were 50, 100 and 25 mg/ml respectively.

Mothana et al. (2009) investigated medicinally important properties of Yemeni plants. Among the properties of interest were antibacterial properties. *E. socotrana* exhibited antibacterial acitivty against several test bacteria, of which *M. flavus* is of interest due to its genera being closely related to that of *K. polaris*. The zone of inhibition was 18 mm which was determined by the study to be significant.

Kamba and Hassan (2010) studied the phytochemical composition as well as the antibacterial activity of extracts made from the leaves, stems and roots of *E. balsamifera*. Of all the extracts, the root extract exhibited the best activity in terms of the lowest MIC (5 mg/ml). Among the susceptible bacteria were *E. coli* and *P. aeruginosa*.

Jahan et al. (2011) focused on the antibacterial activity of different types of extracts, as compared to each other. The different extracts samples tested methanolic, acetone, ethyl acetate, aqueous and gemmo-modified extracts of *E. tirucalli* and another medicinal plant. The methanolic and gemmo-modified extracts were the most effective compared to the other solvents. Both these extracts successfully inhibited the growth of *E. coli* but the gemmo-modified extract had superior activity. Upadhyay et al. (2010) aimed to validate several claims of medicinal properties of *E. tirucalli*. One of their obejctives was to evaluate the antibacterial activity of the crude methanolic extract of the plant's leaves and stem/bark.

Concentrations as low as 2.5 mg/ml exhibited activity against several bacteria. At the lowest concentration, zones of inhibition could be observed for *E. coli*, *P. vulgaris* and *P. aeruginosa*, among others. As described above, Parekh and Chanda (2007) did extensive investigation on the several properties, including antimicrobial, on Indian plants. The methanolic extract of *E. tirucalli* was a successful antibacterial against *E. coli* among others.

E. pulcherma, more commonly known as poinsettia, was used in a study by Yakubu and Mukhtar (2011) in order to evaluate the plants antibacterial properties. The flowers, leaves, stems and whole plants were used to produce both ethanolic as well as aqueous extracts. Both types of extracts made from all parts except the flowers exhibited antibacterial activity against all bacteria tested. An MIC of 5.00mg/ml was observed for *E. coli* for all extracts, except for that of the flowers as mentioned.

It is evident that the results obtained, antibacterial activity of the *E. gummifera* extract against *K. polaris*, *P. paravulva* and *P. vulgaris*, was consistent with several similar studies done on other *Euphorbia* species, thus corroborating the antibacterial activity of the plant. Of specific interest to this study is the similar antibacterial activity of the *E. gummifera* metanolic extract and fractions observed compared to that several of other *Euphorbia* species' extracts against the same bacteria or closely related bacteria.

4.6.3 Bioautography

From the results in Table 4.4 it was clear that most of the major fractions from the silica column chromatography on the *E. gummifera* extract, appeared to exhibit antibacterial activity on both of the identified bacteria, *K. polaris* and *P. paravulva*.

The first group of compounds that eluted from the column was the non-polar compounds due to the non-polar solvent hexane being the major solvent in the eluent. The bacterial broth cultures as well as the INT solution contain a large percentage of water. Water is very polar and as a result the non-polar molecules that are extremely hydrophobic could distort the result. Thus the inhibition zone observed from fractions A to I might not be a result of antibacterial compound(s) but mere different polarities preventing adequate mixture of water with non-polar compounds.

The middle polarity and polar fraction exhibited strong UV reactive properties (Chapter 3). Fluorescence can be due to the presence of aromatic functional groups, aliphatic/alicyclic groups and conjugated double bonds (Sharma, 2000). These functional groups, being associated with more polar compounds could be responsible for the visible inhibition. Inside a solution, unsaturated hydrocarbons such as quinolone, isoquinoline and indole, fluoresce under UV light (Khopka, 1998). Treatment with vanillin reveals

compounds with functional groups such as amines, hydroxyl and carbonyl groups (Pirrung, 2016). Thus, overall the more polar compounds could be responsible for the antibacterial activity, yet the non-polar compounds cannot be ruled out before taking the GC-MS results into consideration.

4.6.4 GC-MS-analysis

From the GC-MS analysis and further research it was evident that *E. gummifera* contained several compounds that have not only been identified in other *Euphorbia* species but also have been tested for antimicrobial activity (Table 4.5). Lupeol had been referred to as a magical drug (Wal et al., 2015). The antibacterial activity of lupeol was tested against several pathogenic bacteria which included strains of *E. coli*, *P. aeruginosa* and others. For both the bacteria, MIC values of 250 µg/ml were observed. Tamokou et al. (2010) investigated both the antioxidant as well as antimicrobial activity of fractions and compounds obtained from the *Albizia adianthifolia* plant. Two compounds were tested, of which one was lupeol. The compound was an active antimicrobial at an MIC of 0.25 mg/ml against *P. mirabilis*. Lupeol has been isolated from several *Euphorbia* species: *E. hirta* (Ragasa and Cornelio, 2013), *E. larica* (Jassbi, 2006), *E. bivonae* (Stefano et al., 2011), *E. chamaesyce* (Tanaka et al., 1999), *E. lagascae* (Duarte, 2008), *E. tirucalli* (Gupta et al., 2013). Lupeol was present in several fractions of interest: C, D, G to L and N to BB which all exhibited antibacterial activity.

Özçelik et al. (2011) evaluated the antibacterial activity several different compounds which included quinic acid. Among the susceptible bacteria were *E. coli*, *P. aeruginosa* and *P. mirabilis*, where the MIC values for the compound was 8, 4 and 8 µg/ml respectively for each. The compound has been found in *E. hirta* (Gopi et al., 2015) as well as *E. macroclada* and *E. gaillardotii* (Ertas et al., 2015). Quinic acid was found in fractions BB, DD and FF that were not potent antibacterial fractions. However, this compound may play a role in the whole extracts' antibacterial activity.

Amyrins are known for their potent antimicrobial activity (Vázquez et al., 2012). Conrado et al. (2015) investigated the antibacterial activity of the extract, fractions and compounds obtained from *Protium hebetatum*. Both α- and β-amyrin was identified in the extract and selected fractions. The extract exhibited antibacterial activity against *S. aureus* and *E. faecalis*. Rivero-Cruz et al. (2009) investigated the antimicrobial activity of several isolated compounds as a possible remedy for microbial oral disease. β-Amyrin exhibited antibacterial activity against several pathogenic bacteria including *E. coli* and *P. aeruginosa*. Both the amyrins have been identified in several *Euphorbia* species. α-Amyrin has been identified in *E. hirta* (Ragasa and Cornelio, 2015), *E. characias* (Fernandes-Freire et al., 1990) and *E.*

grandialata (Ismail et al., 2017). α-Amyrin was only found in fraction H that had potent antibacterial activity.

Rivero-Cruz et al. (2009) isolated several compounds from *Byrsonima crassifolia* and evaluated their antimicrobial potential. One of the tested compounds was β-amyrin, which showed antibacterial activity against several of the test organisms, including *E. coli* and *P. aeruginosa* with MIC values of 500µg/ml and 1mg/ml respectively. Similarly to α-amyrin, β-amyrin has been islolated from several *Euphorbia* species such as *E. hirta* (Martínez-Vázquez et al., 1999; Ragasa and Cornelio, 2013), *E. decipiens* (Ahmad et al., 2002a) and *E. larica* (Jassbi, 2006). β-Amyrin was found in fraction C,E, F and G. Of these, only C and G exhibited antibacterial activity.

Betulin was found by Tene et al. (2009) to possess antimicrobial activity during their study on terpenoids from *Croton macrostachys*. The compound exhibited antibacterial activity against three pathogenic bacteria with MIC values ranging from 31.25 to 500µg/ml. As mentioned above, Rivero-Cruz et al. (2009) isolated compounds from *B. crassifolia* and for the purpose of studying their antimicrobial properties betulin was also isolated and tested. The compound exhibited antibacterial activity against all tested bacteria including *E. coli* and *P. aeruginosa*. However, the MIC values (both 1.03 mg/ml) were much higher as compared to β-amyrin. Betulin has been found in *E. teheranica* (Jassbi, 2000), *E. heteradena* (Ahmad et al., 2000b), *E. rigida* (Gherraf et al., 2010), *E. latifolia* (Zhang et al., 2006) and *E. myrsinites* (Öksüz et al., 1995). Fractions D, E, G to J, L and X contained betulin, all of which had strong antibacterial activity.

Basile et al. (1999) isolated pure flavonoids from several moss species in an attempt to evaluate their antibacterial activity. One such flavonoid was lucenin 2. The flavonoid was antibacterial against all test bacteria including *E. coli* and *P. aeruginosa*. Lucenin 2 has not been isolated or found in any *Euphorbia* species, but only mosses (*B. pomiformis*, *H. ciliate*, *P. affine*, *P. cuspidatum*, *D. scoparium*). The compound was identified in fractions J and O to V, which were all antibacterial.

Roridins are classified as trichothenes which are produced by fungi as defense compounds known as mycotoxins (Xu et al., 2006). These compounds also act as antimicrobials against bacteria and yeasts. Wagenaar and Clardy (2001) extracted metabolites from a *Myrothecium* species to investigate its anticancer and antimicrobial properties. The extract exhibited antibacterial activity against *S. cerevisiae* and two yeasts. Of the extracted metabolites identified, roridin E was one. Roridin E was also found to be produced by *M. roridum* marine fungi (Xu et al., 2006). This interesting compound has not previously been identified as being produced by plants. Identification in *E. gummifera* fractions could indicate an

endophytic fungal producer. Fractions R and CC was found to contain the compound where the former had antibacterial activity.

Shingate et al. (2013) investigated the antimicrobial activity of lanosterol as well as sterols produced from the former. Lanosterol was found to act antibacterial against *E. coli* with an MIC of 8µg/ml and *S. aureus* with and MIC of above 64µg/ml. The compound has been identified in the latex of *E. peplus* (Giner et al., 2000), *E. lathyris* (Giner et al., 1995), *E. characais* latex (Fernandes-Freire et al., 1990) and *E. pekinensis* (Kong and Min, 1996). Fractions C, D and F contained lanosterol, all of which had antibacterial activity.

Muhammad et al. (2016) investigated the chemical composition of the stem/bark of *Ficus platyphylla* and tested the isolated compounds for anti-bacterial and-tyrosinase activity. Lupeol acetate had antibacterial activity against all tested bacteria. It had an MIC value of 450µg/ml for *E.coli* and *P. aeruginosa.* Among the *Euphorbia* species known to contain lupeol acetate are: *E. larica* (Jassbi, 2006), *E. geniculata* (Eliza et al., 2016) and *E. quinquecostata* (Mbwambo et al., 1996). Fractions B, D, E, I and J were found to contain lupeol acetate and all were antibacterial.

Plant-associated soil microorganisms that have a direct positive effect on the overall health, development and productivity of plants are referred to as plant growth promoting microorganisms (PGPM) (Avis et al., 2008). PGPM improve plant growth by enhancing stress tolerance, inducing disease resistance and increase nutrient availability and acquisition. The term rhizobacteria refers to a group of heterogeneous bacteria that have the ability to colonize the root environment (Ahemad and Kibret, 2014; Ahmad et al 2008; Joseph et al., 2007). It is predominantly the Proteobacteria, especially α and β classes that have been characterized by soil microbiome studies, but other major groups include Actinobacteria, Firmicutes, Bacteroidetes, Planctomycetes, Verrucomicrobia and Acidobacteria (Turner et al., 2013). This group of beneficial bacteria can exert their beneficial effects either directly or indirectly. Direct beneficial growth promotion involves enhancing nutrient availability and uptake while indirect growth promotion involves strengthened responses to potential pathogenic entities (Ahmad et al., 2008; Joseph et al., 2007). Well known PGPR include the *Rhizobium* species as well as species belonging to the *Pseudomanas*, *Bacillus*, *Azospirillum*, *Azotobacter*, *Klebsiella*, *Serratia* and *Enterobacter* (Ahemad and Kibret, 2014; Ahmad et al., 2008; Pereg et al., 2015).

Under stressed conditions, beneficial soil microorganisms play an even more pivotal role in supporting plant growth. Stressed conditions can include environmental stresses such as drought, temperature, salinity, excess water, heavy metals, excessive wind etc. as well as biological stresses such as competition, pathogens and pests. As plants are constantly confronted with a changing environment, they

have evolved mechanisms to cope with the stress imposed by such changes. Arid and semi-arid environments impose a certain level of stress that involves water deficit, high temperatures and salinity. Even though al plants have the ability to respond to these stresses, few plants are completely resistant to these stresses (Rodriguez et al., 2004) reflected by the handful of plants that are able to survive in these harsh conditions.

When *E. gummifera* plants die, large amounts of compounds are released into the soil environment through the decomposition process (described previously) due to the plant's high mass. Of these compounds, antimicrobial compounds are prominent. As the PGPM's are killed off, the subsequent plants are unable to colonize these areas due to the absence of these microorganism combined with the prevailing environmental conditions.

4.7 Conclusion

Overall, the results and previous research indicate that *E. gummifera* plant does have antibacterial activity. The crude extract activity corroborates that of several other similar studies of other *Euphorbia* species. Furthermore, the GC-MS analysis results indicated that the fractions contained several compounds that have both been isolated in other *Euphorbia* species as well as having similar antibacterial activities. In addition, the identification of *K. polaris* and *P. paravulva* from a fairy circle matrix soil could shed some light on the maintenance/origin of this phenomenon.

4.8 References

Abdallah, E.M. 2011. Plants am alternative source of antimicrobials. Journal of Applied Pharmaceutical Science 1(6), 16-20.

Abreu, A.C., McBain, A.J., Simoes, M. 2012. Plants as sources of new antimicrobials and resistance-modifying agents. Natural Product Reports 29, 1007-1021.

Adwan, G., Abu-Sanab, B., Adwan, K. 2010. Antibacterial activities of some plant extracts alone and in combination with different antimicrobials against multidrug-resistant *Pseudomonas aeruginosa* strains. Asian Pacific Journal of Tropical Medicine 3(4), 266-269.

Ahamed, B.K.M., Krishna, V., Gowdru, H.B., Rajanaika, H., Kumar aswamy, H.M., Rajshekarappa, S., Dandin, C.J., Mahadevan, K.M. 2007. Isolation of bactericidal constituents from the steam bark extract of *Grewia tiliaefolia* Vahl. Research Journal of Medicinal Plant 1(3), 72-82.

Ahemad, M. and Kibret, M. 2014. Mechanisms and applications of plant growth promoting rhizobacteria: Current perspective. Journal of King Saud University- Science 26, 1-20.

Ahmad, F., Ahmad, I., Khan, M.S. 2008. Screening of free-living rhizosphere bacteria for their multiple plant growth promoting activities. Microbiological Research 163, 173-181.

A). Ahmad, V.U., Hussain, H., Hussain, J., Jassbi, A.R., Bukhari, I.A.,Yasin, A., Choudhary, M.I., Dar, A., 2002. New bioactive diterpenoids from *Euphorbia decipiens.* Zeitschrift für Naturforschung 57, 1066–1071.

B.) Ahmad, V.U., Zahid, M., Khan, T., Asim, M., Ahmad, A. 2002. Chemical constituents of *Euphorbia heteradenia* Boiss. Proceedings of the Pakistan Academy of Sciences. 39, 201–205.

Al-Mughrabi K.I. 2003. Antimicrobial activity of extracts from leaves, stems and flowers of *Euphorbia macroclada* against plant pathogenic fungi. Phytopathologia Mediterranea 42(3), 245-250.

Avis, T.J., Grave,l V., Antoun, H., Tweddell, R. 2008. Multifaceted beneficial effects of rhizosphere microorganisms on plant health and productivity. Soil Biology and Biochemistry 40, 1733-1740.

Basile, A., Giordano, S., López-Sáez, J.A., Cobianchi, R.C. 1999. Antibacterial activity of pure favonoids isolated from mosses. Phytochemistry 52, 1479-1482.

Betoni, J.E.C., Mantovani, R.P., Barbosa, L.N., Di-Stasi, L.C., Fernandes, A. 2006. Synergism between plant extract and antimicrobial drugs used on *Staphylococcus aureus* diseases. Memórias do Instituto Oswaldo Cruz 101(4), 387-390.

Chandramu, C., Manohar, R.D., Krupadanam, D.G., Dashavantha, R.V. 2003. Isolation, Characterization and Bio- logical Activity of Betulinic Acid and Ursolic Acid from *Vitex negundo* L. Phytotherapy Research 17(2), 129-134.

Conrado, G.G., Simplicio, F.G., Costa, K.R.C., Rehder, V.L.G., Espinar, M.F., Souza, G.O., Sampaio, P.T.B. 2015. Antibacterial activity and chemical compounds of leaves and branches of *Protium hebetatum*. Revista Brasileira de Plantas Medicinais 17(4), 865-874.

Duarte, N. 2008. Structural Characterization and Biological Activities of Terpenic and Phenolic Compounds Isolated from *Euphorbia lagascae* **and** *Euphorbia tuckeyana*. PhD Thesis Universidade de Lisboa Faculdade de Farmácia.

Eloff, J.N. 1998. A sensitive and quick microplate method to determine the minimal inhibitory concentration of plant extracts for bacteria. Planta Medica 64, 711-713.

Eliza, E., Fatsiami, R., Yusuf, S., Ferlinahayati, F. 2016. Isolation of triterpenoid from katemas (*Euphorbia geniculata* Ortega) stem extracted using methanol and its toxicity test. Indonesian Journal of Fundamental and Applied Chemistry 1(1), 19-23.

Elulmalai, E.K., Prasad, T.N.V.K., Hemachandran. J., Viviyan Theresa, S., Thirumalai, T., David, E. 2010. Extracellular synthesis of silver nanoparticles using leaves of *Euphorbia hirta* and their antibacterial activities. Journal of Pharmaseuticals Science and Research 2(9), 549-554.

Ertas, A., Yilmaz, M.A., Firat, M. 2015. Chemical profile by LC–MS/MS, GC/MS and antioxidant activities of the essential oils and crude extracts of two *Euphorbia* species, Supplementary material. Natural Product Research 29(6), 529–534.

Fernandes-Freire, M., Novais, J.M., Pais, M.S.S. 1990. Free triterpenols and sterols produced by *in vitro* cultures and laticifer cells from *Euphorbia characias*. Phytochemistry 29(6), 1855-1860.

Freire, M.F.I., Carvalho Mario, G., Berbara, R.L.L., Freire, R.B. 2008. Antimicrobial activity of lupeol acetate from *Vernonia scorpioides* Pers. Asteraceae Revista Brasileirade Farmacia.83, 83-87.

Gherraf, N., Zellagui, A., Mohamed, N. S. Hussien, T. A., Mohamed, T. A., Hegazy, M. F., Rhouati, S., Moustafa, M. F. M., El-Sayed, M. A., Mohamed, A. H. 2010. Triterpenes from *Euphorbia rigida*. Pharmacognosy Research 2(3), 159-162.

Gilani, A.H. and Atta-ur-Rahman. 2005. Trends in ethnopharmacology. Journal of Ethnopharmacology 100, 43-49.

Giner, J., Berkowitz, J.D., Andersson, T. 2000. Nonpolar components of the latex of *Euphorbia peplus.* Journal of Natural Products 63, 267-269.

Giner, J. and Djerassi, C. 1995. A reinvestigation of the biosynthesis of lanosterol in *Euphorbia lathyris*. Phytochemistry 39(2), 333-335

Gopi, K., Renu, K., Vishwanath, B.S., Jayaraman, G. 2015. Protective effect of *Euphorbia hirta* and its components against snake venom induced lethality. Journal of Ethnopharmacology 165, 180-190.

Gupta, N., Vishnoi, G., Wal, A., Wal, P. 2013. Medicinal Value of *Euphorbia tirucalli*. Systematic Reviews in Pharmacy 4(1), 40-47.

Halberstein, R.A. 2005. Medicinal Plants: Historical and Cross-Cultural Usage Patterns. Annals of Epidemiology 15(9), 686-699.

Hall, T.A. 1999. BioEdit: a user-friendly biological sequence alignment editor and analysis program for Windows 95/98/NT. Nucleic Acids Symposium Series 41, 95-98.

Hall-Stoodley, L., Costerton, J.W., Stoodley, P. 2004. Bacterial biofilms: From the natural environment to infectious diseases. Nature Reviews Microbiology 2, 94-108.

Ismail, M., Owis, A.I., Hetta, M., Mohammed, R. 2017. Total phenolics and flavonoids content, antioxidant activity and GC/MS analyses of *Euphorbia grandialata*. Journal of Applied Pharmaceutical Science 7(6), 176-181.

Jabeen, K., Javaid, A., Ahmad, E., Athar, M. 2011. Antifungal compounds from *Melia azederach* leaves for management of *Ascochyta rabiei*, the cause of chickpea blight, Natural Products Research 25(3), 264-276.

Jahan, N., Khalil-Ur-Rehman, Ali, S., Bhatti, I.A. 2011. Antimicrobial potential of gemmo-modified extracts of *Terminalia arjuna* and *Euphorbia tirucalli.* International Journal of Agriculture and Biology 13(6), 1001-1005.

Jarvis, B.B. and Wang, S. 1999. Stereochemistry of the Roridins. Diastereomers of Roridin E. Journal of Natural Products 62(9), 1284-1280.

Jassbi, A.R. 2006. Chemistry and biological activity of secondary metabolites in *Euphorbia* from Iran. Phytochemistry 67, 1977-1984.

Jassbi, A.R. 2000. Phytochemical investigations on some medicinal plants from families Euphorbiaceae and Lamiaceae. PhD Thesis, HEJ Research Institute of Chemistry, Karachi University, Pakistan.

Joseph, B., Patra, R.R., Lawrence, R. 2007. Characterization of plant growth promoting rhizobacteria associated with chickpea (*Cicer arietinum* L.). International Journal of Plant Production 2, 141-152.

Joubert, A. 2008. Investigation on selected biotic and abiotic factors in the maintenance of the "fairy circles" (barren patches) of southern Africa. MSc thesis, University of Pretoria, South Africa.

Kamba, A.S. and Hassan, L.G. 2010. Phytochemical screening and antimicrobial activities of *Euphorbia balsamifera* leaves, stems and root against some pathogenic microorganisms. African Journal of Pharmacy and Pharmacology 4(9), 645-652.

Khopkar, S.M. 1998. Molecular luminance spectroscopy, in: Khopkar, S.M., (Eds.), Basic concepts of analytical chemistry. New Age International.

Khullar, N. 2010. Antimicrobials from plants and their use in therapeutics and drug discovery. The IIOAb Journal 1(3), 31-37.

Kirbag, S., Erecevit, P., Zengin, F., Guvenc, A.N. 2013. Antimicrobial activity of some *Euphorbia* species. African Journal of Traditional, Complementary and Alternative Medicine 10(5), 305-309.

Kong, L.Y. and Min, Z.D. 1996. Studies on chemical constituents of roots of *Euphorbia pekinensis*. Acta Pharmaceutica Sinica 31(7), 524-529.

Kumar, S., Malhotra, R., Kumar, D. 2010. *Euphorbia hirta:* Its chemistry, traditional and medicinal uses, and pharmacological activities. Pharmacognosy Review 4(7), 58-61.

Lin, J., Dou, J., Xu, J., Akber Aisa, H. 2012. Chemical composition, antimicrobial and antitumor activities of the essential oils and crude extracts of *Euphorbia macrorrhiza*. Molecules 17, 5030-5039.

Liu, Q., Zhanga, Y., Yu, N., Bi, Z., Zhu, A., Zhan, X., Wu, W., Yu, P., Chen, D., Cheng, S., Cao, L. 2015. Genome sequence of *Pseudomonas parafulva* CRS01-1, an antagonistic bacterium isolated from rice field. Journal of Biotechnology 206, 89-90.

Lutta, K.P., Bii, C., Akenga, A.T., Cornelius, W.W. 2008. Antimicrobial marine natural product from the sponge *Axinella infundibuliformis*. Records of Natural Products 2(4), 116-127.

Madureira, A.M., Ascenso, J.R., Valdeira, L., Duarte, A., Frade, J.P., Freitas, G., Ferreira, M.J.U. 2003. Evaluation of the antiviral and antimicrobial activities of triterpenes isolated from *Euphorbia segetalis.* Natural Product Research 17(5), 375-380.

Mahesh, B. and Satish, S. 2008. Antimicrobial activity of some important medicinal plants against plant and human pathogens. World Journal of Agricultural Science 4, 839-843.

Margulis, L. and Chapman, M.J. 2009. Kingdoms and Domains: An Illustrated Guide to the Phyla of Life on Earth, Elsevier Science.

Martínez-Vázquez, M., Ramírez Apan, T.O., Lazcano, E.M., Bye, R. 1999. Anti-inflammatory Active Compounds from the *n*-Hexane Extract of *Euphorbia hirta*. Revista de la Sociedad Química de México 43(4), 103-105.

Mbwambo, Z.H., Lee, S.K., Mshiu, E.N., Pezzuto, J.M., Kinghorn, A.D. 1996. Constituents from the stem wood of *Euphorbia quinquecostata* with phorbol dibutyrate receptor-binding inhibitory activity. Journal of Natural Products 59, 1051–1055

Mothana, R.A., Lindequist, U., Gruenert, R., Bednarski, P.J. 2009. Studies of the *in vitro* anti-cancer, antimicrobial and antioxidant potentials of selected Yemeni medicinal plants from the island Soqotra. BMC Complementary and Alternative Medicine 9(7), 1-11.

Muhammad, A., Ya'u, M., Sirat, H.M. 2016. Antibacterial and Antityrosinase of isolated compounds from stem bark of *Ficus platyphylla* Del. Proceedings of 28th ISERD International Conference, Kyoto Japan, 45-49.

Öksüz, S.; Gürek, F.; Gil, R. R.; Pengsuparp, T.; Pezzuto, J. M.; Cordell, G. A. 1995. Four diterpene esters from *Euphorbia myrsinites*. Phytochemistry 38, 1457-1462.

Özçelik, B., Kartal, M., Orhan, I. 2011. Cytotoxicity, antiviral and antimicrobial activities of alkaloids, flavonoids, and phenolic acids. Pharmaceutical Biology 49(4), 369-402.

Parekh, J. and Chanda, S.V. 2007. *In vitro* antimicrobial activity and phytochemical analysis of some Indian medicinal plants. Turkish Journal of Biology 31, 53-58.

Pereg. L. and McMillian. M. 2015. Scoping the potential uses of beneficial microorganisms for increasing productivity in cotton cropping systems. Soil Biology and Biochemistry 80, 349-358.

Petrovska, B.B. 2012. Historical review of medicinal plants' usage. Pharmacognosy Review 6(11), 1-5.

Pirrung, M.C. 2016. Following the Reation, in: Handbook of Synthetic Organic Chemistry, 2nd edition. Elsevier Academic Press.

Pisano, M.B., Cosentino, S., Viale, S., Spanò, D., Corona, A., Esposito, F., Tramontano, E., Montoro, P., Tuberoso, C.I.G., Medda, R., Pintus, F. 2016. Biological activities of aerial parts extracts of *Euphorbia characias.* BioMed Research International 2016, 1-11.

Racaniello, V. 2009. Detecting viruses: the plaque assay. Virology blog: About viruses and viral disease. [Online available: http://www.virology.ws/2009/07/06/detecting-viruses-the-plaque-assay/] [Date accessed: 25 July 2017].

Ragasa, C.Y. and Cornelio, K.B. 2013. Triterpenes from *Euphorbia hirta* and their cytotoxicity. Chinese Journal of Natural medicine 11(5), 528-533.

Reddy, G.S.N., Prakash, J.S.S., Prabahar, V., Matsumoto, G.I., Stackebrandt, E., Shivaji, S. 2003. *Kocuria polaris* sp. nov., an orange-pigmented psychrophilic bacterium isolated from an Antarctic cyanobacterial mat sample. International Journal of Systematic and Evolutionary Microbiology 53, 183-187.

Rivero-Cruz, J.F., Sánchez-Nieto, S., Benítez, G., Casimiro, X., Ibarra-Alvarado, C., Rojas-Molina, A., Rivero-Cruz, B. 2009. Antibaterial compounds isolated from *Byrsonima crassifolia*. Revista Latinoamericana de Química 37(2), 155-163.

Rodriguez, R.J., Redman, R.S., Henson, J.M. 2004. The role of fungal symbiosis in the adaption of plants to high stress environments. Mitigation and Adaptation Strategies for Global Change 9**,** 261–272.

Saga, T. and Yamaguchi, K. 2009. History of antimicrobial agents and resistant bacteria. Japan Medical Association Journal 52(2), 103-108.

Savini, V., Catavitello, C., Masciarelli, G., Astolfi, D., Balbinot, A., Bianco, A., Febbo, F., D'Amario, C., D'Antonio, D. 2010. Drug sensitivity and clinical impact of members of the genus *Kocuria*. Journal of Medical Microbiology 59, 1395-1402.

Sharma, B.K. 2000. Molecular Luminescence Fluorometry and Phosphorimetry, in: Sharma, M. (Eds), Instrumental Methods of Chemical Analysis. Krishna Prakashan Media.

Sherma, J., O'Hea, C.M., Fried, B.J. 1992. Separation, identification and quantification of chloroplast pigment by HPLC with scanning densitometry. Journal of Planar Chromatography - Modern TLC 5, 343‑349.

Shingate, B.B., Hazra, B.G., Salunke, D.B., Pore, V.S., Shizari, F., Deshpande, M.V. 2013. Synthesis and antimicrobial activity of novel oxysterols from lanosterol. Tetrahedron 69, 11155-11163.

Sibanda, T. and Okoh, A.I. 2007. The challenges of overcoming antibiotic resistance: Plant extracts as potential sources of antimicrobial and resistance modifying agents. African Journal of Biotechnology 6(25), 2886-2896.

Sosa, A.A., Bagi, S.H., Hameed, H.I. 2016. Analysis of bioactive chemical compounds of *Euphorbia lathyrus* using gas chromatography-mass spectrometry and Fourier-transform infrared spectroscopy. Journal of Pharmacognosy and Phytoterapy 8(5), 109-126.

Stackebrandt, E., Koch, C., Gvozdiak, O., Schumann, P. 1995. Taxonomic dissection of the genus *Micrococcus*: *Kocuria* gen. nov., *Nesterenkonia* gen. nov., *Kytococcus* gen. nov., *Dermacoccus*

gen. nov., and *Micrococcus* Cohn 1872 gen. emend. International Journal of Systematic Bacteriology 45(4), 682-692.

Stapleton, P.D., Shah, S., Anderson, J.C., Hara, Y., Hamilton-Miller, J.M.T., Taylor, P.W. 2004. Modulation of ß-lactam resistance in *Staphylococcus aureus* by catechins and gallates. International Journal of Antimicrobial Agents 23(5), 462-467.

Stefano, V.D., Pitonzo, R., Schillaci, D. 2011. Chemical constituents and antiproliferative activity of *Euphorbia bivonae*. Chemistry of Natural Products 47(4), 660-664.

Sudhakar, M., Rao, C.V., Rao, P.M., Raju, D.B., Venkateswarlu, Y. 2006. Antimicrobial activity of *Caesalpinia pulcherrima*, *Euphorbia hirta* and *Asystasia gangeticum*. Fitoterapia 77, 378-380.

Suresh, K., Deepa, P., Harisaranraj, R., Vaira Achudhan, V. 2008. Antimicrobial and Phytochemical Investigation of the Leaves of *Carica papaya* L., *Cynodon dactylon* (L.) Pers., *Euphorbia hirta* L., *Melia azedarach* L. and *Psidium guajava* L. Ethnobotanical Leaflets 12, 1184-1194.

Swerdlow, J. 2000. Nature's Medicine: Plants That Heal. National Geographic Society.

Tamakou, J.D., Mpetga, D.J.S., Lunga, P.K., Tene, M., Tane, P., Kuiate, J.R. 2012. Antioxidant and antimicrobial activities of ethyl acetate extract, fractions and compounds from stem bark of *Albizia adianthifolia* (Mimosoideae). Complementary and Alternative Medicine 12(99), 1-10.

Tanaka, R., Kasubuchi, K., Kita, S., Matsunaga, S. Obtusifoliol and related steroids from the whole herb of *Euphorbia chamaesyce*. Phytochemistry 41(3), 457-463.

Tene, M., Ndontsa, B.L., Tane, P., Tamokou, J., Kuiate, J-R. Antimicrobial diterpenoids and triterpenoids from the stem bark of *Croton macrostachys*. Internation Journal of Biological and Chemical Sciences 3(3), 538-544.

Turner T.R., James E.K., Poole P.S. 2013. The plant microbiome. Genome Biology 14 (209), 1-10.

Uchino, M., Shida, O., Uchimura, T., Komagata, K. 2001. Recharacterization of *Pseudomonas fulva* Iizuka and Komagata 1963, and proposals of *Pseudomonas parafulva* sp. nov.and *Pseudomonas cremoricolorata* sp. nov. Journal of General and Applied Microbiology 47, 247-261.

Upadhyay, B., Singh, K.P., Kumar, A. 2010. Ethno-medicinal, phytochemicals and antimicrobial studies of *Euphorbia tirucalli* L. Journal of Phytology 2(4), 65-77.

Vázquez, L.H., Palazon, J., Navarro-Ocaña, A. 2012. The Pentacyclic Triterpenes α, β-amyrins: A Review of Sources and Biological Activities, in: Rao, V. (Eds), A Global Perspective in the role Nutrition and Health, INTECH, pp. 487-505.

Verma, R.N. and Batra, A. 2013. Isolation and analytic characterization of rebaudioside A and GC-MS analysis of methanolic leaves extract of *Stevia rebaudiana* Bert. Annals of Phytomedicine.

Wagenaar, M.M. and Clardy, J. 2001. Two New Roridins Isolated from *Myrothecium* sp. The Journal of Antibiotics 54(6), 517-520.

Wal, A., Srivastava, R.S., Wal, P., Rai, A., Sharma, S. 2015. Lupeol as a magical drug. Pharmaceutical and Biological Evaluations 2(5), 142-151.

Wal, P., Wal, A, Sharma, G., Rai, A.K. 2011. Biological Activities of Lupeol. Systematic Reviews in Pharmacy 2(2), 96-105.

World Health Organization. 2011. WHO Regional Committee for Europe, European strategic action plan on antibiotic resistance. [Online available:

http://www.euro.who.int/__data/assets/pdf_file/0008/147734/wd14E_AntibioticResistance_111380.pdf]. [Date accessed: 8 June 2017].

Xu, J., Takasaki, A., Kobayashi, H., Oda, T.,Yamada, J., Mangindaan, R.E.P., Ukai†, K., Nagai, H., Namikoshi, M. 2006. Four new macrocyclic trichothecenes from two strains of marine-derived fungi of the genus *Myrothecium*. The Journal of Antibiotics 59(8), 451-455.

Yakubu, A. I and Mukhtar, M. D. 2011. In vitro antimicrobial activity of some phytochemical fractions of *Euphorbia pulcherima* L. (Poinsettia). Journal of Medicinal Plants Research 5(12), 2470-2475.

Yusef, H.H., Belal, M.A., El-Sharouny, E.E. 2014. Production of natural pigments from novel local psychrotolerant *Kocuria* spp. Life Science Journal 11(9), 500-507.

Zhang, L. H., Zhang, G. T., Ye, W. C., Yin, Z. Q., Zheng, D., Zhao, S. X. 2006. Chemical constituents from *Euphorbia latifolia*. Natural Product Research and Development 18, 58-60.

Zheng, Y., Huang, W., Yoo, J., Ebersole, J. L., Huang, C. B. 2011. Antibacterial compounds from *Siraitia grasvenorii* leaves. Natural Products Research, 25(9): 890-897.

CHAPTER 5

General conclusion

5.1 Introduction

Fairy circles are classified as one of nature's intriguing unexplained botanical phenomena. Notwithstanding its infamous nature, it is also one of controversy and dispute in the scientific community. This contentious scientific anomaly has led to contradicting theories put forth by a diverse set of global scientists, over the better part of the last 45 years. Even with such worldwide interest, no single theory has been accepted/proven, further baffling the scientific community.

Theories range from social insects, vegetation patterning, volatile gas emissions, microorganisms and plant-based allelopathy. This project aimed to provide information in support of the allelopathy and to the microbial theories.

5.2 General conclusion

Overall, the *E. gummifera* methanol extract exhibited phytotoxic activity that could indicate allelopathic properties. The allelopathic/phytotoxic activity was, however, linked to water stress, thus suggesting a synergistic relationship between the plant's toxicity and water stress. Lucenin 2, a known allelopathic compound, was identified by GC-MS as being present in fractions derived from the plant extract. This compound could be linked to the extract's germination inhibition activity. The plants phytotoxicity was directly linked to the collected fairy circle soil in that similar results were observed for the bio-assays. The most profound inhibition was observed when using soil collected from underneath dead *E. gummifera* plants. Emphasis was put on the decaying process of plants in nature and how compounds are modified once they enter the natural soil environment. Initially these compounds are present in high concentrations which causes germination and growth inhibition. Yet as a web of biotic and abiotic factors shape and breakdown these compounds, their concentrations dwindle down to a level where it could cause the opposite effects on plants until finally disappearing from the environment. This process can explain the appearance and disappearance of fairy circles as part of the allelopathy theory.

The chemistry of *E. gummifera* was all but a mystery until the commencement of this project. Chromatographic methods including TLC, silica column chromatography and GC-MS provided vital information on the chemistry of the plant (identification of 216 compounds). Several different compounds were identified that had previously been identified in members of the *Euphorbia* genus, whereas others are not common to this genus. Among these compounds were potent antibacterial compounds.

Several compounds were identified by GC-MS that exhibited similar antibacterial activity to that previously published. Similarity was in terms of MIC values as well as the tested bacteria. Of the test bacteria used, two were isolated and identified from the rhizosphere of grasses that grow in-between fairy circles. These were the pigmented bacteria *K. polaris* and *P. paravulva*. These bacteria could play a pivotal role in aiding in the survival of plant in terms of phytoprotection and defense compounds (described in Chapter 4). Their susceptibility to the extract and the antibacterial compounds identified could possibly indicate that these bacteria could be absent from inside fairy circles. These pigmented bacteria could play a role in the origin and maintenance of Garub fairy circles, but further studies are needed to provide supporting data.

A general model that could explain the formation, maintenance and disappearance of fairy circles based on the allelopathic and antibacterial porperties of *E. gummifera* is shown in Figure 5.1. Even though the results are promising and do shed light on possible explanations for the origin and maintenance of Garub fairy circles and possibly others, further research is vital to support the findings already made.

These include in-field experiments to demonstrate allelopathic activity as mimicking the exact environmental conditions would allow more accurate results. The chemistry of *E. gummifera* is still not fully investigated. Alternative extraction, separation and identification methods need to be employed. These include HPLC and NMR in order to identify toxic phorbol esters. The antimicrobial activity needs to be evaluated at a bigger scope. This includes a wider variety of bacteria as well as fungi.

Figure 5.1: Proposed model for formation of fairy circles from the death of *E. gummifera* followed by fairy circle formation and finally fairy circle death.

Appendix A

Collection data

Table A1: Specifics of the collection of soil from inside fairy circle

Inside circle (IS)	IS1	IS2	IS3	IS4	IS5	IS6	IS7	IS8	IS9	IS10
1. GPS coordinates	S 26° 36.148' O 16° 0.874'	S 26° 36.166' O 16° 0.839'	S 26° 36.176' O 16° 0.850'	S 26° 36.195' O 16° 0.863'	S 26° 36.220' O 16° 0.859'	S 26° 36.219' O 16° 0.849'	S 26° 36.204' O 16° 0.839'	S 26° 36.202' O 16° 0.830'	S 26° 36.201' O 16° 0.821'	S 26° 36.181' O 16° 0.836'
2. Date and time	17 March 08:52	09:06	09:15	09:28	09:38	09:47	09:56	10:04	10:13	10:22
3. Additional information										
3.1 Comments on soil characteristics	Very small pebbles on top followed by fine sand. Tiny holes visible on surface.	Very small pebbles on top followed by fine sand. Tiny holes visible on surface.	Very small pebbles on top followed by fine sand. Tiny holes visible on surface.	More plants surrounding circle. Circle is oval shaped.	More plants near the circle. Circle is oval shaped.	Small circle.	Big circle. Long oval shaped. Fine sand.	Very big circle.	Sand inside circle has a hard surface that breaks when sample is taken.	Very small pebbles on top followed by fine sand. Tiny holes visible on surface.

3.2 Comments on plants inside circle	No plants inside.	Plants found on edge/matrix have a thick sand layer on roots.	Few plants inside.	Located near an *E. gummifera*	A much-defined matrix of plants. One plant on the inside.		Small plants near edge on inside.	Small plants near edge on inside.		Dry plants that is burned black located on edge.
3.3 Furthers comments			Circle is a bit sunken (not level).	A hard sand formation found on the inside of the circle. Resembles a type of nest. An ant was observed.	Heart shaped and located on a slope.		Located on a slope.	Oval shaped and located on a slope.	Small circle and has the same sand formation as IS4. Animal droppings also found inside circle.	Not a defined circle. Same sand formation as IS4 and IS9.

Table A2: Specifics of the collection of soil from outside fairy circles

Outside circles (OS)	OS1	OS2	OS3	OS4	OS5	OS6	OS7	OS8	OS9	OS10
1. GPS coordinates	S 26° 36.154' O 16° 0.855'	S 26° 36.182' O 16° 0.850'	S 26° 36.172' O 16° 0.843'.	S 26° 36.209' O 16° 0.863'	S 26° 36.220' O 16° 0.853'	S 26° 36.212' O 16° 0.843'	S 26° 36.203' O 16° 0.835'	S 26° 36.201' O 16° 0.825'	S 26° 36.190' O 16° 0.828'	S 26° 36.172' O 16° 0.837'
2. Date and time	09:00	09:11	09:23	09:34	09:44	09:50	10:00	10:08	10:15	10:27
3. Additional information										
3.1 Comments on soil characteristics	Less small pebbles on top. Grasses growing.	Sand very fine. Texture more constant.	Sand very fine. Texture more constant.	Many grasses. Compact soil.	A lot of grass. Compact soil.	Sand less compact.	Sand less compact.	Sand less compact .	Less compact soil.	
3.2 Comments on plants outside circle	Thick layer of sand on plant roots.	Thick layer of sand on plant roots.	Thick layer of sand on plant roots.	Plants are small.	Plants are small.	Less of a thick sand layer on plant roots.		Less of a thick sand layer on plant roots.		
3.3 Further comments		Animal droppings found.	Animal droppings found.	On a slope.	On a slope.	Animal droppings found.	On a slope.	On a slope.		

Appendix B

Statistical data

B1 Germination inhibition assays data

Table B1.1: Germination inhibition assay statistical data- starting concentration 20mg/ml and 2ml water used

Tukey's Multiple Comparison Test	Mean Diff.	q	P value	95% CI of diff
Control vs 0.624	-5.330	1.947	P > 0.05	-17.62 to 6.961
Control vs 1.25	-10.66	3.895	P > 0.05	-22.96 to 1.627
Control vs 2.5	-5.332	1.948	P > 0.05	-17.62 to 6.959
Control vs 5	-5.332	1.948	P > 0.05	-17.62 to 6.959
Control vs 10	-11.33	4.139	P > 0.05	-23.62 to 0.9592
Control vs 20	-4.000	1.461	P > 0.05	-16.29 to 8.291
0.624 vs 1.25	-5.334	1.948	P > 0.05	-17.63 to 6.957
0.624 vs 2.5	-0.001999	0.0007301	P > 0.05	-12.29 to 12.29
0.624 vs 5	-0.001999	0.0007301	P > 0.05	-12.29 to 12.29
0.624 vs 10	-6.002	2.192	P > 0.05	-18.29 to 6.289
0.624 vs 20	1.330	0.4858	P > 0.05	-10.96 to 13.62
1.25 vs 2.5	5.332	1.948	P > 0.05	-6.959 to 17.62
1.25 vs 5	5.332	1.948	P > 0.05	-6.959 to 17.62
1.25 vs 10	-0.6680	0.2440	P > 0.05	-12.96 to 11.62
1.25 vs 20	6.664	2.434	P > 0.05	-5.627 to 18.96
2.5 vs 5	0.0000	0.0000	P > 0.05	-12.29 to 12.29
2.5 vs 10	-6.000	2.192	P > 0.05	-18.29 to 6.291
2.5 vs 20	1.332	0.4865	P > 0.05	-10.96 to 13.62
5 vs 10	-6.000	2.192	P > 0.05	-18.29 to 6.291
5 vs 20	1.332	0.4865	P > 0.05	-10.96 to 13.62

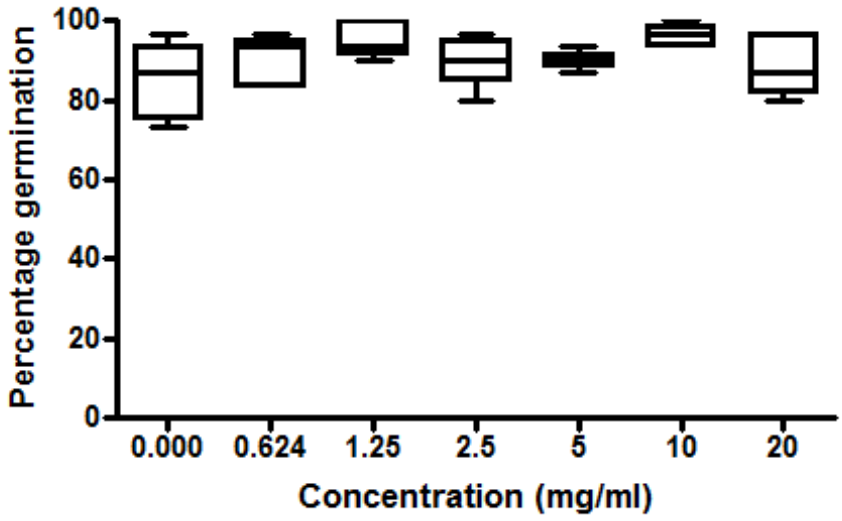

Figure B1.1: Box and whisker diagram of the germination data- Starting concentration 40mg/ml and 2ml water used

Table B1.2: Germination inhibition assay statistical data- starting concentration 40mg/ml and 1ml water used

Tukey's Multiple Comparison Test	Mean Diff.	q	P value	95% CI of diff
Control vs 0.625	12.83	2.426	P > 0.05	-11.65 to 37.32
Control vs 1.25	16.67	3.342	P > 0.05	-6.418 to 39.75
Control vs 2.5	19.34	3.877	P > 0.05	-3.750 to 42.42
Control vs 5	21.33	4.278	P > 0.05	-1.752 to 44.42
Control vs 10	36.17	6.838	P < 0.01	11.68 to 60.66
Control vs 20	57.34	11.50	P < 0.001	34.26 to 80.43
Control vs 40	63.11	10.96	P < 0.001	36.45 to 89.77
0.625 vs 1.25	3.835	0.7250	P > 0.05	-20.65 to 28.32
0.625 vs 2.5	6.503	1.229	P > 0.05	-17.98 to 30.99
0.625 vs 5	8.501	1.607	P > 0.05	-15.99 to 32.99
0.625 vs 10	23.34	4.186	P > 0.05	-2.474 to 49.15
0.625 vs 20	44.51	8.415	P < 0.001	20.02 to 69.00
0.625 vs 40	50.28	8.349	P < 0.001	22.40 to 78.16
1.25 vs 2.5	2.668	0.5350	P > 0.05	-20.42 to 25.75
1.25 vs 5	4.666	0.9356	P > 0.05	-18.42 to 27.75
1.25 vs 10	19.50	3.687	P > 0.05	-4.984 to 43.99
1.25 vs 20	40.67	8.156	P < 0.001	17.59 to 63.76
1.25 vs 40	46.44	8.065	P < 0.001	19.79 to 73.10
2.5 vs 5	1.998	0.4006	P > 0.05	-21.09 to 25.08
2.5 vs 10	16.83	3.183	P > 0.05	-7.652 to 41.32
2.5 vs 20	38.01	7.621	P < 0.001	14.92 to 61.09
2.5 vs 40	43.78	7.602	P < 0.001	17.12 to 70.43
5 vs 10	14.84	2.805	P > 0.05	-9.650 to 39.32
5 vs 20	36.01	7.220	P < 0.001	12.92 to 59.09
5 vs 40	41.78	7.255	P < 0.001	15.12 to 68.44
10 vs 20	21.17	4.003	P > 0.05	-3.316 to 45.66
10 vs 40	26.94	4.473	P > 0.05	-0.9387 to 54.82

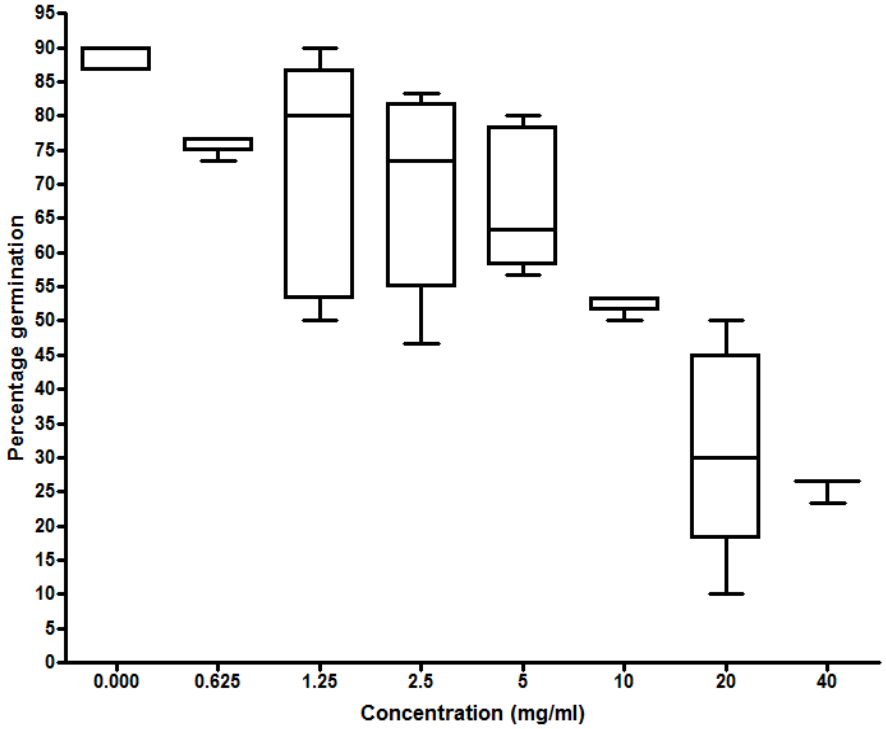

Figure B1.2: Box and whisker diagram of the germination data- Starting concentration 40mg/ml and 1ml water used

Table B1.3: Germination inhibition assay using *S. uniplumis* extract statistical data- Starting concentration 40mg/ml and 1ml water used

Tukey's Multiple Comparison Test	Mean Diff.	q	P value	95% CI of diff
Control vs 0.625	-3.998	1.282	P > 0.05	-18.30 to 10.30
Control vs 1.25	-1.998	0.6408	P > 0.05	-16.30 to 12.30
Control vs 2.5	-3.334	1.069	P > 0.05	-17.63 to 10.97
Control vs 5	-0.001999	0.0006411	P > 0.05	-14.30 to 14.30
Control vs 10	-2.668	0.8556	P > 0.05	-16.97 to 11.63
Control vs 20	1.334	0.4278	P > 0.05	-12.97 to 15.63
Control vs 40	2.782	0.8922	P > 0.05	-11.52 to 17.08
0.625 vs 1.25	2.000	0.6414	P > 0.05	-12.30 to 16.30
0.625 vs 2.5	0.6640	0.2129	P > 0.05	-13.64 to 14.96
0.625 vs 5	3.996	1.282	P > 0.05	-10.30 to 18.30
0.625 vs 10	1.330	0.4265	P > 0.05	-12.97 to 15.63
0.625 vs 20	5.332	1.710	P > 0.05	-8.967 to 19.63
0.625 vs 40	6.780	2.174	P > 0.05	-7.519 to 21.08
1.25 vs 2.5	-1.336	0.4285	P > 0.05	-15.64 to 12.96
1.25 vs 5	1.996	0.6401	P > 0.05	-12.30 to 16.30
1.25 vs 10	-0.6700	0.2149	P > 0.05	-14.97 to 13.63
1.25 vs 20	3.332	1.069	P > 0.05	-10.97 to 17.63
1.25 vs 40	4.780	1.533	P > 0.05	-9.519 to 19.08
2.5 vs 5	3.332	1.069	P > 0.05	-10.97 to 17.63
2.5 vs 10	0.6660	0.2136	P > 0.05	-13.63 to 14.97
2.5 vs 20	4.668	1.497	P > 0.05	-9.631 to 18.97
2.5 vs 40	6.116	1.961	P > 0.05	-8.183 to 20.42

Tukey's Multiple Comparison Test	Mean Diff.	q	P value	95% CI of diff
5 vs 10	-2.666	0.8550	P > 0.05	-16.97 to 11.63
5 vs 20	1.336	0.4285	P > 0.05	-12.96 to 15.64
5 vs 40	2.784	0.8928	P > 0.05	-11.52 to 17.08
10 vs 20	4.002	1.283	P > 0.05	-10.30 to 18.30
10 vs 40	5.450	1.748	P > 0.05	-8.849 to 19.75

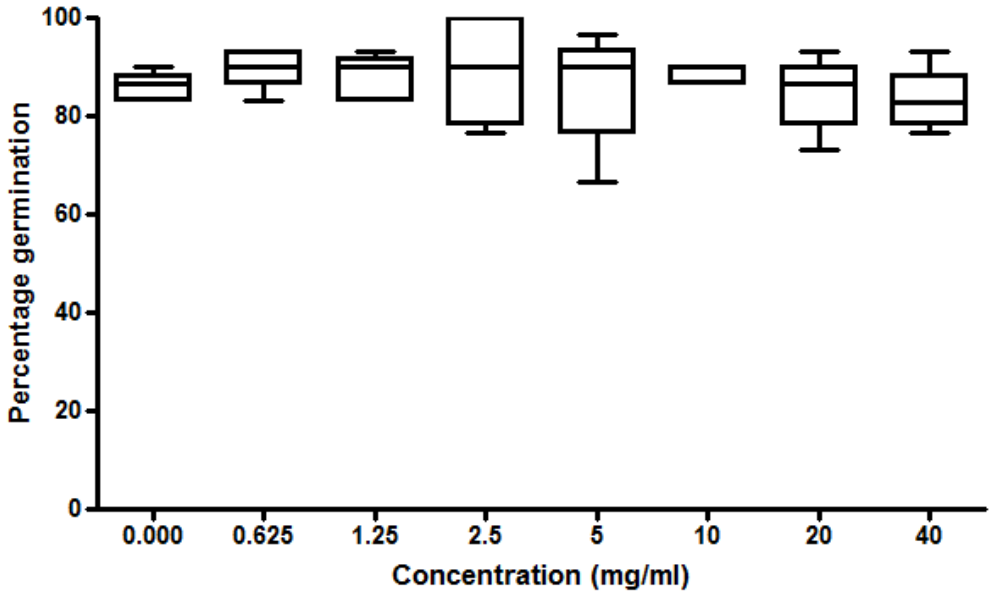

Figure B1.3: Box and whisker diagram of the germination data using *S. uniplumis* extract starting concentration 40mg/ml and 1ml water used

Table B1.4: Germination inhibition assay statistical data for brown colored sticky part of *E. gummifera* extract

Tukey's Multiple Comparison Test	Mean Diff.	q	P value	95% CI of diff
0.00 vs 0.625	4.666	1.208	P > 0.05	-13.05 to 22.38
0.00 vs 1.25	2.666	0.6903	P > 0.05	-15.05 to 20.38
0.00 vs 2.5	2.000	0.5178	P > 0.05	-15.71 to 19.71
0.00 vs 5	5.998	1.553	P > 0.05	-11.71 to 23.71
0.00 vs 10	3.332	0.8627	P > 0.05	-14.38 to 21.04
0.00 vs 20	13.34	3.453	P > 0.05	-4.375 to 31.05
0.00 vs 40	8.000	2.071	P > 0.05	-9.711 to 25.71
0.625 vs 1.25	-2.000	0.5178	P > 0.05	-19.71 to 15.71
0.625 vs 2.5	-2.666	0.6903	P > 0.05	-20.38 to 15.05
0.625 vs 5	1.332	0.3449	P > 0.05	-16.38 to 19.04
0.625 vs 10	-1.334	0.3454	P > 0.05	-19.05 to 16.38
0.625 vs 20	8.670	2.245	P > 0.05	-9.041 to 26.38
0.625 vs 40	3.334	0.8632	P > 0.05	-14.38 to 21.05
1.25 vs 2.5	-0.6660	0.1724	P > 0.05	-18.38 to 17.05
1.25 vs 5	3.332	0.8627	P > 0.05	-14.38 to 21.04
1.25 vs 10	0.6660	0.1724	P > 0.05	-17.05 to 18.38
1.25 vs 20	10.67	2.763	P > 0.05	-7.041 to 28.38
1.25 vs 40	5.334	1.381	P > 0.05	-12.38 to 23.05
2.5 vs 5	3.998	1.035	P > 0.05	-13.71 to 21.71
2.5 vs 10	1.332	0.3449	P > 0.05	-16.38 to 19.04
2.5 vs 20	11.34	2.935	P > 0.05	-6.375 to 29.05
2.5 vs 40	6.000	1.554	P > 0.05	-11.71 to 23.71
5 vs 10	-2.666	0.6903	P > 0.05	-20.38 to 15.05
5 vs 20	7.338	1.900	P > 0.05	-10.37 to 25.05
5 vs 40	2.002	0.5184	P > 0.05	-15.71 to 19.71
10 vs 20	10.00	2.590	P > 0.05	-7.707 to 27.72
10 vs 40	4.668	1.209	P > 0.05	-13.04 to 22.38

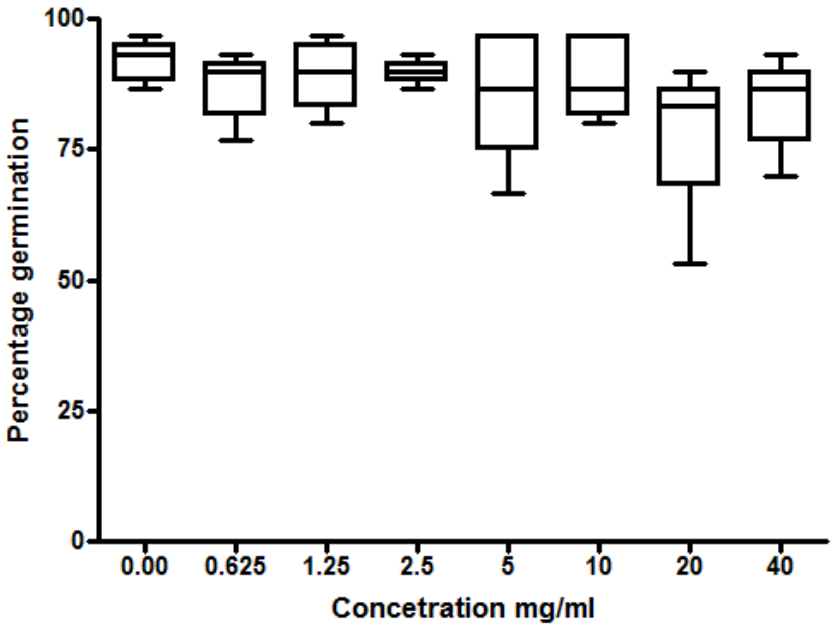

Figure B1.4: Box and whisker diagram of the germination inhibition data for the brown colored sticky part of *E. gummifera* extract

Table B1.5: Germination inhibition assay statistical data for the milky cream colored part of the *E. gummifera* extract

Tukey's Multiple Comparison Test	Mean Diff.	q	P value	95% CI of diff
0.000 vs 0.625	-2.666	0.9735	P > 0.05	-15.22 to 9.893
0.000 vs 1.25	-3.334	1.217	P > 0.05	-15.89 to 9.225
0.000 vs 2.5	-2.666	0.9735	P > 0.05	-15.22 to 9.893
0.000 vs 5.0	-0.6640	0.2425	P > 0.05	-13.22 to 11.89
0.000 vs 10.0	-3.998	1.460	P > 0.05	-16.56 to 8.561
0.000 vs 20.0	0.6680	0.2439	P > 0.05	-11.89 to 13.23
0.000 vs 40.0	2.002	0.7310	P > 0.05	-10.56 to 14.56
0.625 vs 1.25	-0.6680	0.2439	P > 0.05	-13.23 to 11.89
0.625 vs 2.5	0.0000	0.0000	P > 0.05	-12.56 to 12.56
0.625 vs 5.0	2.002	0.7310	P > 0.05	-10.56 to 14.56
0.625 vs 10.0	-1.332	0.4864	P > 0.05	-13.89 to 11.23
0.625 vs 20.0	3.334	1.217	P > 0.05	-9.225 to 15.89
0.625 vs 40.0	4.668	1.704	P > 0.05	-7.891 to 17.23
1.25 vs 2.5	0.6680	0.2439	P > 0.05	-11.89 to 13.23
1.25 vs 5.0	2.670	0.9749	P > 0.05	-9.889 to 15.23
1.25 vs 10.0	-0.6640	0.2425	P > 0.05	-13.22 to 11.89
1.25 vs 20.0	4.002	1.461	P > 0.05	-8.557 to 16.56
1.25 vs 40.0	5.336	1.948	P > 0.05	-7.223 to 17.89

Tukey's Multiple Comparison Test	Mean Diff.	q	P value	95% CI of diff
2.5 vs 5.0	2.002	0.7310	P > 0.05	-10.56 to 14.56
2.5 vs 10.0	-1.332	0.4864	P > 0.05	-13.89 to 11.23
2.5 vs 20.0	3.334	1.217	P > 0.05	-9.225 to 15.89
2.5 vs 40.0	4.668	1.704	P > 0.05	-7.891 to 17.23
5.0 vs 10.0	-3.334	1.217	P > 0.05	-15.89 to 9.225
5.0 vs 20.0	1.332	0.4864	P > 0.05	-11.23 to 13.89
5.0 vs 40.0	2.666	0.9735	P > 0.05	-9.893 to 15.22
10.0 vs 20.0	4.666	1.704	P > 0.05	-7.893 to 17.22
10.0 vs 40.0	6.000	2.191	P > 0.05	-6.559 to 18.56

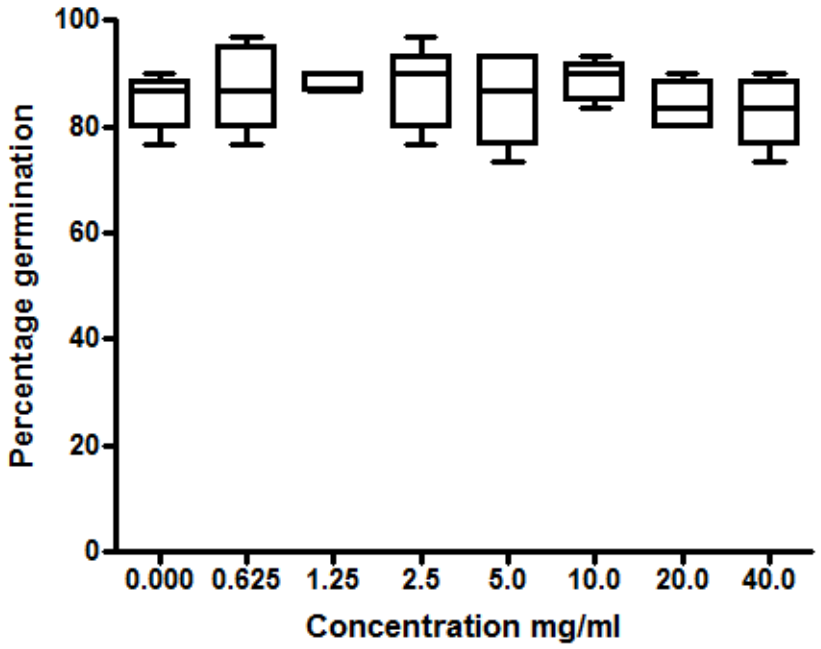

Figure B1.5: Box and whisker diagram for the germination inhibition data for the milky cream colored part of the *E. gummifera* extract

B2 Soil-bed bioassay data

Table B2.1: Soil-bed bioassay established seedling statistical data

Tukey's Multiple Comparison Test	Mean Diff.	q	P value	95% CI of diff
IS vs OS	-10.00	1.425	P > 0.05	-36.48 to 16.48
IS vs DP	23.33	3.324	P > 0.05	-3.150 to 49.81
OS vs DP	33.33	4.749	P < 0.05	6.850 to 59.81

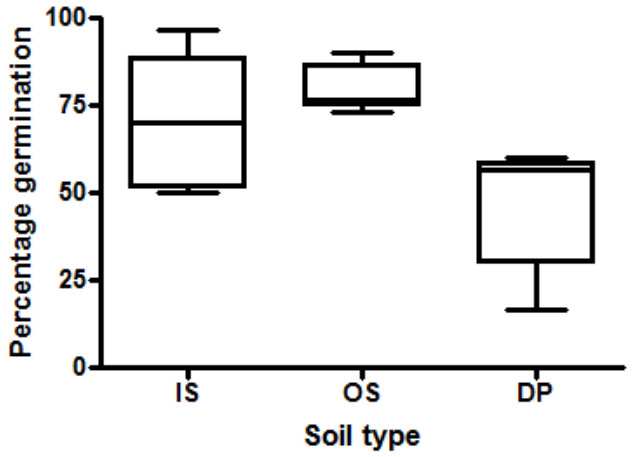

Figure B2.1: Box and whisker diagram for the established seedling data of the soil-bed bioassay

B3 Soil-agar bioassay

Table B3.1: Soil-agar bioassay germination statistical data- nutrient agar used

Tukey's Multiple Comparison Test	Mean Diff.	q	P value	95% CI of diff
Control vs IS	28.00	5.214	P < 0.05	5.274 to 50.72
Control vs OS	21.80	4.060	P > 0.05	-0.9217 to 44.52
Control vs DP	49.33	9.188	P < 0.001	26.61 to 72.05
Control vs RH	18.66	3.476	P > 0.05	-4.058 to 41.39
IS vs OS	-6.196	1.154	P > 0.05	-28.92 to 16.53
IS vs DP	21.33	3.973	P > 0.05	-1.390 to 44.05
IS vs RH	-9.332	1.738	P > 0.05	-32.05 to 13.39
OS vs DP	27.53	5.127	P < 0.05	4.806 to 50.25
OS vs RH	-3.136	0.5841	P > 0.05	-25.86 to 19.59
DP vs RH	-30.66	5.711	P < 0.01	-53.39 to -7.942

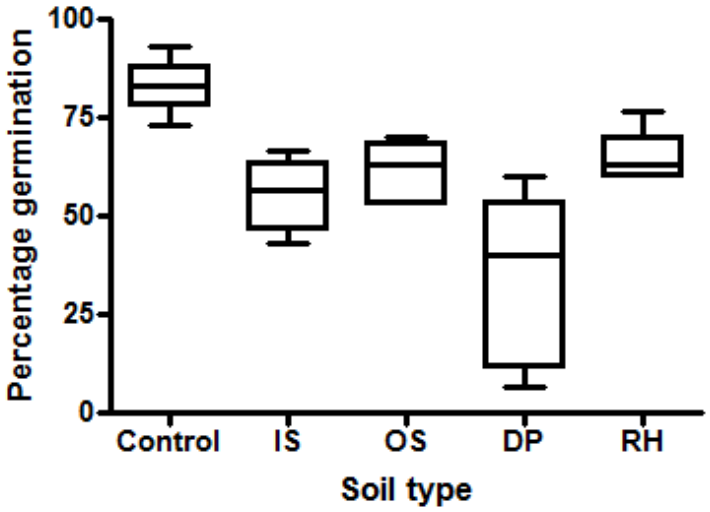

Figure B3.1: Box and whisker diagram of the germination data for the soil-agar bioassay using nutrient agar

Table B3.2: Soil-agar bioassay germination statistical data- pure agar used

Tukey's Multiple Comparison Test	Mean Diff.	q	P value	95% CI of diff
Control vs IS	-1.334	0.6080	P > 0.05	-10.62 to 7.951
Control vs OS	-1.998	0.9106	P > 0.05	-11.28 to 7.287
Control vs DP	-1.932	0.8806	P > 0.05	-11.22 to 7.353
Control vs Rh	-3.334	1.520	P > 0.05	-12.62 to 5.951
IS vs OS	-0.6640	0.3026	P > 0.05	-9.949 to 8.621
IS vs DP	-0.5980	0.2726	P > 0.05	-9.883 to 8.687
IS vs Rh	-2.000	0.9115	P > 0.05	-11.29 to 7.285
OS vs DP	0.06600	0.03008	P > 0.05	-9.219 to 9.351
OS vs Rh	-1.336	0.6089	P > 0.05	-10.62 to 7.949
DP vs Rh	-1.402	0.6390	P > 0.05	-10.69 to 7.883

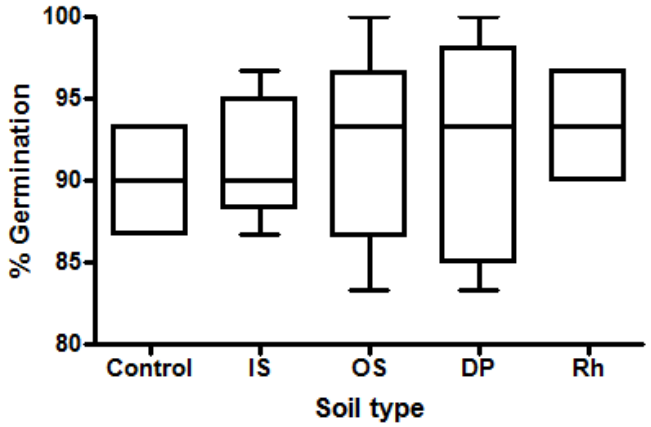

Figure B1.3: Box and whisker diagram of the germination data for the soil-agar bioassay using pure agar

Appendix C

Major column fractions' weights

Table C1: The weights of the pooled major fractions

Pooled fractions	Weight (grams)
1-12	0.0316
13-16	0.3187
17-18	0.0492
19-28	0.5254
29-30	0.0416
31-34	0.0551
35-37	0.0708
38-41	0.0969
42-44	0.1956
45-48	0.1529
49-60	0.0903
61-70	0.0211
71	0.0017
72-82	0.0227
83-89	0.0246
90-96	0.0283
97-99	0.0111
100	0.0035
101-118	0.0528
119	0.0029
120-131	0.0354
132-147	0.0601
148-155	0.0236
156-158	0.0481
159-172	0.2034
173-182	0.0839
183-200	0.2599
201-205	0.0253
206-224	0.1253
225-234	0.0409
235	0.0037
236-248	0.0575
249-250	0.007
251-266	0.0417
267-268	0.0027

Appendix D

Bacterial 16S rRNA gene sequences, PCR and BLAST information

D1 16S rRNA gene sequences

Yellow bacterium:

CATGCAGTCGAGCGGTTGAGGGGAGCTTGCTCCCTGATTCAGCGGCGGACGGGTGAGTCTTG
CCTAGGAATCTGCCTATTAGTGGGGGACAACGTTTCGAAAGGAACGCTAATACCGCATACGT
CCTACGGGAGAAAGCAGGGGACCTTCGGGCCTTGCGCTAATAGATGAGCCTAGGTCGGATT
AGCTAGTTGGTGGGGTAAAGGCTCACCAAGGCGACGATCCGTAACTGGTCTGAGAGGATGA
TCAGTCACACTGGAACTGAGACACGGTCCAGACTCCTACGGGAGGCAGCAGTGGGGAATAT
TGGACAATGGGCGAAAGCCTGATCCAGCCATGCCGCGTGTGTGAAGAAGGTCTTCGGATTGT
AAAGCACTTTAAGTTGGGAGGAAGGGTTGTAGATTAATACTCTGCAATTTTGACGTTACCGA
CAGAATAAGCACCGGCTAACTCTGTGCCAGCAGCCGCGGTAATACAGAGGGTGCAAGCGTT
AATCGGAAT

Orange bacterium:

AGTCGACGATGATGCCCAGCTTGCTGGGCGGATTAGTGGCGAACGGGTGAGCCTTTCGTGAG
TAACCTGCCCTTGACTCTGGGATAAGCCTGGGAAACTGGGTCTAATACTGGATACTACCTCG
CACCGCATGGTGGGTGGTGGAAAGGGTTTTACTGGTTTTGGATGGGCTCACGGCCTATCAGC
TTGTTGGTGGGGTAATGGCTCACCAAGGCGACGACGGGTAGCCGGCCTGAGAGGGTGACCG
GCCACACTGGGACTGAGACACGGCCCAGACTCCTACGGGAGGCAGCAGTGGGGAATATTGC
ACAATGGGCGGAAGCCTGATGCAGCGACGCCGCGTGAGGGATGACGGCCTTCGGGTTGTAA
ACCTCTTTCAGTAGGGAAGAAGCGAGAGTGACGGTACCTGCAGAAGAAGCGCCGGCTAACT
ACGTGCCAGCAGCCGCGGTAATACGTAGGGCGCAAGCGTTGTCCGGAATTATTGGGCGTAA
AGAGCTCGTAGGCGGTTTGTCGCGTCTGCTGTGAAAGCCCGGGGCTCAACCCCGGGTCTGCA
GTGGGTACGGGCAGACTAGAGTGCAGTAGGGGAGACTGGAATTCCTGGTGTAGCGGTGAAA
TGCGCAGATATCAGGAGGAACACCGATGGCGAAGGCAGGTCTCTGGGCTGTTACTGACGCT
GAGGAGCGA

D2 PCR primer information

Table D2.1: PCR Primer information

Primer	Sequence (5'>3')	Melting temperature (°C)	Reference
27F primer (forward)	5'-AGAGTTTGATCMTGCGTCAG	50-52	Frank et al., 2008; Galkiewicz and Kellogg 2008; Stackebrandt and Liesack, 1993; Lane, 1991
1492R primer (reverse)	5'-GGTTACCTTGTTACGACTT	47	

***M= A/C**

D3 BLAST information

Table D3.1: The top 10 most significant alignments after BLAST for the yellow bacterium

Description	E-value	Hit %	Accession
Pseudomonas argentinensis **Strain CH01 16S rRNA, partial sequence**	0.0	99%	NR 03115.1
Pseudomonas straminea **Strain NBRC 16S rRNA, partial sequence**	0.0	99%	NR 113859.1
Pseudomonas punonensis **Strain LMT03 16S rRNA, partial sequence**	0.0	99%	NR 109583.1
Pseudomonas straminea **Strain CB-7 16S rRNA, partial sequence**	0.0	98%	NR 036908.1
Pseudomonas turukhanskensis **Strain IB1.1 16S rRNA, partial sequence**	0.0	98%	NR 152710.1
Pseudomonas flavescens **Strain NBRC 10344 16S rRNA, partial sequence**	0.0	97%	NR 114195.1
Pseudomonas paravulva **Strain AJ 2129 16S rRNA, partial sequence**	0.0	97%	NR 040859.1
Pseudomonas vancouverensis **Strain DhA-51 16S rRNA, partial sequence**	0.0	97%	NR 041953.1
Pseudomonas seleniipraecipitans **Strain CA5 16S rRNA, partial sequence**	0.0	98%	NR 116646.1
Pseudomonas paravulva **Strain NBRC 16636 16S rRNA, partial sequence**	0.0	97%	NR 113856.1

Table D3.2: The top 10 most significant alignments after BLAST for the orange bacterium

Description	E-value	Hit%	Accession
Kocuria polaris **Strain CMS 76or 16S rRNA, partial sequence**	0.0	99%	NR 02824.1
Kocuria rosea **Strain DSM 20447 16S rRNA, partial sequence**	0.0	99%	NR 04487.1
Kocuria dechangensis **Strain NEAU-ST5-33 16S rRNA, partial sequence**	0.0	97%	NR 137239.1
Kocuria aegyptia **Strain YIM 70003 16S rRNA, partial sequence**	0.0	97%	NR 043511.1
Kocuria himachalensis **Strain K07-05 16S rRNA, partial sequence**	0.0	97%	NR 043323.1
Kocuria oceani **Strain FXJ8.095 16S rRNA, partial sequence**	0.0	97%	NR 156033.1
Kocuria turfanensis **Strain HO-9042 16S rRNA, partial sequence**	0.0	97%	NR 043899.1
Kocuria subflava **Strain YIM 13062 16S rRNA, partial sequence**	0.0	96%	NR 14586.1
Kocuria flava **Strain HO-9041 16S rRNA, partial sequence**	0.0	96%	NR 044308.1
Kocuria sediminis **Strain FCS-11 16S rRNA, partial sequence**	0.0	96%	NR 118222.1

D4 References

Frank, J.A., Reich, C.I., Sharma, S., Weisbaum, J.S., Wilson, B.A., Olsen, G.J. 2008. Critical evaluation of two primers commonly used for amplification of bacterial 16S rRNA genes. Applied and Environmental Microbiology 74(8), 2461-2470.

Galkiewicz, J.P. and Kellogg, C.A. 2008. Cross-kingdom amplification using bacteria-specific primers: Complications for studies of coral microbial ecology. Applied and Environmental Microbiology 74(24), 7828-7831.

Lane, D.J. 1991. 16S/23S rRNA sequencing in: Stackebrandt, E. and Goodfellow, M. (Eds.), Nucleic acid techniques in bacterial systematics. John Wiley & Sons, New York, NY.

Stackebrandt, E. and Liesack, W. 1993. Nucleic acids and classification in: Goodfellow, M. and O'Donnell, A.G. (Eds), Handbook of new bacterial systematics. Academic Press, Loden, England.

Appendix E

GCMS analysis data

Table 1E: Details of the compounds identified by the GCMS analysis

Compound name	Compound structure	Fraction, hit % and retention time		
Lupeol	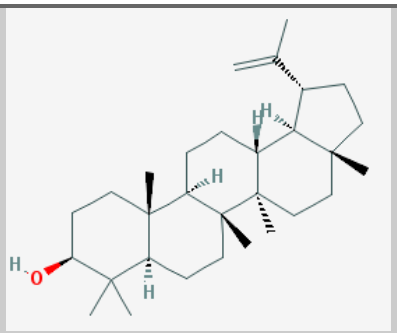	B	80%	22.835
		C	89%	32.555
		E	90%	27.755
		G	90%	23.985
		H	90%	32.505
		I	89%	23.985
		J	87%	32.440
		K	87%	32.440
		L	87%	32.430
		M	74%	32.440
		N	81%	32.455
		O	83%	32.450
		P	85%	32.450
		Q	86%	32.445
		R	83%	32.445
		V	73%	32.440
		W	77%	32.445
α-Amyrin	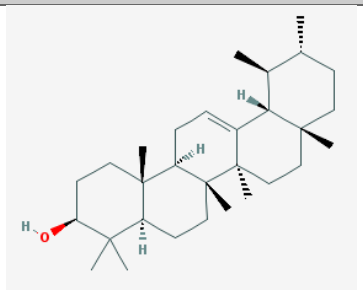	H	92%	31.860
B-Amyrin	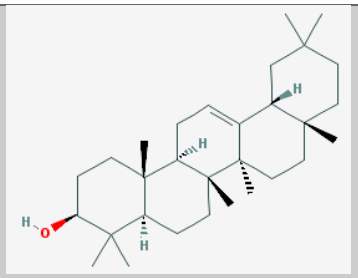	C	92%	21.270
		E	93%	31.920
		F	94%	31.890
		G	93%	31.895

Betulin (Lup-20(29)-ene-3, 28-diol, (3.beta.))	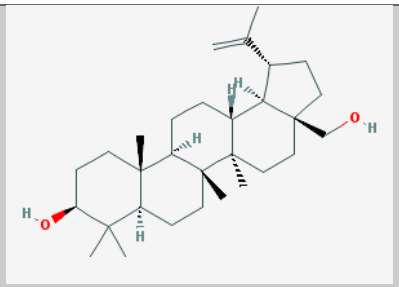	D	83%	31.675
		E	79%	31.660
		G	77%	31.635
		H	89%	28.485
		I	84%	27.730
		J	84%	26.095
		L	80%	28.450
		X	85%	23.880
Lupeol acetate (Lup-20(29)-en-3-ol, acetate, (3.beta))	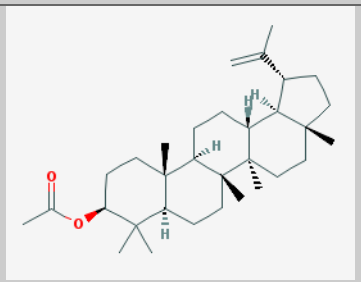	B	94%	24.030
		D	94%	24.105
		E	89%	32.640
		I	88%	32.445
		J	85%	23.875
Hopenone b (A'-Neogammacer-22(29)-en-3-one)	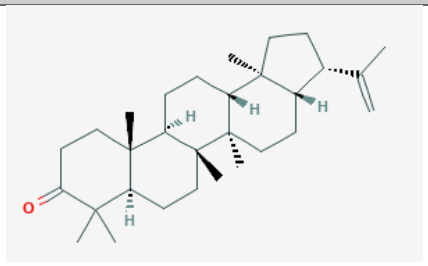	B	80%	31.175
Lanosterol	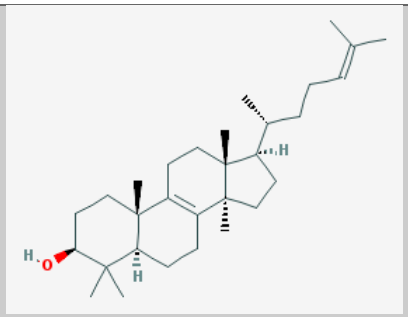	C	90%	31.375
		D	90%	31.375
		F	90%	30.760

Germanicen (Olean-18-ene)	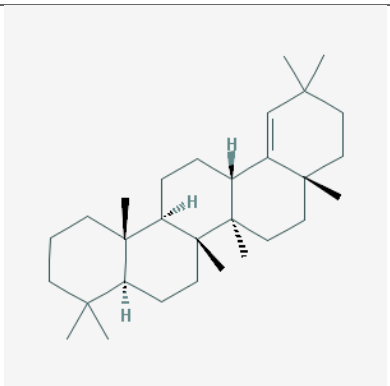	A	80%	31.665
		C	82%	22.380
Olean-12-en-3-one	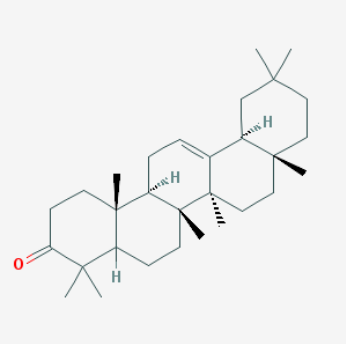	A	91%	31.570
		B	93%	31.600
		K	76%	31.840
Triacontanoic acid, methyl ester (Methyl melissate)	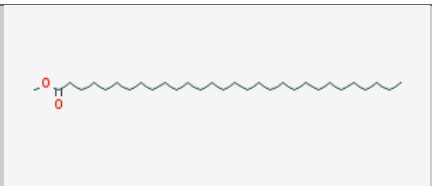	A	87%	31.085
		B	95%	31.175
17-Pentatria-contene	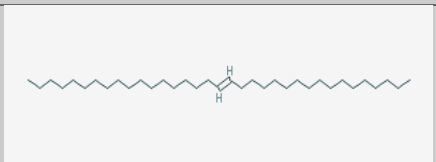	A	96%	30.665
		C	97%	31.040
		D	91%	23.460
Pentatria-contane		A	96%	29.615

Hexatria-contane	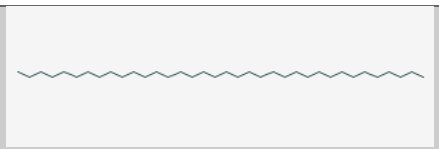	A	95%	28.790
Tetracontane		A	96%	28.390
Nonacosane	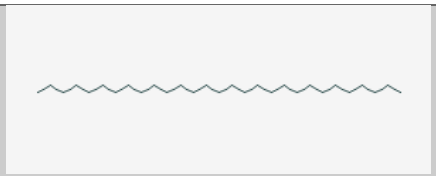	A	97%	26.885
Heneicosyl trifluoroacetate	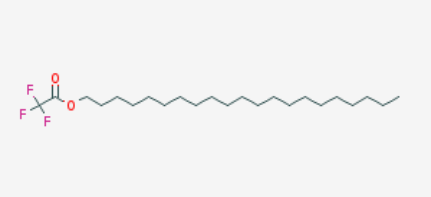	A	97%	26.135
Octatriacontyl pentafluoropropionate	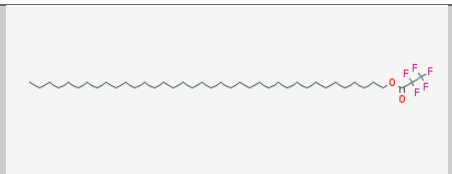	A	95%	23.780

Docosyl heptafluorobutyrate	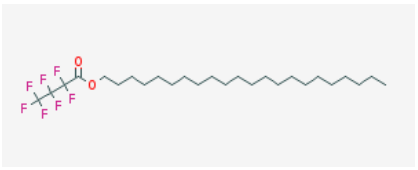	A	97%	25.305
1-Heptacosanol	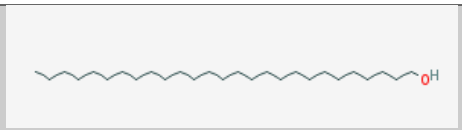	A	97%	24.555
		C	97%	28.790
		D	96%	30.870
		F	89%	28.765
Tetracosane	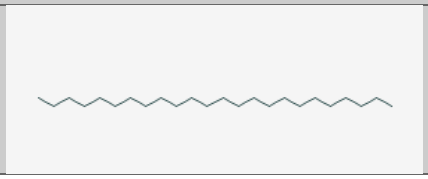	A	96%	23.810
Eicosane		A	96%	22.175
		EE	89%	17.445
		II	90%	19.450
Heneicosane	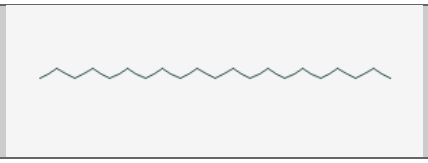	A	98%	20.410
1-Nonadecene	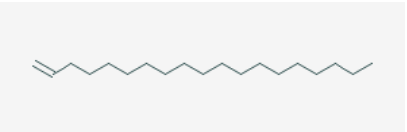	A	98%	19.410
Hexadecane	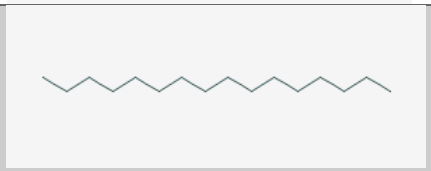	A	97%	15.250
		EE	92%	15.230

D:B-Friedo-B':A'-neogammacer-5-en-3-one	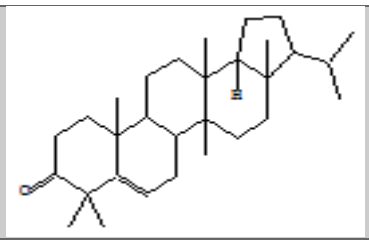	B	87%	32.645
Eicosanoic acid, methyl ester (Arachidic acid methyl ester)	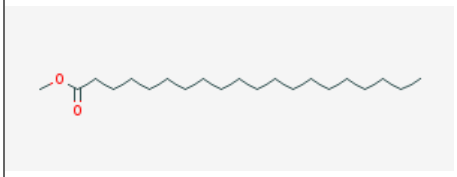	B	80%	32.460
Urs-12-ene	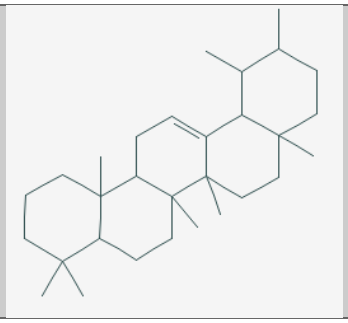	B	82%	30.420
Methyl 18-methylicosanoate	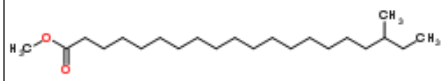	B	82%	30.000
Octacosyl acetate	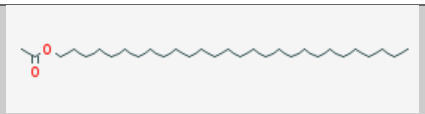	B	82%	29.770
Octadec-9-en-1-al dimethyl acetal		B	81%	29.405
Octacosanoic acid, methyl ester		B	95%	29.040

2-Nonacosanone		B	89%	28.935
2-methylhexacosane		B	90%	28.710
		L	92%	20.395
		M	92%	20.400
Octadecanal	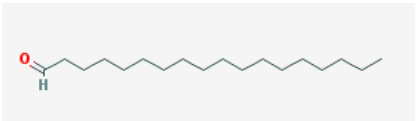	B	87%	28.265
		C	85%	29.685
Methyl 24-methyl-hexacosanoate		B	91%	28.190
Pentacosanoic acid, methyl ester		B	90%	26.430
Tetracosanoic acid, methyl ester Methyl lignocerate	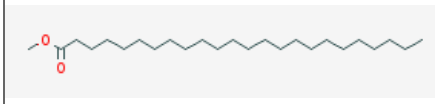	B	93%	25.55
		C	85%	24.855
2-Pentacosanone	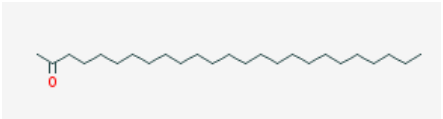	B	87%	25.440
Methyl 21-methyldocosanoate		B	92%	24.795
Cetyl glycidyl ether (Oxirane, [(hexadecyloxy) methyl])	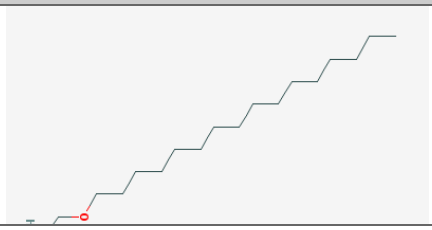	B	82%	24.670
		M	80%	14.025

		N	80%	14.025
Bis(2-ethylhexyl) phthalate/ 1,2-Benzenedicarboxylic acid, bis(2-ethylhexyl) ester	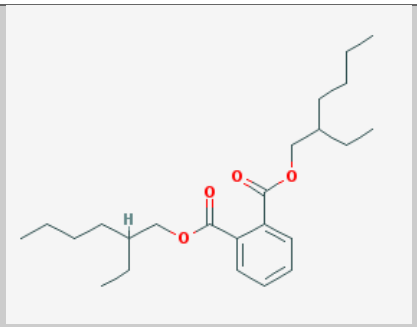	B	92%	24.225
		F	86%	24.225
		K	84%	24.225
		L	81%	24.225
		W	77%	24.225
		EE	78%	24.225
		FF	74%	24.225
		GG	74%	24.225
		HH	74%	24.225
		II	82%	24.225
Methyl 20-methyl-heneicosanoate	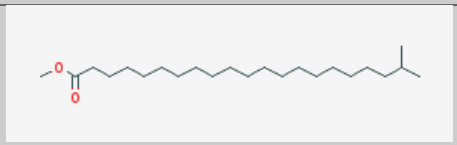	B	80%	24.030
Methyl 18-methylnonadecanoate	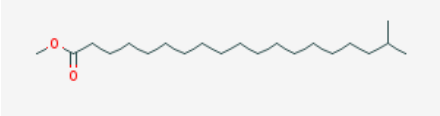	B	90%	22.405
Methyl stearate		B	92%	20.650
		BB	82%	23.650
		DD	90%	20.650
		EE	93%	20.655

		FF	90%	20.650
		GG	95%	20.650
		HH	94%	20.650
		II	96%	20.650
8,11,14-Docosatrienoic acid, methyl ester /Methyl (8E,11E,14E)-8,11,14-docosatrienoate	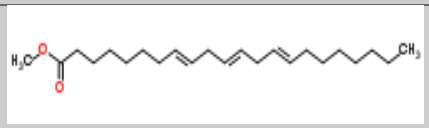	B	88%	20.440
9,12-Octadecadienoic acid	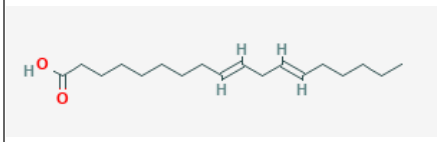	B	95%	20.385
		II	92%	20.380
Dibutyl phthalate	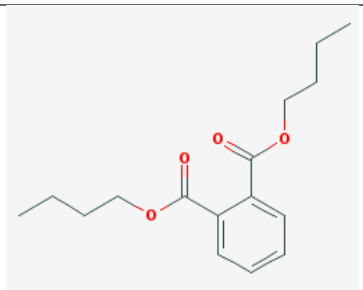	B	97%	19.175
		C	96%	19.175
Hexadecanoic acid, methyl ester / Methyl palmitate	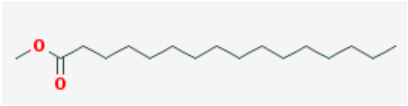	B	97%	18.745
		DD	85%	18.740
		EE	87%	18.740
		FF	87%	18.740
		HH	92%	18.740
		II	96%	18.740
Benzene, 1,2-dimethyl-	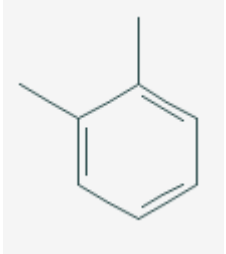	C	97%	5.075
		D	95%	5.020
		E	97%	5.075
		G	95%	5.000
		H	97%	5.070
		Z	71%	5.100
6a,14a-		C	80%	32.040
		D	82%	32.125

Methanopicene, perhydro-1,2,4a,6b,9,9,12a-heptamethyl-10-hydroxy		E	82%	32.065
		F	81%	32.030
		G	82%	32.025
		H	82%	31.975
		K	77%	31.940
		L	81%	31.940
		M	71%	31.945
		N	75%	31.940
		O	75%	31.945
		P	78%	31.940
		Q	75%	31.950
		R	73%	31.945
		W	71%	31.945
Oxalic acid, 2-phenylethyl tridecyl ester	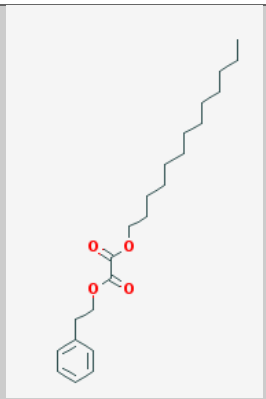	D	95%	28.695
cis-1-Chloro-9-octadecene	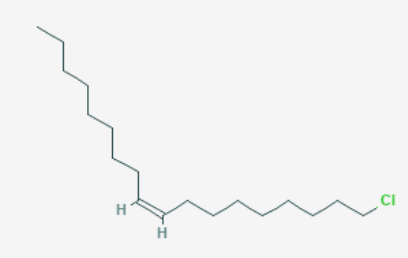	D	86%	27.945
		E	87%	28.765
		M	77%	30.755
		W	83%	20.260
03027205002 FLAVONE 4'-OH,5-OH,7-DI-O-GLUCOSIDE		C	80%	31.250
		D	73%	24.865
		F	78%	27.980
		H	85%	28.760
		I	83%	30.755
		J	77%	25.295
		K	74%	28.170
		L	78%	30.755

		M	81%	26.730
		N	79%	27.160
		O	82%	22.785
		P	81%	26.735
		Q	79%	22.575
		R	80%	22.575
		S	74%	28.175
		T	74%	25.750
		U	74%	26.735
		V	73%	26.730
		X	72%	24.550
		Y	79%	24.045
		Z	75%	24.050
13,27-Cycloursan-3-ol, acetate, (3.beta.,13.beta.,14.beta.)	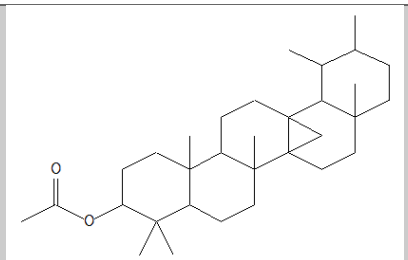	C	83%	22.030
		D	82%	22.015
Octadecanoic acid, 3-hydroxy-2-tetradecyl-, methyl ester, (2R,3R)	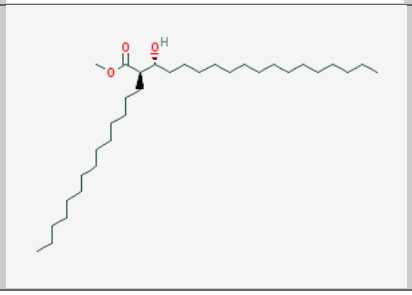	C	72%	30.490
IRON IODIDE COMPLEX I	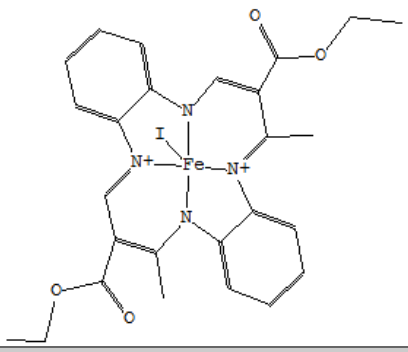	C	80%	30.850
		M	77%	18.985
		P	70%	18.985
Ethyl iso-		C	72%	30.490

allocholate		S	80%	18.750
		T	72%	16.685
		W	73%	19.845
		Y	76%	17.010
		Z	71%	22.685
Fumaric acid, hexadecyl 2-phenylethyl ester		C	92%	30.030
beta-Sitosterol	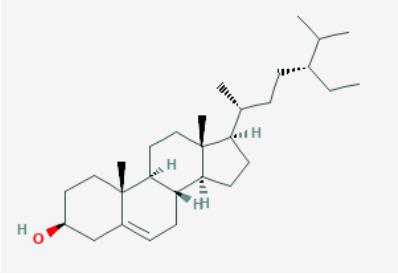	E	89%	31.360
		F	89%	31.345
		G	91%	31.335
Moretenal/a'-Neogammacer-22(29)-en-3-ol, (3.beta.,21.beta.)		E	85%	22.835
		G	83%	22.570
		H	83%	22.475
9,19-Cyclolanostan-3-ol, acetate, (3.beta.)	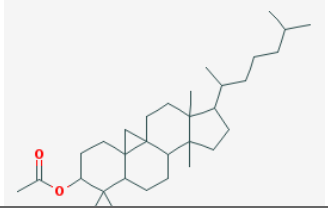	F	71%	27.220
		H	80%	24.435
		J	76%	31.720

		L	78%	23.345
ISOCHIAPIN B	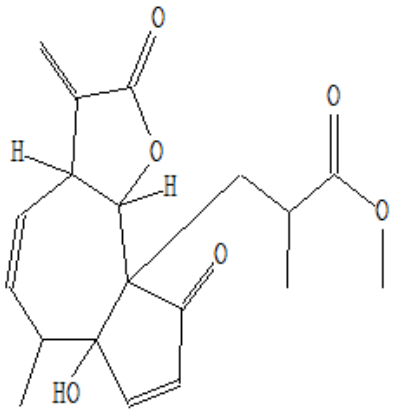	F	73%	25.290
		K	74%	25.290
		L	82%	25.290
		M	88%	24.055
		N	83%	23.840
		O	89%	21.230
		P	88%	21.230
		Q	88%	21.385
		R	77%	21.240
		S	88%	21.055
		T	88%	23.060
		U	88%	22.985
		V	85%	20.445
		W	86%	22.150

		X	82%	19.455
Decane	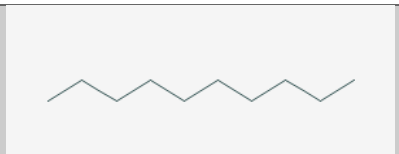	F	91%	6.835
		O	92%	6.790
		P	92%	6.760
		R	95%	6.780
		S	92%	6.780
		T	93%	6.840
		U	94%	6.825
		V	90%	6.780
		W	97%	8.450
		X	95%	6.825
		Y	94%	6.780
		Z	92%	6.830
		AA	94%	6.845
		BB	94%	6.790
		CC	94%	6.850
		DD	95%	6.820
		EE	96%	6.785
		FF	95%	6.785
		GG	96%	6.825
		HH	95%	6.785
		II	95%	6.835
9,19-Cyclolanostan-3-ol-11-one, acetate	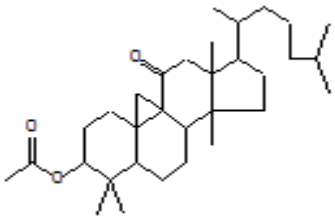	F	73%	31.485
		G	74%	31.480
(22-Z)-DEHYDROCHOLESTEROL-1-ETHER		G	80%	30.810
		M	75%	27.395
		O	74%	25.485
		P	77%	25.490
		Q	75%	25.485
		R	75%	25.490
		S	81%	18.420
		T	77%	20.650
		U	74%	25.490
9,19-Cyclolanost-		G	71%	27.120

24-en-3-ol, acetate, (3.beta.)		I	80%	30.545
Ursane-3,12-diol /4,4,6a,6b,8a,11, 12,14b-Octamethyl-docosahydropicene-3,13-diol	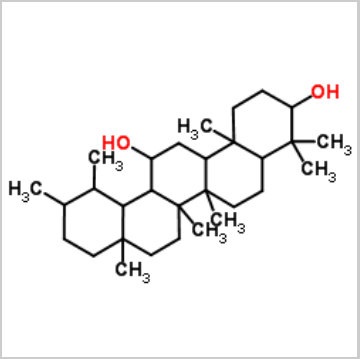	G	80%	25.740
		H	80%	25.640
(14.beta.)11,12-Epoxyolean-3-ol, acetate		G	76%	25.620
Lanostan-3.beta.-ol, 11.beta.,18-epoxy-19-iodo-, acetate	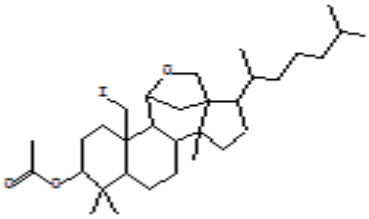	G	81%	23.510
		H	83%	23.585
Rhamnol/Cinchol /Cupreol/Quebrachol/Angelicin/beta.-Sitosterin /Stigmast-5-en-3-ol (3.beta.)	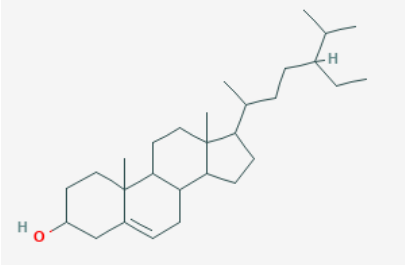	H	83%	31.315

9,19-Cyclo-27-norlanostan-25-one, 3-(acetyloxy)-24-methyl-, (3.beta.,24R)	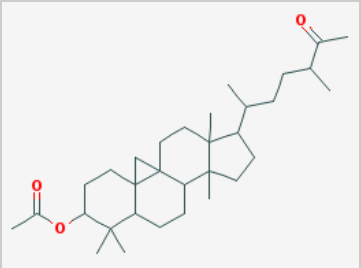	H	78%	30.850
		I	81%	23.425
Longiborneol/ Juniperol	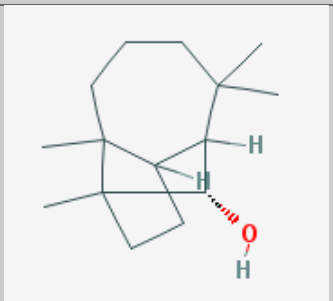	H	78%	30.550
		N	71%	28.450
Nonanoic acid	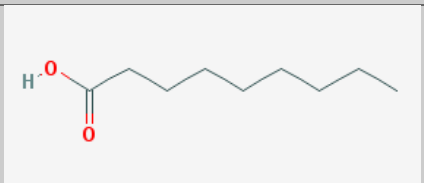	H	94%	10.960
17-(1,5-Dimethyl-3-phenylthiohex-4-enyl)-4,4,10,13,14-pentamethyl-2,3,4,5,6,7,10,11,12,13,14,15,16,17-tetradecahydro-1H-cyclopent(a)phenanthren-3-ol	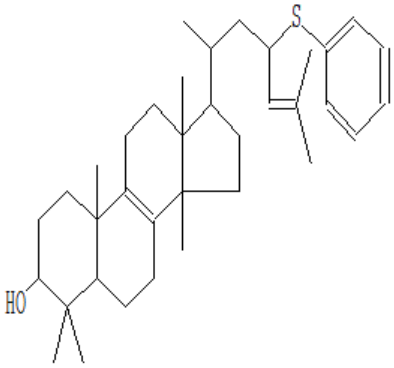	I	80%	32.565
		J	82%	32.565
		K	80%	32.565
		L	77%	32.555
		M	77%	31.258
		N	73%	31.258

METHYL COMMATE B	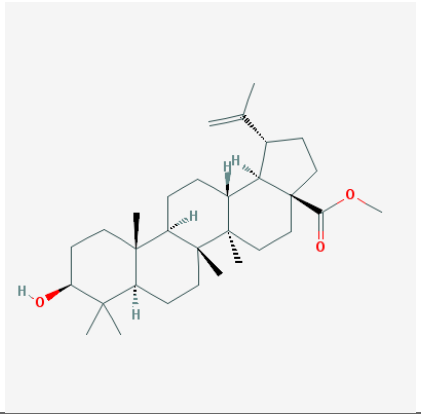	I	79%	31.940
		J	78%	31.945
Methyl commate C	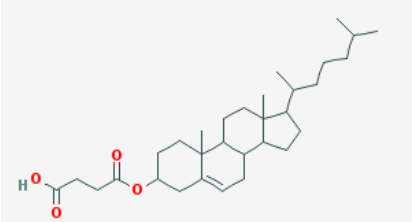	I	81%	31.845
1,2-Benzenedicarboxylic acid, butyl 2-ethylhexyl ester	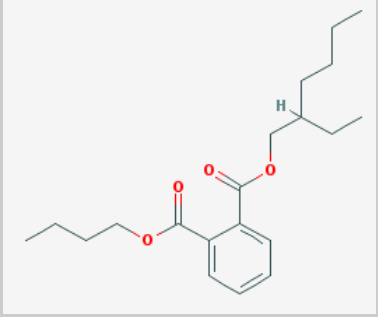	I	87%	19.170
		J	86%	19.165
7-Nonenoic acid, methyl ester	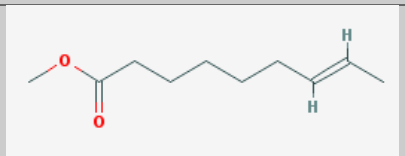	I	82%	14.020
Methyl commate D	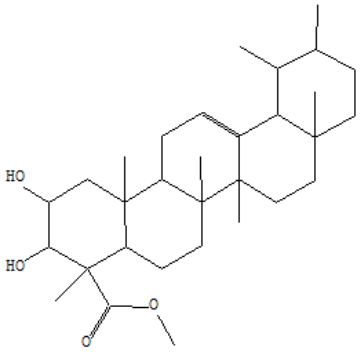	J	80%	31.845

30-Norlupan-28-oic acid, 3-hydroxy-21-methoxy-20-oxo-, methyl ester, (3.beta.)	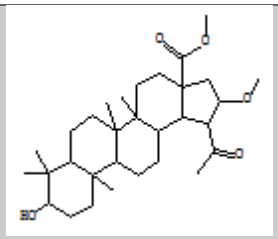	J	79%	25.630
		Y	78%	22.280
Lucenin 2	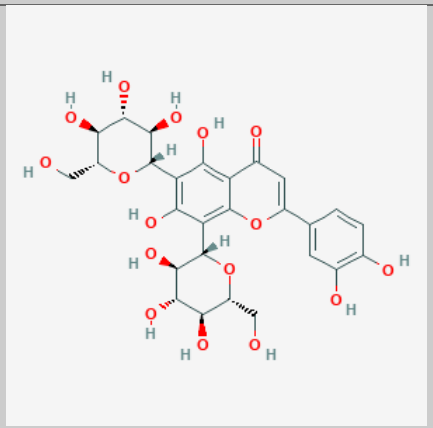	J	76%	24.225
		O	80%	24.230
		P	81%	24.230
		Q	82%	24.230
		R	79%	24.230
		S	81%	24.230
		T	79%	24.230
		U	80%	24.230
		V	77%	24.225
Dotriacontane		K	79%	19.450
		L	82%	19.455
		M	90%	17.445
		N	91%	20.400
		O	90%	17.445
		P	88%	21.295
		Q	89%	17.450
		R	89%	20.400
		S	90%	17.450
		T	90%	17.450
		U	89%	17.450
		V	90%	17.450
		W	89%	19.455
		X	87%	17.445
		Y	83%	17.445
		X	86%	17.450
		CC	86%	17.445
		DD	84%	19.455
		EE	84%	19.455
		FF	84%	19.455
		HH	84%	19.455

1,2-Benzenedicarboxylic acid, butyl octyl ester	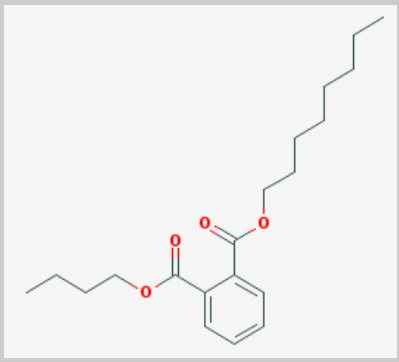	K	90%	19.170
7,8-Epoxylanostan-11-ol, 3-acetoxy-	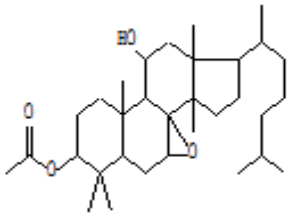	L	79%	25.635
		M	76%	27.495
		N	80%	23.270
		Q	76%	23.120
		R	77%	23.120
		S	79%	23.115
14-.BETA.-H-PREGNA	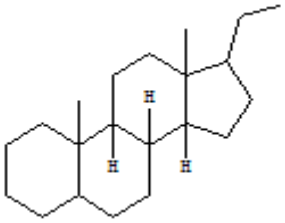	L	89%	23.060
		M	93%	20.270
		N	89%	23.060
		O	87%	21.620
		P	85%	22.160
		R	87%	21.385
		S	88%	22.985
		T	89%	21.625
		U	85%	21.300
Tetrapentacontane, 1,54-dibromo	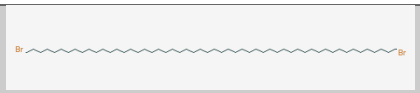	L	91%	21.375
		M	90%	21.380
		N	88%	20.485
		Q	85%	21.300
		T	85%	21.295
BUTYL ISODECYL PHTHALATE/1,2-Benzenedicarboxylic acid, butyl 8-methylnonyl ester	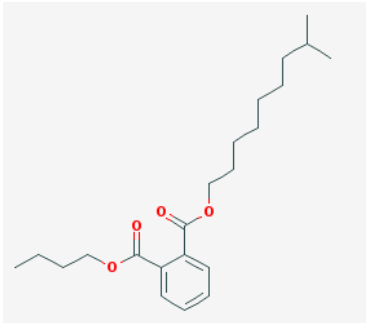	L	89%	19.170

Nonadecane	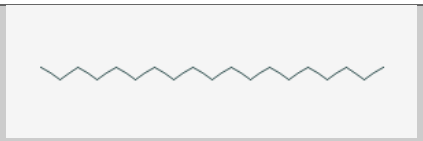	L	90%	18.475
		M	91%	18.475
		W	94%	15.230
		Y	86%	15.230
Docosane	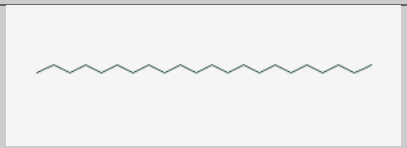	L	91%	17.445
		N	91%	15.230
		Q	90%	15.235
		R	90%	15.235
		T	92%	15.230
		U	89%	14.035
		V	93%	15.230
		W	89%	17.450
		BB	86%	15.225
		FF	90%	17.445
		GG	89%	17.455
Z,Z-6,28-Heptatriactontadien-2-one	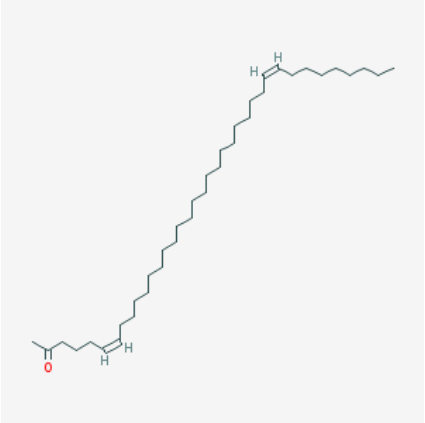	L	82%	15.345
4-(3-Methoxycarbonylpropyl)-4-butanolide	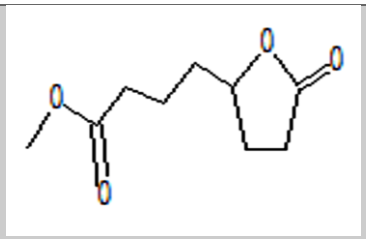	L	89%	15.110
		M	83%	15.115
		N	84%	15.120
		O	74%	15.125

1',1"'-bis[1-Methylethenyl)-1,1"-(2,3-dimethylbutan-2,3-diyl)-bis[ferrocene]		M	72%	28.705
2-Monostearoylglycerol/ Octadecanoic acid, 2-hydroxy-1-(hydroxymethyl)ethyl ester	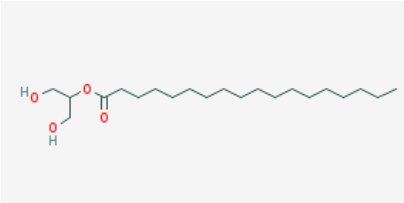	M	78%	25.485
		FF	75%	25.295
Bis(tridecyl) phthalate	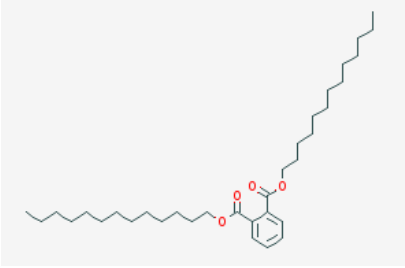	M	82%	24.225
		N	79%	24.225
Heptadecanoic acid, 15-methyl-, methyl ester	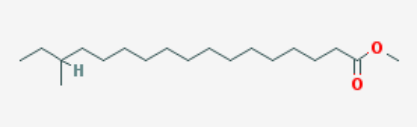	M	87%	20.655
Methyl 14-methyl-eicosanoate		M	82%	18.740
		N	85%	20.655
		O	83%	20.650
		U	81%	20.655
Stigmastane-3,6-dione, (5.alpha.)		M	81%	17.340
		O	77%	16.800

		P	78%	17.370
Z-7-Hexadecenal	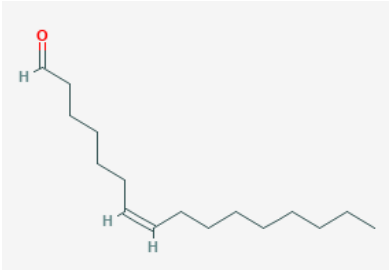	M	78%	15.945
		O	81%	17.945
		R	80%	17.945
		T	82%	17.370
		V	82%	21.385
		W	82%	17.370
		Y	78%	17.365
2,5-Furandione, 3-(dodecenyl)di-hydro/ Dodecenylsuc-cinic anhydride	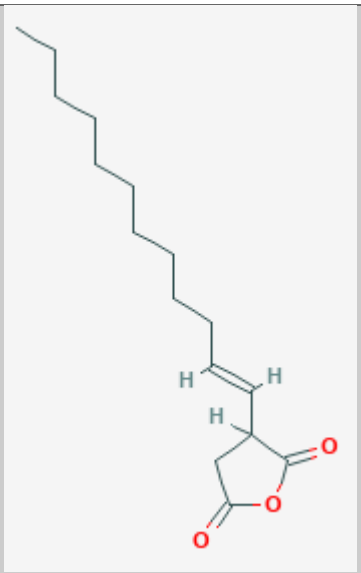	M	80%	17.115
		W	78%	18.290
		X	77%	15.140

4-(4-Methoxycarbonyl butyl)-4-butanolide	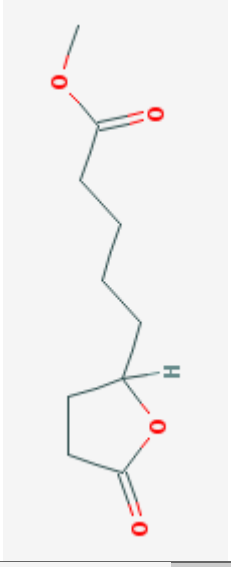	M	74%	16.445
2-Dodecen-1-yl(-)succinic anhydride/ 2,5-Furandione, 3-dodecenyl	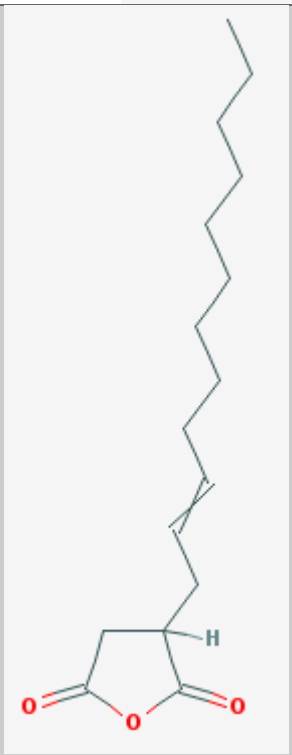	M	81%	16.290
		R	72%	14.420
		S	82%	18.295
4-Oxo-beta-isodamascol	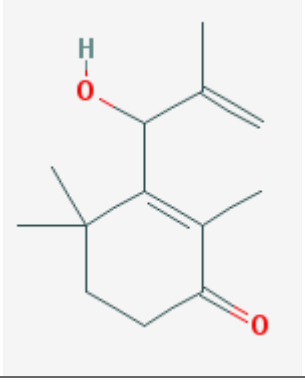	M	74%	15.515
		W	75%	17.810
		Z	71%	17.420

E,E,Z-1,3,12-Nonadecatriene-5,14-diol	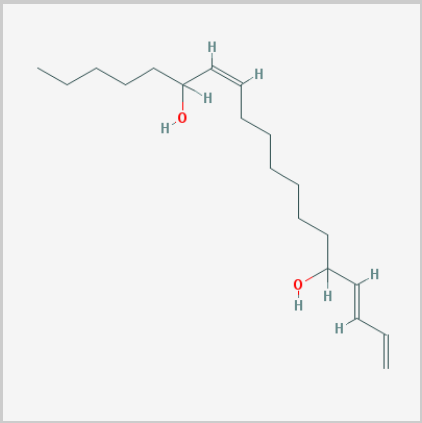	M	82%	15.345
		N	82%	15.345
		O	81%	15.345
		X	76%	17.870
Octadecane		M	91%	15.320
		O	91%	15.235
		S	92%	15.235
		U	93%	15.235
		W	91%	16.370
		Z	85%	15.230
		AA	87%	15.230
		CC	89%	15.230
		DD	92%	15.230
		GG	92%	15.230
		HH	91%	17.445
		II	91%	17.445
Tetradecane	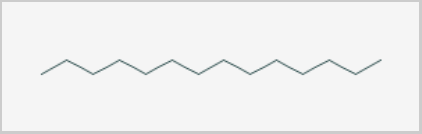	M	91%	12.765
		N	91%	12.765
		O	92%	12.765
		P	93%	12.765
		Q	93%	12.765
		R	93%	12.765
		S	93%	12.770
		T	94%	12.765
		U	94%	12.765
		V	94%	12.765
		W	95%	12.760
		X	89%	12.760
		Y	86%	12.760
		Z	89%	12.760
		AA	87%	12.760
		BB	89%	12.760
		CC	87%	12.760
		DD	90%	12.760
		EE	93%	12.760
		FF	91%	15.230

		GG	90%	12.760
		HH	92%	12.760
		II	91%	12.760
3.alpha.-(Trimethylsiloxy)cholest-5-ene/ Silane, trimethyl [[(3.beta.)-stigmast-5-en-3-yl]oxy]-	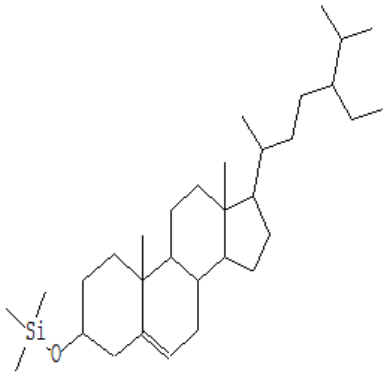	O	79%	31.285
		V	74%	25.295
Methyl behenate/ Docosanoic acid, methyl ester	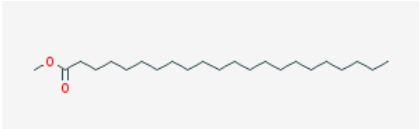	N	80%	18.740
		U	80%	18.757
1-Heptatriacotanol		O	82%	23.850
		X	76%	15.685
Cyclopropanebutanoic acid, 2-[[2-[[2-[(2pentylcyclopropyl)methyl]cyclopropyl]methyl]cyclopropyl]methyl]-, methyl ester	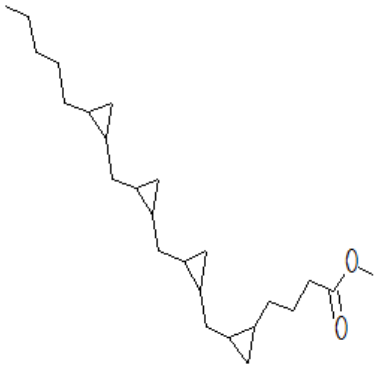	O	78%	18.740
		S	78%	20.655
		V	81%	18.740
		W	79%	20.655
		X	76%	18.740
(2,2,6-Trimethyl-bicyclo[4.1.0]hept-1-yl)-methanol	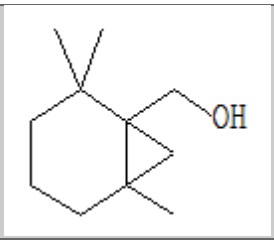	O	78%	17.365

Ppropiolic acid, 3-(1-hydroxy-2-isopropyl-5-methylcyclo hexyl)	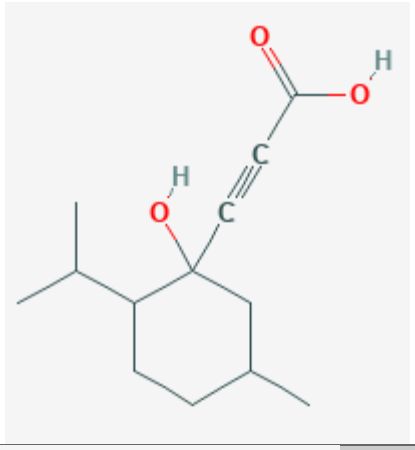	O	77%	17.280
6-epi-shyobunol	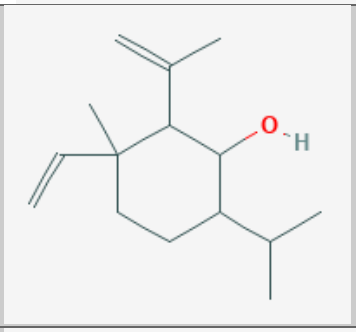	O	76%	17.120
		P	75%	17.120
1-Heptadec-1-ynyl-cyclopentanol	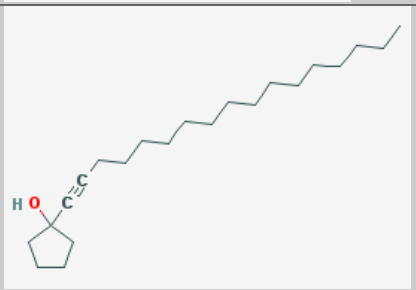	O	78%	15.880
		S	79%	16.225
(2,6,6-Trimethylcyclohex-1-enylmethanesulfonyl)benzene	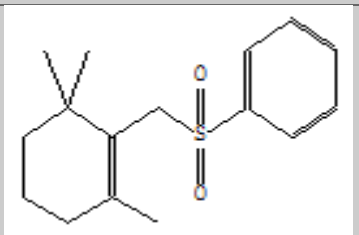	O	81%	15.485
4,6,6-Trimethyl-bicyclo[3.1.1]heptan-2-ol	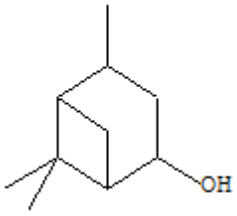	O	71%	13.690

Benzeneethanol, 4-hydroxy	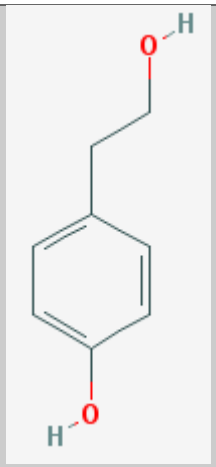	O	93%	13.140
		P	91%	13.140
1-Phenyl-3-buten-1-ol	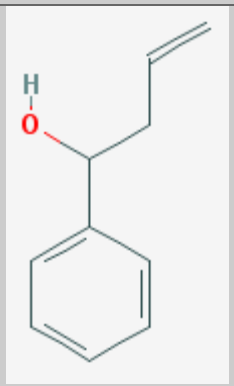	O	81%	11.565
		P	80%	11.560
Tritetracontane	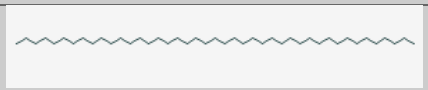	O	84%	11.415
		S	84%	11.420
Dodecane	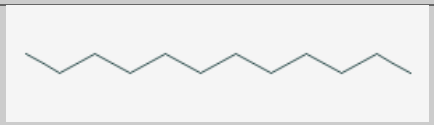	O	95%	8.460
		P	90%	9.990
		Q	90%	9.985
		R	91%	9.985
		S	92%	9.990
		T	92%	9.990
		U	93%	9.985
		V	94%	9.990
		W	93%	9.985
		X	94%	9.985
		Y	90%	9.985
		Z	90%	9.985
		AA	91%	9.985
		BB	93%	9.985
		CC	90%	9.985
		DD	93%	9.980
		EE	92%	9.985

		FF	93%	9.985
		GG	93%	9.990
		HH	93%	9.985
		II	94%	9.985
2-Pentene, 2,3-dimethyl	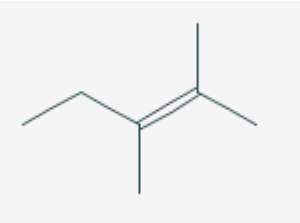	O	82%	5.095
10-epi-.gamma.-eudesmol	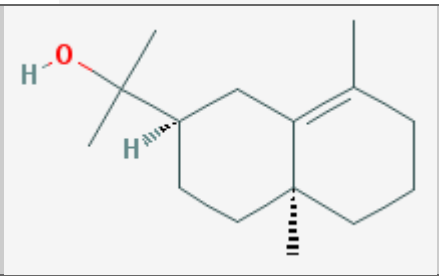	P	71%	29.080
Silane, [(3.alpha.)-cholest-5-en-3-yloxy]trimethyl-	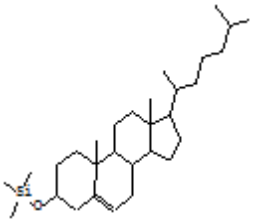	N	79%	25.645
		O	76%	25.640
		P	75%	26.485
		Q	77%	25.185
		R	74%	25.185
		S	76%	25.640
		T	74%	25.180
		U	74%	25.185

		W	75%	23.530
		Y	77%	26.660
		Z	74%	23.205
Cortisol/ Pregn-4-ene-3,20-dione, 11,17,21-trihydroxy-, (11.beta.)-	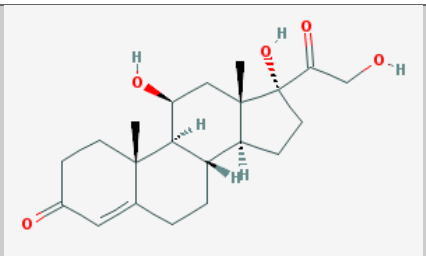	P	75%	23.115
Psilostachyin A/ **Spiro[7H-cyclohepta[b]furan-7,2'(5'H)-furan]-2,5'(3H)-dione, octahydro-8-hydroxy-6,8-dimethyl-3-methylene-, [3aS-(3a.alpha.,6.beta.,7.alpha.,8.alpha.,8a.alpha.)]-**	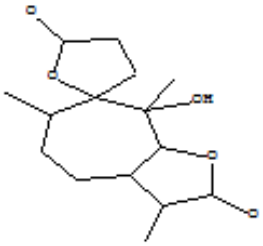	P	77%	22.575
1b,4a-Epoxy-2H-cyclopenta[3,4]cyclopropa[8,9]cycloundec[1,2-b]oxiren-5(1aH)-one, 2,7,9,10-tetrakis(acetyloxy)decahydro-3,6,8,8,10a-	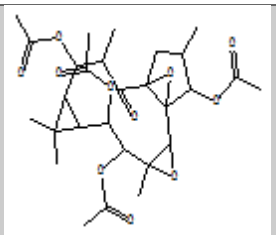	P	78%	16.805

pentamethyl-				
Farnesane/ Dodecane, 2,6,10-trimethyl	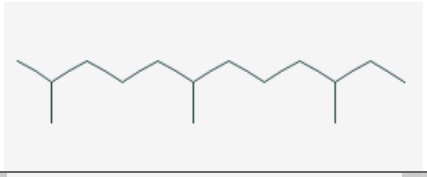	P	86%	11.420
2-Hexanol, 2,5-dimethyl	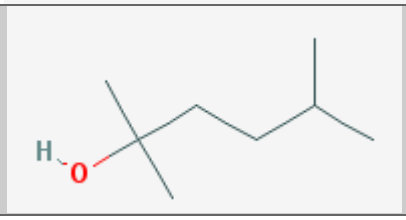	P	84%	10.235
Undecane	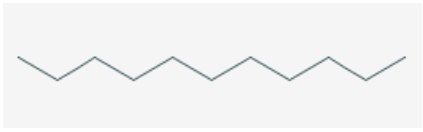	P	94%	8.465
		R	95%	8.460
		S	95%	8.460
		T	96%	8.460
		U	96%	8.455
		V	96%	8.460
		W	97%	8.450
		X	96%	8.455
		Y	95%	8.455
		Z	95%	8.455
		AA	94%	8.455
		BB	95%	8.455
		CC	94%	8.460
		FF	92%	8.460
		GG	93%	8.470
		HH	95%	8.455
		II	95%	8.455
3-Chloro-1-cyclohexyloxy-3-methyl-2-nitrosobutane	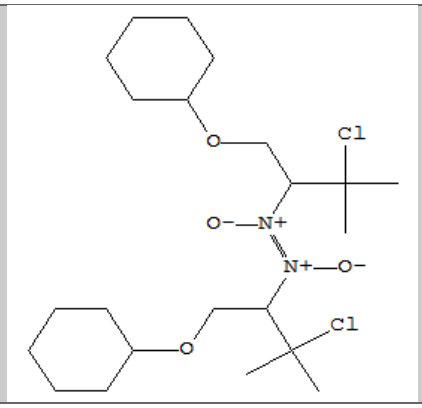	P	82%	5.100
		T	80%	5.110
		V	77%	5.110

7-Methoxy-1-methyl-2-pentyl-3H,4-hydro-pyrido[3,4-b]indole	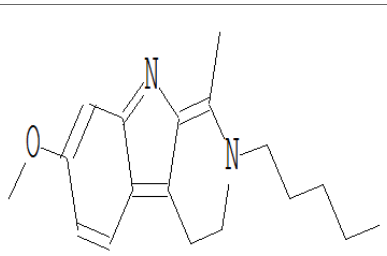	Q	71%	21.235
		S	74%	21.235
		T	70%	21.230
3,6-Dimethyl-5-hepten-1-ol acetate	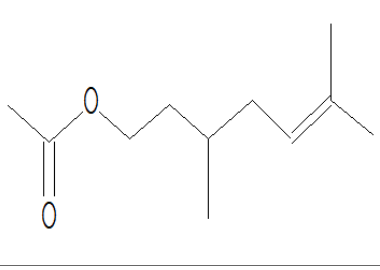	Q	82%	15.995
		R	80%	15.995
		S	79%	15.885
Diethyl carbitol/ Ethane, 1,1'-oxybis[2-ethoxy	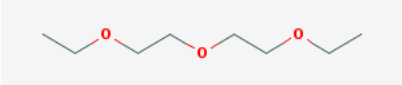	Q	75%	14.495
Cyclopropane, 2-chloro-1,1,3-trimethyl	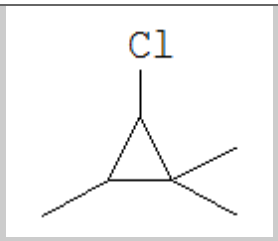	Q	80%	5.070
		U	81%	5.085
RORIDIN E	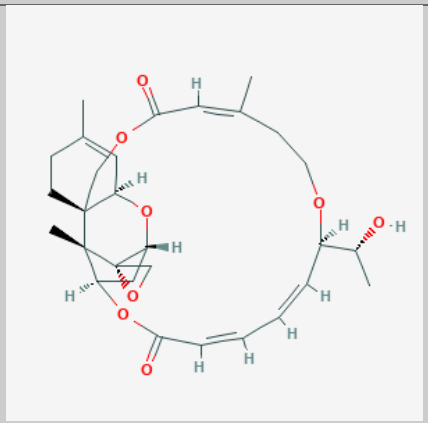	R	76%	17.120

		CC	78%	20.380
(-)-Vincadifformine	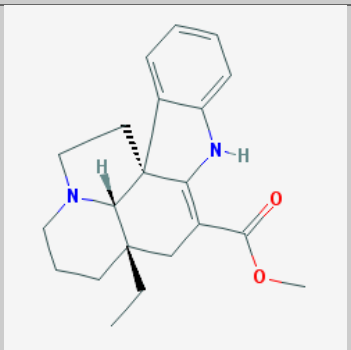	R	81%	15.885
1,3,5-Triazine-2,4-diamine, 6-chloro-N-ethyl	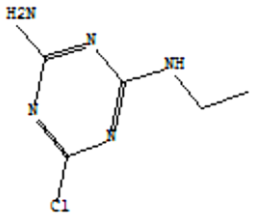	R	76%	15.805
Benzaldehyde, 4-hydroxy-2-methoxy	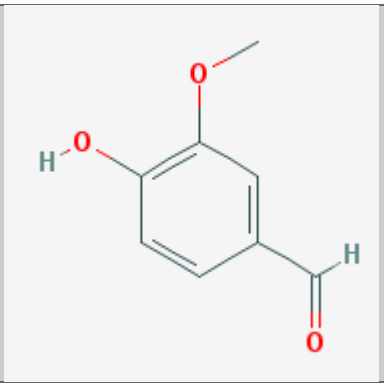	R	80%	12.855
2-Methoxy-4-vinylphenol	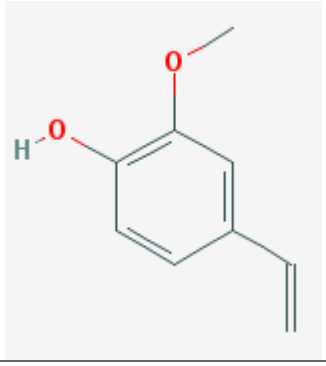	R	72%	11.700

1,7-OCTADIENE, 2,3,3-TRIMETHYL	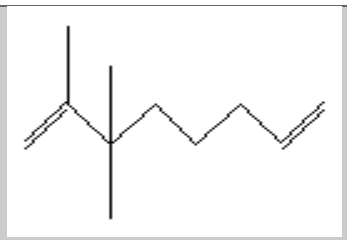	R	77%	5.105
Ergosta-5,24(28)-dien-3-ol, (3.beta.)	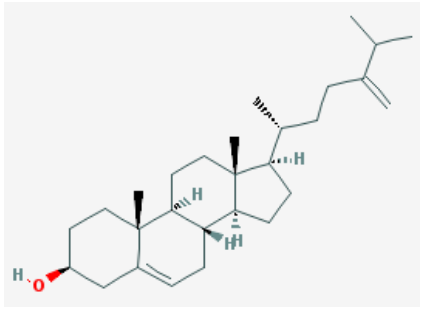	S	73%	18.125
Aspidospermidin-17-ol, 1-acetyl-16-methoxy-	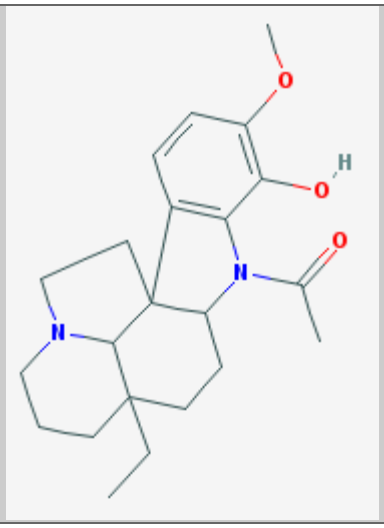	S	81%	10.910
		T	79%	17.940
		U	79%	17.365
		V	81%	17.365
		Z	78%	17.365
1,4-Dioxaspiro[4.5]decane, 8-(methylthio)	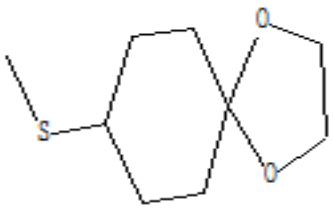	S	75%	10.060
		T	80%	16.120

1-(3,4-DIHYDROXY-5-HYDROXYMETHYL-TETRAHYDRO-FURAN-2-YL)-4,5-DIHYDROXY-1H-PYRIMIDIN-2-ONE	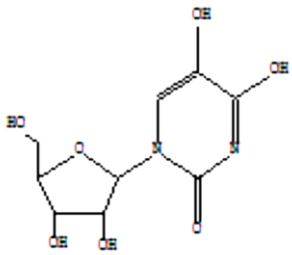	S	70%	9.865
Durene/ Benzene, 1,2,4,5-tetramethyl	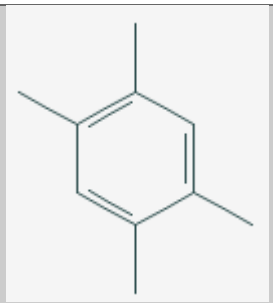	S	79%	8.845
		T	83%	7.270
		V	91%	8.845
		W	94%	8.840
		Z	78%	8.840
1,4-Dioxane, 2-ethyl-5-methyl	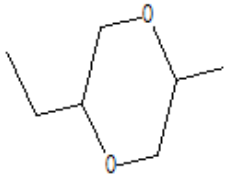	S	81%	8.485
Hydroperoxide, 1-ethylbutyl	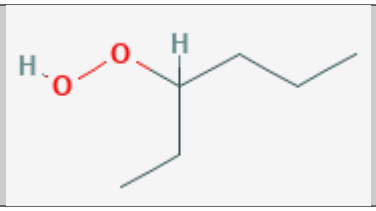	S	80%	5.275
1-Butene, 2,3,3-trimethyl	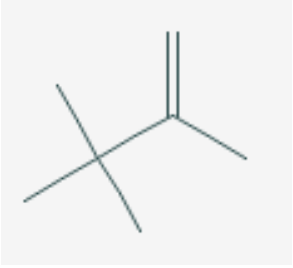	S	90%	5.100

Spirost-8-en-11-one, 3-hydroxy-, (3.beta.,5.alpha., 14.beta.,20.beta. ,22.beta.,25R)	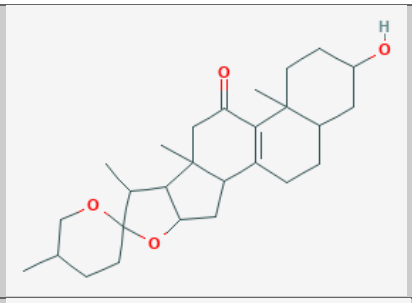	T	75%	18.125
		U	72%	18.125
Tetratria-contane		T	88%	14.030
Benzaldehyde, 4-hydroxy-3-methoxy/ vanillin	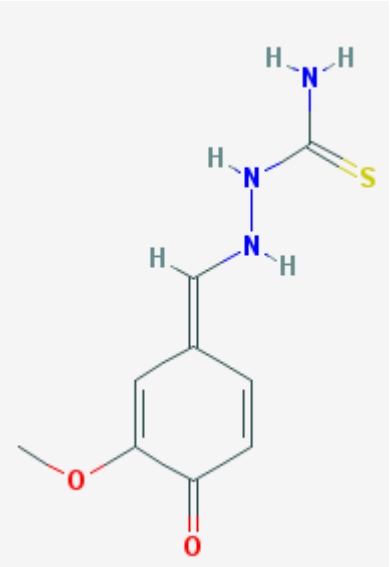	T	86%	12.850
Tetratetraconta ne	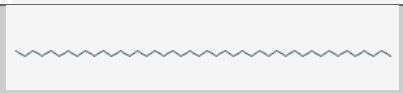	T	88%	11.420
1,3-Cyclopentadiene, 1,2,3,4-tetramethyl-5-methylene	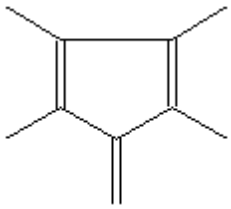	T	85%	8.845
Methoxyacetic acid, 2-tridecyl ester		U	87%	11.420

2-HYDROXYMETHYL-6-(3-NITRO-PHENOXY)-TETRAHYDRO-PYRAN-3,4,5-TRIOL	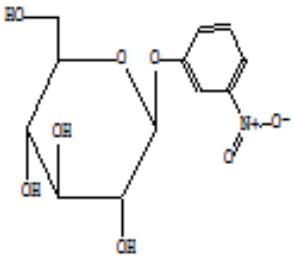	U	70%	9.860
		V	75%	9.865
Benzene, 1,2,3,5-tetramethyl	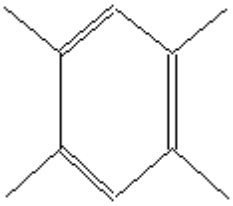	U	88%	8.840
1,1-Cyclobutanedicarboxamide, 2-phenyl-N,N'-bis(1-phenylethyl		U	73%	6.695
QUERCETIN 7,3',4'-TRIMETHOXY	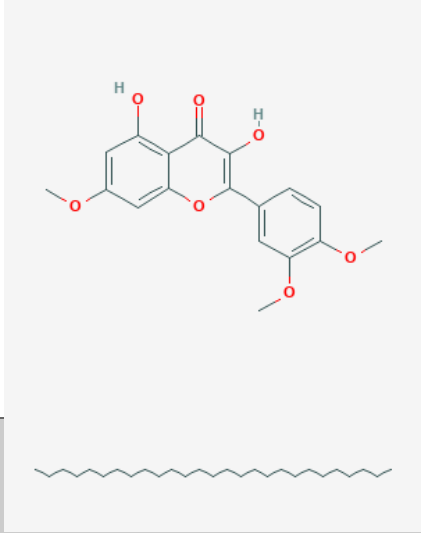	V	73%	19.845
Heptacosane		V	88%	14.030

Benzene, 4-ethyl-1,2-dimethyl	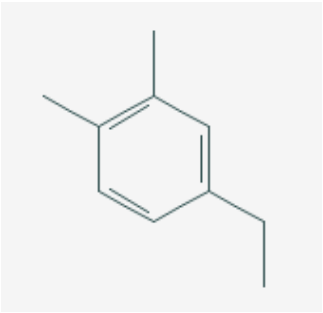	V	83%	8.280
		W	92%	8.275
Benzene, 1,3,5-trimethyl	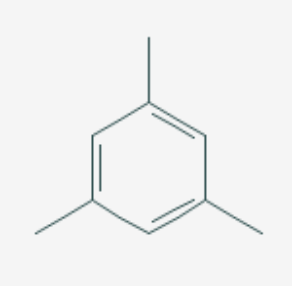	V	75%	6.710
		W	92%	7.255
beta.-Agarofuran, dihydro/ 6a,14a-Methanopicene, perhydro-1,2,4a,6b,9,9,12a-heptamethyl-10-hydroxy-	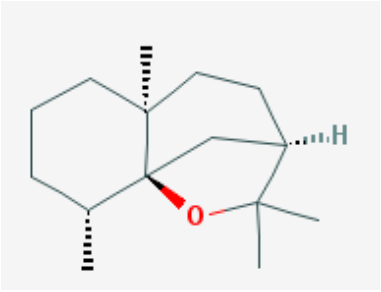	W	71%	26.730
Lanosta-7,9(11)-dien-18-oic acid, 22,25-epoxy-3,17,20-trihydroxy-, .gamma.-lactone, (3.beta	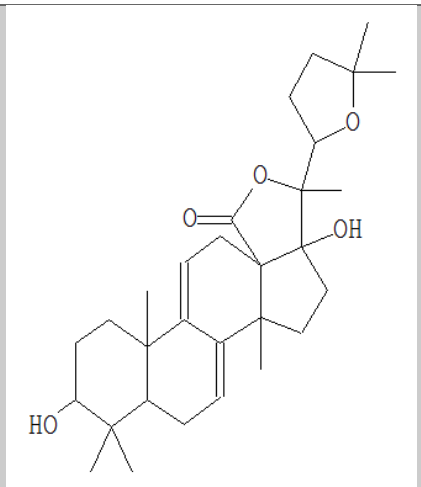	W	70%	25.490

Octadecyl acetate	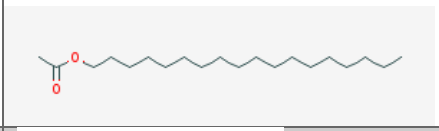	W	81%	21.385
1-(HYDROXYMETHYL)-2,5,5,8A-TETRAMETHYLDECAHYDRO-2-NAPHTHALENOL	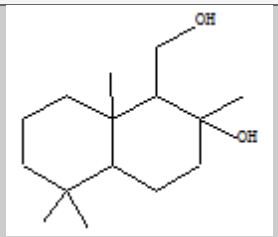	W	77%	16.785
Pentadecane	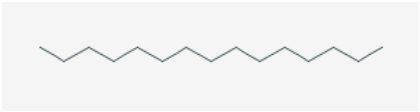	W	93%	14.030
Naphthalene	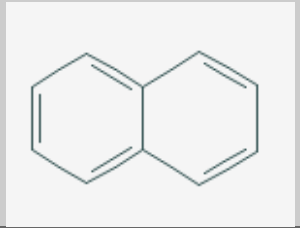	W	83%	9.860
3-tert-Butyl-5-chloro-2-hydroxybenzophenone	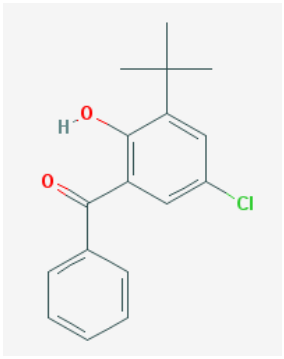	W	72%	7.980
1,3-Pentanediol, 2,2,4-trimethyl	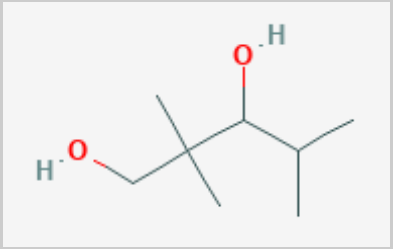	W	72%	7.775

Acetamide, N-benzyl-2-(4H-[1,2,4]triazol-3-yl)-	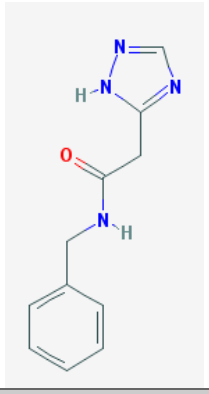	W	76%	5.085
7-Dehydrocholesteryl isocaproate	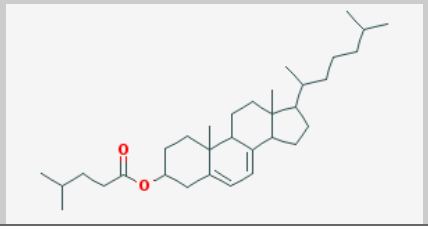	X	73%	21.610
Tricosane		X	90%	15.230
1,2,3-Benzenetriol /Pyrogallol	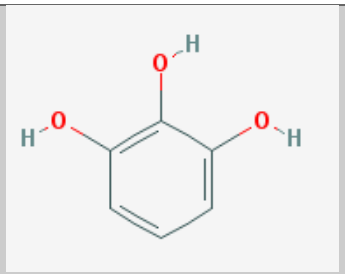	X	91%	12.525
		Y	96%	12.510
		Z	80%	12.510
		AA	95%	12.515
		BB	95%	12.515
		CC	94%	12.515
		DD	87%	12.535
		FF	84%	12.540
1,1,6-trimethyl-3-methylene-2-(3,6,9,13-tetramethyl-6-ethenye-10,14-dimethylene-pentadec-4-enyl)cyclohexane	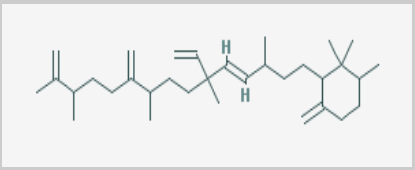	Y	76%	26.565
Octadecanoic acid, 2,3-dihydroxypropyl	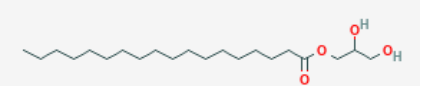	Y	76%	25.480
		Z	80%	25.485
		BB	81%	25.480
		CC	77%	25.480

ester/ Glyceryl monostearate;		DD	71%	25.480
		EE	75%	25.485
		GG	71%	25.485
13-[(1-Phenylethylimino)methyl]tricyclo[8.2.2.24,7]hexadeca-1(13),4,6,10(14),11,15- hexaen-5-ol	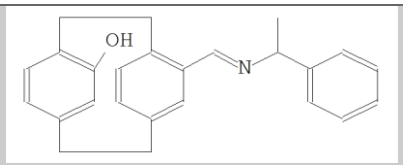	Y	70%	22.805
Methyl 5-(2-phenylpropionyl) hexanoate	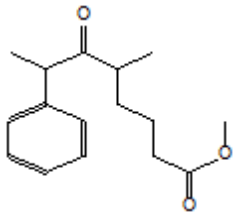	Y	70%	22.575
Sambucinol/ Trichothec-9-ene-3,13-diol, 11,12-epoxy-, (3beta,11beta,12R)	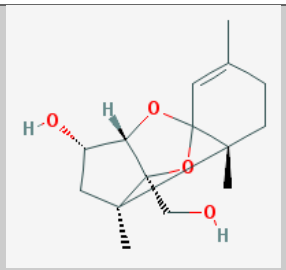	Y	73%	22.370
		Z	71%	22.375
Hexane, 2-phenyl-3-propyl	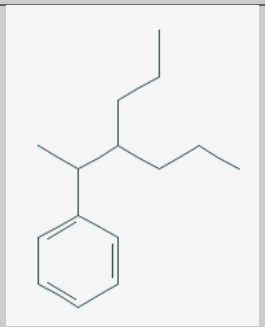	Y	75%	21.415

4-((1E)-3-Hydroxy-1-propenyl)-2-methoxyphenol	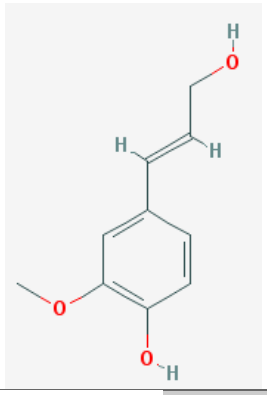	Y	81%	16.890
ENDO-ISOCAMPHONONE	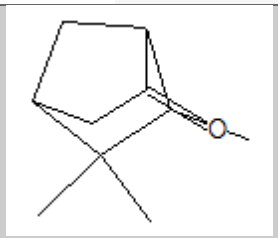	Y	73%	15.885
Megastigma trienone	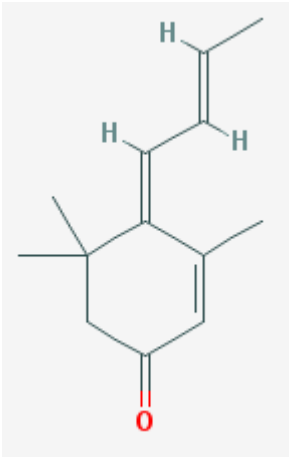	Y	91%	15.690
		Z	89%	15.690
		AA	78%	15.685
Acetovanillone/ Ethanone, 1-(4-hydroxy-3-methoxyphenyl)	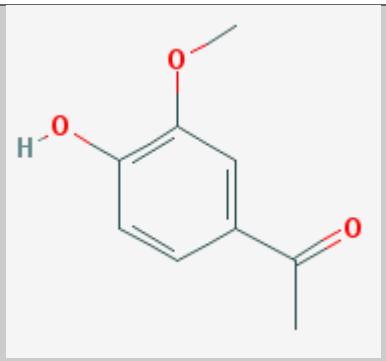	Y	84%	15.190
		Z	89%	15.190
		AA	79%	15.185
		BB	76%	15.185
trans-2-Dodecenoic acid	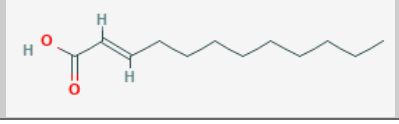	Y	84%	14.720

D-Allose	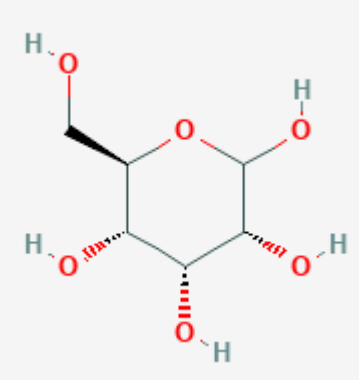	Y	90%	13.810
		Z	91%	13.830
		AA	88%	13.825
		BB	87%	13.795
		CC	84%	13.795
		DD	84%	13.790
		EE	86%	13.785
		FF	84%	13.790
Hydrazine, 1-(3-hydroxybenzyl)	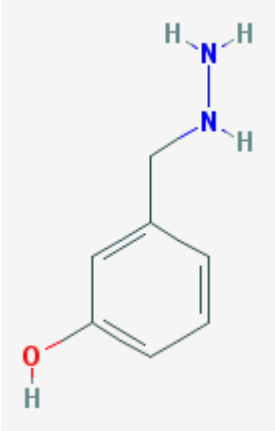	Y	74%	13.145
9-Oxabicyclo[4.2.1]non-7-en-3-ol	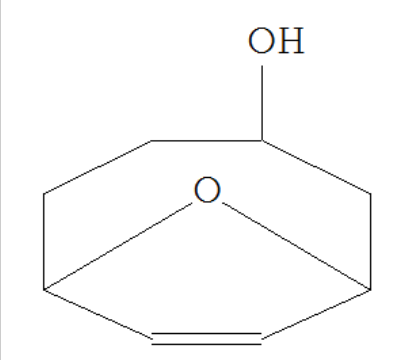	Y	85%	10.265
		Z	85%	10.275
		AA	84%	10.250

2-Butenal, 2-methyl-4-(2,6,6-trimethyl-1-cyclohexen-1-yl)	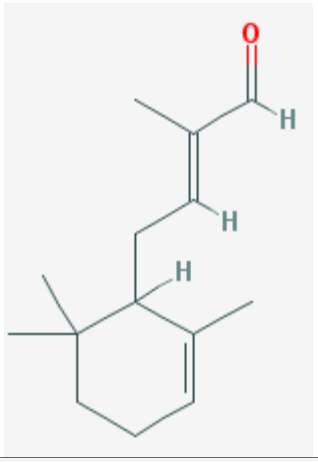	Z	70%	26.715
Cholest-5-en-3-ol (3.beta.)-, 9-octadecenoate, (Z)-	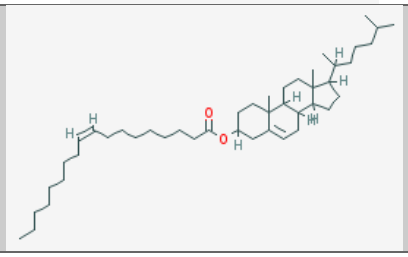	Z	71%	21.240
H-Benzocycloheptene-2-one, decahydro-9a-methyl-, trans	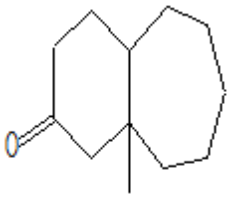	Z	71%	17.870
2-(5'-Hydroxy-1',1',5'-trimethylhexyl)-3-methylcyclopropenyl methyl ketone	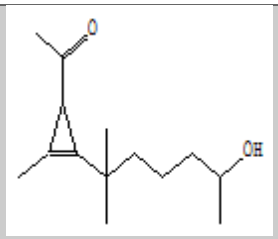	Z	76%	17.820
2,5-Dimethyl-4-methoxyphenol	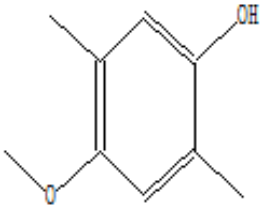	Z	71%	16.365

Desulphosinigrin	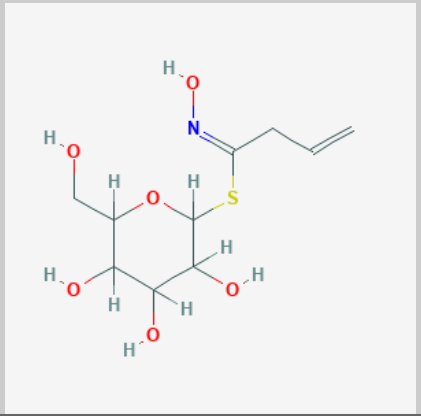	Z	76%	15.435
PERMETHYLATED AND REDUCED PRODUCT OF DEGRADATION PRODUCT FROM H3-GLYCOLIPID BY L-L-FUCOSIDASE AND BY B-GALACTOSIDASE		Z	73%	14.715
Stearic acid / Octadecanoic acid		Z	74%	14.025
ANHYDROGLUCOPYRANOSE, TBS 1X		Z	72%	13.625

BUTANEDIOIC ACID, 2,3-DIMETHOXY-, DIETHYL ESTER	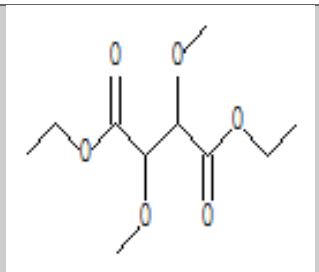	Z	73%	11.365
1-Methoxy- 5-trimethylsilyloxy-3-phenylpentane	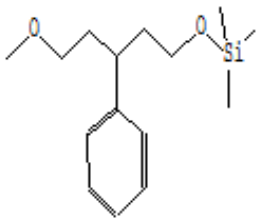	Z	71%	9.195
2-Deoxy-2-fluoro-1,6-anhydro-.beta.-d-glucopyranose	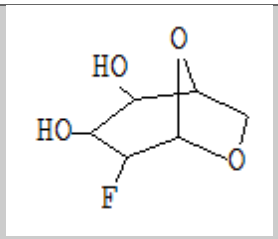	Z	74%	9.035
4-Methylmannitol	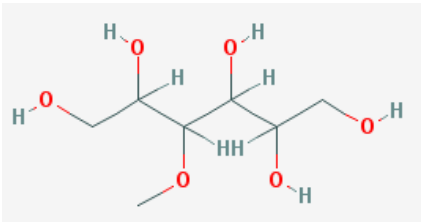	Z	71%	8.915
Cyclohexanamine, N-3-butenyl-N-methyl	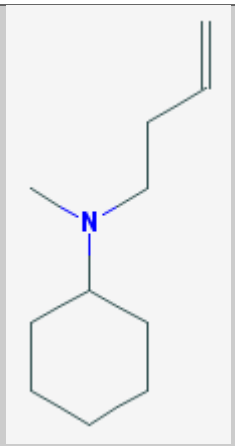	Z	83%	8.125
		AA	85%	8.125

2,5-Methylene-d,l-rhamnitol	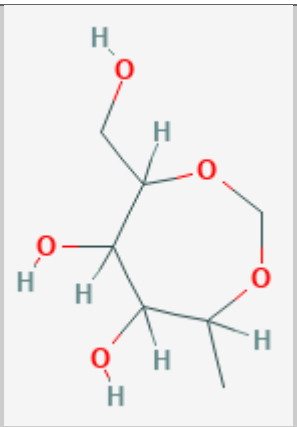	Z	73%	6.715
Lactose / D-Glucose, 4-O-.beta.-D-galactopyranosyl	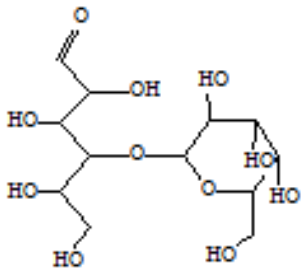	AA	79%	17.445
		BB	81%	17.445
METHYL 3-ACETYLHYDROXYPALMITATE / Monopalmitolein	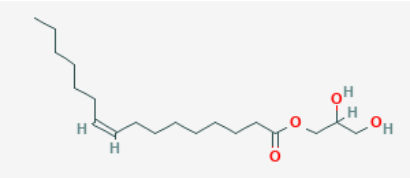	AA	74%	15.050
		CC	74%	15.050
Phenol, 2,6-dimethoxy	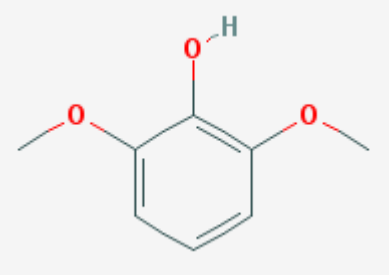	AA	76%	12.180
		BB	93%	12.185
		CC	82%	12.190

18,18'-Bi-1,4,7,10,13,16-hexaoxacyclononadecane		AA	72%	9.350
3-n-Butylthiolane	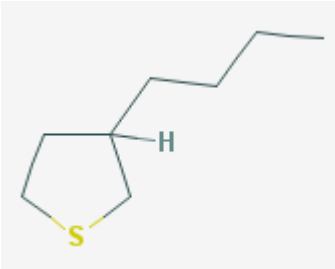	AA	72%	9.195
3-Dimethylsilyloxytetradecane		AA	72%	8.920
2,4-Dihydroxy-2,5-dimethyl-3(2H)-furan-3-one	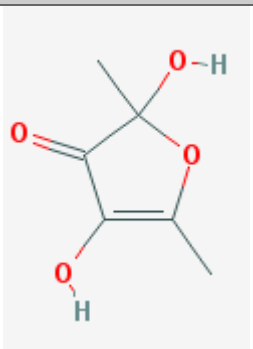	AA	76%	6.530
Benzenepropanoic acid, 3,5-bis(1,1-dimethylethyl)-4-hydroxy-, methyl		BB	70%	18.980
		CC	74%	18.985
		DD	78%	18.985

ester		EE	76%	18.985
		FF	77%	18.985
		GG	77%	19.980
		HH	74%	18.985
		II	78%	18.980
9,10-Secocholesta-5,7,10(19)-triene-1,3-diol, 25-[(trimethylsilyl)oxy]-, (3.beta.,5Z,7E)	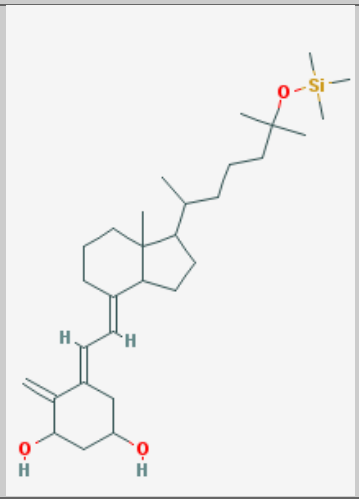	BB	70%	18.785
Pentadecanoic acid, 14-methyl-, methyl ester	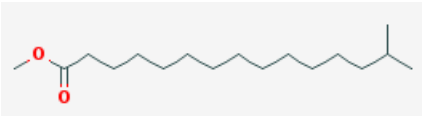	BB	76%	18.740
		CC	80%	18.740
7-Methyl-Z-tetradecen-1-ol acetate	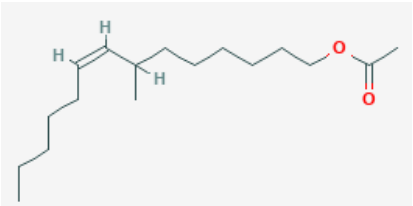	BB	75%	15.050
4-Fluoro-1-methyl-5-carboxylic acid, ethyl(ester)	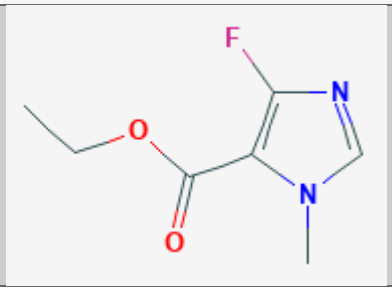	BB	72%	14.770

8-Methyl-6-nonenoic acid	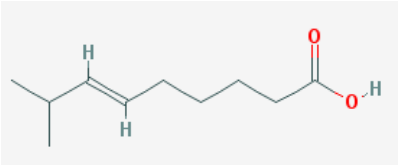	BB	71%	13.590
2-Trifluoroacetoxytridecane		BB	70%	13.270
		EE	71%	13.115
Propanoic acid, nonyl ester	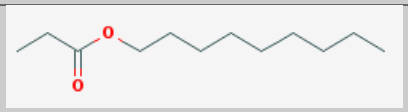	BB	74%	13.120
2-Heptanol, 5-ethyl	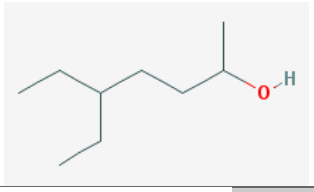	BB	79%	9.560
N-(3-BUTENYL)-N-METHYLCYCLOHEXANAMINE	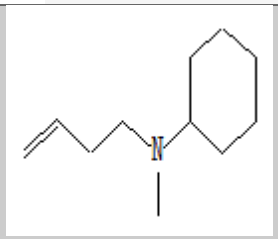	BB	79%	8.125
M-XYLENE / BENZENE, 1,3-DIMETHYL	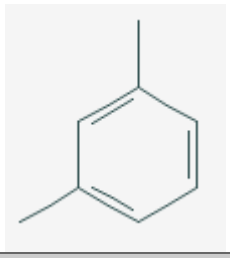	BB	82%	5.120
Hexadecanoic acid, 2-hydroxy-1-(hydroxymethyl)ethyl ester/ 2-Monopalmitin		CC	77%	23.895
		DD	75%	23.895

Heptadecanoic acid, 10-methyl-, methyl ester	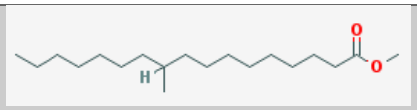	CC	79%	20.650
Acetic acid, chloro-, hexadecyl ester	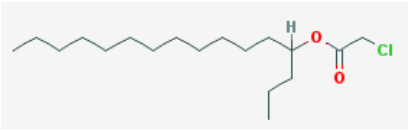	CC	76%	20.260
		HH	86%	20.260
Quinic acid	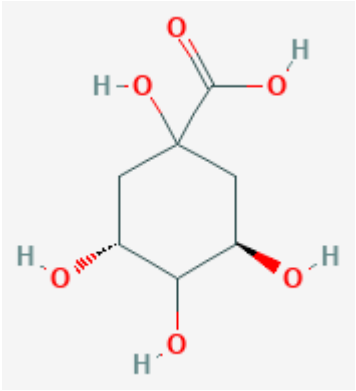	CC	83%	15.280
		DD	83%	15.265
		FF	80%	15.270
Lauroyl peroxide	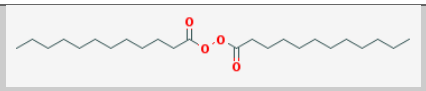	CC	71%	13.120
1,2-Benzenedicarboxylic acid, dioctyl ester	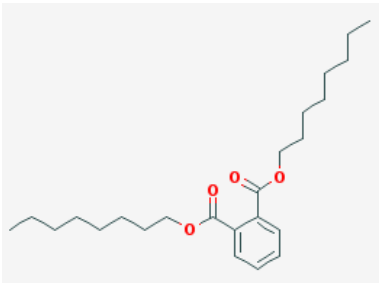	DD	73%	24.225
		GG	74%	24.220

7-Hexadecenoic acid, methyl ester		DD	79%	20.435
Cyclopropaneoctanoic acid, 2-[[2-[(2-ethylcyclopropyl)methyl]cyclopropyl]methyl]-, methyl ester		DD	85%	20.380
		FF	86%	20.380
1-Pentadecanol	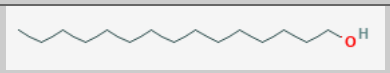	DD	81%	20.260
Acetic acid, 2-propylpentyl ester	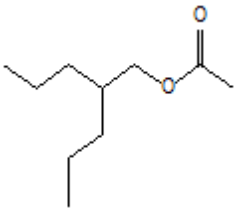	DD	70%	13.115
		FF	73%	13.115
		GG	75%	13.120
2-Propenoic acid, octyl ester		DD	79%	9.570
		GG	82%	9.575
9-Octadecenoic acid (Z)-, methyl ester	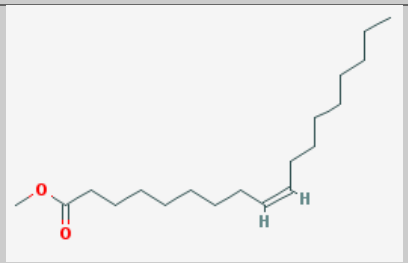	EE	78%	20.435
		FF	81%	20.435

Z,Z-8,10-Hexadecadien-1-ol	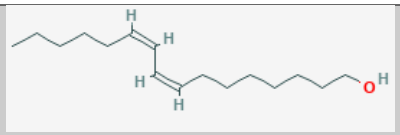	EE	80%	20.385
Chloroacetic acid, pentadecyl ester	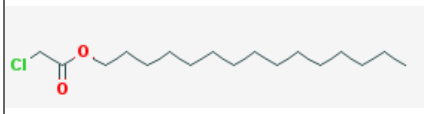	EE	81%	20.260
(trans)-2-nonadecene	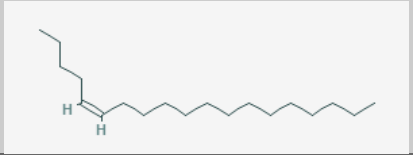	EE	79%	15.145
2-Nonene	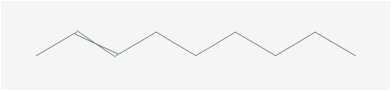	EE	82%	10.400
3-Chloropropionic acid, heptadecyl ester	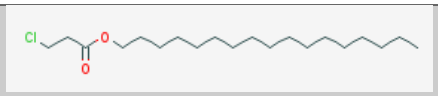	FF	80%	20.260
2-Chloropropionic acid, pentadecyl ester	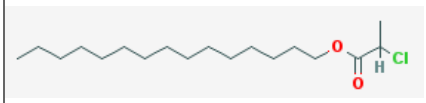	FF	80%	17.375
3-octyl acetate	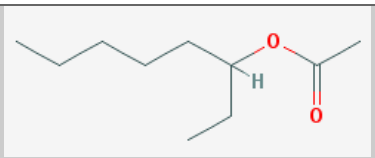	FF	83%	9.570
1-Heptadecanol	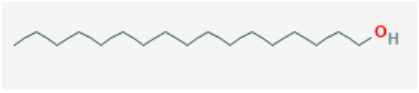	GG	85%	20.260

7,9-Di-tert-butyl-1-oxaspiro(4,5)deca-6,9-diene-2,8-dione	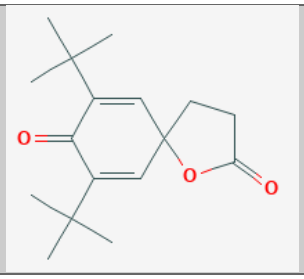	GG	70%	18.785
1,6-ANHYDRO-BETA-D-GLUCOPYRANOSE / LEVOGLUCOSAN	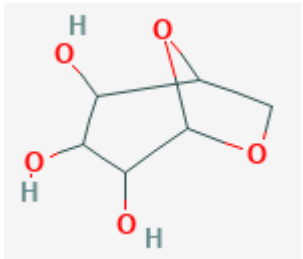	GG	84%	13.785
		HH	84%	13.785
		II	82%	13.780
6-Octadecenoic acid, methyl ester	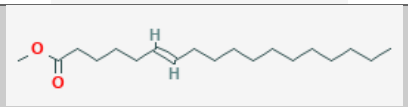	HH	84%	20.435
Hexadecadienoic acid, methyl ester	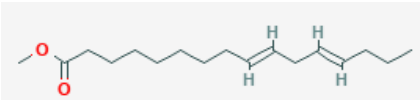	HH	88%	20.380
8-Heptadecanol, 8-methyl-	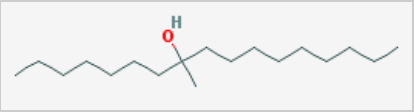	HH	72%	13.115
		II	72%	13.115
7-Octadecenoic acid, methyl ester	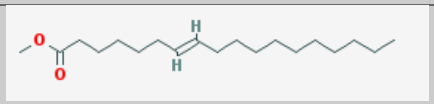	II	89%	20.430
9,12-Octadecadienoic acid (Z,Z)-, methyl ester	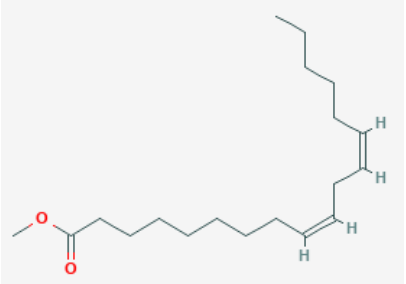	II	92%	20.380
1-Eicosanol	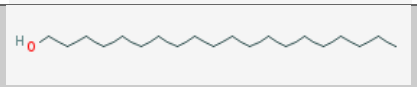	II	80%	20.260